AD NUMBER

ADB017795

NEW LIMITATION CHANGE

TO

Approved for public release, distribution unlimited

FROM

Distribution authorized to U.S. Gov't. agencies only; Test and Evaluation; 22 APR 1977. Other requests shall be referred to Aeronautical Systems Division, Attn: XRH, Wright-Patterson AFB, OH 45433.

AUTHORITY

ASD/WPAFB USAF ltr, 17 Aug 1977

(2)

INNOVATIVE AIRCRAFT DESIGN STUDY, TASK II

Nuclear Aircraft Concepts

LOCKHEED-GEORGIA COMPANY
Marietta, Georgia 30063

April 1977

Final Report on Contract F33615-76-C-0112
24 June 1976 to 15 April 1977

Prepared for

THE UNITED STATES AIR FORCE
Air Force Systems Command
Aeronautical Systems Division
Wright-Patterson AFB, Ohio 45433

SECURITY CLASSIFICATION OF THIS PAGE (When Data Entered)

REPORT DOCUMENTATION PAGE

READ INSTRUCTIONS BEFORE COMPLETING FORM

1. REPORT NUMBER

2. GOVT ACCESSION NO.

3. RECIPIENT'S CATALOG NUMBER (9)

4. TITLE (and Subtitle) (6)

INNOVATIVE AIRCRAFT DESIGN STUDY, TASK II, Nuclear Aircraft Concepts.

5. TYPE OF REPORT & PERIOD COVERED
Final Report.
24 June 1976 to 15 April 1977.

6. PERFORMING ORG. REPORT NUMBER (14) LG77ER0008

7. AUTHOR(s) John C. Muehlbauer, David N. Byrne, Eugene P. Craven, Charles C. Randall, Sterling G. Thompson of Lockheed and Robert E. Thompson, Bill L. Pierce, Jack M. Ravets & Richard J. Steffan of Westinghouse

8. CONTRACT OR GRANT NUMBER(s) (15) F33615-76-C-0112 Mod

9. PERFORMING ORGANIZATION NAME AND ADDRESS
Lockheed-Georgia Company
86 South Cobb Drive
Marietta, Georgia 30063

10. PROGRAM ELEMENT, PROJECT, TASK AREA & WORK UNIT NUMBERS

11. CONTROLLING OFFICE NAME AND ADDRESS
Deputy for Development Planning
Aeronautical Systems Division
Air Force Systems Command, United States Air Force
Wright-Patterson AFB, Ohio 45433

12. REPORT DATE (11) April 1977

13. NUMBER OF PAGES
266

14. MONITORING AGENCY NAME & ADDRESS (if different from Controlling Office)
(12) 254p.

15. SECURITY CLASS. (of this report)
Unclassified

15a. DECLASSIFICATION/DOWNGRADING SCHEDULE

16. DISTRIBUTION STATEMENT (of this Report)
(10) John C. Muehlbauer, Charles C. Randall
David N. Byrne, Sterling G. Thompson
Bill L. Pierce

17. DISTRIBUTION STATEMENT (of the abstract entered in Block 20, if different from Report)

18. SUPPLEMENTARY NOTES

19. KEY WORDS (Continue on reverse side if necessary and identify by block number)
Innovative Aircraft, Nuclear Aircraft, Airborne Nuclear Propulsion, Nuclear-Powered Aircraft, Advanced Transport Aircraft, Chemical-Fueled Aircraft, Advanced Technology Aircraft, NuERA II Reactor Systems, Composite Materials, Laminar Flow Control, Spanloader Aircraft, Aircraft Costing

20. ABSTRACT (Continue on reverse side if necessary and identify by block number)
Parametric analyses and design refinement studies were performed for conventional, canard, and spanloader aircraft configurations to determine the lightest ramp weight configuration with a nuclear propulsion system. Mission requirements for these analyses were: 400,000 and 600,000-lb payloads, 0.75 cruise Mach number, 1000 n.m. emergency chemically-fueled range, and a 9000-ft field length. The parametric investigation included variations of cruise altitude, engine bypass ratio and turbine inlet temperature, wing loading, wing sweep angle, and wing aspect ratio. The canard

DD FORM 1 JAN 73 1473 EDITION OF 1 NOV 65 IS OBSOLETE

210 065

SECURITY CLASSIFICATION OF THIS PAGE (When Data Entered)

20. Abstract

configuration was between one and ten percent lighter in ramp weight than the other candidates at both payloads.

Analyses of several Rankine and Brayton nuclear propulsion cycles showed an open Brayton cycle to be preferable because of its low weight and extensive data base. The selected cycle and the canard configuration were used to develop an aircraft subject to the following mission requirements: 400,000-lb payload, 0.75 cruise Mach number, 10,000-ft field length, and 1000 n.m. emergency range. The resulting reference aircraft with a ramp weight of 1,556,491 lb served as a basis for assessing the design sensitivity of alternate mission requirements, technology applications, and nuclear operating philosophies. A 13.1-percent weight reduction was achieved through an alternate nuclear operating philosophy which included shaped shielding, use of emergency range chemical fuel for shielding, and reactor utilization during all flight phases. A similar weight savings of 13.5 percent relative to an all-aluminum aircraft was realized by the reference aircraft with 40 percent of its structure in composite materials. Smaller weight effects were experienced for the other technologies investigated and for variations in the mission requirements.

Economic costs were derived based on a production run of 250 aircraft, a 10,500 n.m. average trip range, and an annual utilization of 1080 hrs for military application. The unit acquisition cost was estimated to be 139 million dollars and the 20-year life-cycle cost for the fleet was 71.2 billion dollars. Using a 3000-hr annual utilization rate consistent with commercial expectations, a unit flyaway cost of 115.6 million dollars was estimated for civil application. The corresponding life-cycle cost for the fleet was 93.8 billion dollars. By adopting the special nuclear design features of the alternate nuclear aircraft, it was determined that a cost savings of 7.9 percent would be accrued.

Comparisons were made of the reference and alternate nuclear aircraft with JP-fueled aircraft to determine that design range value which will result in JP-fueled aircraft with the same ramp weights or life-cycle costs as the nuclear aircraft. The results showed the equal ramp weight cross-over ranges to be 9200 and 7850 n.m. relative to the reference and alternate nuclear aircraft, respectively. For mission ranges exceeding these values, the nuclear aircraft will be lighter in weight. The converse is true for shorter ranges. Similarly, the life-cycle cost ranges were 11,950 and 11,100 n.m., respectively. However, a 300-percent fuel price increase reduced these ranges to 6100 and 4700 n.m., respectively. Thus, as the severity of the energy shortage increases fuel prices, the future prospects for airborne nuclear propulsion will improve.

* (Brayton cycle and canard configuration)

SUMMARY

Parametric analyses and design refinement studies were performed for conventional, canard, and spanloader aircraft configurations to determine the lightest ramp weight configuration with a nuclear propulsion system. In external appearance, the conventional aircraft is a larger-scale C-5 type aircraft. The canard aircraft has a conventional fuselage for carrying cargo, a high wing positioned on the aft-end of the fuselage, a forward-fuselage mounted canard surface for horizontal control, and vertical tail surfaces mounted on each wingtip and the aft fuselage. The spanloader aircraft carries containerized cargo throughout its entire wing span, has a short fuselage for outsized cargo, and uses wingtip-mounted verticals and a fuselage-mounted canard for lateral and directional control.

The parametric design mission requirements for these configurations were payloads of 400,000 and 600,000 lb of containerized and/or outsized cargo, a cruise Mach number of 0.75, an emergency range of 1000 n.m. on chemical fuel, and a 9000-ft field length compatibility. Parametric variations of cruise altitude, engine bypass ratio and turbine inlet temperature, wing loading, wing sweep angle and wing aspect ratio were considered to determine the minimum ramp weight aircraft for each of the three candidate configurations.

Upon completion of the parametric analysis and several aircraft design refinements, the three aircraft configurations were compared for the two mission payload values. The canard configuration was selected for analysis since it had the lowest ramp weights of the three configurations for both payloads. For the larger payload of 600,000 lb, the canard aircraft was one percent lighter than the spanloader aircraft and 4.3 percent lighter than the conventional aircraft. For the smaller payload of 400,000 lb, the canard was 4.8 and 9.8 percent lower than the conventional and spanloader aircraft, respectively.

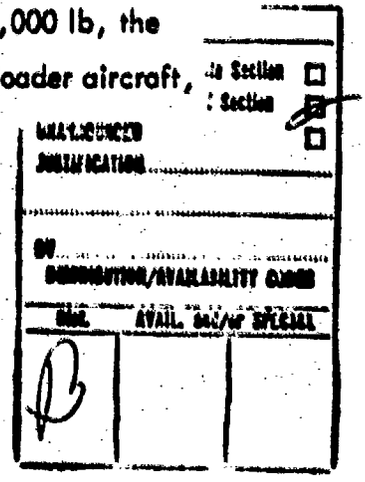

Analyses of several Rankine and Brayton nuclear propulsion cycles resulted in the selection of an open Brayton cycle for a reference aircraft. The selection was made on the basis of the extensive data background and low weight of the cycle. Of all the cycles considered, only a non-recuperated closed Brayton cycle with a dual-mode engine was found to be lighter in weight than the selected cycle. However, due to the inadequate data base for this closed Brayton cycle, it must be studied further before it can be considered as a viable candidate.

The selected canard configuration was used to develop an aircraft design for the reference mission requirements of a 400,000-lb payload, a 0.75 cruise Mach number, a 10,000-ft field length, and an emergency range of 1000 n.m. on chemical fuel. The resulting reference aircraft design with a ramp weight of 1,556,491 lb served as a basis for assessing the design sensitivity to variations in the mission requirements, in advanced technology applications, and in the nuclear operation and design philosophy. A 13.1-percent reduction in ramp weight to 1,353,119 lb was achieved by adopting an alternate nuclear operational design philosophy. Features of this alternative included special shaping of the shield, use of the emergency range chemical fuel for shielding, and full-power reactor operation for all normal flight phases with half-power for emergencies.

The use of composite materials for 40 percent of the structural weight of the reference aircraft produced a 13.5-percent scvings in aircraft ramp weight relative to an all-aluminum aircraft. Studies of the application of other advanced technologies indicated substantially smaller potential benefits than for composites. The other technologies considered and the effects on aircraft ramp weight were: laminar flow control on wing and verticals saved 3.6 percent, engine bypass ratios between 5.8 and 18 varied the weight by less than 2 percent, a 200°F increase in engine turbine inlet temperature during nuclear cruise saved about one percent. Of all these candidate technologies, it appears that only composite materials offer sufficient potential benefits to offset its expected additional research and development cost.

Sensitivity studies on mission requirements showed a 10.4-percent increase in ramp weight for doubling the emergency range to 2000 n.m. and less than a 1.75-percent weight variation for takeoff distances between 8000 and 12,000 ft. These studies also showed, relative to the reference aircraft with a cruise Mach number of 0.75, a weight savings of 1.65 percent by reducing the Mach number to 0.65, and a weight penalty of 4.6 percent at a 0.85 Mach number.

Both military and civil cost data were estimated for the reference nuclear aircraft. The unit military acquisition cost was 139 million dollars and the 20-year life-cycle cost for the fleet was 71.2 billion dollars. These values were derived based on a production run of 250 aircraft, an annual utilization of 1080 hours, and an average trip of 10,500 n.m. For compatibility with normal commercial practice, an annual utilization of 3000 hours was used in calculating civil cost data. The resulting civil flyaway cost was 115.6 million dollars per copy for the reference aircraft, and the life cycle cost for the fleet was 93.8 billion dollars. By adopting the special nuclear design features of the alternate nuclear aircraft, a cost savings of 7.9 percent was achieved relative to the reference aircraft.

Two studies were conducted for the reference aircraft to assess the effects of higher fuel prices and changes in nuclear R&D. A 10-percent increase in life-cycle cost was produced for a 100-percent increase in fuel price. While 2.25 billion dollars for nuclear R&D is substantial, its effect on the total life-cycle costs is small as indicated by the study results which showed a 2-percent change in life-cycle costs for 50-percent variations in the nuclear R&D.

Characteristically, a nuclear aircraft does not have a range limitation. For comparison with a JP-fueled aircraft, which is range limited, it is of interest to establish the values of the cross-over range, that is, the design range for the JP-fueled aircraft which will give it the same ramp weight or life-cycle cost as the nuclear aircraft. To establish these cross-over ranges, a conventional JP-fueled aircraft configuration was developed for several mission ranges and for the same payload as the nuclear aircraft. The results showed the equal ramp weight cross-over ranges to be 9200 and 7850 n.m.

relative to the reference and alternate nuclear aircraft, respectively. To perform missions with ranges exceeding these cross-over values, the nuclear aircraft will be lighter in weight than a JP-fueled aircraft. The converse is true for shorter range values.

In terms of equal life-cycle costs, the cross-over ranges relative to the reference and alternate nuclear aircraft were found to be 11,950 and 11,000 n.m., respectively. However, for a 300-percent increase in fuel price as a result of energy shortages, these cross-over ranges are reduced to 6100 and 4700 n.m., respectively. Thus, as the energy shortage becomes more severe in the future, the prospects for airborne nuclear propulsion are improved.

FOREWORD

This final report documents the findings of a study by the Lockheed-Georgia Company of innovative nuclear-powered aircraft designs. Support for this study was provided by the Air Force Aeronautical Systems Division under contract F33615-76-C-0112 and by Lockheed's Independent Development Program. The latter was used to develop the JP-fueled competitive aircraft and the alternate-temperature data used for the nuclear engines in the sensitivity studies.

The Advanced Energy Systems Division of the Westinghouse Electric Corporation, under subcontract to Lockheed, performed the propulsion cycle analyses portion of this study. Westinghouse was also responsible for developing variations in the design of the base-point NuERA II reactor system consistent with the alternate shielding and operational philosophies addressed during the study.

Dr. L. W. Noggle served as the Air Force Study Manager on this program. Dr. J. C. Muehlbauer and Mr. R. E. Thompson fulfilled similar roles for Lockheed and Westinghouse, respectively. Additional Lockheed personnel who participated in this study and their areas of responsibility were as noted.

D. N. Byrne	Aerodynamics
E. P. Craven	Design
H. V. Davis, Jr.	Value Engineering
E. E. McBride	Stability and Control
C. C. Randall	Propulsion
R. E. Stephens	Structures
S. G. Thompson	Economics

Additional Westinghouse participants included:

B. L. Pierce	Propulsion Cycle Analysis
J. M. Ravets	Shielding and Reactor Design
R. J. Steffan	Nuclear Costing

TABLE OF CONTENTS

LIST OF FIGURES

LIST OF TABLES

1.0 INTRODUCTION

Several recent international events are prompting the United States to reassess its global commitments and its goals for the future. Actions taken during the Middle East conflict in 1973 showed that friendly foreign powers can no longer be relied upon to permit overflights and the use of their bases in times of crisis. Pressures exerted by emerging third world nations are also restricting areas accessible to the United States.

Of equal importance, is the rising economic and military dependence of the U. S. on imported energy supplies, as evidenced during and since the 1974 Arab oil embargo. Clearly, alternate forms of energy must be sought and developed if the U. S. is to regain its former level of independence and continue to function as a stabilizing influence worldwide.

In the midst of this changing world environment, the airlift responsibilities of the United States Air Force are unchanged, but are becoming increasingly more difficult to fulfill. Optimum utilization of technology developments is essential in future military transport aircraft if the Air Force is to undertake its airlift responsibilities within practical and economic limitations. Nuclear power is both an alternate energy source and an advanced technology which, if applied to aircraft, offers the potential for the Air Force to meet its commitments on long range or endurance missions in times of reduced chemical fuel availability.

In recognition thereof, and as part of its normal planning and analysis of possible future inventory vehicles, the Air Force commissioned this study on conceptual designs of nuclear-powered aircraft to satisfy mission requirements envisioned for the post-2000 time period. The minimum takeoff-gross-weight aircraft concept was determined from several candidates, was sized for a reference mission, and was used to evaluate the benefits achievable through the adaptation of various advanced technologies and alternate nuclear operational philosophies. Complete 20-year life-cycle costs and direct operating costs were generated for the reference aircraft. In addition, a conventional JP-fueled aircraft was designed for the reference mission to serve as a point of comparison for the nuclear aircraft.

2.0 STUDY APPROACH

The objectives of this study were to:

- Determine the minimum takeoff gross weight nuclear aircraft configuration of several candidates with due consideration given to multi-mission capabilities and military/civil commonality.
- Adapt the selected configuration to a reference mission and evaluate the direct operating costs and life cycle costs.
- Identify the most promising technologies which should be pursued to enhance mission accomplishment.

Guidelines for the conduct of this study and the overall plan followed to achieve the objectives are reviewed in the remainder of this section.

2.1 STUDY GUIDELINES

Guidelines for the conduct of this study were defined by the Air Force,* adopted from the NASA Span-Distributed Loading Aircraft Program,** or suggested by Lockheed and Westinghouse. For ease of presentation, these guidelines have been grouped according to whether they constrain the mission, the aircraft configuration, the nuclear propulsion system, or the economic evaluation.

2.1.1 Mission Constraints

- Cruise Mach number: 0.75
- Payload: 400,000 lb and 600,000 lb
- Payload type:
  - 463L pallets (10 lb/ft^3 cargo density, 375 lb tare weight)
  - 8-ft x 9.5-ft x 20-ft or 40-ft containers (10 lb/ft^3 cargo density, 1.5 lb/ft^3 tare weight)

* "Innovative Aircraft Design Study, Task II," Air Force Request for Proposal F33615-76-R-0112, March 31, 1976. (Ref. 1)

** "Technical and Economic Assessment of Swept-Wing Span-Distributed Load Concepts for Civil and Military Air Cargo Transports," NASA Request for Proposal, June 24, 1976. (Ref. 2)

- o Emergency recovery range: 1000 n.m.
- o Field length over 50-ft obstacle: 9000 ft (sea-level, 93°F hot day)

2.1.2 Configuration Constraints

- o Cargo compartment outsized capability to be at least equivalent to that of the C-5 aircraft
- o Cargo compartment floor strength to be adequate for one or more fully equipped M-60 main battle tanks
- o Cargo compartment to have 10,000-lb and 25,000-lb tie-down points throughout
- o Cargo compartment environment minimums to be 50°F and 18,000-ft pressure altitude
- o Air drop capability not required
- o Capability required to air launch either long range cruise or M-X missiles
- o Capability required for aerial refueling and conversion to a tanker within 24 hr
- o Structural design to conform to current military and commercial specifications with a 2.5-g load factor
- o Aircraft design life to be 60,000 operational hours

2.1.3 Nuclear System Constraints

- o Reactor system: Liquid-metal-cooled Nuclear Extended Range Aircraft (NuERA) II reactor*
- o Reactor operational lifetime: 10,000 hr
- o Dose rate criteria: 5 mr/hr at 20-ft distances from reactor center
- o Engine turbine inlet temperature limited to 1600°F by heat exchanger during nuclear-powered cruise
- o Reactor inoperative during takeoffs, climb, emergency cruise, descent and landings

* J. E. Werle, et al, "High Temperature Liquid Metal Cooled Reactor Technology," Westinghouse Astronuclear Laboratory Report on Contract AF 33(615)-69-C-1430, Vol. 1-3, March 1970. (Ref. 3)

2.1.4 Economic Constraints

- Cost base: January 1975 dollars
- Annual utilization: 3000 hr - civil, 1080 hr - military
- Crew size: 4 persons
- Fleet size: 250 aircraft
- Operating life cycle: 20 yr
- Fuel prices: JP - \$3.30/10^6 BTU (\$0.40/gal)
  Nuclear - \$0.65/10^6 BTU

2.2 STUDY PLAN

The general approach followed to achieve the study objectives is illustrated in Figure 2-1. Numbers and letters in the lower right-hand corner of each activity block on the study plan correspond to section and appendix designations of this report.

Parametric studies were performed, subject to the study guidelines, for one conventional and three unconventional aircraft configurations to determine the minimum takeoff gross weight version. The four configurations had identical technology features and levels, as identified in an assessment of technologies projected to have reached state-of-the-art status by the year 2000. Standard technology items so identified and included throughout this study were supercritical airfoils, composite materials, high-thrust-level engines, and relaxed static stability.

Several nuclear propulsion cycle concepts were investigated as part of this study. Two of the concepts embodied dual-mode engines, that is, engines which can operate on both nuclear heat and JP fuel. The other concepts required separate dedicated engines capable of operating on just nuclear heat or just JP fuel. The recommended propulsion cycle and the selected configuration identified in the parametric study were used in the design of an aircraft for a reference mission supplied midway through this study by the Air Force.

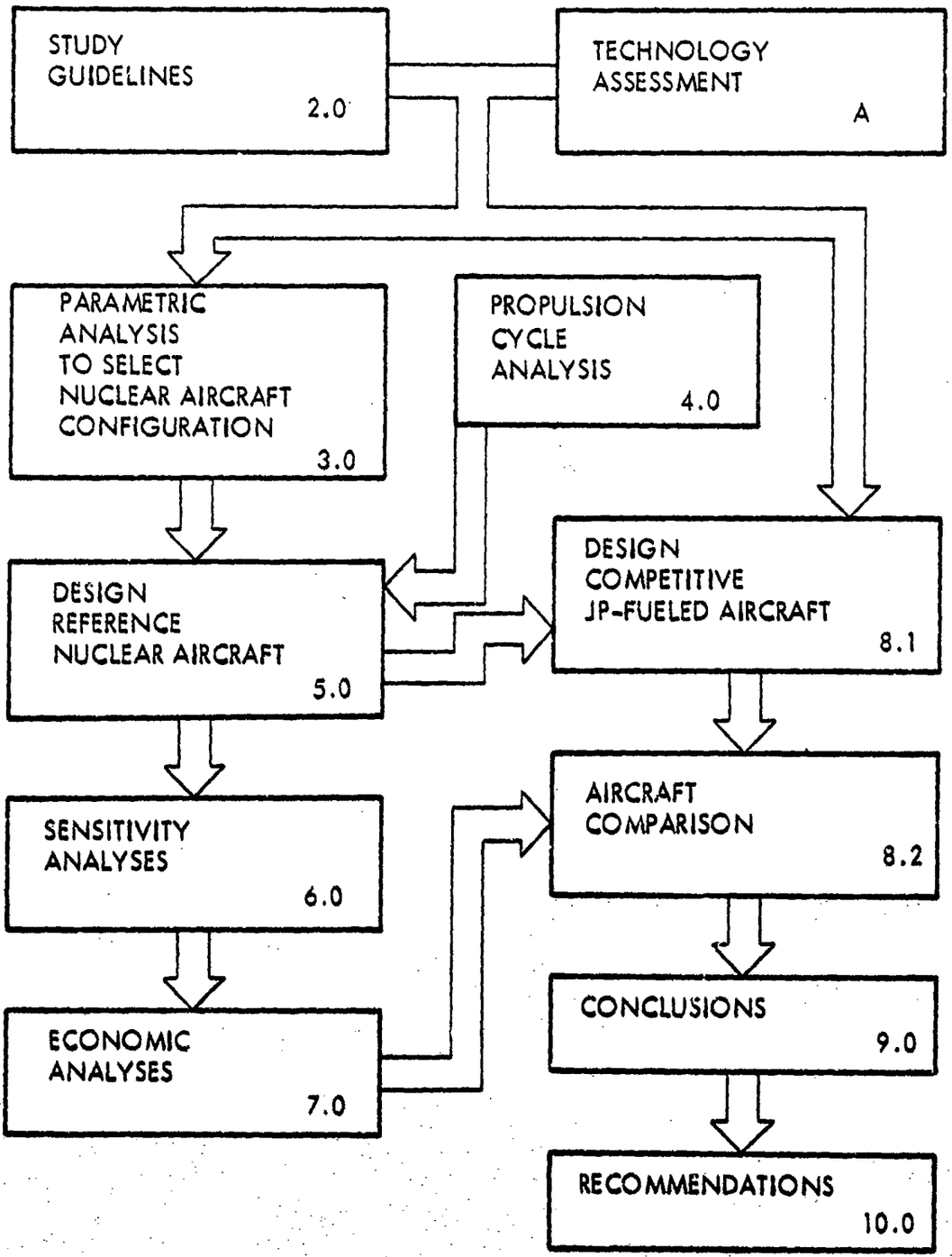

Figure 2-1. Study Plan

Sensitivity studies were performed for the reference aircraft to assess the effects of variations in the performance requirements, technology levels, and nuclear operating philosophy. Subsequently, direct operating costs and 20-year life-cycle costs were derived as part of the economic analysis of the reference aircraft.

A conventional JP-fueled aircraft was designed for the reference mission to serve as a basis for comparing the technical and economic competitiveness of the nuclear-powered aircraft. Results of the comparison of the two aircraft were responsible for the conclusions and many of the recommendations for future studies. Other recommendations were identified during the parametric, design, and sensitivity portions of this study.

3.0 CONFIGURATION ANALYSES

This section contains the results of studies directed toward the first part of the study objective, that is, to determine the minimum weight nuclear aircraft configuration from several candidates, subject to the study guidelines. Several cargo compartment layouts were evaluated for each candidate configuration and efforts were made to minimize the fuselage wetted area and pressurized volume. Subsequently, parametric studies on aircraft geometry and performance were undertaken for each configuration to determine the minimum weight design. For each of these optimum designs, refinements were made and sensitivity studies were conducted prior to selecting one configuration for development to satisfy the reference mission, as discussed in Section 5.0.

3.1 BASELINE CONFIGURATIONS

Four candidate aircraft configurations were analyzed in this study to determine the one most amenable to the application of nuclear propulsion for the specified missions. Plan views of these configurations are shown in Figure 3-1. For identification purposes in the remainder of this report, these configurations have been designated as conventional, canard, spanloader and dual-spanloader. The last title, as shown by the fourth planform in the figure, applies to a spanloader aircraft derivative having dual reactors, one in each wing.

The conventional aircraft is so designated because of its similarity to the large transport aircraft in service today. This aircraft has a T-tailed empennage mounted on the aft fuselage. Large turbofan engines are mounted beneath the wing. The reactor is located approximately in the middle of the fuselage near the aircraft center of gravity. All of the cargo is carried in the fuselage with any outsized equipment transportable forward of the reactor while containerized or palletized cargo is accommodated either forward or aft of the reactor.

The canard aircraft achieves its horizontal flight control through a canard surface mounted beneath the forward portion of the fuselage. Vertical surfaces at the wingtips

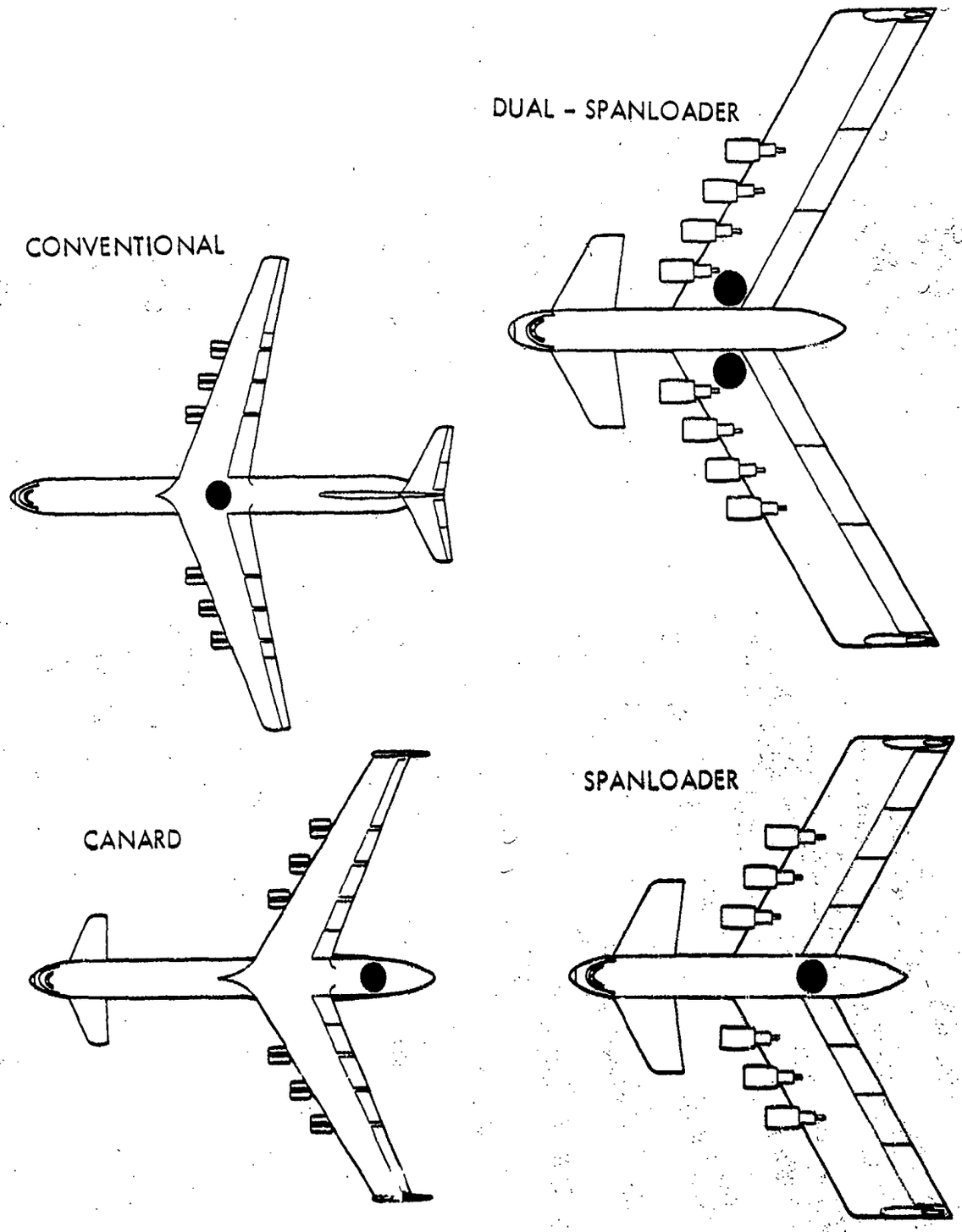

Figure 3-1. Study Configurations

fulfill a double function of providing directional control and reducing the induced drag by effectively increasing the wing aspect ratio. An outstanding advantage of this configuration is that the reactor location is aft of the cargo compartment and is coincident with the aft end of the fuselage. Thus, all of the cargo is loaded into the fuselage forward of the reactor, thereby requiring only one loading position.

The spanloader aircraft is so designated because of its characteristic feature of having containerized or palletized cargo loaded throughout the entire span of the wing. The reactor is positioned in the aft end of the fuselage, and the remainder of the fuselage is capable of carrying outsized equipment. Flight control surfaces on this aircraft are similar to those on the canard aircraft. The engines are mounted on top of the thick supercritical wing to keep the cargo compartment floor height to a level serviceable by existing ground-based loading equipment. The last feature is a variation from Lockheed's* previous design of a JP-fueled spanloader which did not have a requirement to use existing loading equipment.

The dual-spanloader represents an attempt to extend the spanloader design philosophy of distributing the payload and fuel in the wing to achieve a balance between inertia and flight loads, thereby minimizing aircraft structural weight. Two reactors, with a total power equivalent to that needed for propulsion, are located in the wing in an effort to distribute the total reactor weight. This increases the wing span and reduces the induced drag through the higher wing aspect ratio.

Further details are presented in Section 3.2 on the common features of these candidate configurations and on the implications of the technology levels used, as per the technology assessment results in Appendix A.

* W. M. Johnston, J. C. Muehlbauer, et al, "Technical and Economic Assessment of Span-Distributed Loading Cargo Aircraft Concepts," NASA CR-145034, Lockheed-Georgia Company, 1976. (Ref. 4)

3.2 BASIC DATA

Standard design criteria and data were used in the parametric studies to develop the optimum design for each aircraft configuration. The data base and the pertinent criteria in the areas of structures and materials, aerodynamics, propulsion system, and flight controls are reviewed under these headings.

3.2.1 Structures and Materials

Basic structural design criteria were selected for use in determining the weights of the aircraft and in computing the structural loads, rigidity requirements, and sizes for point-design. These criteria were chosen for conformity with current military specifications.* Specific criteria included limit load factors between +2.5 and -1.0 g's for maneuvers and +1.5 g's for landing and taxi. Structural design speed criteria were 350 kts in cruise and 410 kts in a dive.

In addition to the design criteria, certain assumptions were made concerning permissible stress levels in the structural materials. Current cargo aircraft wings, using conventional aluminum and construction techniques, are designed with tensile strength limits between 45,000 and 55,000 psi, depending upon the design lifetime. The relatively low limits are due primarily to fracture and fatigue properties of current metals over long operational lifetimes exceeding 30,000 hr. Significant increases in these levels are projected through future advances** in design practices, analytical techniques, manufacturing methods, and metallurgical research. By the year 2000, when nuclear aircraft could become a reality, aluminum tensile strength limits of 70,000 psi are reasonable goals for a design life of 50,000 to 60,000 hr. This strength guideline was adopted in sizing aluminum structural elements.

---

* "Airplane Strength and Rigidity" series, MIL-A-8860 series, Department of Defense. (Ref. 5)
"Airworthiness Standards: Transport Category Airplanes," Federal Aviation Regulations, Part 25 (FAR 25), Federal Aviation Administration, Department of Transportation, 1974. (Ref. 6)

** E. A. Starke, Jr., "The Fatigue Resistance of Aircraft Materials, The Current Frontier," LG76RR0001, Lockheed-Georgia Company, Sept. 1976. (Ref. 7)

Developments in the field of advanced composites are expected to equal or exceed those in conventional materials during the rest of this century. Improvements in relative economics coupled with the higher strength-to-weight ratios of composites compared to conventional metals, will produce a high level of composite material usage in future aircraft. For these reasons, it was assumed that 40-percent of the structural weight of the aircraft in this study would be graphite/epoxy with a design stress level of 140,000 psi.

Weights for the major structural components of the point design version of each configuration were estimated through the use of statistical equations which have been used extensively for JP-fueled aircraft. Weights of the nuclear subsystem and the support equipment were predicted using the equations in Section 4.1 and Appendix D, respectively. An additional weight, equal to 3 percent of the nuclear subsystem weight, was added to the fuselage weight. This approach was found in Reference 8* to be a reasonable approximation of the weight of structure needed to attach the nuclear subsystem inside the fuselage.

Pressurized fuselage shells were limited to 22,000 psi stress levels in aluminum and 25,000 psi in composites at the cargo compartment pressure differential of 4.5 psi, equivalent to a pressure altitude of 18,000 ft. These stress levels are an increase over proven satisfactory levels for pressurized compartment designs in existing aircraft. The derivation of these stress levels was based on both fatigue and damage tolerant considerations. The level for the composite material is deemed conservative, but was chosen in view of the small data base for designing damage tolerant shell structures with composites.

3.2.2 Aerodynamics

The basic airfoils used in this study employ the supercritical technology level appropriate for the late 1990 time frame. The spanloader configuration is based on a

* J. C. Muehlbauer, "Analytical Investigation of Containment Concepts and Criteria for Airborne Nuclear Reactor Systems," Technical Report AFFDL-TR-71-56, Lockheed-Georgia Company, June 1971. (Ref. 8)

21-percent thick supercritical section, while the thinner airfoils used for the conventional and canard configurations are based on 14-percent and 18-percent sections. These baseline airfoils have been defined and wind-tunnel tested by Lockheed. Versions of the basic airfoil have been scaled, as necessary, to satisfy the design requirements for the parametric sizing process.

Typical variations in cruise Mach number and lift for the basic airfoils are shown in Figure 3-2 for two of the scaling variables, sweep angle and thickness. These curves were derived to give maximum thickness ratio at a drag rise of 10 counts. Two pertinent limitations are noted on Figure 3-2. The first constraint is that the maximum thickness ratio normal to the leading edge, t/c_n, for the wing be limited to 30 percent. The thickness ratio normal to the leading edge is equivalent to the streamwise thickness-to-chord ratio divided by the cosine of the wing sweep angle. The 30-percent limit may be explained by referring to Figure 3-3, which illustrates the increase of profile drag with increasing thickness ratios. At the 30-percent limit, the pressure drag produced by the high thickness ratio value has increased the profile drag by 25 percent over the drag contribution from friction, resulting in unacceptably poor performance levels.

Another limit to be considered is the section lift coefficient for which an optimistic value of 1.0 has been used for illustrative purposes. Realistically, a section lift coefficient value in the 0.7 to 0.8 range is better suited to the 2000 time period, based on estimated technology levels.

Performance levels projected for both the swept-wing, span-loaded concept and the canard configuration are partially attributable to the end plating from the wingtip-mounted vertical stabilizers. Hoerner* has provided an equation for calculating the effective wing aspect ratio, AR_{eff}, resulting from the end plating. Excellent agreement has been found between Hoerner's equation and the results of detailed wing loading analyses. This equation is -

* S. F. Hoerner, "Fluid-Dynamic Drag," published by the author, 1958. (Ref. 9)

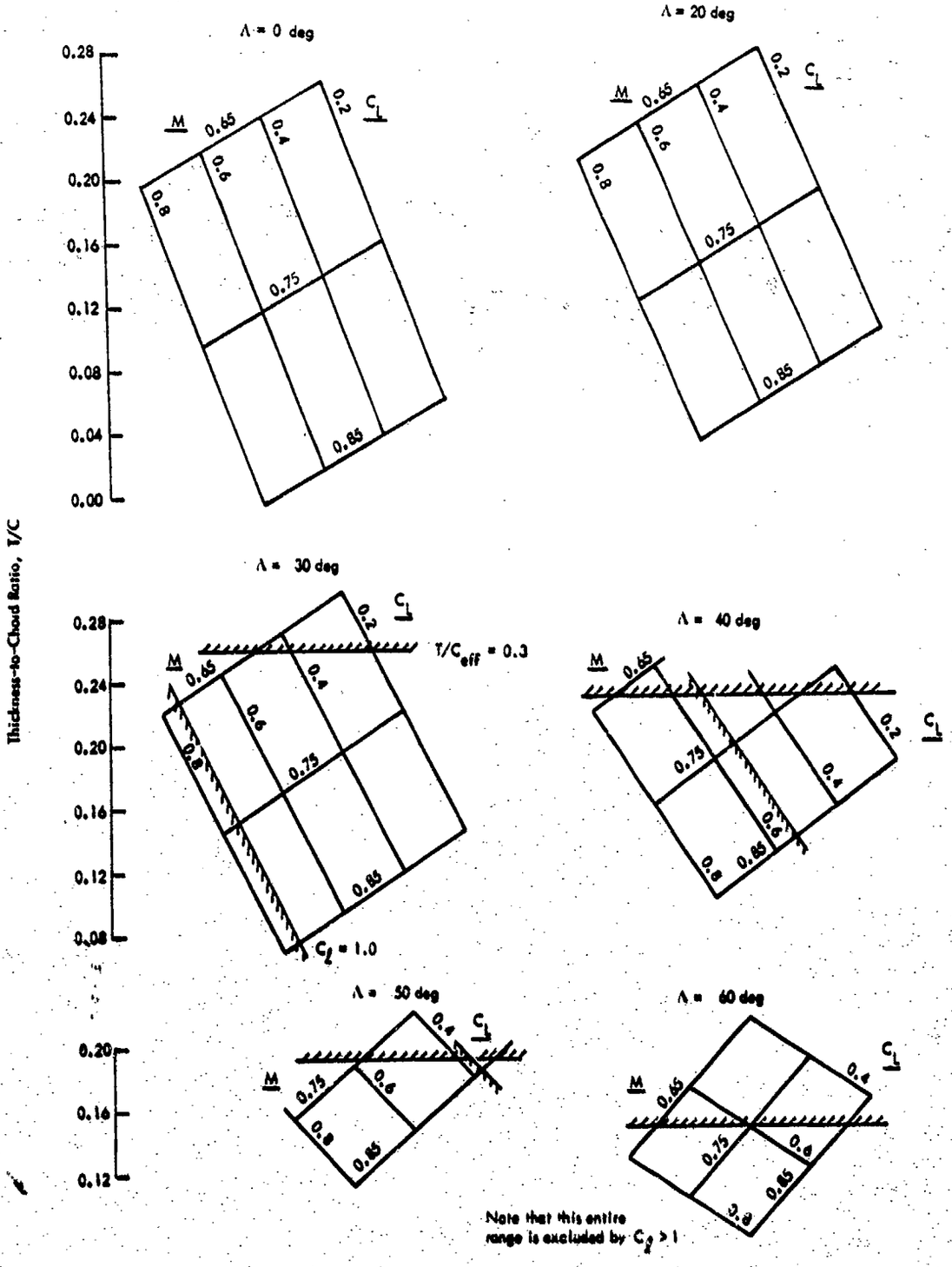

Figure 3-2. Allowable Lift, Mach Number, Sweep Angle Combinations

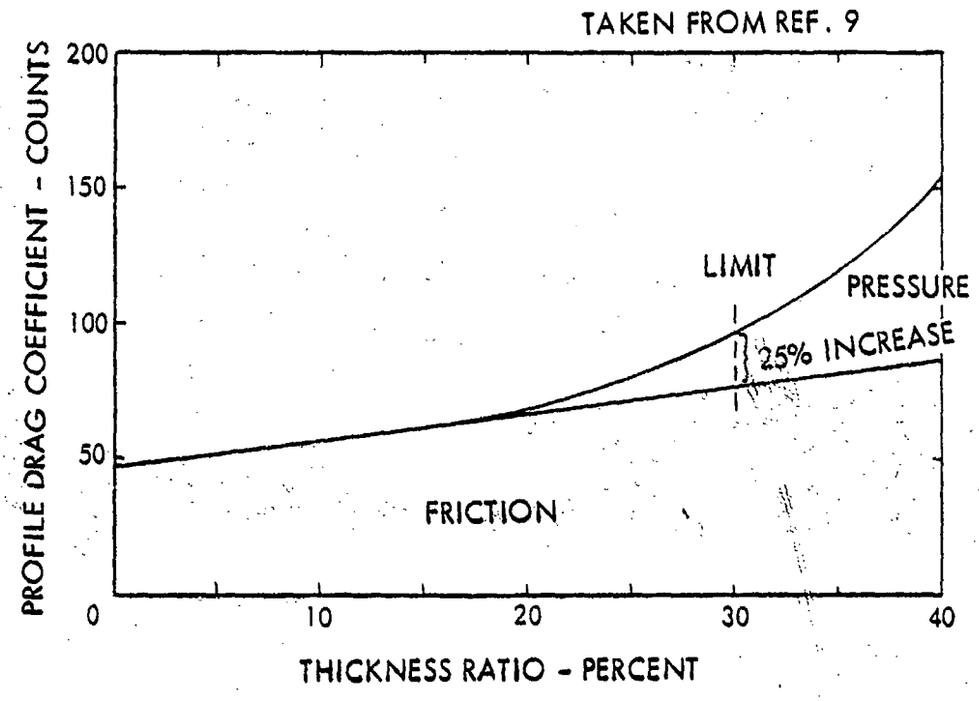

Figure 3-3. Thickness Ratio Limitation Due to Pressure Drag

$$AR_{eff} = AR_{geom} \ (1.0 + 0.9\, h/b)$$

where: AR_{geom} is the actual geometric wing aspect ratio,

h is the height of the vertical endplate, and

b is the wing span.

Drag characteristics of the aircraft were estimated on a component buildup basis. The skin friction drag was determined for the wetted area and characteristic Reynolds number for each component and was referenced to the aircraft wing area. Appropriate shape factors were applied to the skin friction drag to obtain the profile drag for each component. The sum of these component profile drags formed the basic profile drag. Roughness and interference drag corrections, equal to 3 and 5 percent of the basic profile drag, respectively, were included. The trim drag penalty and miscellaneous drag were assigned on the basis of the particular configuration, as was the efficiency factor used for the calculation of the induced drag. Table 3.1 summarizes these values.

TABLE 3.1. CONFIGURATION TRIM AND MISCELLANEOUS DRAG COEFFICIENTS AND EFFICIENCY FACTORS

Configuration	Spanloader	Canard	Conventional
$C_{D_{trim}} + C_{D_{mis}}$	0.0005	0.0005	0.0016
Efficiency Factor	0.89	0.92	0.95

In addition, drag penalties due to the variation of the wing profile drag with lift coefficient and Mach number were included. A compressibility drag increment of 10 counts was included for all configurations.

The high lift system for all configurations consisted of a 30-percent-chord double-slotted flap arrangement. Additionally, a 15-percent-chord leading-edge device was used on the conventional and canard configurations to augment the flap system. This device was excluded from the spanloader, however, as it was of small value due to the inherently high wing thickness ratio typical of span-loaded aircraft.

3.2.3 Propulsion System

Figure 3-4 is a schematic representation of an aircraft nuclear propulsion system based upon an open Brayton thermodynamic cycle. This cycle has received the greatest attention in recent studies. Since it has the best data base of all candidate cycles, the open Brayton was selected for use in the parametric studies of Section 3.4. However, several alternate propulsion cycles were analyzed and compared with the open Brayton cycle, as discussed in Section 4.0, to select the cycle to be used in the design of the reference aircraft of Section 5.0.

For purposes of discussion, the propulsion system of Figure 3-4 is composed of three elements: the nuclear subsystem, the engines, and cycle equipment for transferring energy from the reactor to the engines. The reactor, its shielding, the containment vessel, and all other equipment internal to the containment vessel are considered to be part of the nuclear subsystem. Basic data on each of the three elements of the system are presented subsequently.

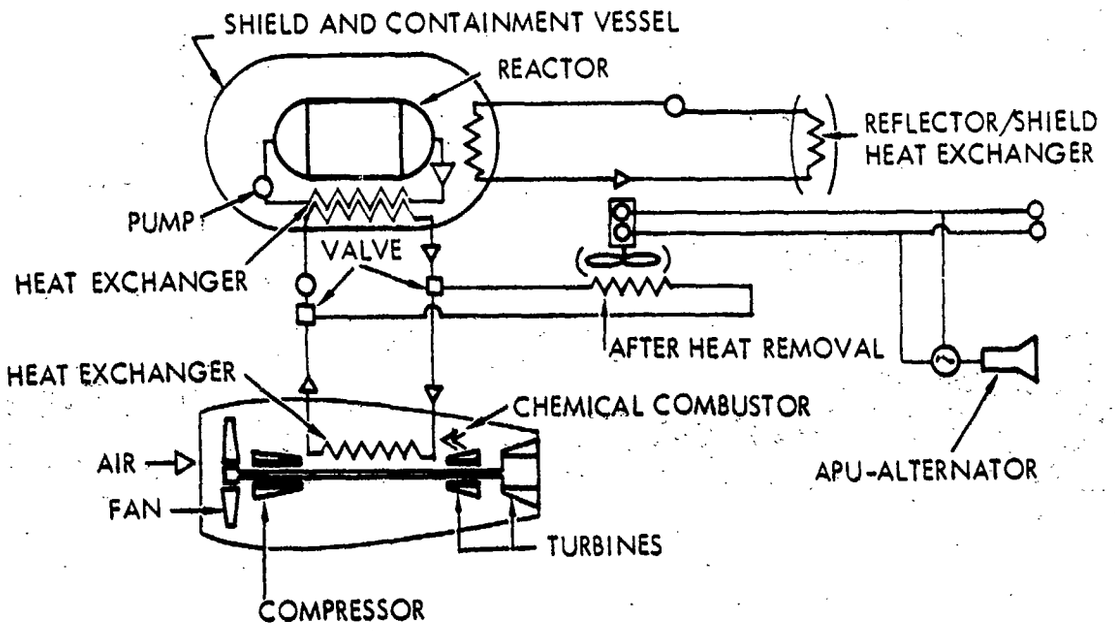

Figure 3-4. Nuclear Propulsion System Schematic

3.2.3.1 Nuclear Subsystem (NSS)

The reference reactor used in this study is a liquid-metal-cooled fast reactor as typified by the NuERA II concept (Ref. 3), which is described in further detail in Appendix B.

In the NuERA II studies, Westinghouse formulated a nuclear subsystem design computer program COP-DS (Component Parametric - Design Subroutines) with seven parameters or input variables. The program was developed to perform a process of core design, reactivity control system design, shielding analysis and design, specification of the primary coolant loop, including primary heat exchangers, auxiliary component shielding, and containment vessel design. The seven major input parameters for which values are selected by the users of COP-DS are the following:

- Reactor Power Level
- Reactor Full Power Operating Lifetime

- o Allowable Average Atom Percent Burnup in the Fuel
- o Core Outlet Temperature
- o Coolant Velocity
- o Dose Rate Criterion
- o Impact Velocity of the Containment Vessel

A discussion of the allowable ranges of these variables is found in Volume II of Ref. 3.

For specified values of the seven input parameters, the program does a weight optimization on two internal parameters, the maximum fuel centerline temperature and the thickness of the fuel cladding. For the optimized configuration, a detailed output format is available which provides information on the thermal, nuclear, and mechanical characteristics of the core; thicknesses of the various shield layers in the primary radial, transverse radial and axial directions; and weight and dimensional data of these and all other components in the system.

In this study a reactor full power operating lifetime of 10,000 hr was used. Other parameter values from the NuERA reference design which were used for this study included: an 11.4-percent allowable average atom burnup, a core outlet temperature of 1800°F, a coolant velocity of 27.8 ft/sec, and a dose rate criterion of 5 mr/hr at 20 ft forward and aft of reactor centerline during operation and 5 mr/hr at 20 ft in any direction 30 minutes after shutdown. An impact velocity of 250 ft/sec was used for establishing the containment vessel thickness.

Using these parameters in the COP-DS computer code, the component weights and dimension were calculated for various reactor power levels. The nuclear subsystem weight (all components out to and including the containment vessel) and the containment outer diameter variations with reactor power are shown in Figures 3-5 and 3-6 for use in aircraft parametric studies.

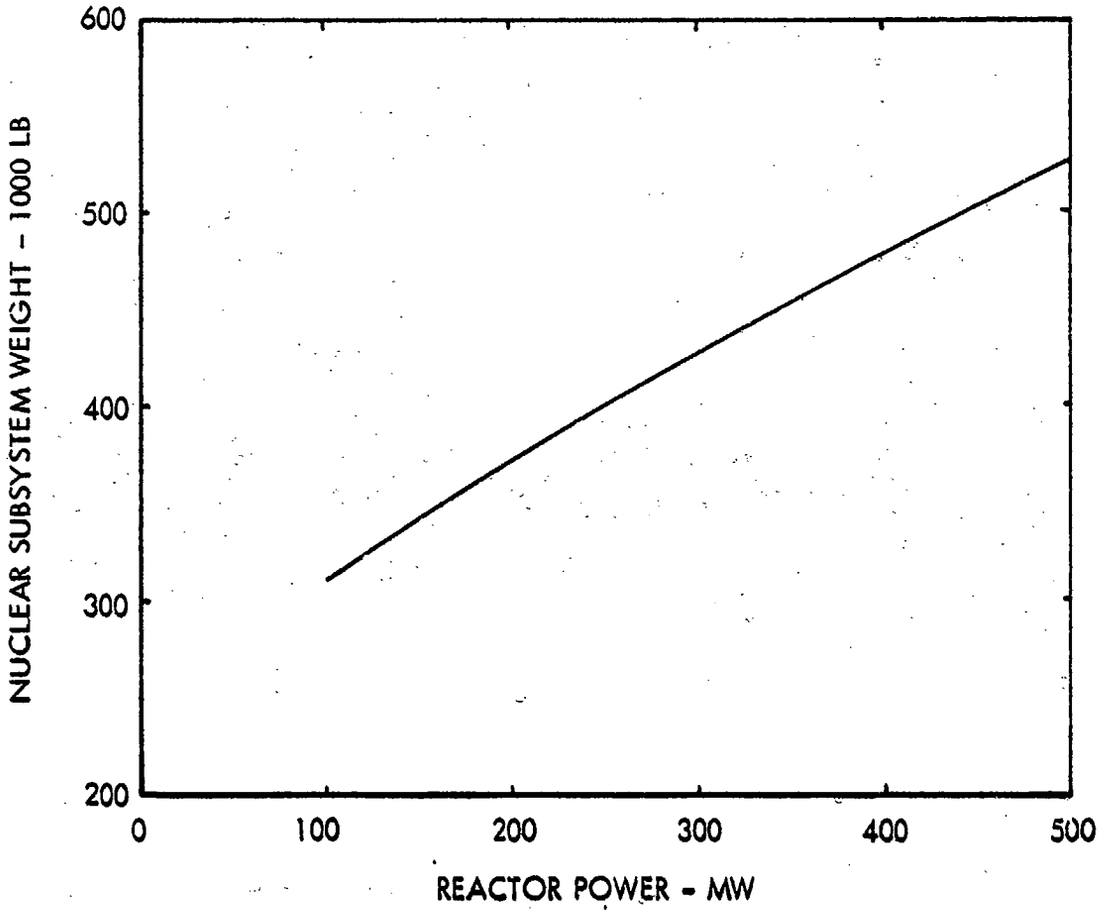

Figure 3-5. NuERA Nuclear Subsystem Weight Variation

3.2.3.2 Engines

Data for advanced turbofan engines with four discrete bypass ratio values of 5.8, 8.4, 13 and 18 were used as a base in scaling the propulsion systems for each aircraft in this study. These base engines are single stage fans and are consistent with gas generator technology predicted for the late 1990 time period. Characteristically, these engines use chemical JP fuel for takeoff, climb and emergency cruise; normal cruise thrust is provided from energy generated by the nuclear reactor.

A recent NASA-Ames Short-Haul Systems Study* (NASSS) provided the background engine data for this study. The thermodynamic cycle trends and the variations of bypass

* T. P. Higgins et al, "Study of Quiet Turbofan STOL Aircraft for Short Haul Transportation," NASA CR-2355, Lockheed Aircraft Corporation, 1973. (Ref. 10)

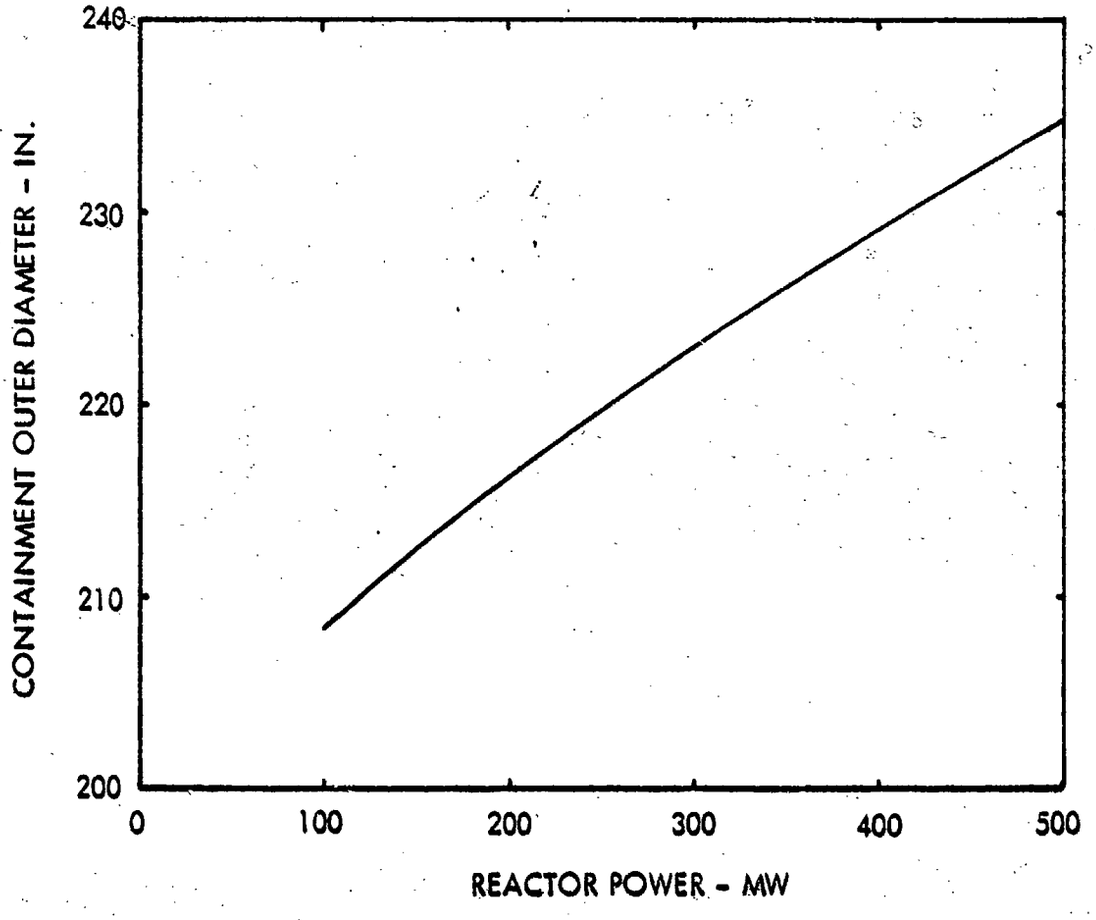

Figure 3-6. NuERA Containment Vessel Outer Diameter Variation

ratios, fan pressure ratios, weights, and dimensions of the 1985 technology level NASSS engines were adjusted to late 1990 technology levels, as projected by various engine manufacturers, including a 100,000-lb maximum thrust per engine limitation imposed by test facility sizes. From the adjusted engine data, four design points were chosen as the basic JP-fueled gas turbine engines which were subsequently modified for nuclear propulsion. Several pertinent parameters of these engines in the nuclear-powered mode are shown in Table 3.2.

Conversion of the four basic JP-fueled engines for nuclear operation required consideration of the effects of reduced allowable turbine inlet temperature (TIT), increased burner pressure losses due to the NaK/air heat exchanger, and changes in engine geometry. Due to material limitations of the heat exchanger added to the engine for nuclear operation, the maximum allowable TIT on nuclear power is projected to be

TABLE 3.2. PARAMETRIC TURBOFAN ENGINE CANDIDATES

Takeoff: JP Fuel; TIT = 1800°F	Cruise: Nuclear Powered; TIT = 1600°F			
Bypass Ratio	5.8	8.4	13	18
Rated Thrust - lb	79,807	79,807	79,807	79,807
Bare Engine Weight - lb	17,861	16,048	14,163	13,193
Maximum Diameter - ft	12.04	12.97	14.26	15.46
Cruise Altitude = 36,089 ft Mach Number = 0.75				
Cruise Thrust - lb	15,787	14,943	12,792	11,027
Cruise Chemical SFC - lb/hr/lb	0.701	0.651	0.625	0.623
Cruise Nuclear SEC* - kw/lb	3.8	3.5	3.4	3.4

* Specific energy consumption (SEC) for the reactor is defined as the reactor energy per unit thrust equivalent to the energy available from the chemical fuel per unit of thrust.

1600°F in the year 2000. Since this temperature is much lower than the 2600°F value expected for a corresponding JP-fueled engine, a straight TIT reduction resulted in a mis-match between cruise power and takeoff, thereby producing very large engines and vehicles with excessive takeoff performance. Consequently, the baseline engines were redesigned to obtain a better match of takeoff and cruise turbine inlet temperatures.

This was accomplished by using the NASSS parametric engine data for the range of TITs and design bypass ratios of interest. These data were used to generate scaling factors for cruise thrust, specific fuel consumption (SFC), and engine dry weights, diameters, and lengths for fixed values of engine rated thrust. The effects of the heat exchanger pressure loss were included in the SFC, engine diameter and weight factors without imposing untenable penalties on the engine cycle thermal efficiencies. These factors were then used to modify the four JP-fueled engine data sets to obtain redesigned nuclear-powered engine data sets with lower TITs for chemical fuel operation. This redesign approach produced significant reductions in both engine and aircraft sizes as engine design TITs approached 1600°F, while maintaining reasonable takeoff performance.

Typical effects on aircraft design are presented in Table 3.3 for variations in the engine takeoff TIT. For each engine takeoff TIT value, cruise on JP fuel was at a TIT of 200°F less than for takeoff while cruise on nuclear power was always at a TIT of 1600°F. The number of engines and their thrust levels were chosen, subject to the 100,000-lb thrust per engine maximum limitation, to provide the total cruise thrust for each of the point design aircraft. The obvious mismatch between engine takeoff and cruise thrust requirements produced heavy ramp weight aircraft with field length performance capabilities considerably shorter than specified. Relative to the point design aircraft in the first column, the one in the fourth column exhibits a better match between takeoff and cruise thrust requirements, closer agreement with the specified field length of 9000 ft, and approximately a 12-percent reduction in ramp weight. To meet the specified 9000-ft field length, the design takeoff TIT of the aircraft in the fourth column would be increased slightly above 1800°F.

The data shown in Tables 3.2 and 3.3 include allowances for nominal environment system airbleed and accessory power extraction for an installed engine. Additional engine data have been included in Appendix C. The engine weights do not include the heat exchanger weight, which is determined and tabulated separately (see Appendix D). The engine performance data do reflect nacelle drag penalties as per the following discussion.

TABLE 3.3. EFFECTS OF TURBINE INLET TEMPERATURE (TIT) ON ENGINE AND AIRCRAFT*

TIT, °F				
Takeoff - JP	2600	2200	2000	1800
Cruise - JP (NUC-1600)	2400	2000	1800	1600
Number of Engines	10	8	6	4
Thrust, 1000 lb				
Total Rated	866	728	532	378
Total Cruise	79	78	74	71
Total Engine Weight, 1000 lb	153	128	104	78
Ramp Weight, 1000 lb	1935	1892	1788	1708
Field Length, ft	3746	4473	6133	9228

* Conventional aircraft, 400,000-lb payload, 20 deg sweep, aspect ratio = 10
Engine bypass ratio = 8.4

In the NASSS effort and a later study by Pratt & Whitney*, it was shown that aircraft with high bypass engines installed in separate exhaust, short-duct nacelles were more efficient than aircraft with similar engines installed in mixed exhaust, long-duct

* D. E. Gray, "A Study of Turbofan Engines Designed for Low Energy Consumption," NASA CR-135002, Pratt & Whitney Aircraft Corporation, April 1976. (Ref. 11)

nacelles. Thus, the short-duct nacelle, similar to that of the L-1011/RB211 or the DC10/CF6, was chosen for all candidates. The engine performance data were corrected to account for drag penalties associated with this type nacelle, which is closely wrapped around the engine to minimize the total system weight. These nacelles do not include any special acoustic treatment since noise level requirements were not specified for this study.

3.2.3.3 Cycle Equipment

Nuclear propulsion system components which are outside of the containment vessel can total to a significant weight. These components include the secondary loop (piping, valves and pumps and motors), shield cooling system, reactor decay heat removal system, and the reactor instrumentation and control system. The engine mounted NaK-to-air heat exchangers can also be considered to be part of the secondary system, but for this study have been considered to be part of the engines.

The weights of these components vary with the reactor power and, in the case of the secondary heat transfer system components, with the length of the piping runs required. Since these weights are not estimated as part of the COP-DS calculations, parametric relationships were needed so that the aircraft configuration studies could properly include the variations in the weights of these components. The parametric relationships and their derivations are included in Appendix D.

3.2.4 Flight Controls

Design criteria for sizing the directional, lateral, and longitudinal flight control surfaces were selected based on the guidelines of Military Specification MIL-F-8785B.*

* "Flying Qualities of Piloted Airplanes," Military Specification MIL-F-8785B (ASG), 1969. (Ref. 12)

The directional control system consisted of 25-percent-chord rudders on the vertical surfaces of each configuration. The vertical tails were sized to provide adequate static directional stability (C_{n_β} = 0.0015/deg), and the rudders were sized to provide adequate yaw control during cross-wind landings and critical engine-out cases. On the spanloader and canard configurations, the wingtip positions of the verticals provide the maximum tail arms with minimum weight penalties and increase the effective aspect ratio of the wing.

The lateral control surfaces were designed to satisfy a roll performance requirement of 30 deg of bank in 4 sec. This is a minimum requirement, but based on C-5 flight test experience, it results in adequate handling qualities. The lateral control systems were extended over the trailing edge of the outboard 25-percent of the wing span for all configurations. The system consisted of fast-acting flaperons and spoilers for the spanloader and canard configurations. Ailerons were used on the conventional configuration.

The longitudinal control system consisted of a canard mounted on the forward portion of the fuselage for both the spanloader and canard configurations. A free-floating canard was used so that aircraft stability would not be reduced. Adequate pitch control to accomplish nose-wheel lift-off at the most forward center-of-gravity position was provided by spanwise blowing at the aerodynamic center of the canard surface.

For the conventional configuration, the horizontal tail was sized to provide at least a 5-percent static stability margin at the most aft center-of-gravity position. A 25-percent-chord elevator provided sufficient control power at the most forward center of gravity position for nose-wheel lift-off at 120 percent of the stall speed.

3.3 ANALYSIS OF BASELINE CONFIGURATIONS

The flight stations for all configurations are intended to accommodate a crew of four, including a flight engineer with responsibility for overseeing the operation of the reactor. While space requirements for the flight station were estimated for use in sizing the pressurization equipment, no attempt was made to lay out the flight station

since such an effort would have been considerably beyond the level of detail expended on other aspects of the aircraft design.

It is recognized that alternate crews and crew accommodations will be required on the long endurance missions normally envisioned for nuclear aircraft. Additional space exists behind the flight station for use by an alternate crew on a cargo transport mission. If the aircraft is used on command, control, and communications missions, the entire cargo compartment region could be reconfigured specifically for the mission with adequate personnel facilities.

Sizing the cargo compartment and the fuselage was extremely sensitive to the cargo arrangement and the design criteria. In addition to the criteria noted in Section 2.1, other criteria were also used to develop cargo arrangements for the aircraft. These additional criteria were established as a result of familiarity with military and commercial aircraft cargo requirements. They are as follows:

- A minimum of 80 linear feet provided for outsized cargo. This area will have a ceiling height of 13.5 ft at the center of the compartment. Other cargo areas will have a minimum height of 10 ft to accommodate the container dimensions.
- A minimum clear access width of 19 ft.
- Passageway widths of 14 in. between cargo rows and solid bulkheads.
- Fore and aft clearances of 3 in. between containers. Transverse clearances of 3 in. between containers with a passageway being provided on the outboard sides of the cargo compartment.
- A minimum space of 5 ft on either side of the reactor for instrumentation and controls.
- A maximum cargo floor height of 13 ft above ground level to be compatible with in-service loading equipment.

3.3.1 Canard and Conventional Configurations

Fuselage cross-sections and planforms were developed and analyzed for two, three, and four-row cargo arrangements for both the conventional and canard configurations. In developing these arrangements, efforts were made to minimize the wetted area and the pressurized volume of the fuselage since these are the major factors in assessing the drag and structural efficiency of a fuselage design. Consistent with the optimization effort, the lateral clearance at the loading doors was restricted to 19 ft, adequate for simultaneously loading two rows of containerized cargo.

A 30-ft long section was allotted for the reactor in the conventional configuration. This spacing was consistent with the guideline to allow a 5-ft minimum space on each side of the reactor for instruments and controls. The canard configuration required only a 25-ft long section for the reactor because of the aircraft design characteristics. In both aircraft, the reactor must be located near the aircraft center of gravity because of balance problems. The center of gravity of the conventional aircraft is near the center of the cargo compartment, but in the canard the center of gravity is near the aft end of the cargo compartment. Thus, the canard does not experience dose-rate space limitations on the aft end of the reactor.

The two-row arrangement produced extremely long aircraft which experienced rotation difficulties during takeoffs subject to the 9000-ft field length requirement and reasonable landing gear length restrictions. The four-row arrangement exhibited a large cross section and a much shorter floor length than the two-row arrangement. However, considerable drag penalties were incurred by the four-row arrangement due to the incompatibility of the low fuselage fineness-ratio value with a cruise speed of Mach 0.75. Consequently, the three-row arrangement emerged as the best fuselage for the conventional and canard aircraft. The fuselage cross-section for this arrangement, as shown in Figure 3-7, readily accommodates both military and civil cargo height requirements.

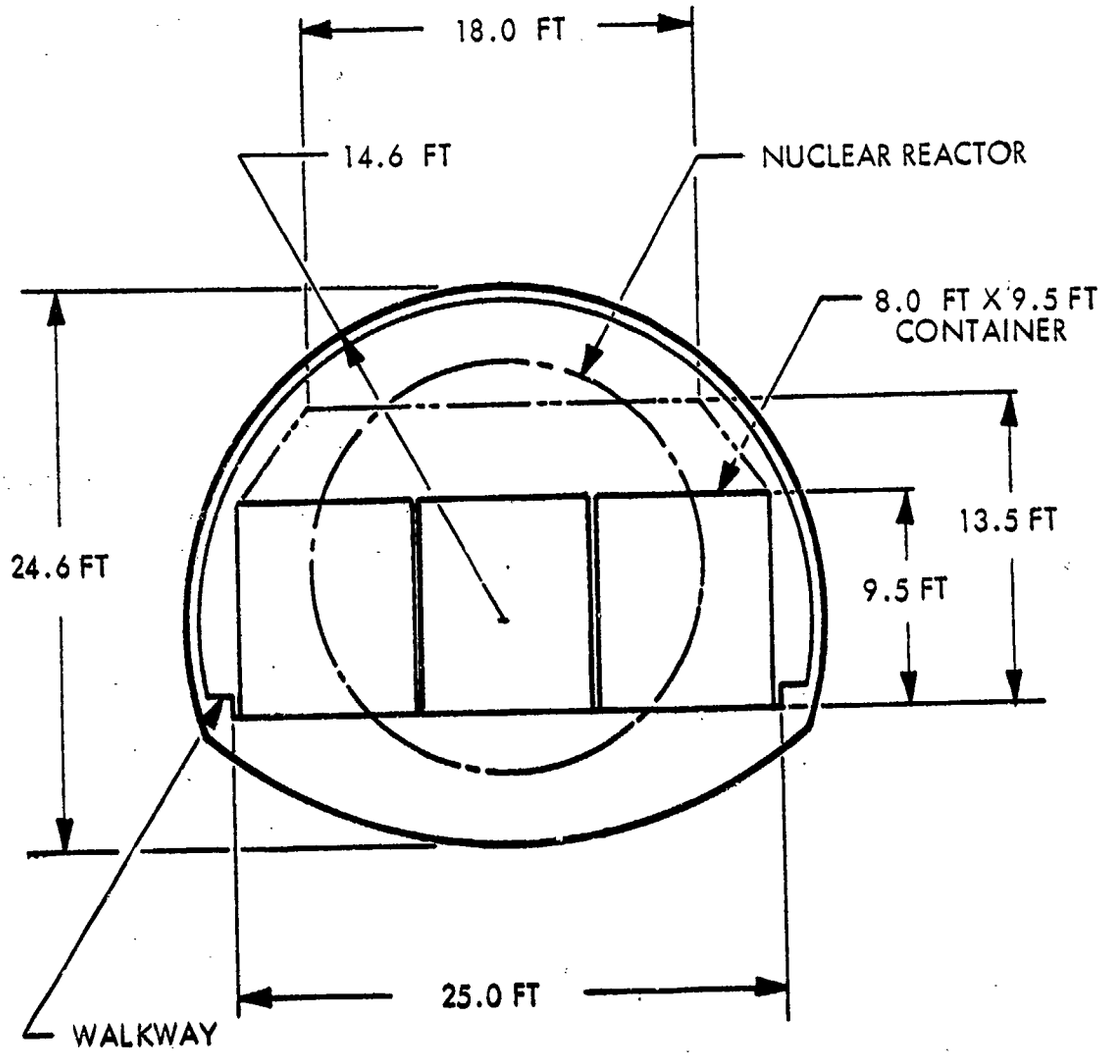

Figure 3-7. Fuselage Cross-Section for Conventional and Canard Configurations

A typical nose section for either the conventional or canard aircraft is shown in Figure 3-8. The transition from the 25-ft constant section at the cargo floor to the 19-ft opening provides space for cargo in other than 40-ft long containers. Inasmuch as this condition also applies to the aft section of the cargo compartment in the conventional configuration, a substitution was made of two 20-ft long containers in lieu of a 40-ft container, thereby taking advantage of otherwise wasted space. This reduced the overall length of the fuselage with an accompanying savings in aircraft weight. Schematic layouts of the containers are shown in Figure 3-9 for both configurations.

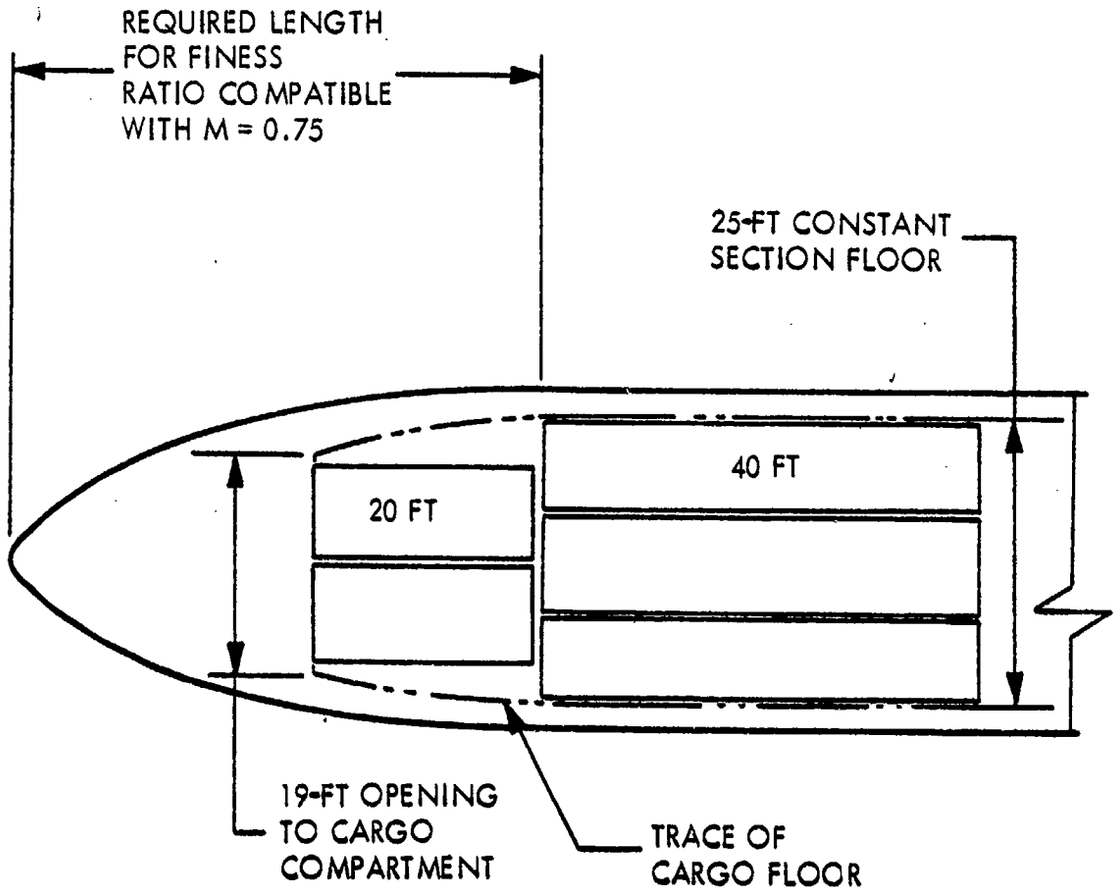

Figure 3-8. Nose Section Floor Plan for Conventional and Canard Configurations

3.3.2 Spanloader Configuration

Cargo compartment layouts for the spanloader configurations drew heavily from recent studies on this configuration (Ref. 4). To meet the outsized military equipment requirements, the fuselage compartment was fixed at 80-ft long, 13.5-ft high, and 17-ft wide. This size will accommodate two 40-ft long containers in each of two parallel rows. A 25-ft long section for the reactor was provided just aft of the cargo compartment, similar to the arrangement on the canard configuration.

In a spanloader aircraft, most of the payload is carried in the wing. Thus, there is an interaction between cargo compartment layout and wing design which does not exist for a conventional aircraft.

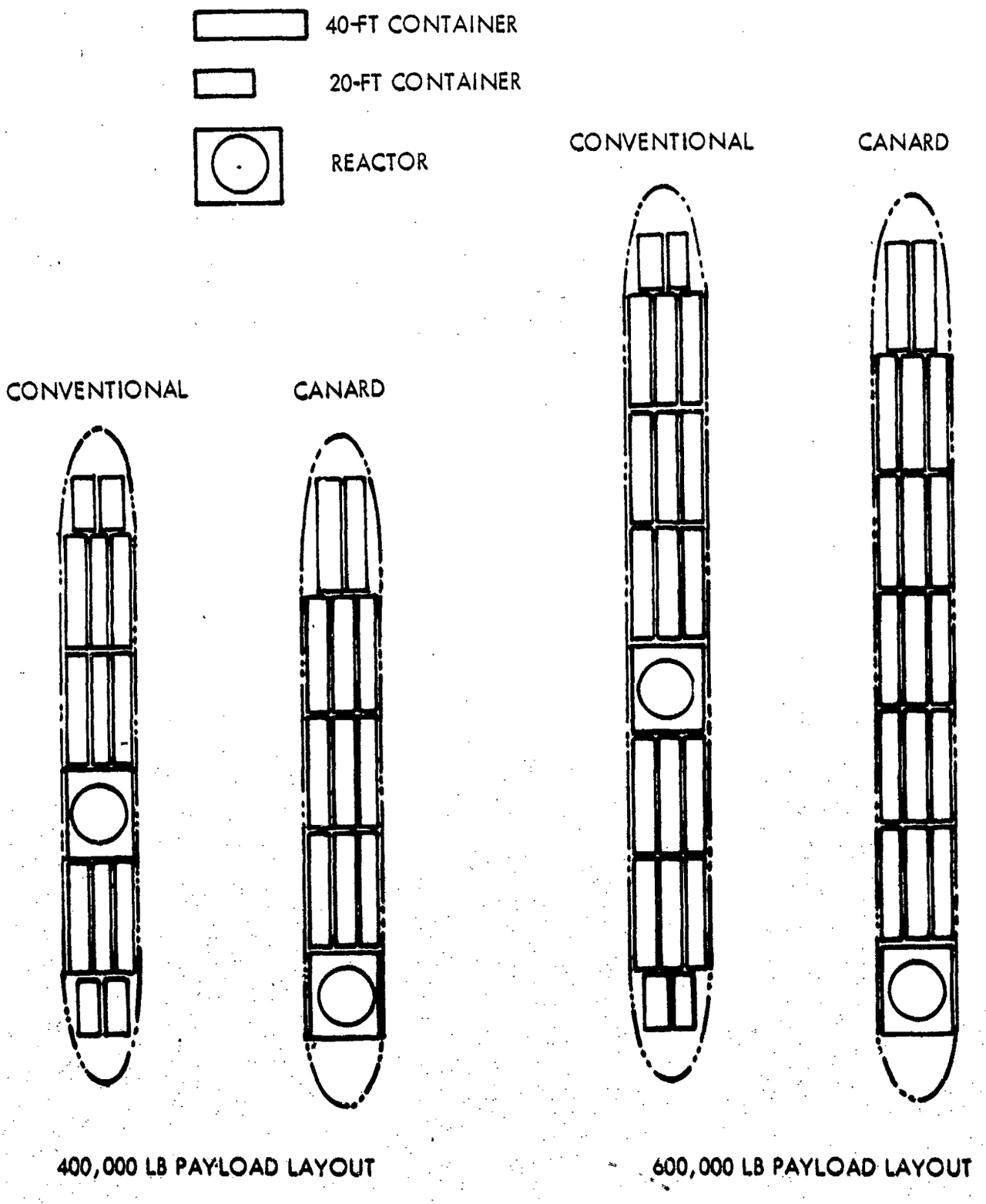

Figure 3-9. Fuselage Floor Plans for Conventional and Canard Configurations

For a specified payload weight, density and container size, the wing span dimension is a function of the wing sweep angle and the number of parallel rows of containers. Table 3.4 lists the span lengths calculated for the candidate spanloader versions in this study. The range of wing sweep angles and one and two rows of containers were selected for consideration based on the optimization studies performed in Ref. 4.

TABLE 3.4. SPANLOADER SPAN DIMENSIONS, FT

Wing Sweep Angle, deg	Aircraft Payload (1000 lb) and Distribution			
	400		600	
	1 Row	2 Rows	1 Row	2 Rows
0	332	172	572	332
20	319	168	544	319
30	298	159	505	298
40	268	145	452	268
50	231	128	325	231

All of the spanloader parametric designs used scaled versions of a 21-percent-thick supercritical airfoil section designated LG5-621. This baseline airfoil has been defined and wind-tunnel-tested by Lockheed. Figure 3-10 gives the streamwise chord lengths for this airfoil when scaled for the ranges of wing thickness ratio and sweep angle values for one and two rows of cargo. Extensive use was made of this figure during the iteration process of developing the parametric spanloaders discussed in Section 3.4.2.3. The iterative process resulted from the interdependence of aircraft weight, wing loading and area, and wing thickness ratio with its associated chord dimension and drag level.

The dual-spanloader configuration was considered to be only a variation of the basic spanloader. After the optimum basic spanloader design was determined in the parametric analysis, it was modified for the dual-reactor concept. Two 40-ft long sections were added in the wing to accommodate two reactors which replaced the single reactor in the aft fuselage.

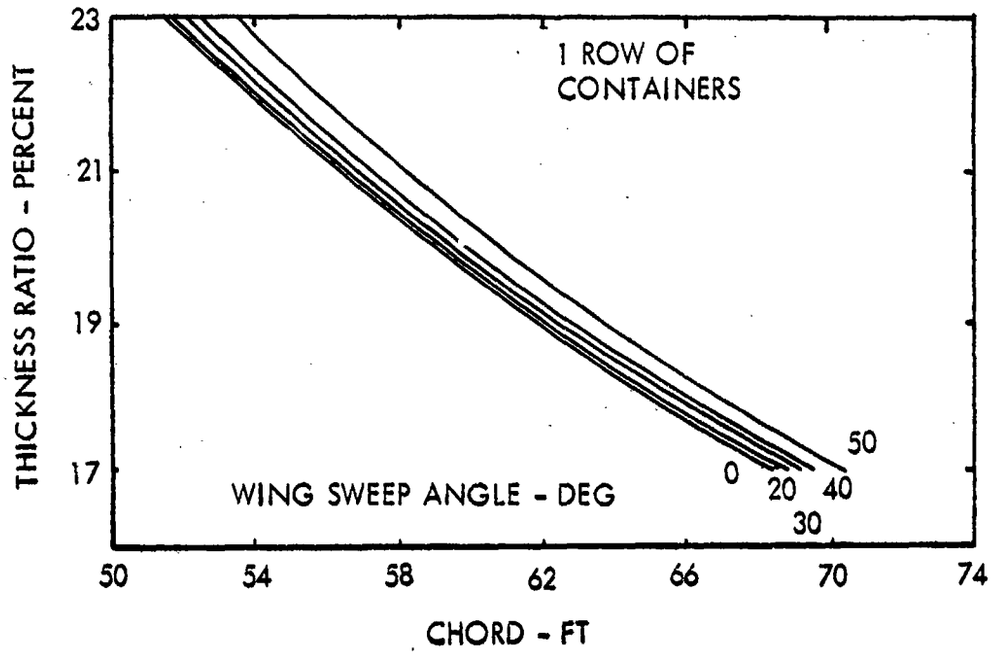

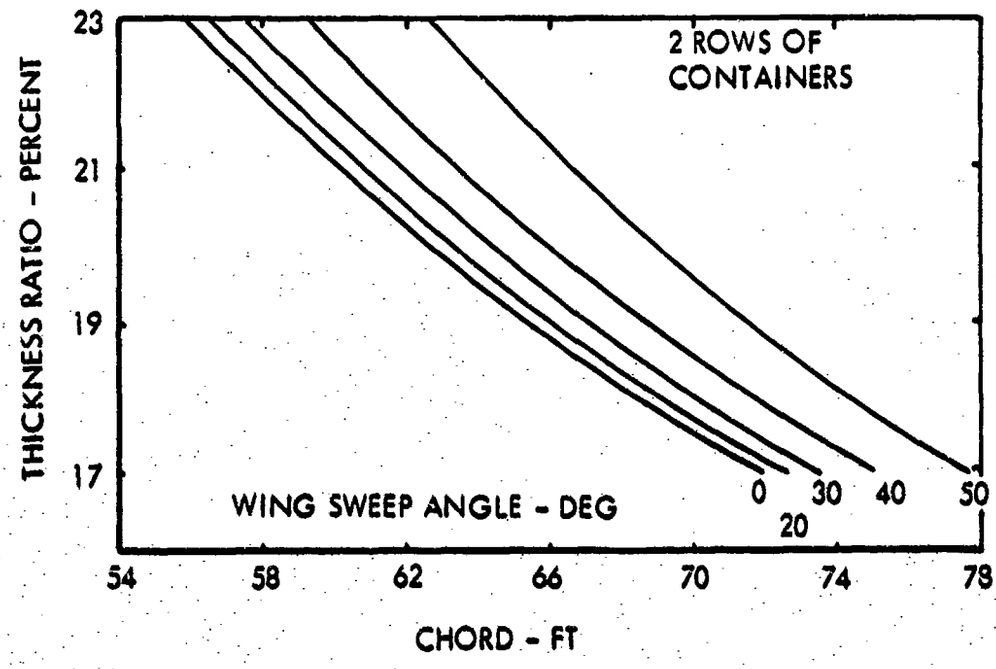

Figure 3-10. Spanloader Wing Chord Dimensions

3.4 PARAMETRIC STUDY

Parametric variations of aircraft geometric and performance characteristics were investigated to minimize the ramp weight of each candidate aircraft configuration. In the preceding section, cargo compartment arrangements were developed for each configuration for the 400,000 and 600,000-lb mission payload requirements. Efforts to develop optimum aircraft designs to accommodate these cargo compartments are the subject of this section. Additional guidelines for these aircraft were the mission requirements to cruise at Mach 0.75, to have an emergency recovery range of 1000 n.m. on JP fuel, and to operate within a 9000-ft field length.

The parameters listed in Table 3.5 were used to generate the array of aircraft designs from which the minimum weight point was selected. The entire range of values was not covered for each configuration. The engine design turbine inlet temperature is the value for cruise on chemical fuel. Usually, the takeoff value is about 200°F greater than the cruise value.

TABLE 3.5. PARAMETRIC STUDY VARIABLES

Cruise Altitude, 1000 ft	24 to 36
Engine Bypass Ratio (BPR)	5.8 to 18
Engine Design Turbine Inlet Temperature, °F	1600 to 1900
Wing Sweep Angle, deg	0 to 50
Wing Loading, lb/ft^2	80 to 150
Wing Aspect Ratio	4 to 12

3.4.1 Preliminary Analyses

Two methods were investigated for varying engine thrust level on chemical fuel to meet the field length restriction. The first was the traditional method of defining an initial power setting, that is the ratio of cruise thrust required to cruise thrust available. A

power setting of 95 percent would mean that the aircraft had an excess thrust of 5 percent. The second method was to vary the engine turbine inlet temperature (TIT) at slightly higher values on chemical fuel than on nuclear power, as discussed in Section 3.2.3. Figure 3-11 shows the effects on aircraft weight and field length from varying TIT and power setting independently for a 400,000-lb payload conventional configuration. The curves indicate that variations in TIT produce greater decreases in field length for smaller weight penalties than do variations in power setting. Based on these findings, the power setting was set equal to one for the parametric study, and variations in TIT were used to achieve specific field lengths.

Some wing loading - altitude combinations produced aircraft designs with cruise lift coefficients considerably higher than projected state-of-the-art for the year 2000. As a guideline, the maximum cruise lift coefficient was limited to the value given by the relationship

$$C_{L_{max\ cruise}} = 0.8 \cos^2 \Lambda$$

where Λ is the wing sweep angle measured in degrees at the wing quarter chord.

Another guideline was established to achieve acceptable landing performance. Nuclear aircraft have a heavy landing weight since they experience minimal fuel burnoff. Therefore, an approach speed limitation of 140 knots was chosen as a reasonable design restriction.

To simplify the parametric study and reduce the number of aircraft point designs, preliminary studies were made to select an engine bypass ratio and cruise altitude. For this preliminary analysis, a 400,000-lb payload conventional configuration was chosen with design characteristics within the range of parametric variables of Table 3.5. As shown on Figure 3-12, less than a 4-percent total variation in aircraft weight resulted for the four engine bypass-ratio values of 5.8, 8.4, 13 and 18 under consideration. Most of the variation occurred between the two lower values. Increasing the bypass ratio above 8.4 saved less than one-half of one percent of the aircraft ramp weight. This small benefit was deemed irrelevant compared to the technology risk required for

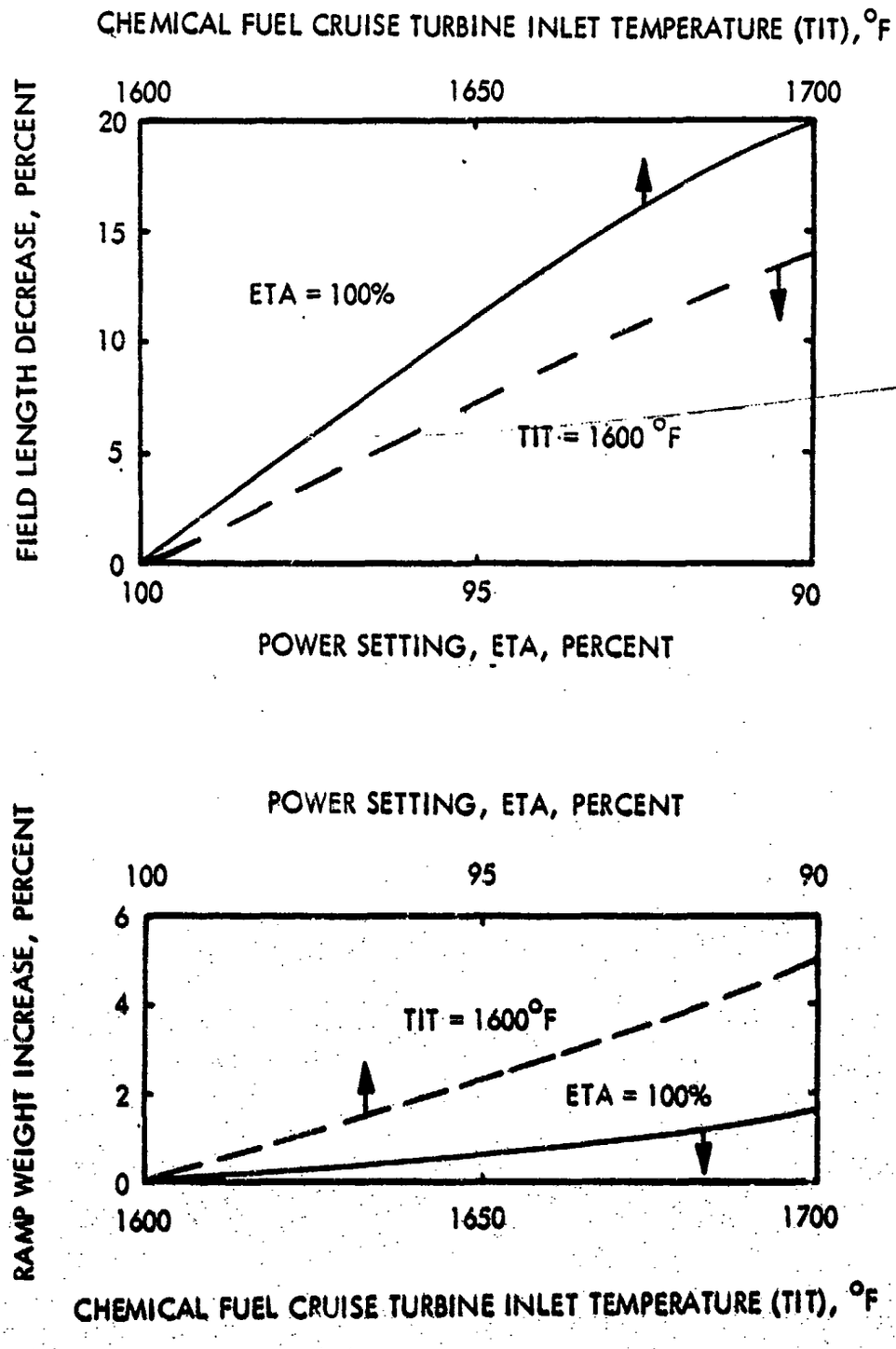

Figure 3-11. Results of Analysis on Power Setting and Turbine Inlet Temperature as Parameters for Engine Sizing. Conventional Configuration, 400,000-lb Payload, AR = 10, $\Lambda = 20^{\circ}$, BPR = 4, Altitude = 36,000 ft.

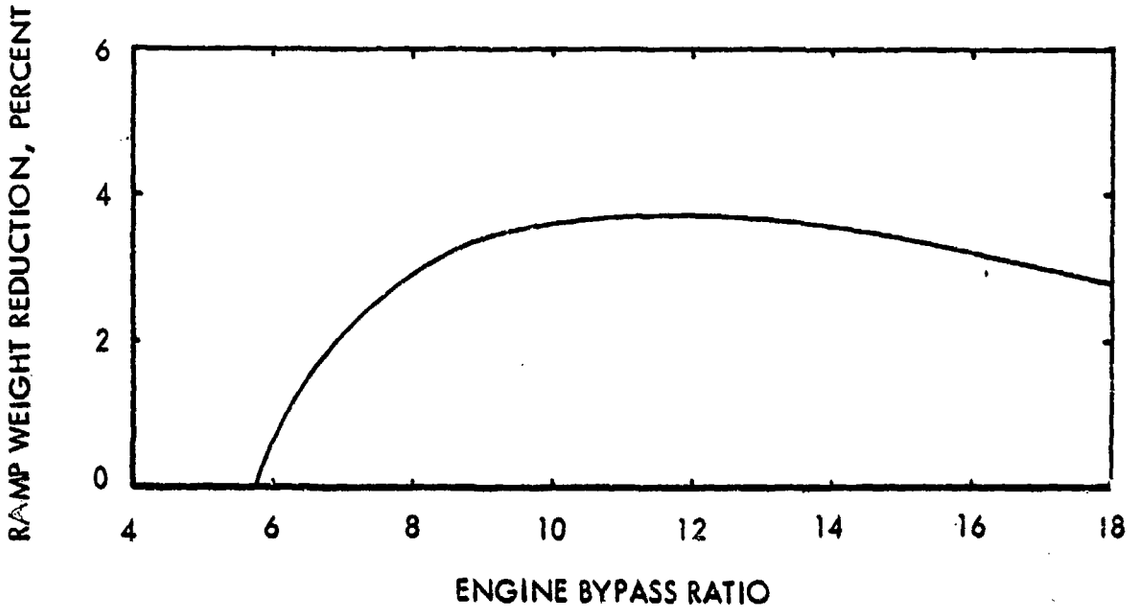

Figure 3-12. Effect of Engine Bypass Ratio on Aircraft Weight. Conventional Configuration, 400,000-lb Payload, AR = 10, $\Lambda = 20^{\circ}$, Altitude = 36,000 ft.

development of the higher bypass ratio engines. Similar trends were observed for the canard and spanloader configurations. Consequently, the 8.4 bypass-ratio engine was selected for the parametric study.

Another preliminary study was performed to select a single cruise altitude for use in the parametric study. For the analysis, each of the three configuration designs were fixed with 8.4 bypass-ratio engines and with other features in the mid-range of the variables listed in Table 3.5. The effect on aircraft ramp weight was investigated for altitude variations between 24,000 and 36,000 ft.

Altitude-optimization results are shown in Figure 3-13 for the 600,000-lb payload span-loader configuration and for the 400,000-lb payload canard and conventional configurations, all subject to a 9000-ft field length requirement. Minimum weights for the three configurations occurred at altitudes of 28,000 and 31,000 ft. Since the configurations were relatively insensitive to altitude variations near the optimum values,

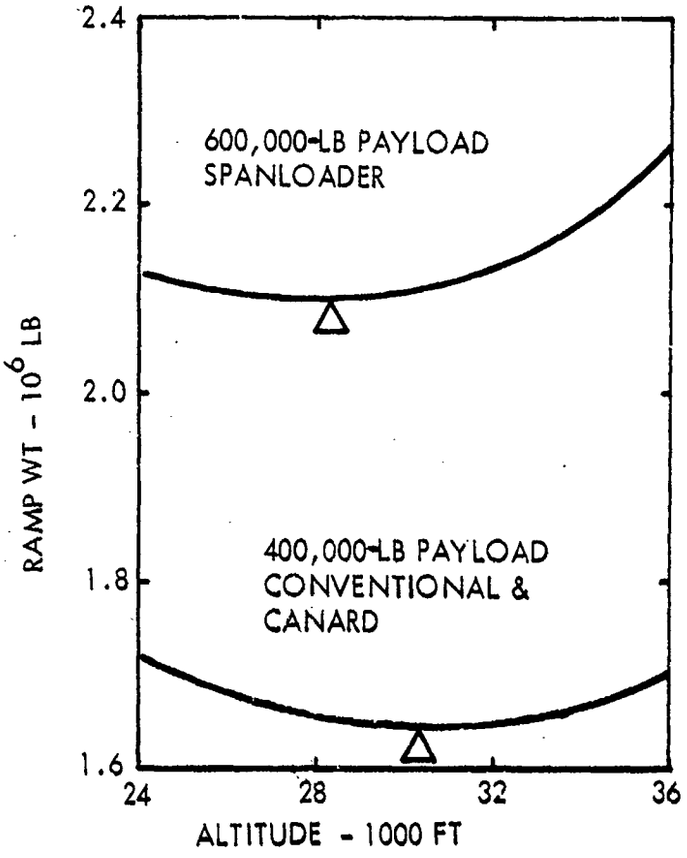

Figure 3-13. Altitude Optimization Results

an altitude of 31,000 ft was selected for uniformity in the parametric study and to make nuclear aircraft flight more compatible with the traffic patterns of existing aircraft.

3.4.2 Parametric Results and Selected Design

Lockheed's Generalized Aircraft Sizing and Performance (GASP) computer program was used to generate the parametric aircraft designs for the two mission payloads of 400,000 and 600,000 lb. Common characteristics of all three configurations are listed in Table 3.6. For each configuration and payload, designs were developed for more than 100 points in the matrix defined by the ranges of values in Table 3.5 for aspect ratio, wing loading, sweep angle and engine design turbine inlet temperature. The minumum ramp weight design for each payload was defined by the parametric results for the canard, conventional and spanloader configurations.

TABLE 3.6. PARAMETRIC STUDY COMMON CHARACTERISTICS

Cruise Mach Number	0.75
Cruise Altitude	31,000 ft
JP Fuel Range	1000 N.M.
Field Length	9000 ft
Engine Bypass Ratio	8.4

3.4.2.1 Canard Configuration

Aircraft designs were generated for the 600,000-lb payload canard configuration for wing sweep angles of 20, 30, and 40 deg and for chemical cruise engine TIT's of 1800, 1850, and 1900°F. The matrix of design points was further broadened by considering variations of wing loading and aspect ratio for each of the nine possible combinations of TIT and sweep angle. Typical results are shown in Figure 3-14 for the one combination of a 30-degree sweep angle and an 1800°F TIT. Both takeoff distance over a 50-ft obstacle and ramp weight data are presented for the parameters of wing loading (W/S) and aspect ratio (AR). In working to define the optimum design point, a line of constant takeoff distance, for the study requirement of 9000 ft, was drawn on the takeoff plot and projected on the ramp weight curves. The lowest point, or bucket, on this projected 9000-ft takeoff distance curve defined the minimum ramp weight aircraft for the particular sweep angle and TIT values. Wing loading and aspect ratio values for this optimum aircraft were interpolated from the ramp weight plot. This procedure was repeated to determine the minimum weight aircraft for the other combinations of TIT and sweep angle.

Data for these minimum weight aircraft were then plotted in a summary matrix, as shown in Figure 3-15, to define the optimum TIT and sweep angle for minimizing the aircraft weight. Superimposed on this matrix are curves for the approach speed limit, as discussed previously, and for the vertical tail span limit. The span limit was set at 20-percent of the wing span for structural stability and flutter prevention, for practical geometric sizing, and for compatibility with experimental data on end-plating effects.

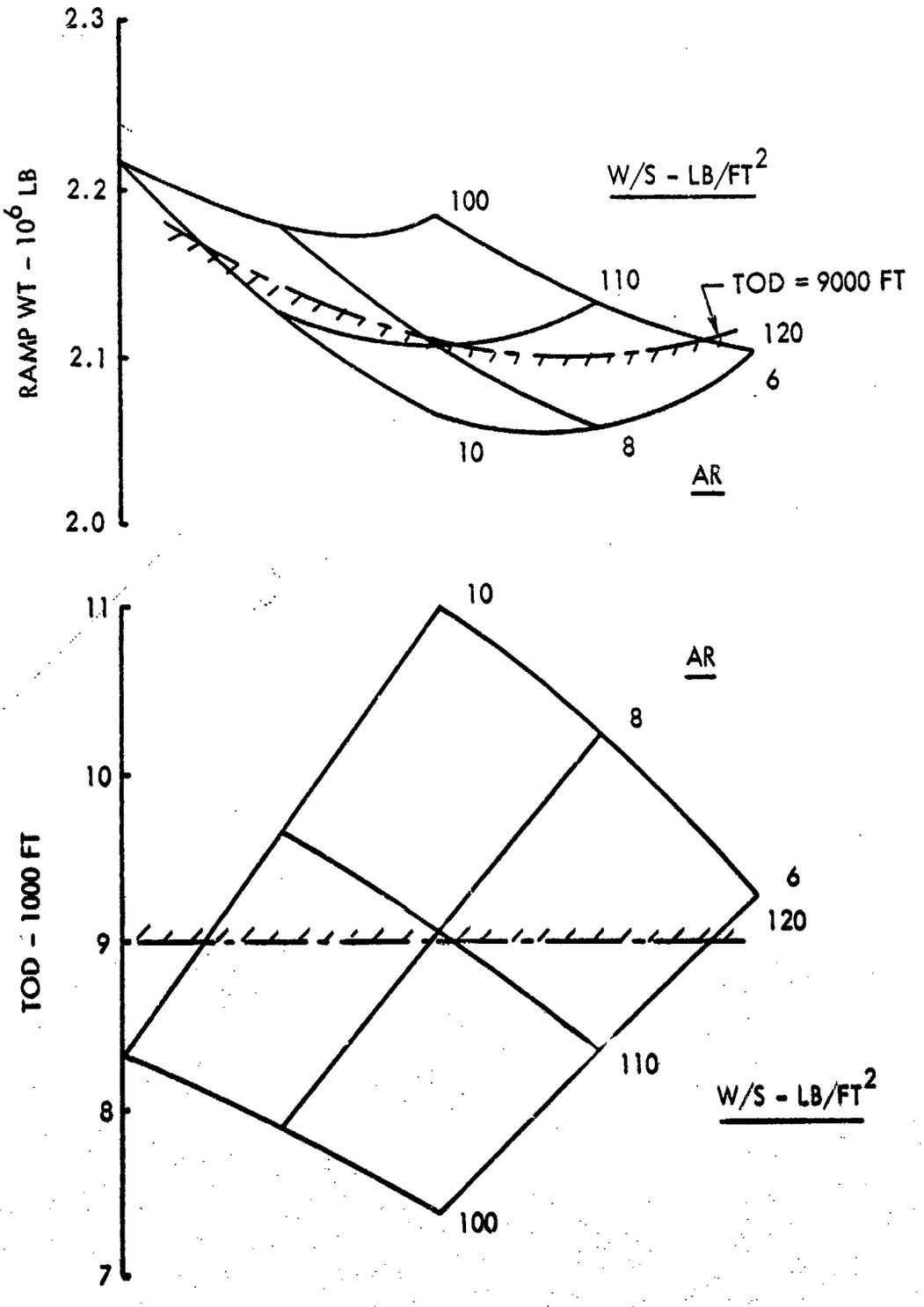

Figure 3-14. Typical Parametric Results for 600,000-lb Payload Canard, TIT = 1800 °F, 30° Sweep Angle.

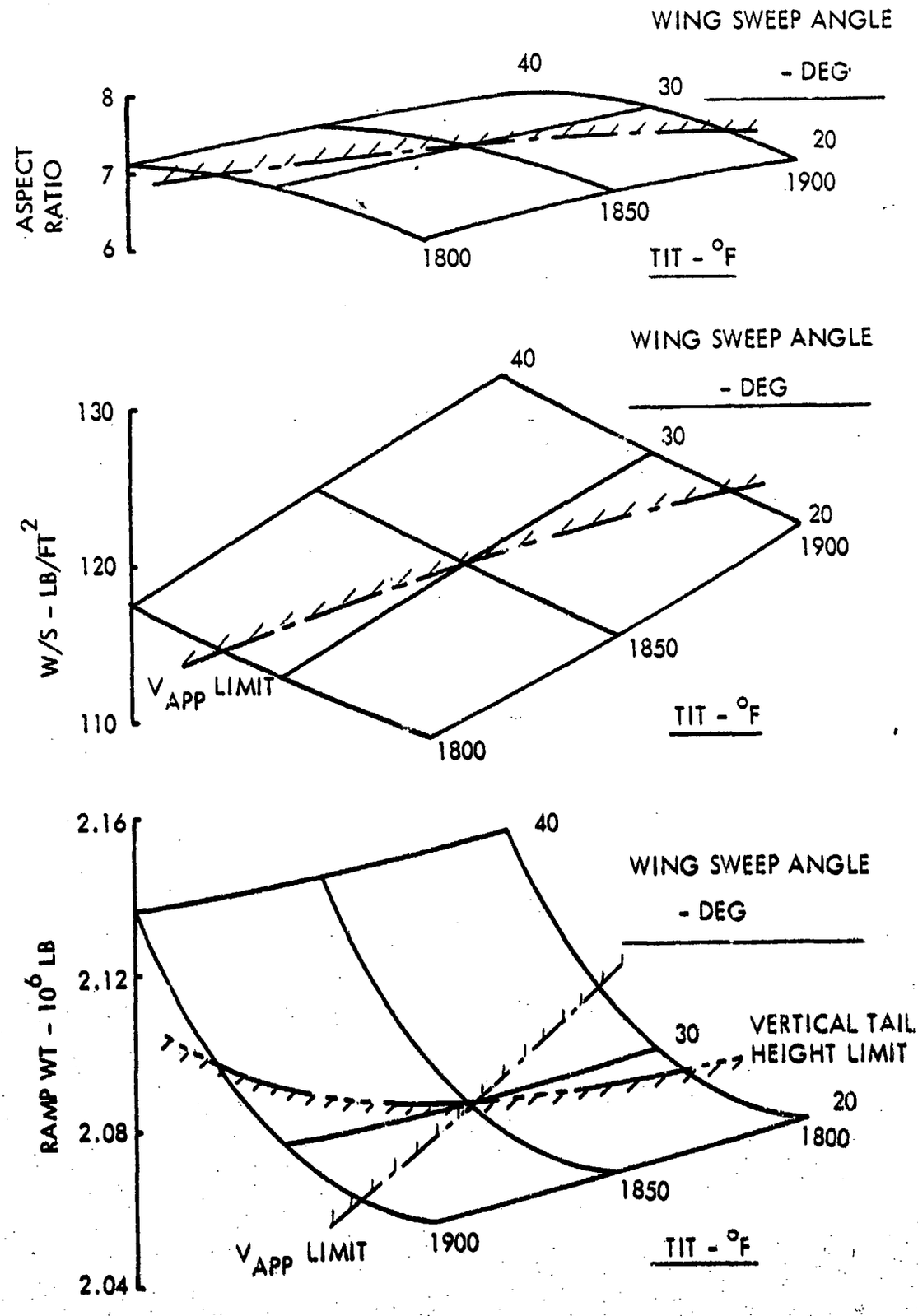

Figure 3-15. Parametric Results for Selecting Optimum 600,000-lb Payload Canard

As a result of these limitations, the minimum weight version of the 600,000-lb payload canard aircraft has a wing sweep angle of 30 deg and a TIT of 1850°F. A three view drawing of the aircraft is included in Figure 3-16. Additional characteristics are listed in Table 3.7.

Parametric studies to define the optimum 400,000-lb payload canard were simplified considerably by the results from the larger canard study. The best aircraft would have the minimum sweep angle of 30 deg and the maximum wing loading allowed under the approach speed constraint. As a result of these deductions, the parametric matrix was reduced to variations of aspect ratio and TIT. The optimum small canard was selected from the field length and ramp weight parametric data in Figure 3-17. Additional characteristics of this aircraft are summarized in Table 3.7.

3.4.2.2 Conventional Configuration

The conventional configuration sizing process was simplified as a result of the parametric similarities between it and the canard configuration. Field length and ramp weight parametric data are presented in Figure 3-18 for the 600,000-lb payload aircraft for a wing sweep angle of 20-deg and a TIT of 1700°F. The minimum weight aircraft defined on Figure 3-18 was compared with similar data for other constant TIT values, as shown in Figure 3-19. After applying the approach speed limit to determine the optimum TIT for this sweep angle, similar data for other sweep angles were combined on Figure 3-20. The minimum weight occurred at a sweep angle of 10 deg. Since there was less than a 0.3-percent variation in ramp weight at 10 and 20-deg sweep angles, the 20-deg angle was chosen to achieve better performance at a cruise Mach number of 0.85 in the sensitivity study of Section 6.1.1. This selected design point aircraft is depicted in Figure 3-21.

The sizing process for the 400,000-lb payload aircraft was identical to that for the 600,000-lb payload aircraft. Figure 3-22 shows the effect of the approach speed limitation in establishing the TIT and minimum ramp weight aircraft. Characteristics of both aircraft are summarized in Table 3.8.

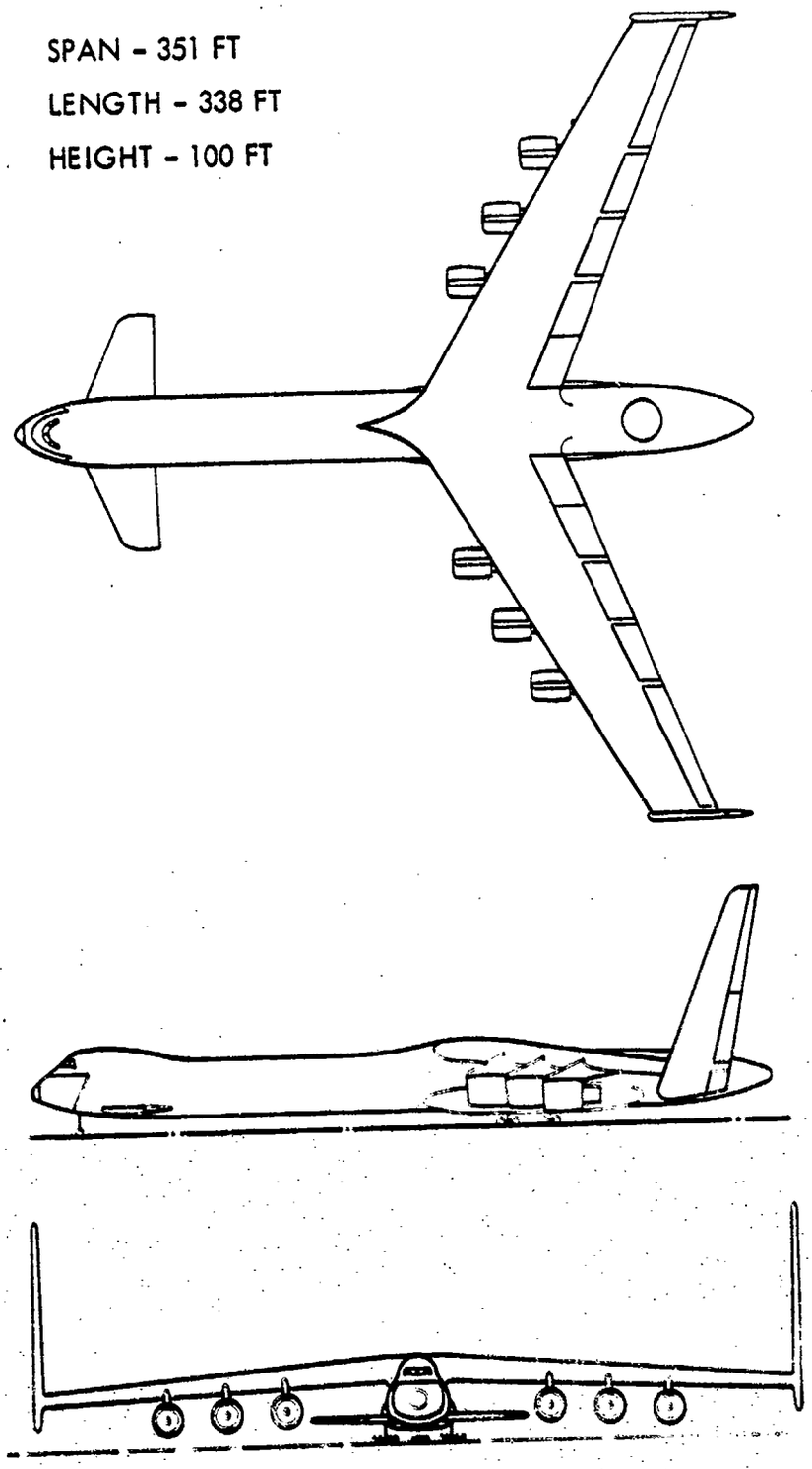

Figure 3-16. Optimum 600,000-lb Payload Canard Aircraft

TABLE 3.7. SUMMARY DATA FOR OPTIMUM CANARD CONFIGURATIONS

	Configuration Payload	
	600,000 lb	400,000 lb
Wing Sweep Angle, deg	30	30
Wing Loading, psf	120	120
Cruise Lift Coefficient	0.508	0.508
Aspect Ratio	7.35	7.90
L/D	24.1	24.2
Weights, 1000 lb		
Nuclear Subsystem	427.9	390.5
OWE	1,314.5	1,015.2
JP Fuel	171.4	126.2
Ramp	2,085.9	1,541.4
Propulsion		
Reactor Size, MW	282	208
No. Engines	6	6
Engine Thrust, 1000 lb	90.3	66.5
Engine Design JP TIT, ^{o}F	1850	1850
Areas, ft^2		
Wing	16,750	12,380
Verticals	3570	2640
Canard	1740	1430

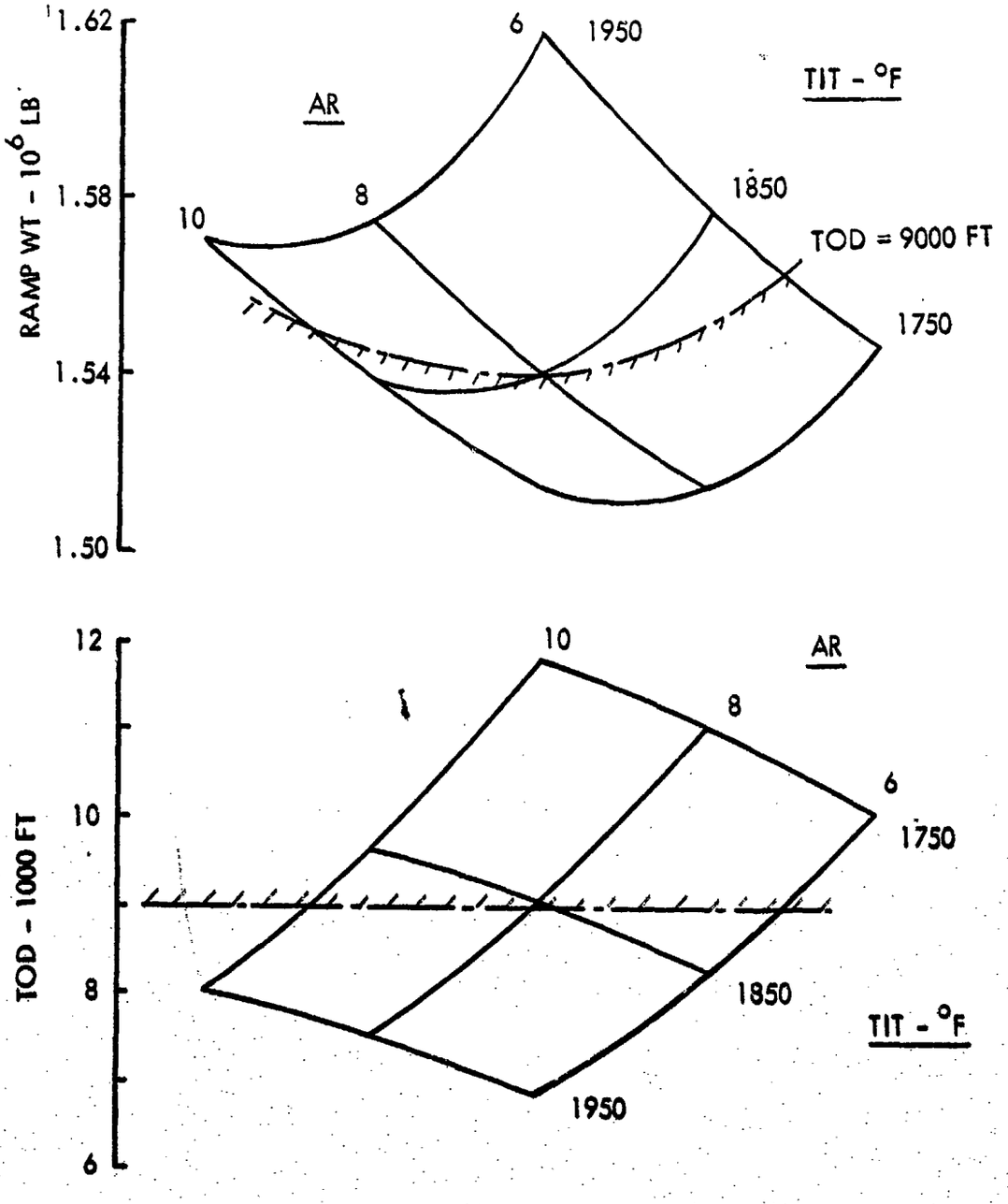

Figure 3-17. Parametric Results for Selecting Optimum 400,000-lb Payload Canard Aircraft

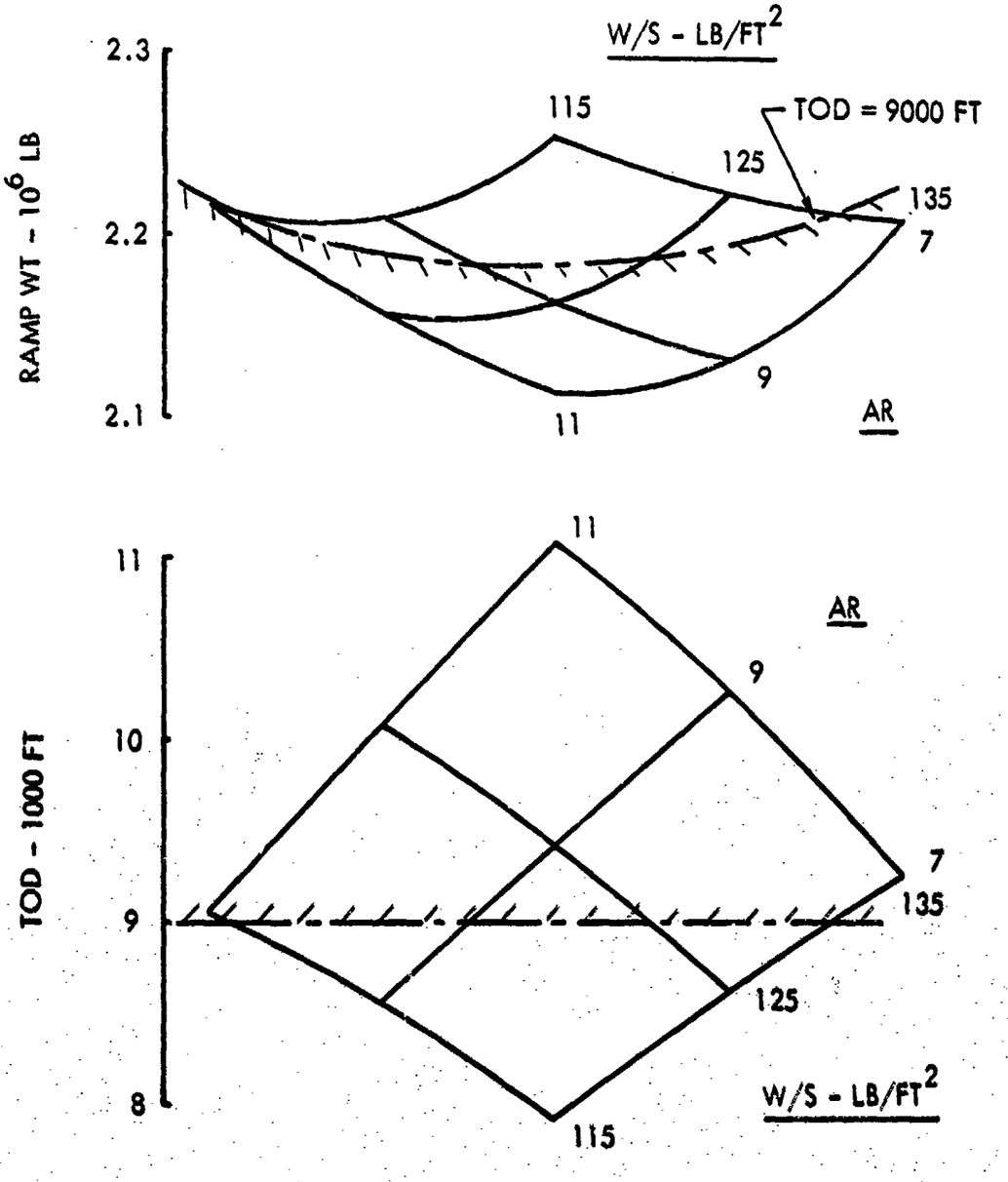

Figure 3-18. Typical Parametric Results for 600,000-lb Payload Conventional Aircraft. TIT = 1700°F, Sweep Angle = 20°

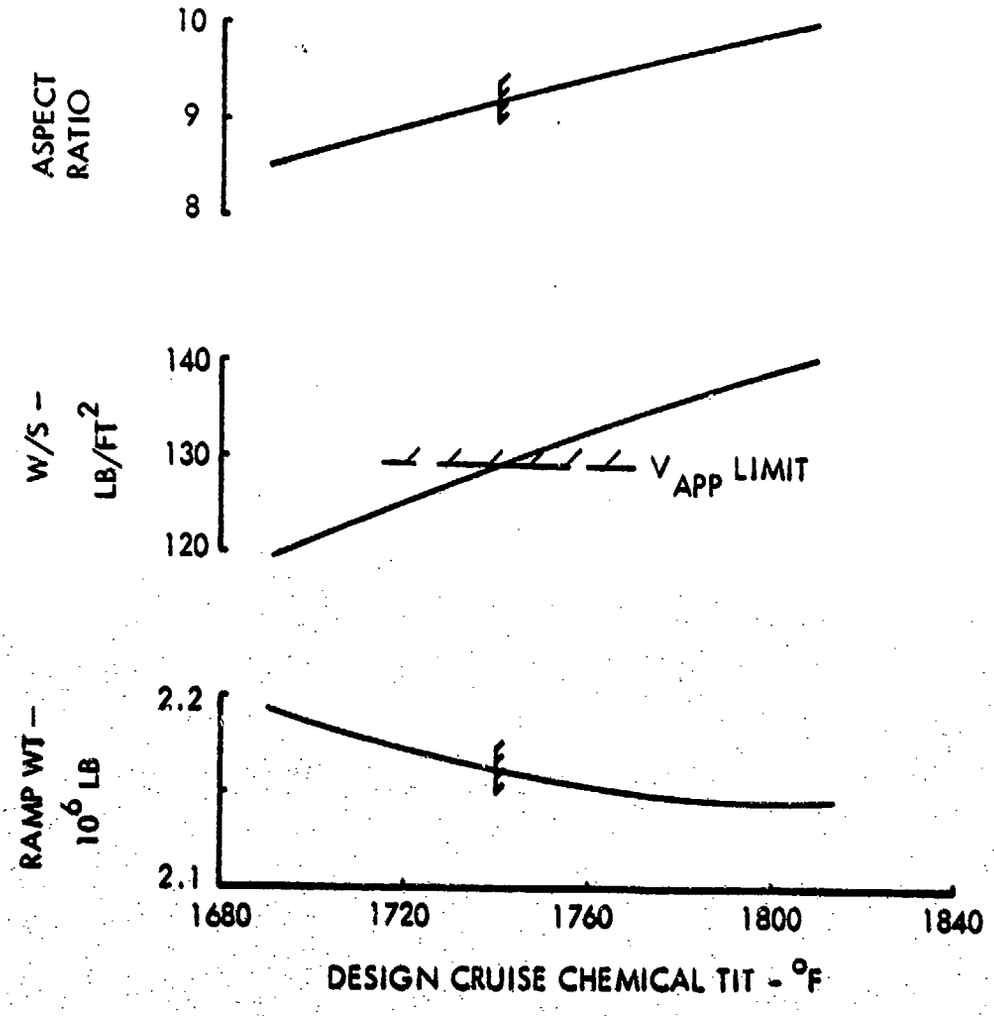

Figure 3-19. TIT Optimization for 600,000-lb Payload Conventional Aircraft. Sweep Angle = 20°

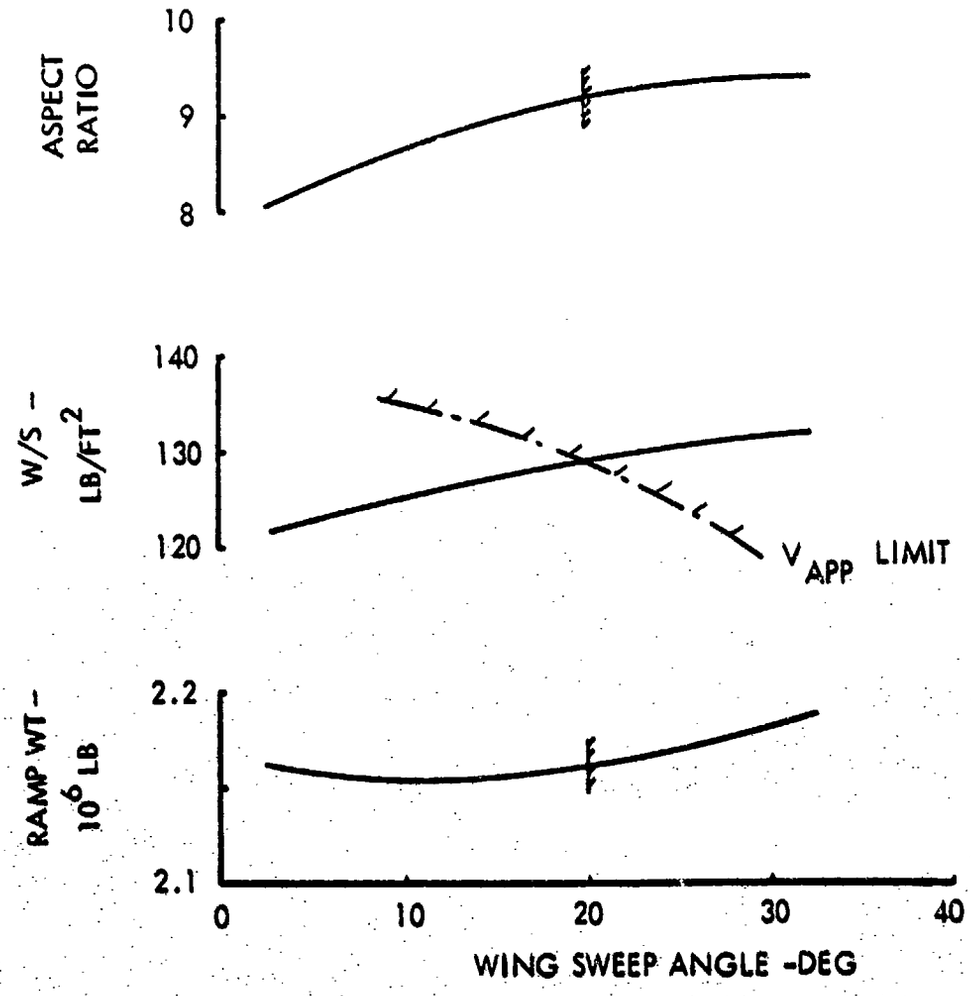

Figure 3-20. Sweep Angle Optimization for 600,000-lb Payload Conventional Aircraft.
TIT = 1740°F

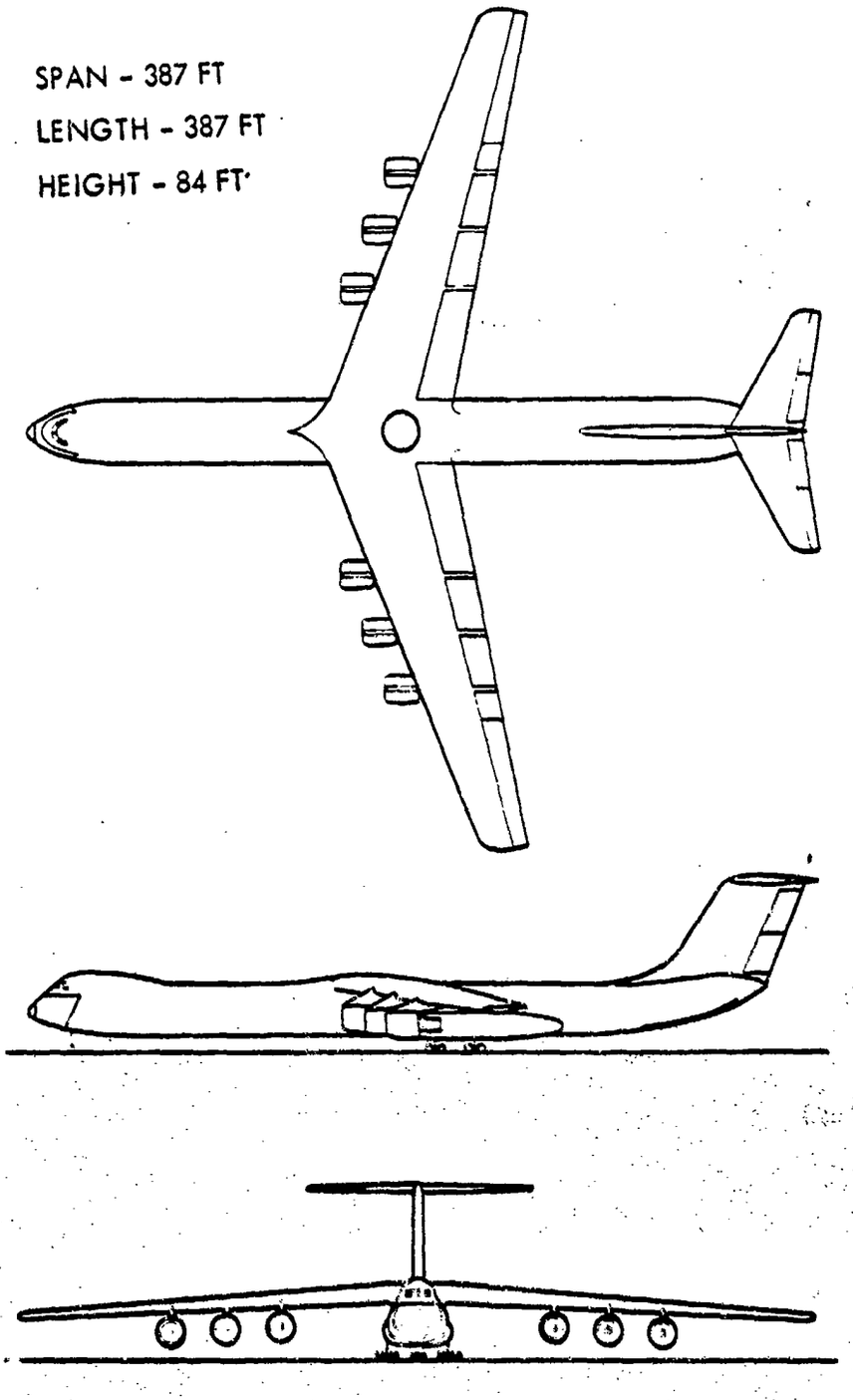

Figure 3-21. Optimum 600,000-lb Payload Conventional Aircraft

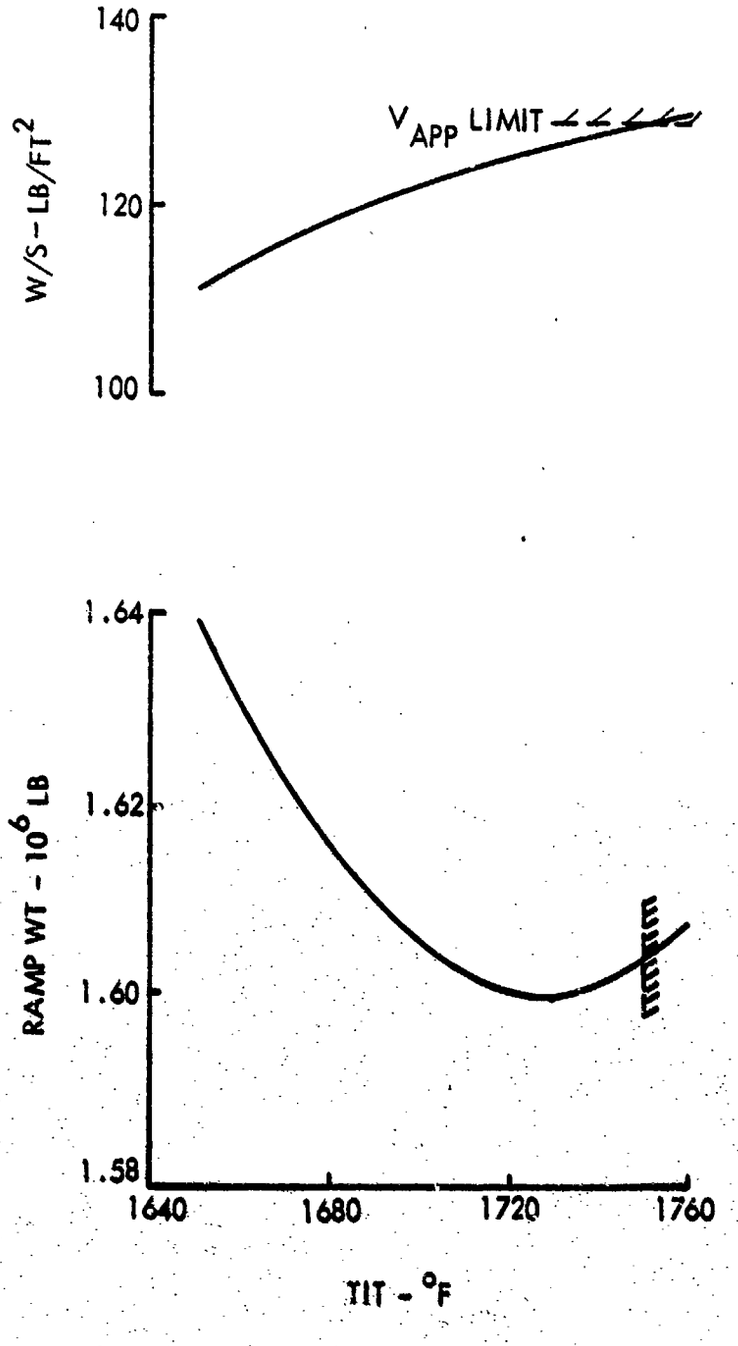

Figure 3-22. TIT Selection for 400,000-Lb Payload Conventional Aircraft

TABLE 3.8. SUMMARY DATA FOR OPTIMUM CONVENTIONAL CONFIGURATIONS

	Configuration Payload	
	600,000 lb	400,000 lb
Wing Sweep Angle, deg	20	20
Wing Loading, psf	129	127
Cruise Lift Coefficient	0.546	0.537
Aspect Ratio	9.18	9.00
L/D	22.5	21.9
Weights, 1000 lb		
Nuclear Subsystem	446.2	408.2
OWE	1,382.5	1,067.6
JP Fuel	178.7	132.4
Ramp	2,161.2	1,600.0
Propulsion		
Reactor Size, MW	318	243
No. Engines	6	4
Engine Thrust, 1000 lb	87.0	97.5
Engine Design JP TIT, °F	1740	1725
Areas, ft^2		
Wing	16,310	12,330
Vertical	2050	1920
Horizontal	2640	1780

3.4.2.3 Spanloader Configuration

The sizing process for the spanloader configuration differed considerably from that for the canard and conventional configurations since the wing geometry of the spanloader is dictated primarily by the cargo distribution and box size. Each combination of parametric values required that the wing airfoil be scaled to a size sufficient to encompass the cross-sectional area of the wing cargo box. Similarly, the wing span in each case had to be sized to accommodate the length of the wing cargo box. In performing the parametric study, the minimum chord, span and thickness dimensions used for the wing were based on the data previously presented in Figure 3-10 and Table 3.4.

Typical parametric data from the sizing process are presented in Figure 3-23. This particular set of data is for the 600,000-lb payload spanloader with two rows of cargo and a 40-deg sweep angle.

All of the data points on the figure represent aircraft with aerodynamically-designed wings, but these aircraft do not necessarily have wing geometries sufficient to accommodate the prescribed cargo distribution. To determine the candidate design points, the wing chords of the program-generated designs were compared with the chord requirements for cargo enclosure for the particular value of wing thickness-to-chord ratio. For this matching process, the chord and thickness-to-chord ratio values of the program-generated designs were plotted on Figure 3-24 for each of the TIT values. The dashed line on the figure represents the chord requirements for cargo enclosure, as given by Figure 3-10. The intersection of the lines are the points where the chord values match. These intersection point values were then transferred to the middle plot on Figure 3-23 to establish the line of candidate spanloader aircraft. To determine the aircraft capable of satisfying the study constraints on field length, the 9000-ft takeoff distance line was constructed on the lower chart and then projected to the other two charts on the figure. The intersection of the chord line and the takeoff distance line defines the only acceptable aircraft for this sweep angle.

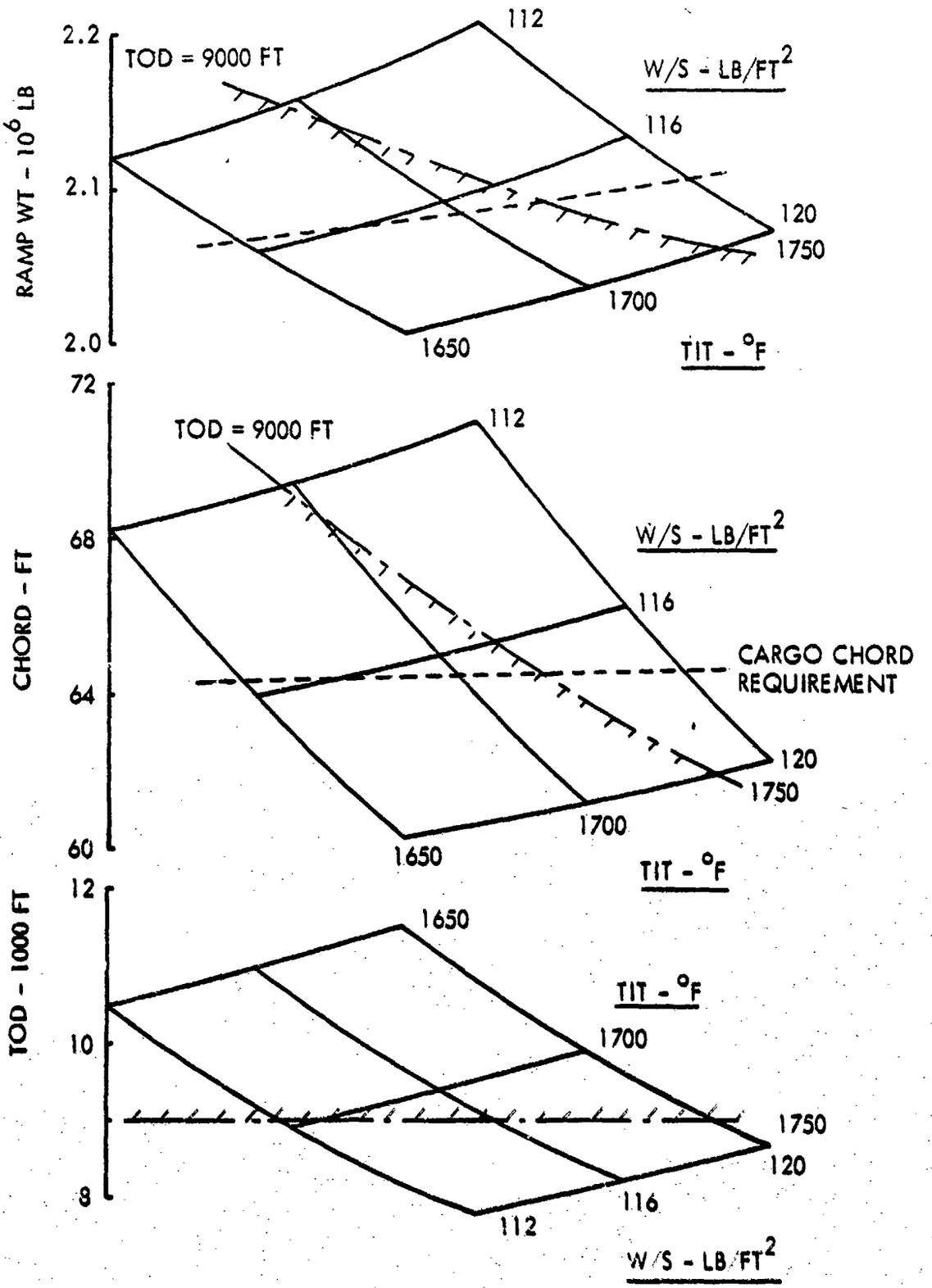

Figure 3-23. Typical Parametric Results for 600,000-lb Payload Spanloader Aircraft. Two Rows, 40° Sweep Angle.

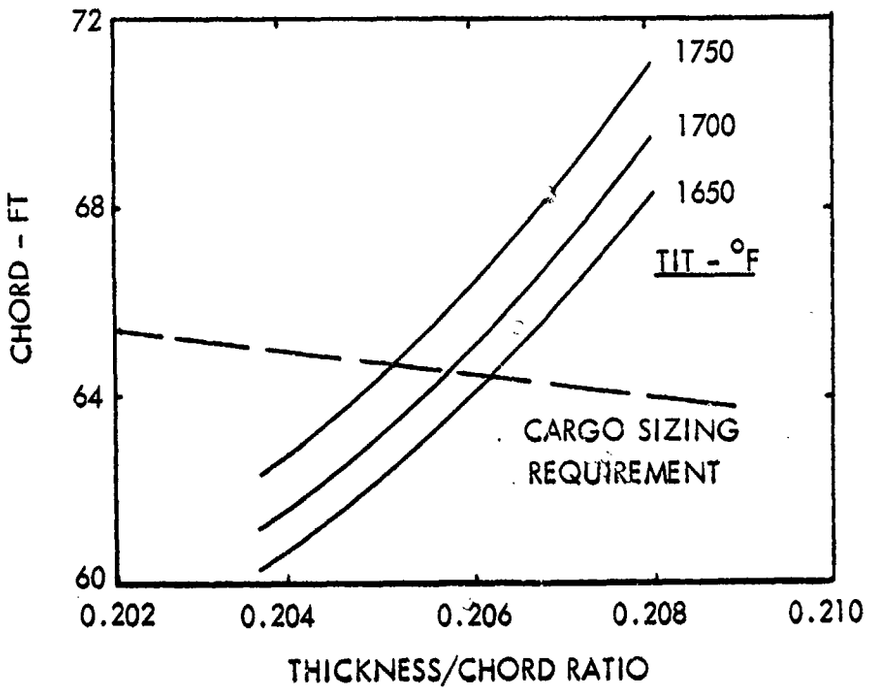

Figure 3-24. Typical Spanloader Chord Matching

The aircraft defined by the data set in Figure 3-23 was compared with similarly-defined aircraft for other sweep angles for both a single and double row of cargo in the wing. This comparison is shown in Figure 3-25. As evident in this figure, the minimum weight design had a wing sweep angle of 30 deg and a double row cargo distribution. This optimum point was somewhat below the approach speed limit of 140 kts. Such was not the case for the single row cargo distribution where the approach speed limitation restricted the maximum sweep angle to 44 deg. Characteristics of the selected aircraft are summarized in Table 3.9, and the aircraft is depicted in Figure 3-26.

A similar optimization process was followed for the 400,000-lb payload spanloader. Only the single row cargo distribution was considered in detail for this payload. The double row distribution was rejected during the initial sizing process when it became evident, that due to the small geometric aspect ratio values of less than three, the approach speed limit and reasonable wing loadings could not be achieved even with very heavy aircraft. Figure 3-27 shows that a 30-deg sweep angle gives the minimum weight

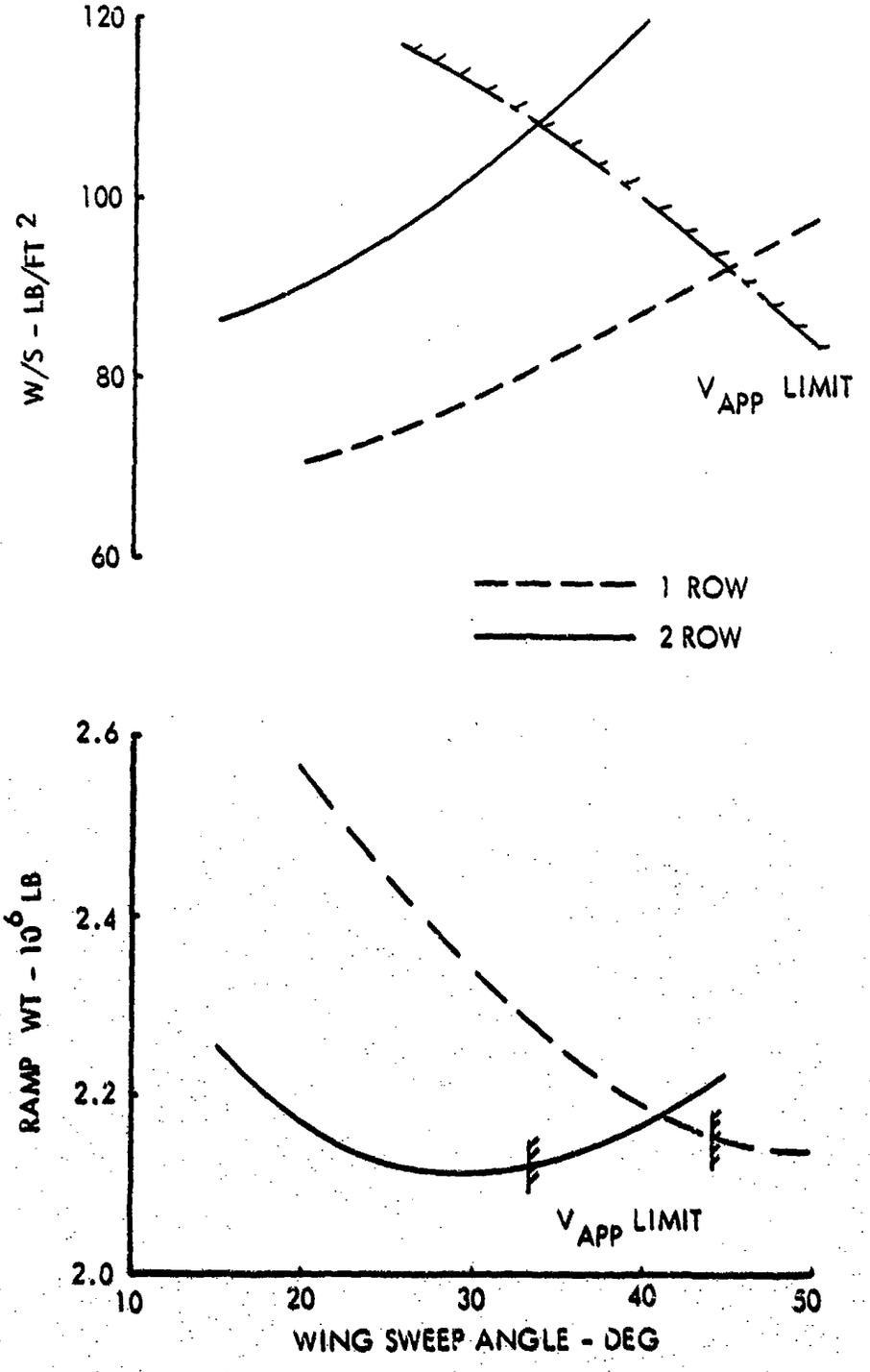

Figure 3-25. Optimization of 600,000-lb Payload Spanloader Aircraft

TABLE 3.9. SUMMARY DATA FOR OPTIMUM SPANLOADER CONFIGURATIONS

	Configuration Payload		
	600,000 lb		400,000 lb
No. Reactors	1	2	1
Wing Sweep Angle, deg	30	30	30
Wing Loading, psf	102.7	103.7	90.9
Cruise Lift Coefficient	0.434	0.439	0.385
Aspect Ratio	4.47	5.68	5.0
L/D	19.6	21.9	20.2
Weights, 1000 lb			
Nuclear Subsystem	464.5	900.0	424.9
OWE	1,309.8	1,864.4	1,114.2
JP Fuel	203.4	236.4	158.4
Ramp	2,113.2	2,700.9	1,672.6
Propulsion			
Reactor Size, MW	354	405	276
No. Engines	6	8	6
Engine Thrust, 1000 lb	90.6	83.6	63.6
Engine Design JP TIT, ^{o}F	1696	1737	1635
Areas, ft^2			
Wing	19,850	25,160	17,770
Verticals	3910	5440	3660
Canard	2940	3820	1980

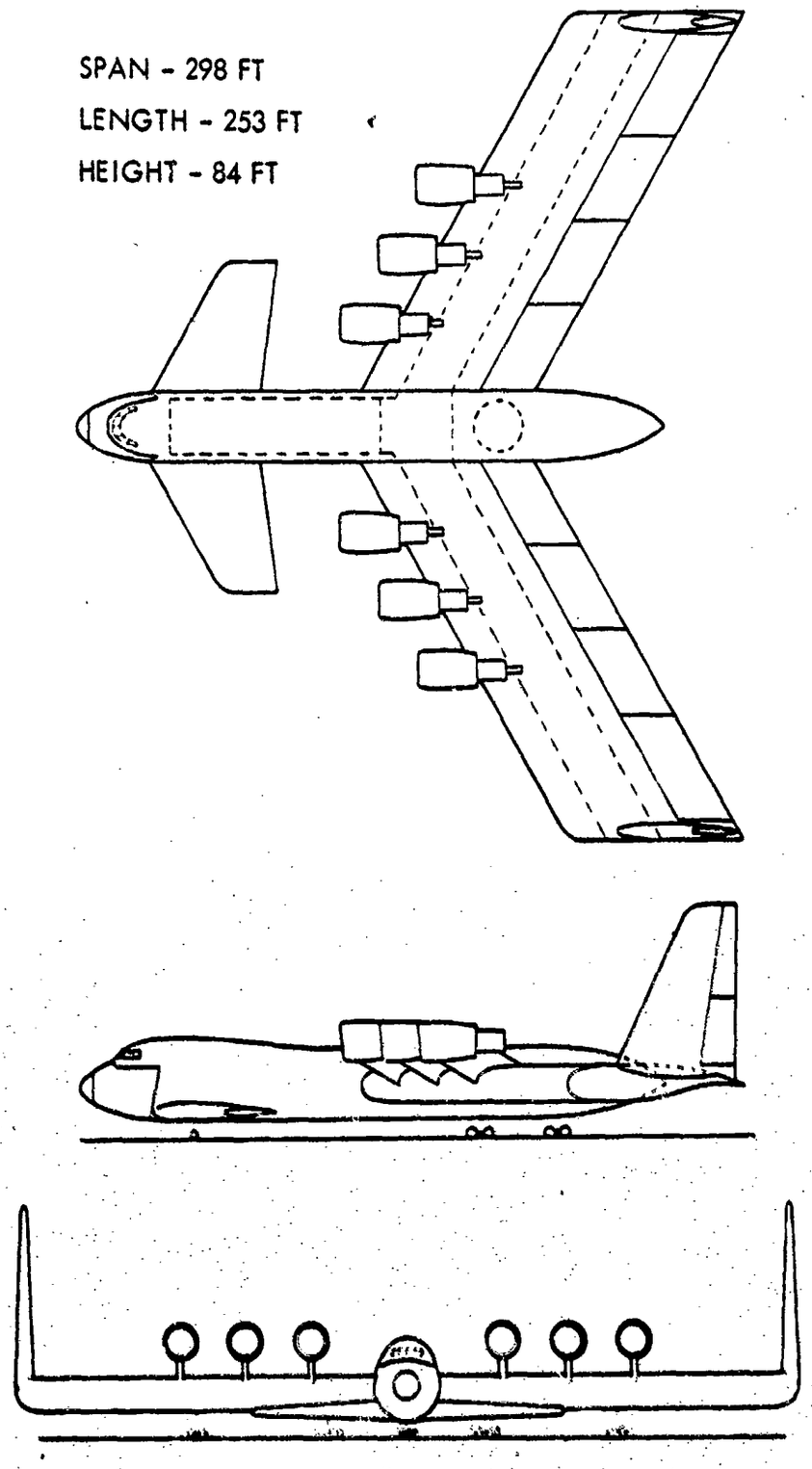

Figure 3-26. Optimum 600,000-lb Payload Spanloader Aircraft

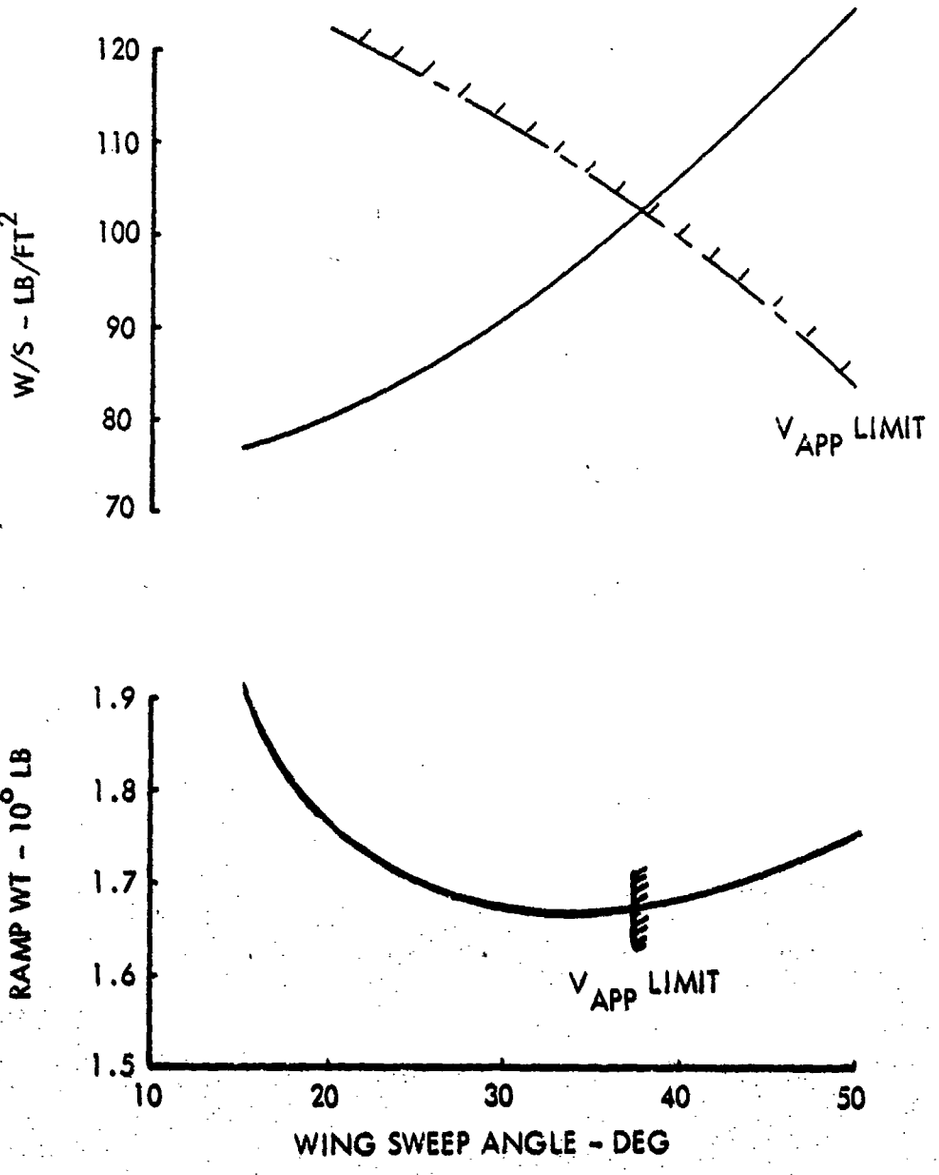

Figure 3-27. Optimization of 400,000-lb Payload Spanloader Aircraft

aircraft within the approach speed constraint. Characteristics of this aircraft are also summarized in Table 3.9.

As a design perturbation, the 600,000-lb payload spanloader was modified slightly to accommodate dual reactors in the wing in place of the single reactor in the aft fuselage. The purpose of this investigation was to determine if additional improvements in aircraft performance could be achieved through distribution of the reactor weight. It was

assumed that the nuclear subsystem shape could be changed without a weight penalty from a sphere to an oblate spheriod of a size that would fit in the wing. As part of this design modification, the span was increased by 80 ft.

Figure 3-28 shows the resulting dual-reactor spanloader. The weight characteristics of the aircraft, as summarized in Table 3.9, clearly indicate that the desired effect was not achieved. The severe weight penalty imposed by dual reactors and the additional span length increased aircraft ramp weight from 2,113,190 lb to 2,700,878 lb. Consequently, this concept was dropped from further consideration.

3.4.3 Full Reactor Usage Sensitivity

Prior to selecting one configuration as optimum, an alternate reactor utilization philosophy was considered and the effects on the aircraft were assessed. For the parametric study, the reactor was assumed to be inoperative during taxi, takeoff, climb, descent, landing and cruise over the recovery range. These operations were performed solely on JP fuel.

In the sensitivity analysis, the reactor was sized, as before, to meet the cruise thrust requirements. However, the reactor was assumed to be fully operational during taxi, takeoff, climb, descent, and landing maneuvers, and at half power for the recovery range cruise. Additional power requirements in excess of the reactor capability were provided through JP-fuel augmentation.

The results of this sensitivity analysis are listed in Tables 3.10 and 3.11 for the 600,000 and 400,000-lb payload configurations, respectively. While all six aircraft realized benefits in terms of reduced weight for this alternate reactor usage philosophy, no one aircraft benefited substantially more than any other. Thus, this sensitivity study did not provide any results that would strongly influence the selection of the optimum configuration.

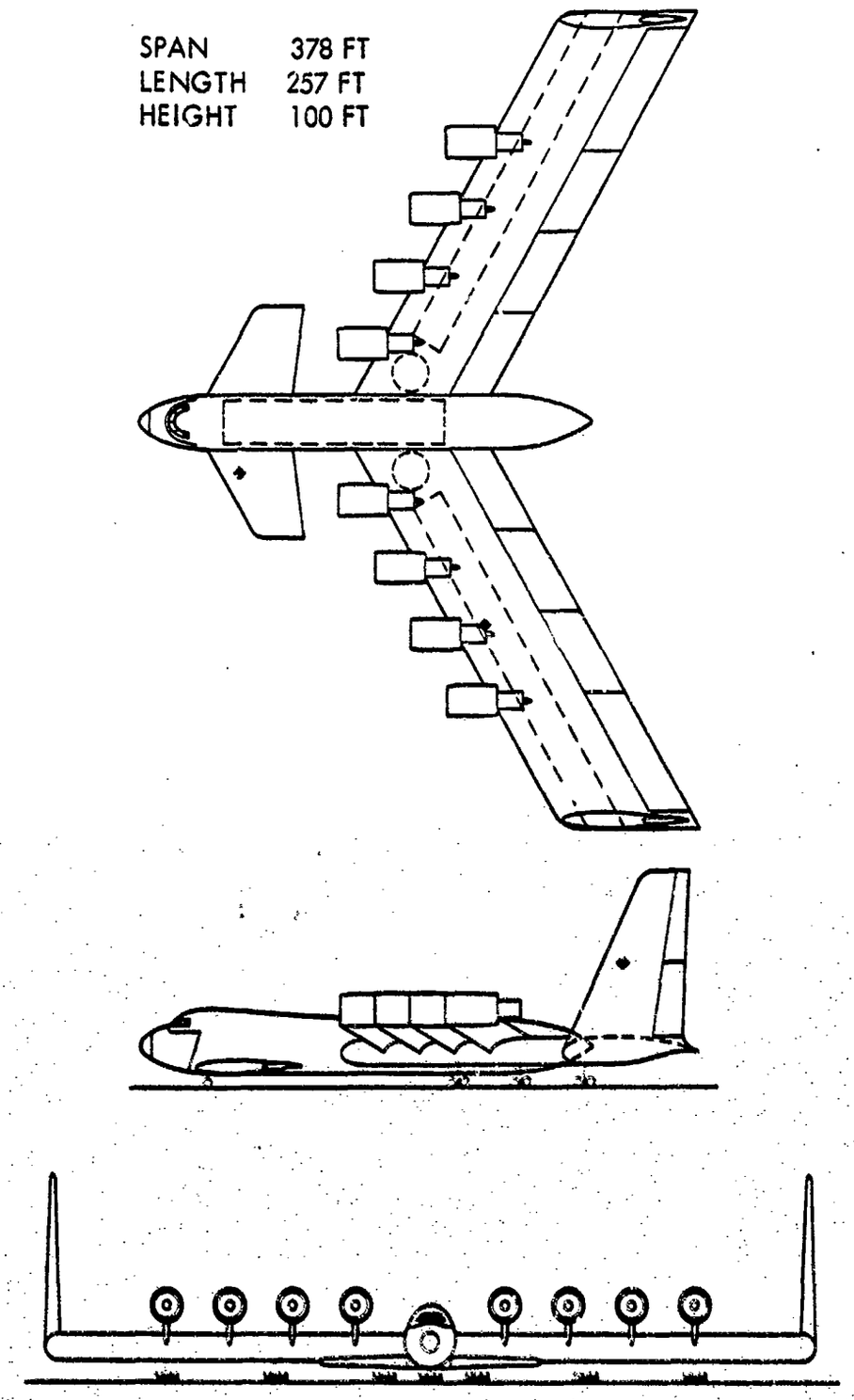

Figure 3-28. Dual-Reactor Spanloader

TABLE 3.10. JP FUEL SENSITIVITY - 600,000-LB PAYLOAD AIRCRAFT

	Selected* Aircraft	Alternate** Aircraft	Percent Reduction
Conventional			
OWE, 1000 lb	1,382.5	1,317.4	4.7
JP Fuel, 1000 lb	178.7	49.5	72.3
Ramp Wt, 1000 lb	2,161.2	1,966.9	9.0
Field Length, ft	9000	8660	4.2
Canard			
OWE, 1000 lb	1,314.5	1,256.0	4.5
JP Fuel, 1000 lb	171.4	33.2	80.6
Ramp Wt, 1000 lb	2,085.9	1,889.2	9.4
Field Length, ft	9000	8490	5.9
Spanloader			
OWE, 1000 lb	1,309.8	1,256.2	4.1
JP Fuel, 1000 lb	203.4	52.2	74.3
Ramp Wt, 1000 lb	2,113.2	1,908.4	9.7
Field Length, ft	9000	7626	15.1

* Takeoff, climb, and emergency cruise on JP fuel

** Takeoff and climb with full-power reactor and JP fuel, emergency cruise with half-power reactor and JP fuel

TABLE 3.11. JP FUEL SENSITIVITY - 400,000-LB PAYLOAD AIRCRAFT

	Selected* Aircraft	Alternate** Aircraft	Percent Reduction
Conventional			
OWE, 1000 lb	1,067.6	1,023.3	4.1
JP Fuel, 1000 lb	132.4	37.8	71.5
Ramp Wt, 1000 lb	1,600.0	1,461.1	8.7
Field Length, ft	9000	8433	6.3
Canard			
OWE, 1000 lb	1,015.2	975.4	3.9
JP Fuel, 1000 lb	126.2	25.2	80.0
Ramp Wt, 1000 lb	1,541.4	1,400.6	9.1
Field Length, ft	9000	8355	7.2
Spanloader			
OWE, 1000 lb	1,114.2	1,084.8	2.6
JP Fuel, 1000 lb	158.4	42.4	73.2
Ramp Wt, 1000 lb	1,672.6	1,527.2	8.7
Field Length, ft	9000	7538	16.5

* Takeoff, climb, and emergency cruise on JP fuel

** Takeoff and climb with full-power reactor and JP fuel, emergency cruise with half-power reactor and JP fuel

3.5 CONFIGURATION SELECTION

The selected aircraft for the three configurations had very similar ramp weights, as a comparison of the weights in Table 3.10 or Table 3.11 showed for each payload. The difference in ramp weight between the lightest and heaviest 600,000-lb payload configurations was only 3.6 percent. For the 400,000-lb payload configuration, this difference was 8.5 percent. Thus, one configuration did not emerge as clearly superior to the other two.

Characteristically for an aircraft parametric study, some design parameters are fixed at values which, on the average for the ranges of parameters being investigated, will yield reasonable aircraft designs. Typical of the quantities fixed are the tail volume coefficients, the wing and landing gear positions relative to the fuselage, and engine placement. This approach is mandated to limit the scope of the parametric study. As a result, the optimum aircraft indicated by the trends of the parametric data usually requires some minor refinements for an acceptable design. Several such refinements were made on each of the configurations prior to selecting the optimum one.

3.5.1 Configuration Refinements

Weight balances were performed on the six aircraft, and the results were used in a check of the tail sizes to assure adequate stability and control capability. Subsequently, small adjustments were made to the tail volume coefficients and wing location on the fuselage.

With the change in coefficient for the vertical surfaces on the canard aircraft, it became apparent that three vertical tails would be needed to keep within the vertical span limitation. The third vertical surface was mounted on the aft fuselage and swept at a 30-deg angle to increase its moment arm. Both of the wingtip-mounted verticals were restricted to a 20-deg sweep angle to minimize possible wing flutter problems.

The stability and control check and the weight balances dictated some shifts in wing position and/or gear location for both the canard and conventional configurations. Generally, the wing shift was away from the reactor, thereby increasing the length and weight of the nuclear system ducting between the reactor and the engines. To counteract this weight increase, the engines were moved inboard on all configurations. Concurrently, the spacing between engines was increased due to aerodynamic interference considerations.

The vertical surfaces on the spanloader configurations were inadvertently specified for an aft-chord position on the wingtip. To preclude the flutter problems that were encountered previously (Ref. 4) with the verticals in an aft position, both verticals were moved as far forward as possible on the wingtips.

Figures 3-29 through 3-34 depict the six aircraft following the refinement efforts. Weight statements of these aircraft are compared in Tables 3.12 and 3.13 for the 600,000-lb and 400,000-lb payloads, respectively. Other characteristics of the aircraft are summarized in Tables 3.14 and 3.15.

3.5.2 Selected Configuration

A comparison of the ramp weights in Tables 3.12 and 3.13 shows that the canard aircraft had the lightest weight for both payloads. For the larger payload, the canard aircraft was one percent lighter than the spanloader aircraft and 4.3 percent lighter than the conventional aircraft. For the smaller payload, the canard aircraft was 4.8 and 9.8 percent lighter than the conventional and spanloader aircraft, respectively.

While the differences in weights for the three configurations were not large, the emergence of the canard aircraft as the lightest weight configuration for both payloads dictated its selection as the optimum configuration. For smaller payloads, the conventional configuration might prove superior. The data also indicate that the spanloader configuration might be better for larger payloads than those considered in this study.

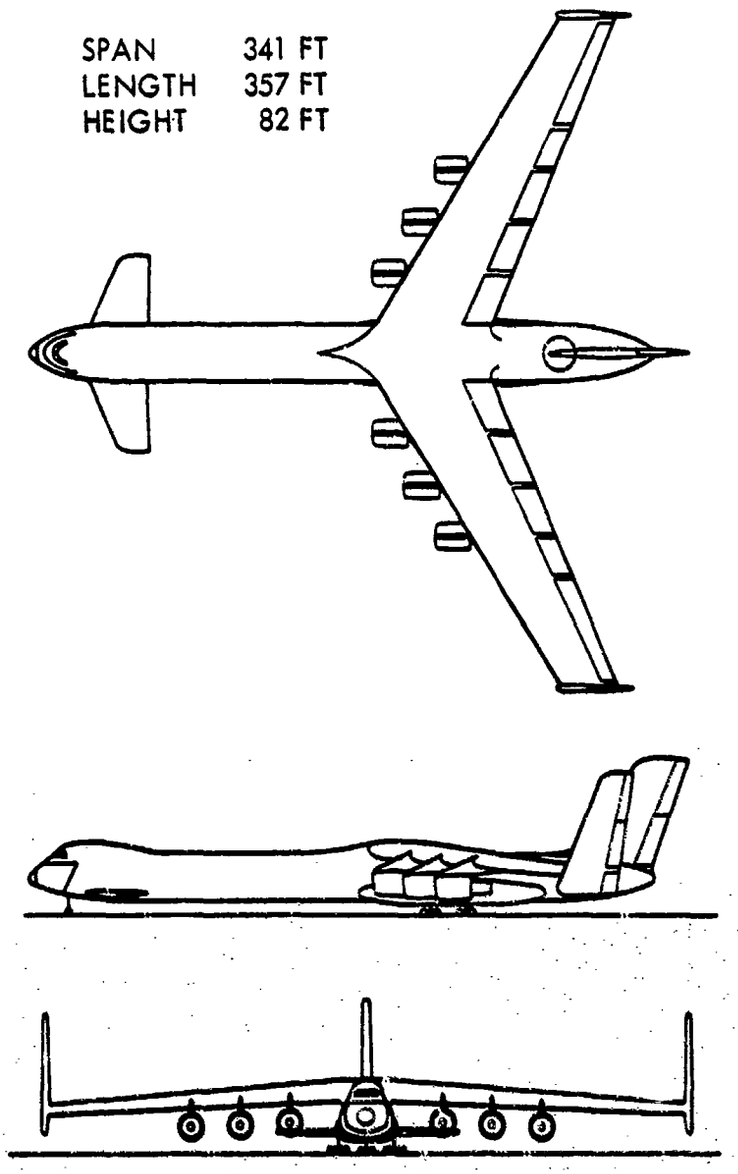

Figure 3-29. Refined Canard Configuration, 600,000-lb Payload

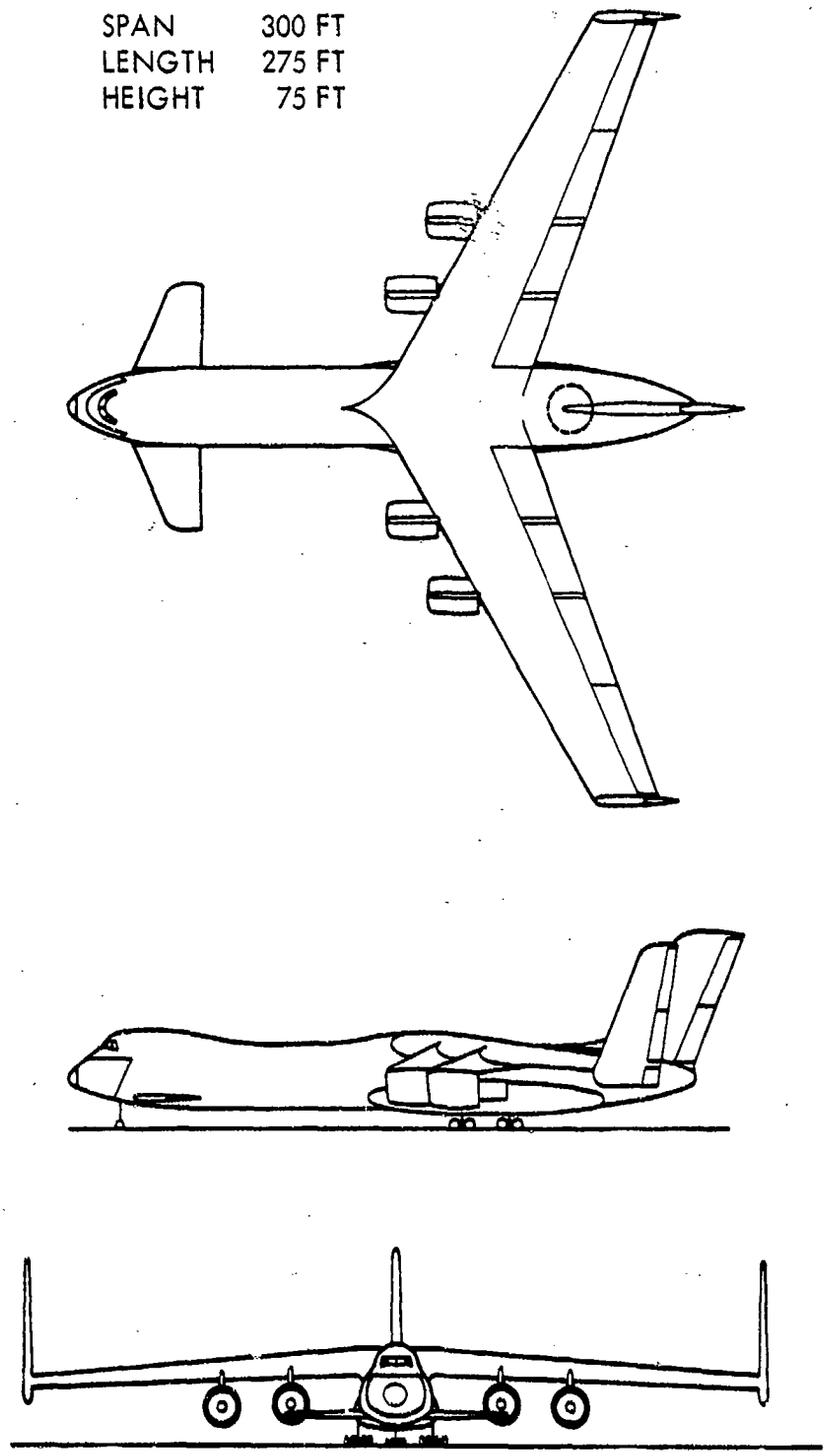

Figure 3-30. Refined Canard Configuration, 400,000-lb Payload

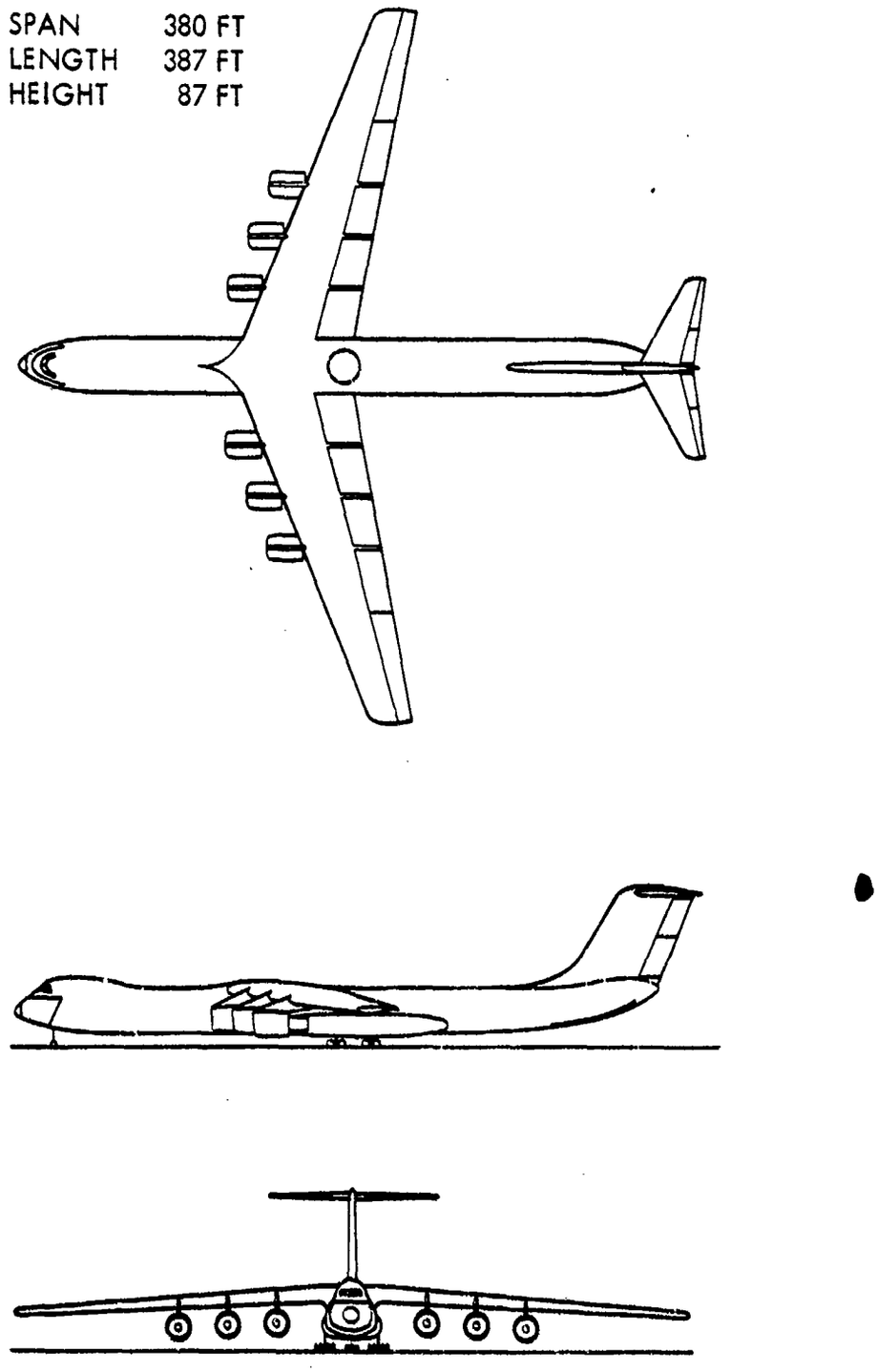

Figure 3-31. Refined Conventional Configuration, 600,000-lb Payload

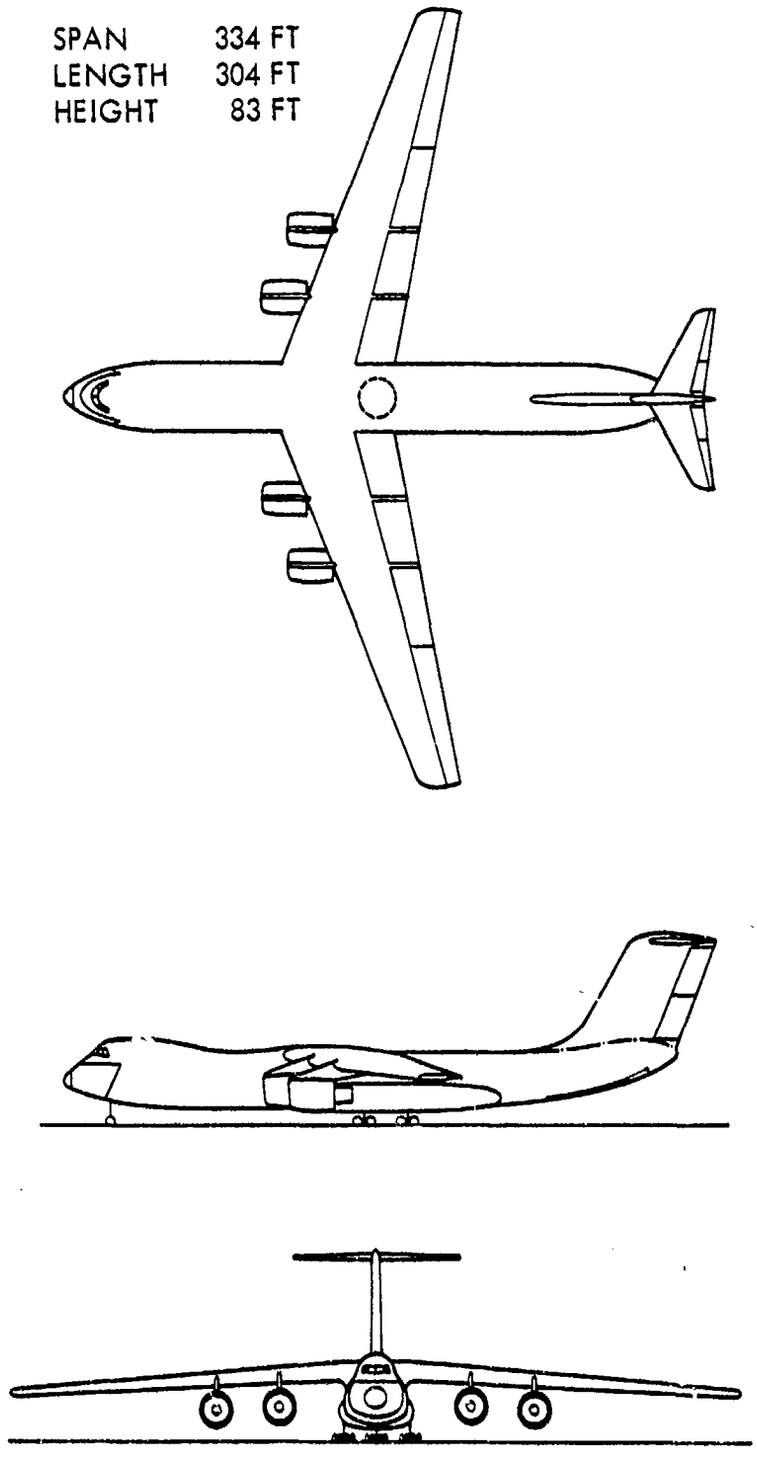

Figure 3-32. Refined Conventional Configuration, 400,000-lb Payload

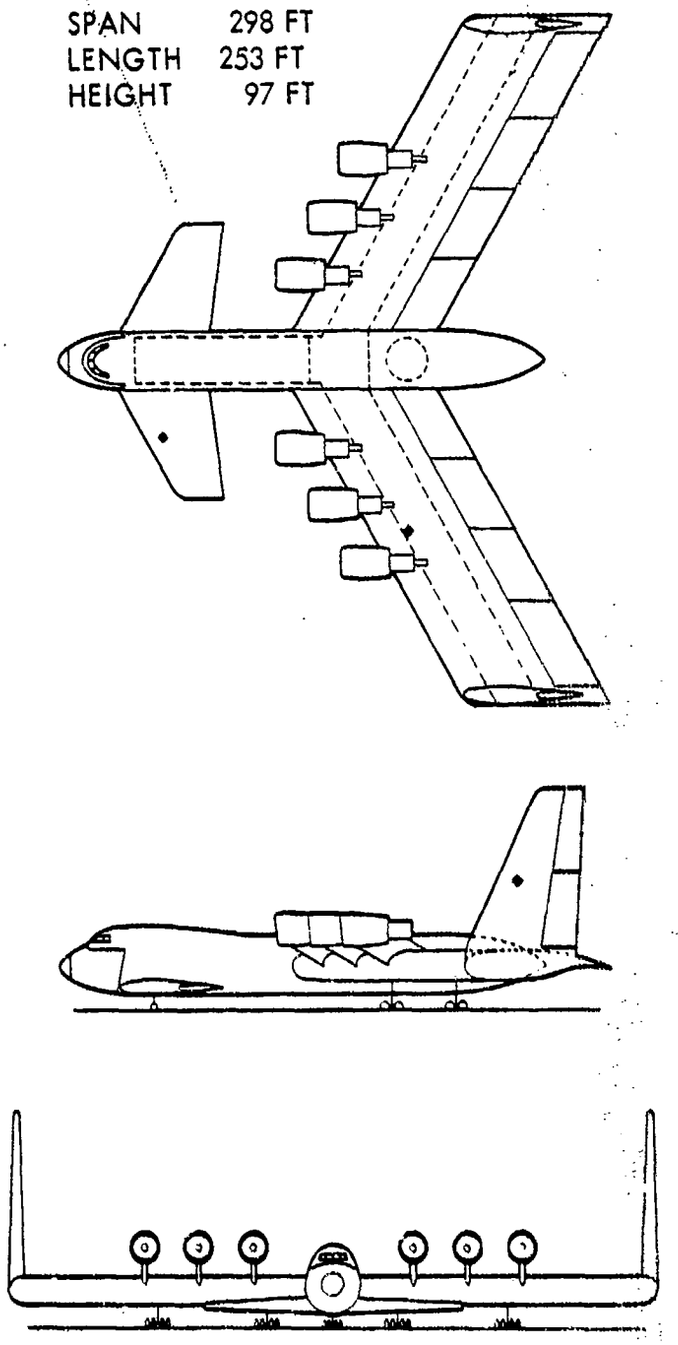

Figure 3-33. Refined Spanload Configuration, 600,000-lb Payload

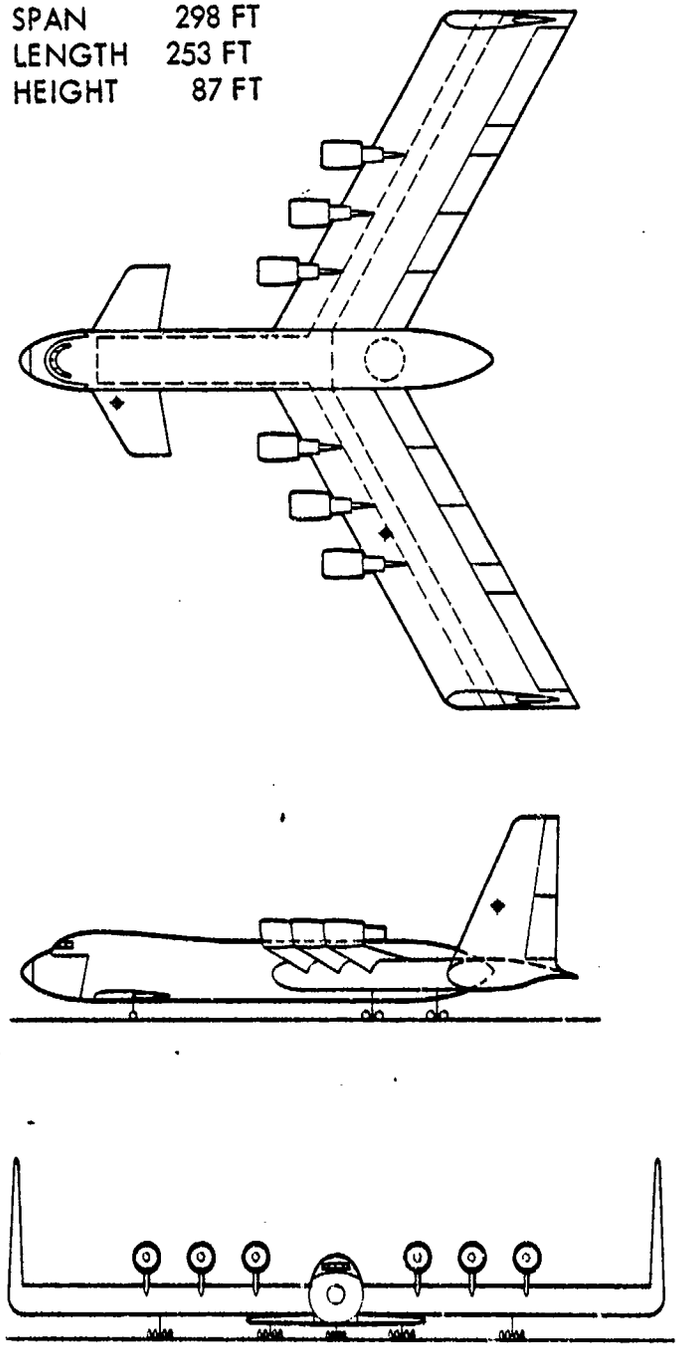

Figure 3-34. Refined Spanloader Configuration, 400,000-lb Payload

TABLE 3.12. WEIGHT SUMMARIES OF 600,000-LB PAYLOAD REFINED CONFIGURATIONS

Configuration	Conventional	Canard	Spanloader
Structure			
Wing	270,013	200,478	234,926
Horizontal Tail	11,811	11,299	15,384
Vertical Tail	9,496	16,473	12,802
Fuselage	180,917	162,861	90,525
Landing Gear	113,703	91,697	92,240
Nacelle & Pylon	36,029	33,643	37,644
Propulsion			
Engine Installed	130,235	120,503	135,670
Nuclear Subsystem	456,037	446,290	469,038
Engine HX & Ducts	164,640	201,064	190,249
Aux. Cooling	18,586	17,594	19,902
Fuel System	3,715	3,689	3,925
Systems & Equipment	63,816	62,651	65,879
Operating Weight	1,458,998	1,368,243	1,368,182
Payload	600,000	600,000	600,000
JP Fuel Weight	188,772	186,149	210,684
Ramp Weight	2,247,770	2,154,392	2,178,866

TABLE 3.13. WEIGHT SUMMARIES OF 400,000-LB PAYLOAD REFINED CONFIGURATIONS

Configuration	Conventional	Canard	Spanloader
Structure			
Wing	184,493	134,658	210,811
Horizontal Tail	7,931	7,622	11,640
Vertical Tail	8,048	12,403	11,264
Fuselage	122,548	106,842	82,276
Landing Gear	70,065	66,750	72,963
Nacelle & Pylon	26,234	24,456	27,164
Propulsion			
Engine Installed	95,651	88,337	93,416
Nuclear Subsystem	409,533	402,171	429,127
Engine HX & Ducts	114,564	124,699	143,246
Aux. Cooling	13,819	13,054	15,839
Fuel System	3,174	3,141	3,463
Systems & Equipment	50,089	48,876	56,936
Operating Weight	1,106,150	1,033,009	1,158,144
Payload	400,000	400,000	400,000
JP Fuel Weight	137,763	134,981	164,052
Ramp Weight	1,643,913	1,567,990	1,722,196

TABLE 3.14. CHARACTERISTICS OF 600,000-LB PAYLOAD REFINED CONFIGURATIONS

Configuration	Conventional	Canard	Spanloader
Wing Sweep, deg	20	30	30
Wing Loading, psf	129.0	120.0	105.1
Cruise Lift Coefficient	0.546	0.508	0.445
Aspect Ratio	8.50	6.70	4.45
L/D	22.04	22.24	19.69
Propulsion			
Reactor Size, MW	337	318	363
No. Engines	6	6	6
Engine Thrust, 1000 lb	91.4	84.9	94.3
Engine Design JP TIT, °F	1733	1722	1705
Areas, ft^2			
Wing	16,972	17,351	19,965
Vertical	2,260	5,025	5,082
Horizontal	2,014	1,925	2,977

TABLE 3.15. CHARACTERISTICS OF 400,000-LB PAYLOAD REFINED CONFIGURATIONS

Configuration	Conventional	Canard	Spanloader
Wing Sweep, deg	20	30	30
Wing Loading, psf	129.0	120.0	92.7
Cruise Lift Coefficient	0.546	0.508	0.392
Aspect Ratio	9.00	7.10	4.96
L/D	22.13	22.29	20.12
Propulsion			
Reactor Size, MW	246	231	284
No. Engines	4	4	6
Engine Thrust, 1000 lb	99.6	92.6	66.5
Engine Design JP TIT, ^{o}F	1731	1722	1645
Areas, ft^2			
Wing	12,409	12,634	17,916
Vertical	1,951	3,668	4,527
Horizontal	1,304	1,257	2,211

4.0 PROPULSION CYCLE ANALYSIS

Three propulsion cycle concepts were investigated to identify the minimum weight propulsion system. The three concepts, as shown schematically in Figure 4-1, were the open Brayton, closed Brayton, and Rankine cycles.

The open Brayton cycle has received the greatest attention in past studies and was, therefore, used as a base case against which the other two cycles were compared. These cycle comparisons were necessarily accomplished before the final study design point aircraft was selected. Therefore, a reference design point was selected at which comparisons were to be made. The reference case requirements are summarized in Table 4.1.

The nuclear propulsion system was sized to provide sufficient thrust for cruise plus a 300 fpm climb capability. The reason for the higher thrust requirement for "Single Mode Dedicated Engines" was to account for the additional drag of the dedicated chemical-fueled engines which were required. The NuERA II type of reactor was used as the reference system for the reasons stated earlier. Weight and volume were estimated by the COP-DS computer code for the criteria given in Section 3.2.3.1.

As shown in Figure 4-1, intermediate heat transfer loops were assumed for all propulsion cycles. With the intermediate heat transfer loops, the COP-DS results for NuERA nuclear subsystem weight and volume can be used directly for any of the propulsion cycle concepts.

In both closed cycles, essentially all of the reactor energy is transferred to the fan air stream. Part of the reactor power is input through the fan and the remaining reactor energy is transferred to the fan air flow through the precooler. Since both closed cycles have this characteristic, the air portion of the propulsion system may be investigated independent of the specific closed cycle, by assuming closed cycle efficiencies (fan power/input thermal power) and a precooler pressure loss ratio. There are interactions between the closed cycle and fan air, such as approach temperature difference limits

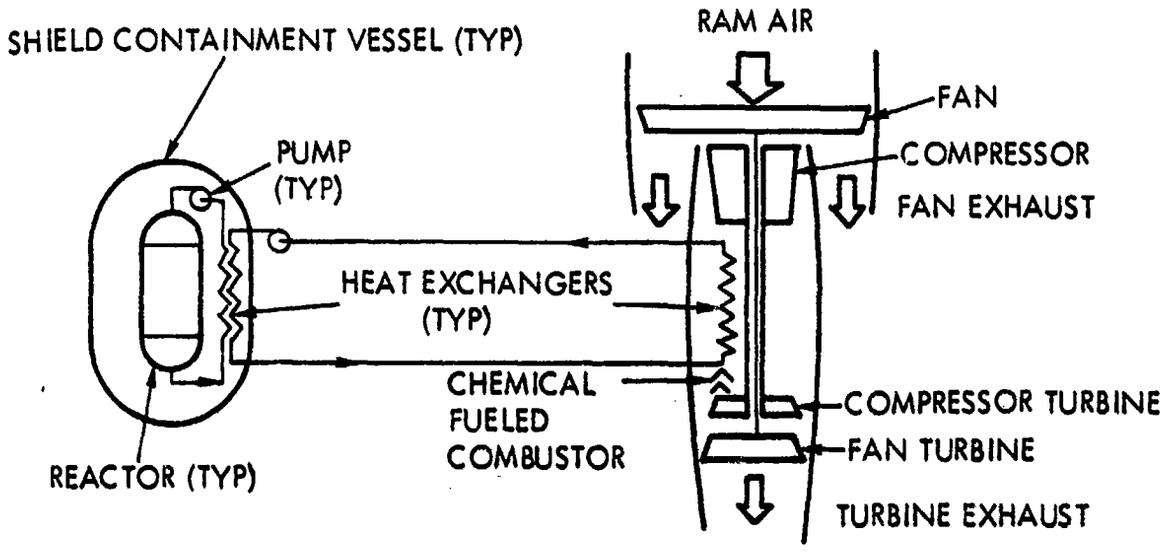

OPEN BRAYTON CYCLE

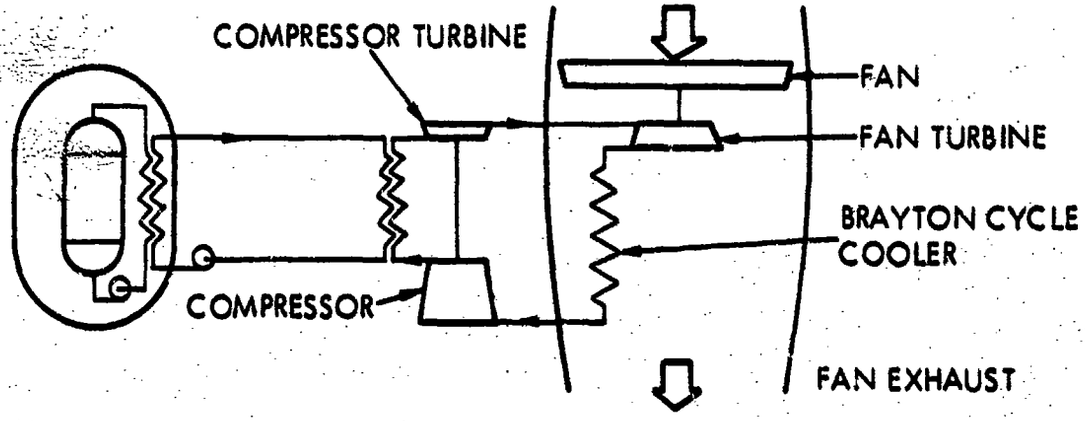

CLOSED BRAYTON CYCLE

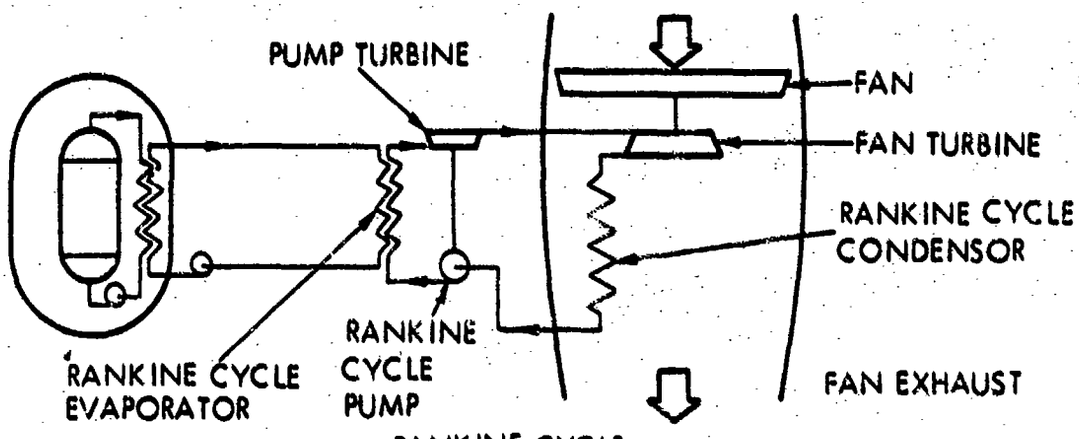

RANKINE CYCLE

Figure 4-1. Candidate Propulsion Cycle Schematics

TABLE 4.1. REFERENCE DATA FOR CYCLE COMPARISONS

Altitude	30,000 ft
Mach Number	0.75 Standard Day
Dual Mode Engines:	
• Number of Engines	6
• Cruise Thrust per Engine (net)	18,000 lb
Single Mode Dedicated Engines:	
• Number of Nuclear Engines	6
• Cruise Thrust per Engine (net)	22,000 lb
• Number of Chemical Engines	6
• Weight of Chemical Engine (each)	16,500 lb
Fan Efficiency	93%
Turbine Efficiency	93%
Compressor Efficiency	90%
NuERA II is the Reference Nuclear System	
• Impact Velocity	250 ft/sec
• Effective Full Power Hours	10,000
• Dose Rate (20-ft forward and aft of reactor center)	5 mr/hr
Piping (50-ft/engine)	300 ft

and condenser pinch-point temperature difference limits, but this type of initial scoping provides insight into the overall characteristics of the complete propulsion system.

The required thermal input power per engine to produce a cruise thrust of 22,000 lb with dedicated-mode engines is shown in Figure 4-2 as a function of the fan pressure ratio for several cycle efficiencies. The curves illustrate that high cycle efficiencies reduce the required reactor input thermal power, and thus, reactor weight. The curves also show

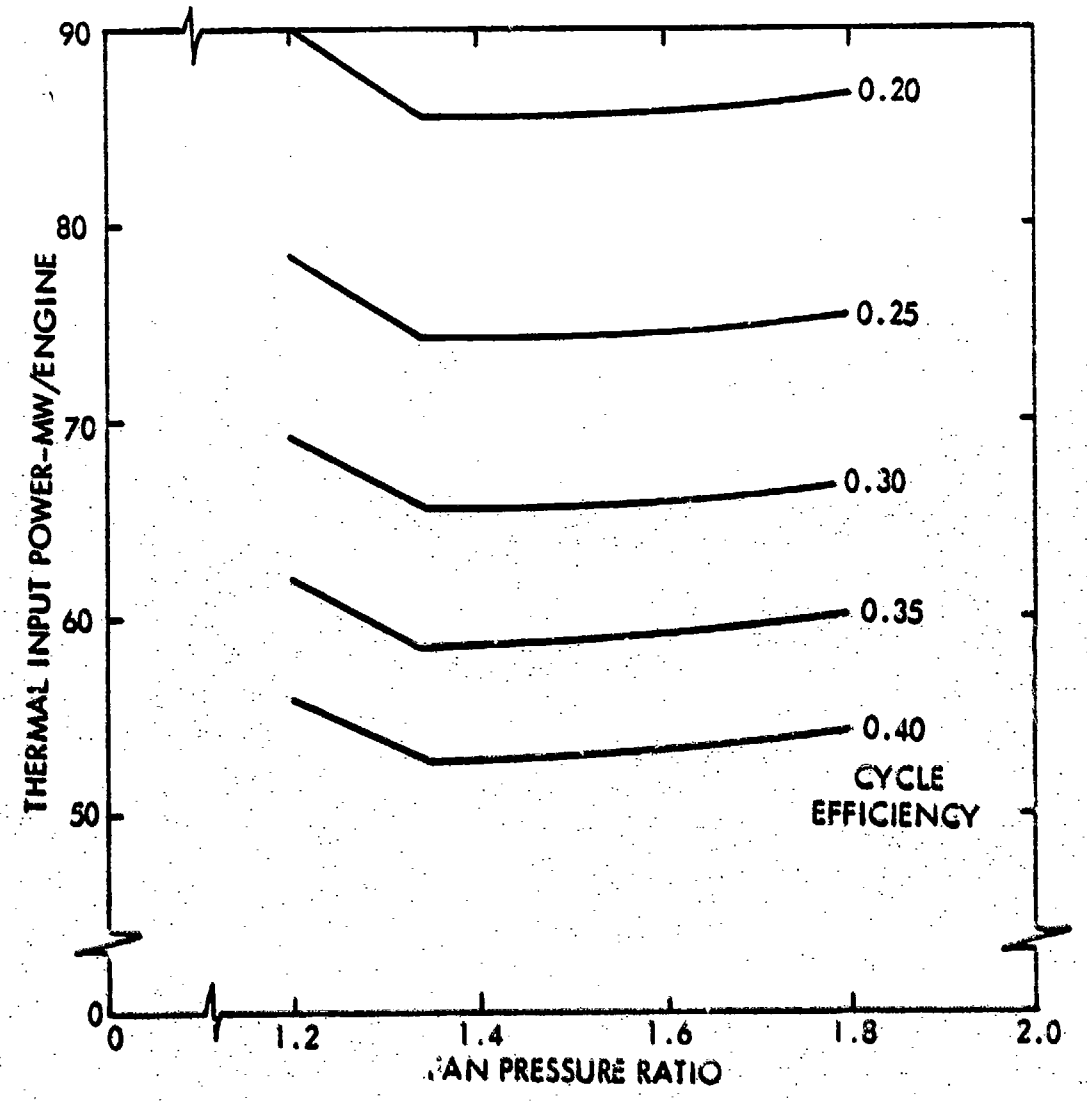

Figure 4-2. Engine Thermal Input Power Sizing.
(Engine Thrust = 22,000 lb)

that increasing the fan pressure ratio to the point where the fan nozzle velocity becomes sonic, reduces the required thermal power, and above that point, the thermal requirements increase slowly for a fixed cycle efficiency. However, as the fan pressure ratio is increased, the fan exit air temperature (sink temperature for the closed cycle) increases, which reduces cycle efficiency.

The fan air flow rate required to produce 22,000 lb of thrust is shown in Figure 4-3 as a function of fan pressure ratio. The fan air flow rate decreases with increasing fan pressure ratio, and higher efficiency cycles have greater air flow rates than lower efficiency cycles for a given fan pressure ratio. Over the range of fan pressure ratios

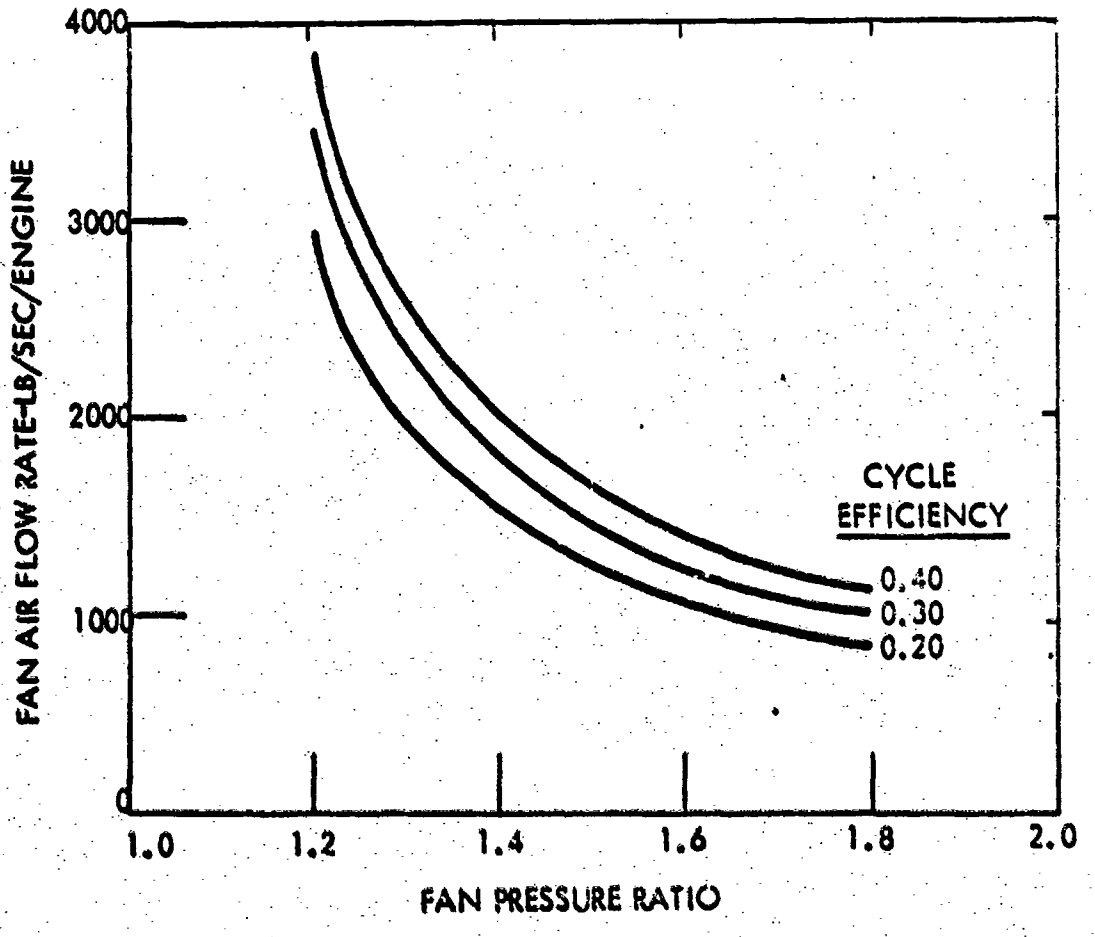

Figure 4-3. Fan Air Flow Rate Requirements. (Engine Thrust = 22,000 lb)

and cycle efficiencies, the fan power is relatively constant ($\pm$ 10%) for the fixed thrust requirement. Further, the fan, fan structure, and nacelle weight and size are proportional to air flow rate and are reduced as the fan pressure ratio is increased. Based on these two figures, the weight of the propulsion system will probably minimize at a fan pressure ratio greater than 1.4, barring approach temperature or pinch-point temperature difference limitations.

The transfer of the waste heat from the closed cycle into the fan air significantly reduces the reactor thermal power requirements. For example with a 30-percent closed cycle efficiency, if the waste heat from the cycle is not transferred to the air, the reactor thermal rating increases by 39 percent to produce the same thrust as an engine that does use the waste heat in the fan air.

4.1 PROPULSION COMPONENT SCALING RELATIONSHIPS

The NuERA II reactor system weight was shown previously in Figure 3-5 as a function of reactor thermal power. This reactor system weight includes the containment vessel and all components inside the containment (reactor, shield, pumps, valves, intermediate heat exchangers, etc.). The NuERA II system weight is quite linear between the thermal ratings of 200 to 750 MW. Since the range of interest in this application appears to be in the 200 to 500 MW rating, the following linear relationship was used to estimate the reactor system weight for cycle comparison

$$W_R = 285200 + 505\ (Q_R)$$

where W_R is in pounds and Q_R is the reactor thermal rating in megawatts.

The weight of the reactor system auxiliary components external to the containment vessel was estimated based on the relationships given in Appendix D.

$$W_T = 2000 + 80.9\ (Q_R)^{0.934}$$

The components included in the auxiliary weight are the shield cooling system, decay heat removal system, reactor instrumentation and control system, secondary pumps and motors.

The weight relationship of the fan rotor, stator, gear box and support structure used in this analysis is:

$$W_f = 4300 \left(\frac{W_{air}}{1100}\right)^{1.5} \left(\frac{P_f}{33,500}\right)^{1.5}$$

where W_f is in pounds, W_{air} is the air flow rate in lb/sec and P_f is the fan power in horsepower.

The nacelle weight penalty relationship, which is needed with the incorporation of the precooler in the nacelle, is:

$$W_n = 0.31\ D_n^2\ L_n$$

where W_n is in pounds, D_n is the nacelle diameter in feet and L_n is the additional nacelle length in feet.

In the closed Brayton cycle analysis, the helium compressor and turbine weight was estimated by:

$$W_c = 1.86 \cdot 10^{-4}\ (P_c)^{1.5}$$

where W_c is in pounds and P_c is the compressor horsepower. The helium power turbine weight relationship is:

$$W_p = 1.35 \cdot 10^{-4}\ (P_p)^{1.5}$$

where W_p is in pounds and P_p is the power turbine horsepower.

The weight of the liquid metal piping was calculated based on the equation given in Appendix D. The piping total length (L_p) was assumed to be 300 ft for the hot leg and also for the cold leg.

$$W_{pl} = \left(3.70\left(\frac{Q_R}{N_E}\right)^{0.628} + 2.94\left(\frac{Q_R}{N_E}\right)^{0.792}\right) 300$$

where W_{pl} is in pounds and N_E is the number of engines.

4.2 CLOSED BRAYTON CYCLES

In the closed Brayton cycles, helium is used as the working fluid since it is an inert gas and has good thermal properties. Mixtures of inert gases (Helium and Xenon) could be used without affecting heat exchanger volumes, but would reduce the number of compressor and turbine stages. However, the mixture of inert gases would not significantly affect powerplant weights and would increase the complexity of the systems required.

Figure 4-4 shows a schematic for the closed recuperated Brayton cycle. The helium working fluid is pressurized by the compressor, flows through the recuperator, where the helium is partially heated, and then flows to the engine heat exchanger where the helium is further heated to 1600°F. Next, the helium is expanded through the turbines which drive the compressor and air fan. After leaving the turbines, the helium flows through the recuperator to the pre-cooler where the reject heat is released to the fan air flow. Finally, the helium returns to the compressor.

In this Brayton cycle analysis, all heat exchangers were assumed to be counterflow shell and tube type. The parameters which were varied to obtain a minimum weight powerplant for specified thrust included: fan pressure ratio, helium compressor pressure ratio, heat exchanger length, Reynolds number, and tube spacing. Both axially-finned and bare tube precoolers were investigated. The overall efficiency of this cycle is sensitive to the pressure drop in the fan discharge air stream. Since the fin surfaces have a fin efficiency less than unity, more total surface area and a larger air-side

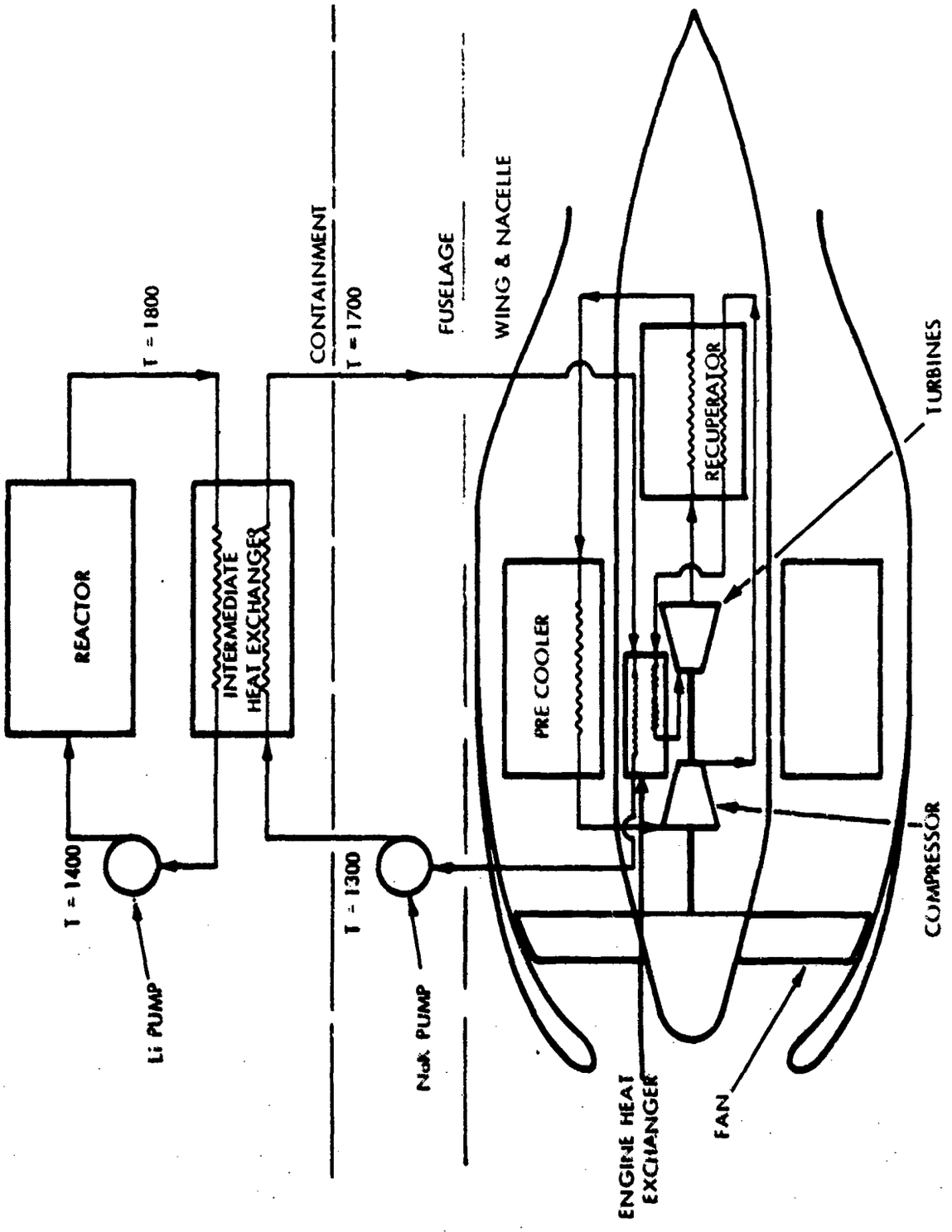

Figure 4-4. Closed Recuperated Brayton Cycle Schematic

pressure drop are required with finned surfaces than with bare tubes. Also, bare tubes have the advantage that all of the surface area is effective in maximizing the heat transfer per unit area or per unit pressure drop. These factors were responsible for the bare tube configuration producing the lighter weight powerplant.

The weight comparison of the base open Brayton and recuperated closed Brayton powerplants is shown on Table 4.2. The engine state points are shown on Table 4.3 for the recuperated closed Brayton cycle.

Figure 4-5 shows the schematic for the closed non-recuperated Brayton cycle. In this concept, the helium turbine and compressor were assumed to be located in the aircraft fuselage. This allowed relatively low pressure and temperature helium to be piped to the individual power turbines. The helium, after expansion in the power turbines, is cooled in the precoolers by the fan air and then returned to the compressors. The temperature of the returning helium is less than 120°F, so that with concentric piping runs, insulation of the pipe lines is not required except for a stagnant gas gap liner in the inner hot pipe. Although the non-recuperated Brayton cycle is not as thermally efficient as the recuperated cycle, the total powerplant weight is slightly less than the recuperated cycle. The weight breakdown is shown in Table 4.2 and the state points are listed in Table 4.4.

Since both types of closed Brayton systems with dedicated engines produce more thrust per pound of powerplant weight than the base open cycle, a dual-mode non-recuperated Brayton system was investigated. Using the dual-mode concept, the engine thrust requirement was reduced from 22,000 to 18,000 lb and the requirement for the six chemical engines was dropped, thereby saving the 99,000 lb for chemical engine weight. A conceptual layout of a dual-mode non-recuperated Brayton engine is shown in Figure 4-6. In the comparison in Table 4.2 of open and closed Brayton dual-mode engines, the calculated powerplant weight of the closed cycle is about 7 percent less than the open cycle. However, the confidence in the weight estimate for the dual-mode closed Brayton system is not on the level of that of the open Brayton system because the closed system has not been studied as much as the open cycle system.

TABLE 4.2. BRAYTON CYCLE WEIGHT COMPARISONS (10^3 LB)

	Base Case Open Brayton (Dual Mode)	Recup. Closed Brayton (Dedicated)	Non-Recup. Closed Brayton (Dedicated)	Non-Recup. Closed Brayton (Dual Mode)
NSS	462	477	499	460
Engine HX	77	3	3	3
Precooler/Condenser	---	22	24	20
Recuperator	---	22	---	---
Piping	36	39	16	15
Auxiliaries	21	25	25	21
Chem. Engines	---	99	99	---
Fan, Gears, Struct.	---	35	29	---
Turbs. and Comps.	---	13	28	17
Engines w/o HX	109	---	---	116
Nacelle Penalty	---	6	6	5
Total	705	741	729	657

TABLE 4.3. CLOSED RECUPERATED BRAYTON CYCLE STATE POINTS

		Temperature °F	Pressure psia	Flow Rate lb/sec/engine
Compressor	Inlet	124	621	73.7
	Outlet	404	1523	---
Cycle Turbine	Inlet	1600	1499	73.7
	Outlet	1320	1010	---
Power Turbine	Inlet	1320	1010	73.7
	Outlet	1048	644	---
Recuperator				
• LP	Inlet	1048	644	73.7
	Outlet	507	627	---
• HP	Inlet	404	1522	73.7
	Outlet	945	1511	---
Pre Cooler				
• Helium Side	Inlet	507	626	73.7
	Outlet	124	623	---
• Air Side	Inlet	78	10.76	1290
	Outlet	192	10.32	---
Engine Heat Exchanger				
• Helium Side	Inlet	945	1510	73.7
	Outlet	1600	1500	---
• NaK Side	Inlet	1700	130	713
	Outlet	1300	102	---
Fan	Inlet	-2	6.34	1290
	Outlet	78	10.76	---

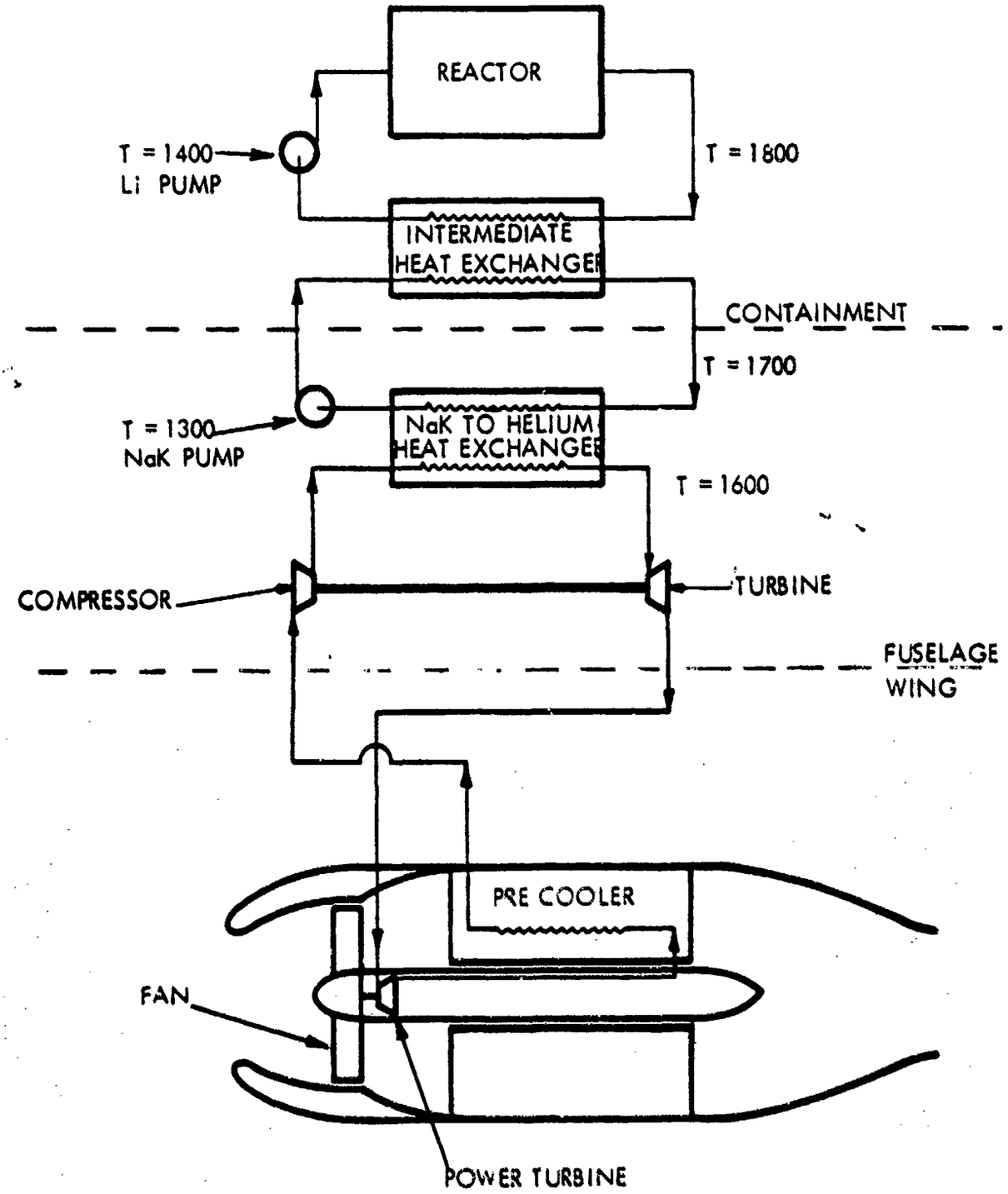

Figure 4-5. Closed Non-Recuperated Brayton Cycle Schematic

TABLE 4.4. CLOSED NON-RECUPERATED BRAYTON CYCLE STATE POINTS

		Temperature °F	Pressure psia	Flow Rate lb/sec/engine
Compressor	Inlet	117	323	56.6
	Outlet	646	1511	---
Cycle Turbine	Inlet	1600	1499	56.6
	Outlet	1071	647	---
Power Turbine	Inlet	1071	646	56.6
	Outlet	742	327	---
Pre-Cooler				
• Helium	Inlet	742	327	56.6
	Outlet	117	324	---
• Air	Inlet	77	10.68	1214
	Outlet	228	10.30	---
Engine Heat Exchanger				
• Helium	Inlet	646	1510	56.6
	Outlet	1600	1500	---
• NaK	Inlet	1700	130	797
	Outlet	1300	102	---
Fan	Inlet	-2	6.34	1214
	Outlet	77	10.68	---

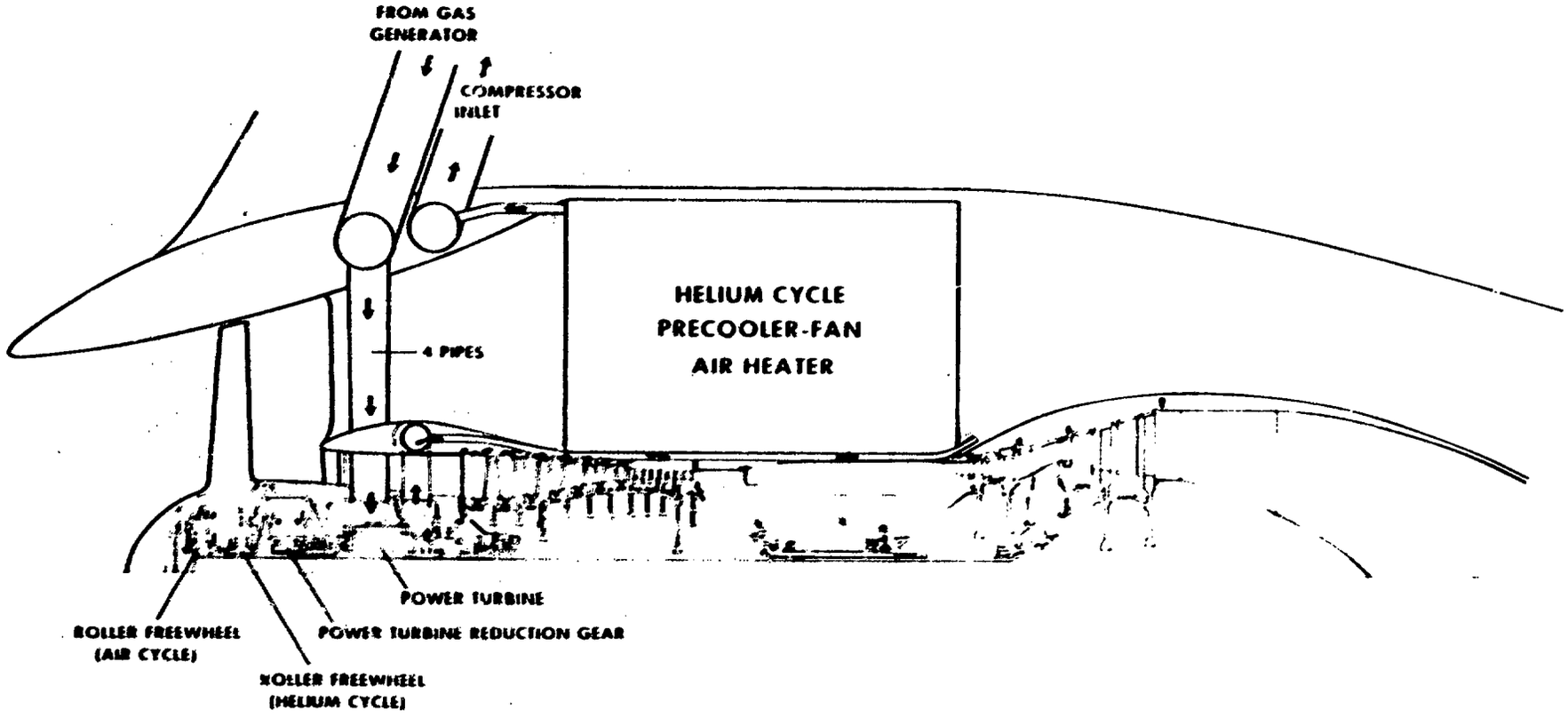

Figure 4-6. Dual Mode Closed Non-Recuperated Brayton Engine Concept

Future studies on the closed Brayton dual-mode system are recommended to increase the confidence of the weight estimate due to its potential advantages over the open cycle system. These advantages include low temperature helium piping in place of high temperature liquid metal piping. Since the fan is driven by an air turbine on takeoff and a helium turbine at cruise, both can be optimized for their particular function in the closed cycle dual-mode system while the design of the open Brayton system requires a compromise between cruise and takeoff performance.

4.3 RANKINE CYCLES

The Rankine cycle propulsion system considered for this application is a simple cycle and system with no feedwater heating, reheating, or moisture removal from the turbine. The steam Rankine cycle is schematically shown in Figure 4-7. Since the Rankine cycle rejects the waste heat through condensers to the fan air flow, the condensing temperature must be sufficient to allow reasonably-sized condensers to be placed in the nacelles.

Figure 4-8 is a typical temperature-entropy diagram which shows the condenser pinch-point temperature difference and the approach temperature difference for the steam Rankine system. With a fixed condensing temperature, increasing the fan pressure ratio increases the fan exit air temperature. This decreases the approach temperature difference, reduces the air flow rate for the fixed thrust requirement, and increases the slope of the air temperature curve to produce a reduction in the pinch-point temperature difference. Therefore, the minimum weight Rankine cycle propulsion system will have a relatively low fan pressure ratio between 1.3 and 1.5.

The thermal input power per engine requirements for various fan pressure ratio values are shown in Figure 4-9 for two different approach temperature difference values. This figure shows that by increasing the approach temperature difference the required reactor thermal power increases and that the higher fan pressure ratios encounter pinch-point temperature difference limits.

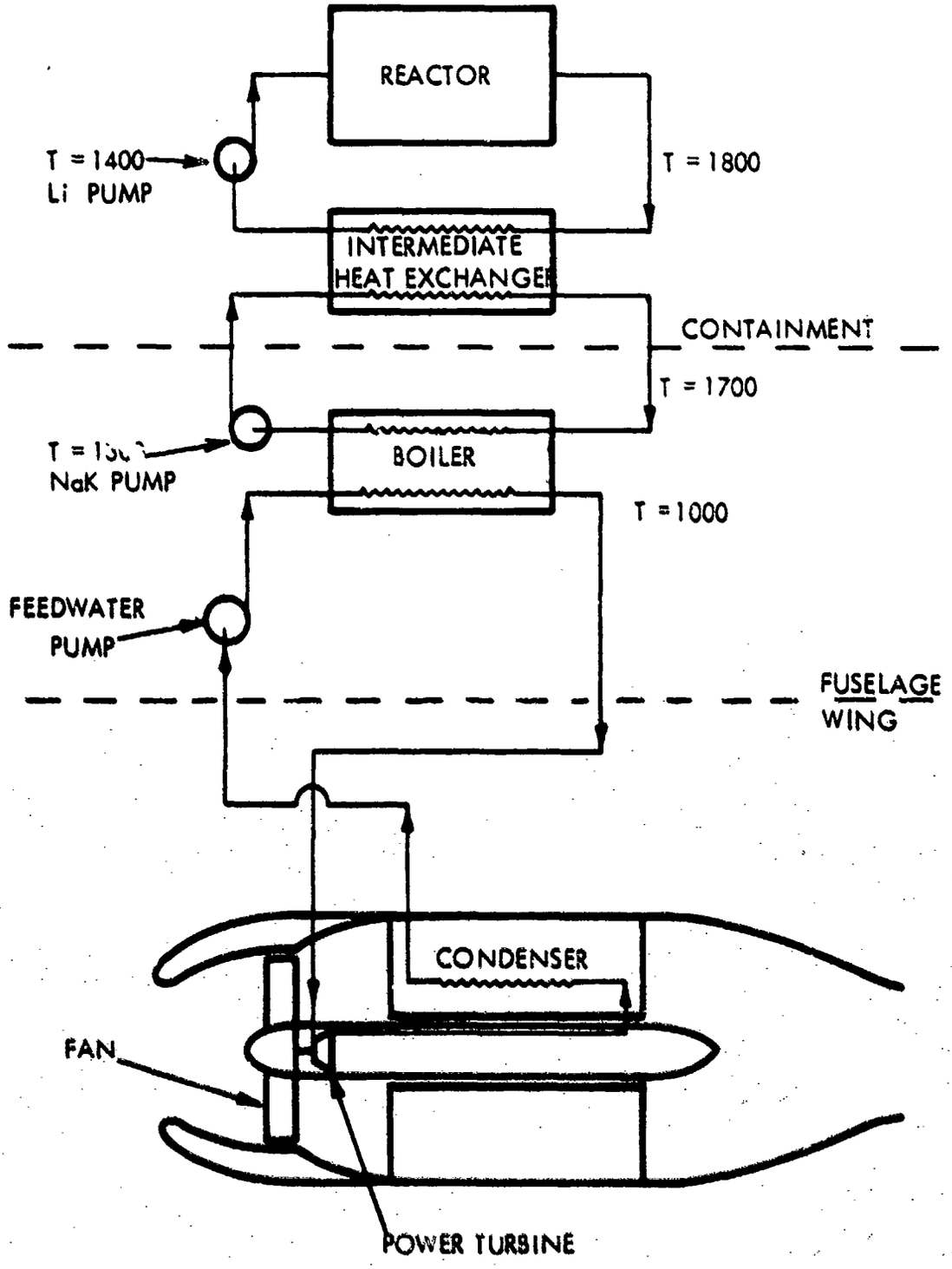

Figure 4-7. Steam Rankine Cycle Schematic

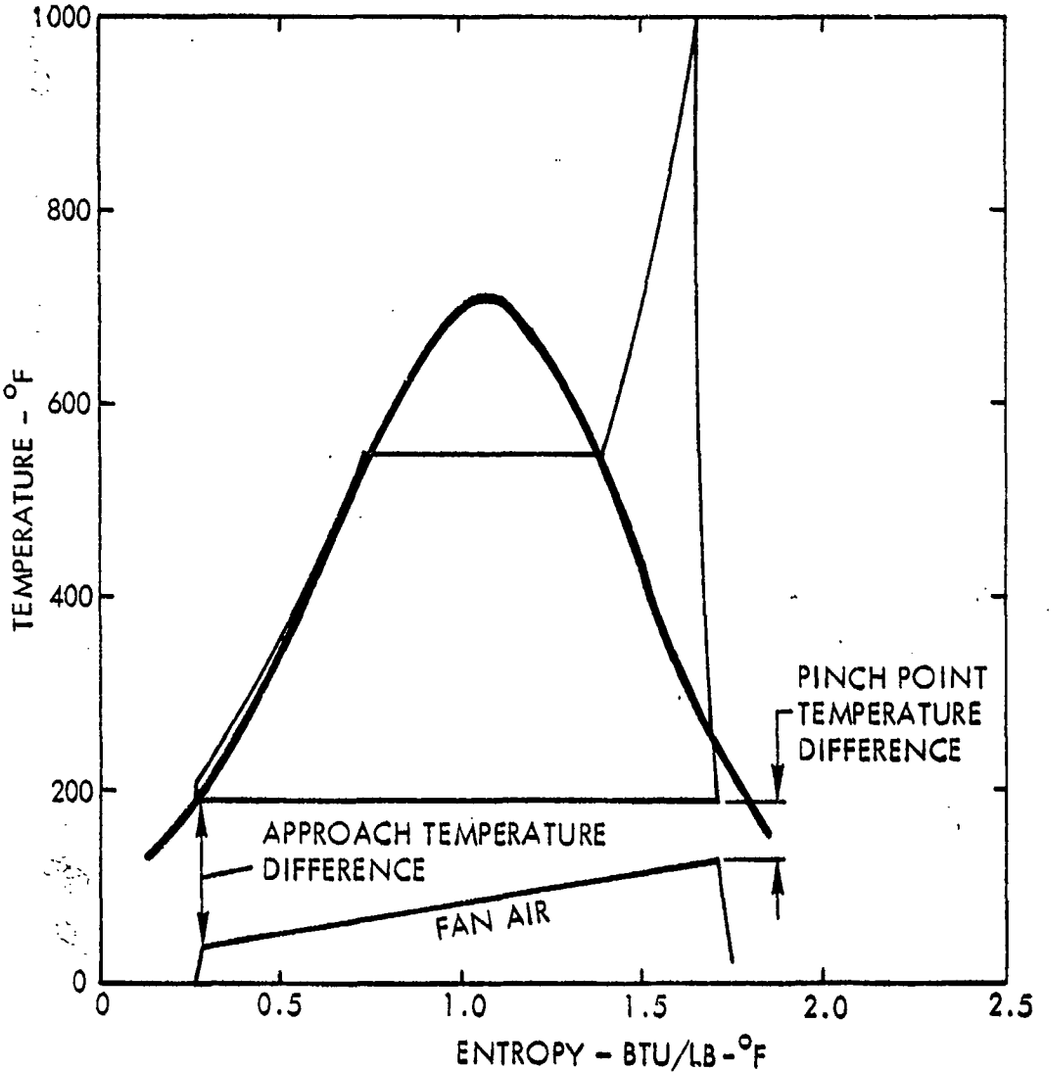

Figure 4-8. Steam Rankine Propulsion Temperature - Entropy Diagram

The corresponding values of propulsion system weight are shown in Figure 4-10. Both approach temperature difference values produce about the same minimum propulsion system weights (~950,000 lb). Approach temperature difference values above 225°F were investigated but required significantly more thermal energy and an increased reactor weight. The 150°F approach temperature difference was judged to be about the minimum,

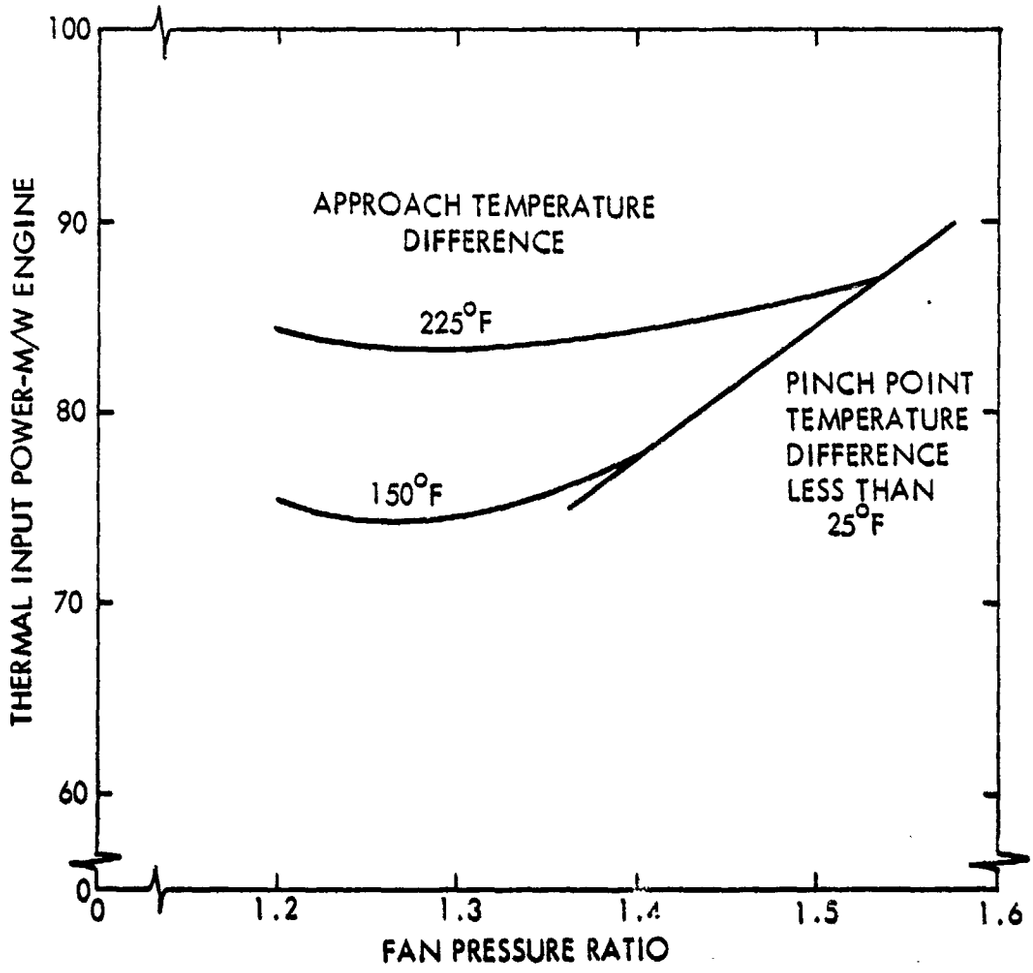

Figure 4-9. Engine Thermal Input Power Sizing for Steam Rankine Cycle

since lower values would require fan pressure ratios less than 1.3 and would increase propulsion system weight. These analyses were based on steam turbine inlet temperatures of 1000°F. A turbine inlet temperature of 1600°F was also investigated to determine if a very optimistic turbine temperature would make this cycle attractive. The weight of the 1600°F turbine inlet temperature system was estimated to be 908,000 lb, which is significantly above the base Brayton open cycle propulsion weight of 705,000 lb.

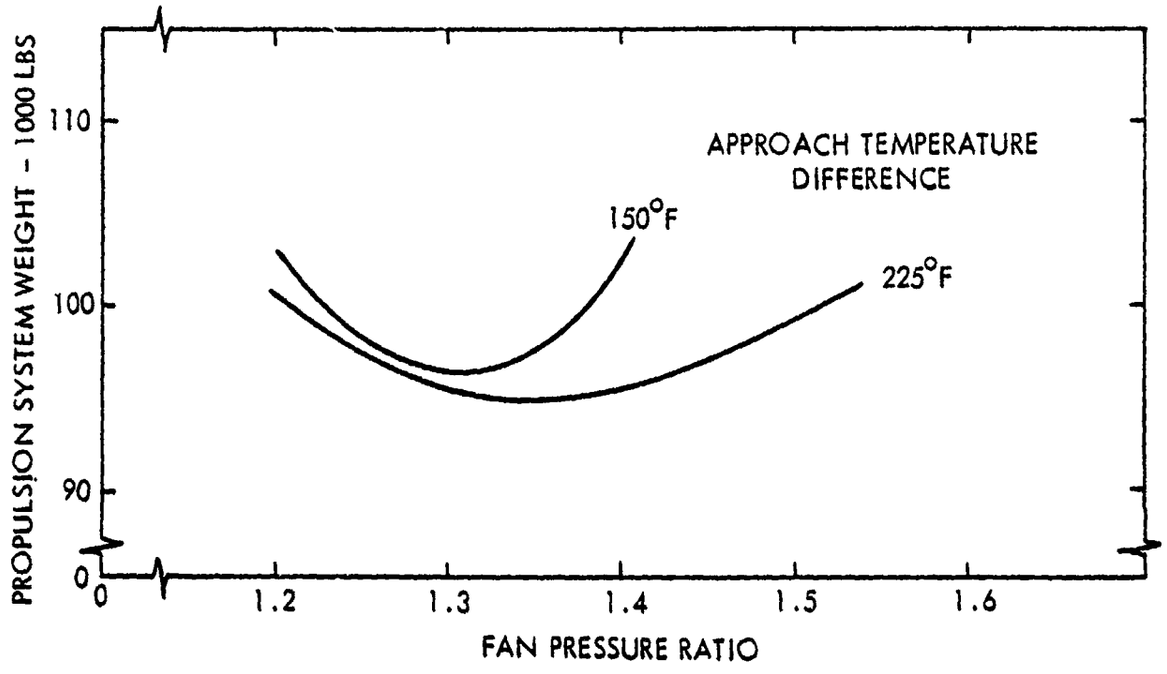

Figure 4-10. Steam Rankine Cycle Propulsion Weight

The use of steam for this application (even with the relatively high condensing temperature) requires large turbine exhaust areas and therefore large heavy turbines. A search was made for fluids which would have higher saturation pressures at these condensing temperatures and thus low turbine exhaust areas. Several were found which required exhaust areas less than 20 percent of that required for steam. Three of these fluids - ammonia, cyanogen, and sulfur dioxide - appeared attractive for this application. They are nominally stable to temperatures above 1000°F, are common industrial chemicals, are available in quantity, and are relatively inexpensive. Furthermore, they have low freezing temperatures (cyanogen at -30°F and the other two below -100°F). Since the Rankine fluid is heated in a liquid metal heater, it must be compatible with liquid metal. Compatibility with liquid metal means that the fluid will not react in a catastrophic manner if a leak occurs. With sulfur dioxide (SO_2) and sodium (Na), the products are solids up to temperatures above 2100°F (Na_2O sublimes at 2327°F and Na_2S melts at 2156°F). Therefore at normal operating temperatures, if a leak occurs, no gas will evolve

and only unreacted SO_2 will be gaseous. Since the three fluids will produce about the same powerplant weight, only SO_2 was selected for further analysis in the Rankine cycle.

With the SO_2 Rankine cycle, the fluid is heated supercritically without a phase change, thereby reducing the complexity of the heater as compared to steam. The fluid is expanded in the turbine as before, but now the expansion ends in the superheated region. This allows either recuperation or higher fan pressure ratios (see Figure 4-11) due to shifts of the

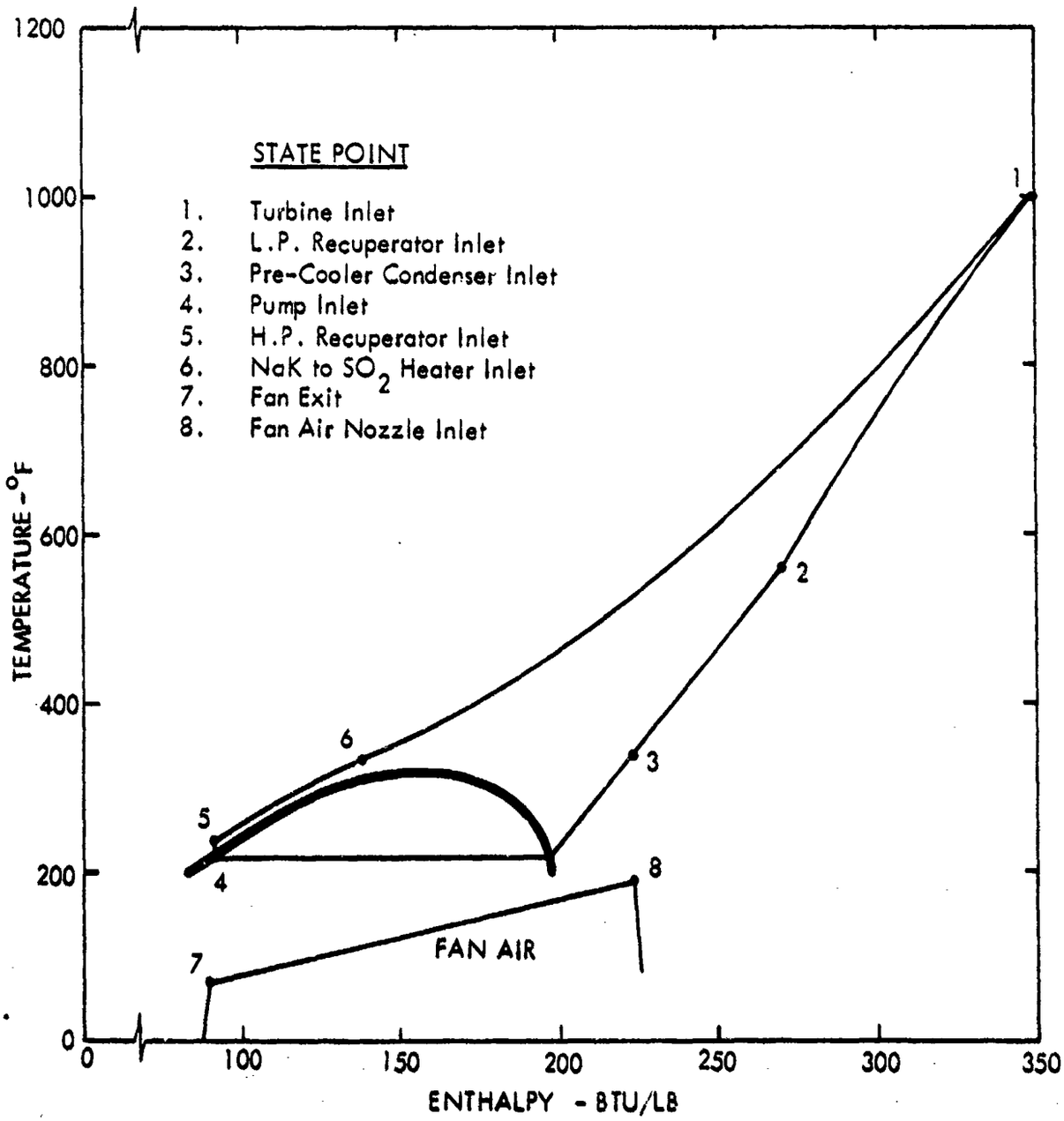

Figure 4-11. Sulfur Dioxide Recuperated Rankine Cycle Temperature - Enthalpy Diagram

pinch-point temperature difference toward the center of the condenser/precooler.

The required thermal input power per engine and the system weights are shown in Figures 4-12 and 4-13 for both the recuperated and non-recuperated sulfur dioxide Rankine cycles for variations in fan pressure ratio. The propulsion system weights of the various Rankine cycles and the open Brayton cycle are compared in Table 4.5. The Rankine cycle propulsion system weights are about 18 percent heavier than the open Brayton cycle propulsion system.

The comparison of the open Brayton, closed Brayton and Rankine cycle propulsion systems weights are affected by the ground rules and assumptions used. For example, since no

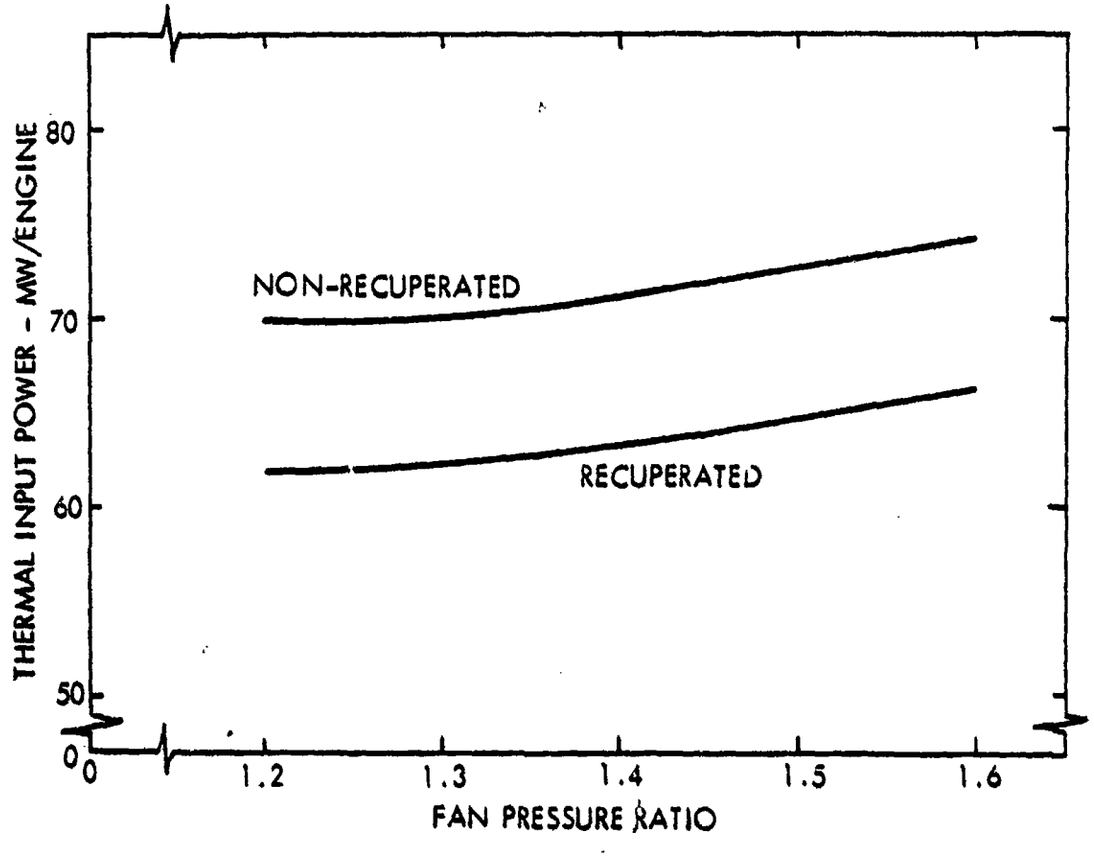

Figure 4-12. Sulfur Dioxide Cycle Engine Thermal Input Power Sizing

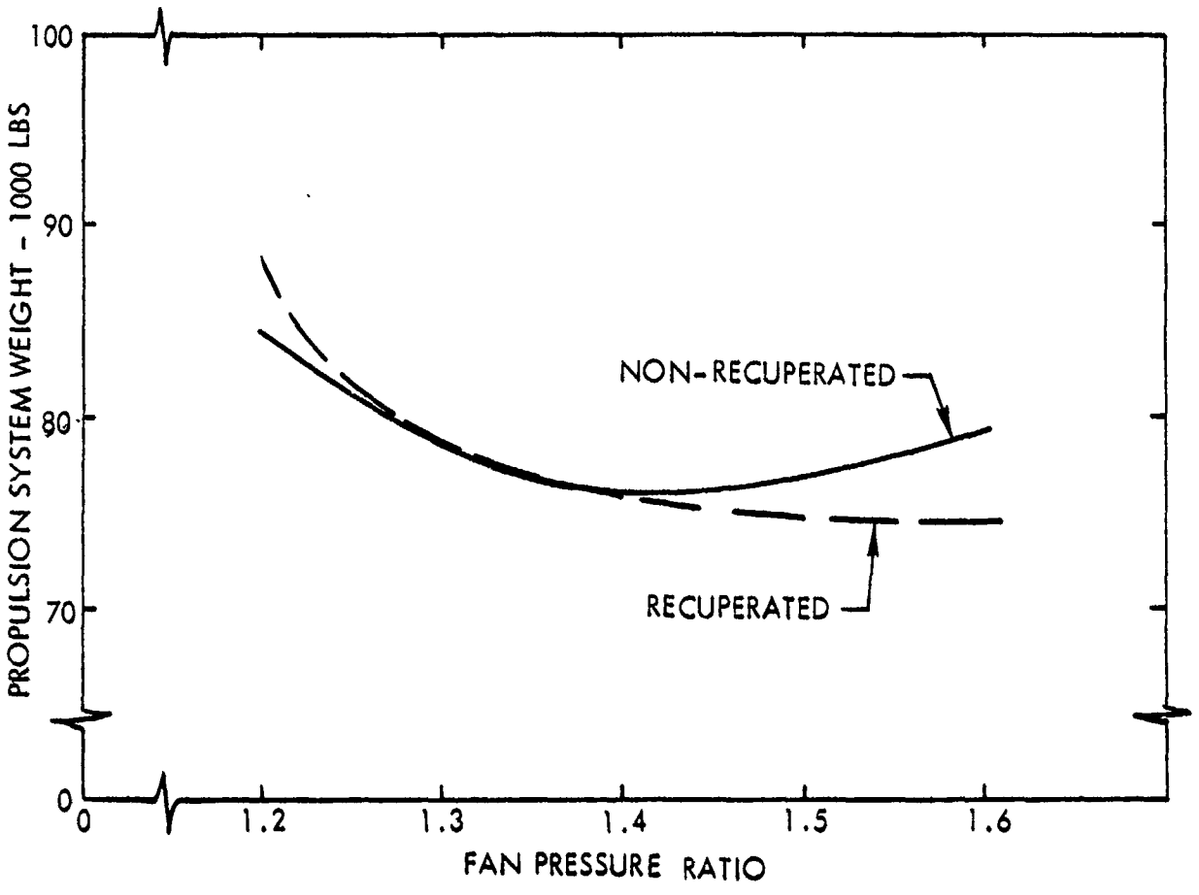

Figure 4-13. Sulfur Dioxide Rankine Cycle Propulsion Weight

specific airframe configuration was used in this comparison, a total piping run of 300 ft was assumed for an average of 50 ft per engine. If a specific airframe requires a piping run of 100 ft per engine, the base open Brayton propulsion system weight would increase by 36,000 lb to a total of 741,000 lb. Correspondingly, only about 7000 lb would be added to the non-recuperated closed Brayton propulsion systems to produce a total weight of 731,000 lb for the dedicated-mode and 662,000 lb for the dual-mode system. Therefore, the integration of the propulsion plant and a specific aircraft configuration may affect the choice of the type of propulsion plant for an optimum aircraft system.

TABLE 4.5. RANKINE CYCLE WEIGHT COMPARISONS (10^3 LB)

	Base Case Open Brayton (Dual Mode)	Steam Rankine (Dedicated)	SO_2 Rankine (Dedicated)	SO_2 Recuperated Rankine (Dedicated)
NSS	462	538	504	489
Engine HX	77	73	63	53
Condenser/Precooler	---	52	48	61
Recuperator	---	---	---	6
Piping	36	18	15	16
Auxiliaries	21	29	25	24
Chem. Engines	---	99	99	99
Fan, Gears, Struct.	---	58	51	35
Turbines and Pumps	---	51	10	11
Engines w/o HX	109	---	---	---
Nacelle Penalty	---	20	24	27
[illegible]	705	938	839	821

4.4 SUMMARY OF COMPARISONS

Comparative total propulsion system weights are shown on Tables 4.2 and 4.5 The only alternative which is lighter in weight than the base case open Brayton cycle is the non-recuperated closed Brayton cycle dual-mode engine. However, the difference in weight was judged to be insufficient in view of its limited data base to warrant its selection for use in the reference aircraft of this study. The open Brayton cycle was selected for use as the base system in the reference aircraft because the more extensive study base for this cycle gives it a greater degree of certainty and acceptability.

It is recommended that future studies be accomplished to confirm, and quantify with more certainty, the characteristics of the non-recuperated closed Brayton dual-mode engine. The investigations of this study have been sufficient to show that such a propulsion system is potentially very attractive from weight considerations. In addition there are several other attractive characteristics of such a system. Among these are:

- All of the piping in the wings is at relatively low temperature (on the order of 200°F or less as opposed to 1700°F for the hot liquid metal pipe of the open Brayton system). This characteristic would greatly simplify the wing piping design.
- The piping in the wings contains only inert gas rather than liquid metal.
- In the dual-mode closed Brayton system the chemically-fueled engines operate only on chemical fuel. Therefore, the engines can be optimized for the turbine inlet temperatures achievable with chemical fuel without having to be degraded to also allow operation at the lower turbine inlet temperature associated with nuclear operation.
- The closed Brayton power conversion system is highly adaptable to alternative thrustors. This study has been accomplished assuming the use of a ducted fan propulsor. The closed Brayton power conversion system could alternatively be used to drive a "Prop-Fan."

- The closed Brayton system is compatible with a direct cycle gas cooled reactor.

The Rankine cycle systems do not appear to be competitive from a weight standpoint.

5.0 REFERENCE AIRCRAFT DESIGN

A reference mission was defined by the Air Force during the study for use in developing a reference aircraft design. The reference mission specifications were:

- Payload: 400,000 lb
- Field Length: 10,000 ft
- Recovery Range: 1000 n.m.

The canard aircraft selected in the preceding parametric study was used as the basic configuration for the reference aircraft. Additional parametric studies were performed to develop that basic configuration into an optimized aircraft design for the reference mission.

5.1 DESIGN DEVELOPMENT

Parametric studies were conducted to re-evaluate the effects of cruise altitude and engine bypass ratio on the reference aircraft. The 30-deg sweep angle and cruise Mach number of 0.75 for the selected basic configuration were retained for these studies.

Figures 5-1 to 5-3 show the variations in aircraft wing loading and ramp weight for a matrix of engine bypass ratio and TIT values at altitudes of 26,000, 31,000 and 36,000 feet. Each of the matrix points on these figures represent minimum weight aircraft with a 10,000-ft field length capability for the two specified matrix values. The ramp weight value for each of these matrix points was determined parametrically following the same procedure discussed in Section 3.4.2 for the canard configuration and illustrated in Figure 3-14.

The study approach speed limit of 140 kts resulted in a wing loading limit of 120 psf for this particular configuration. The projection of the wing loading limit to the ramp weight graph established a curve for determining the minimum weight point. The minimum weight values for each altitude were plotted in Figure 5-4, from which it is evident that 31,000 ft is the optimum altitude.

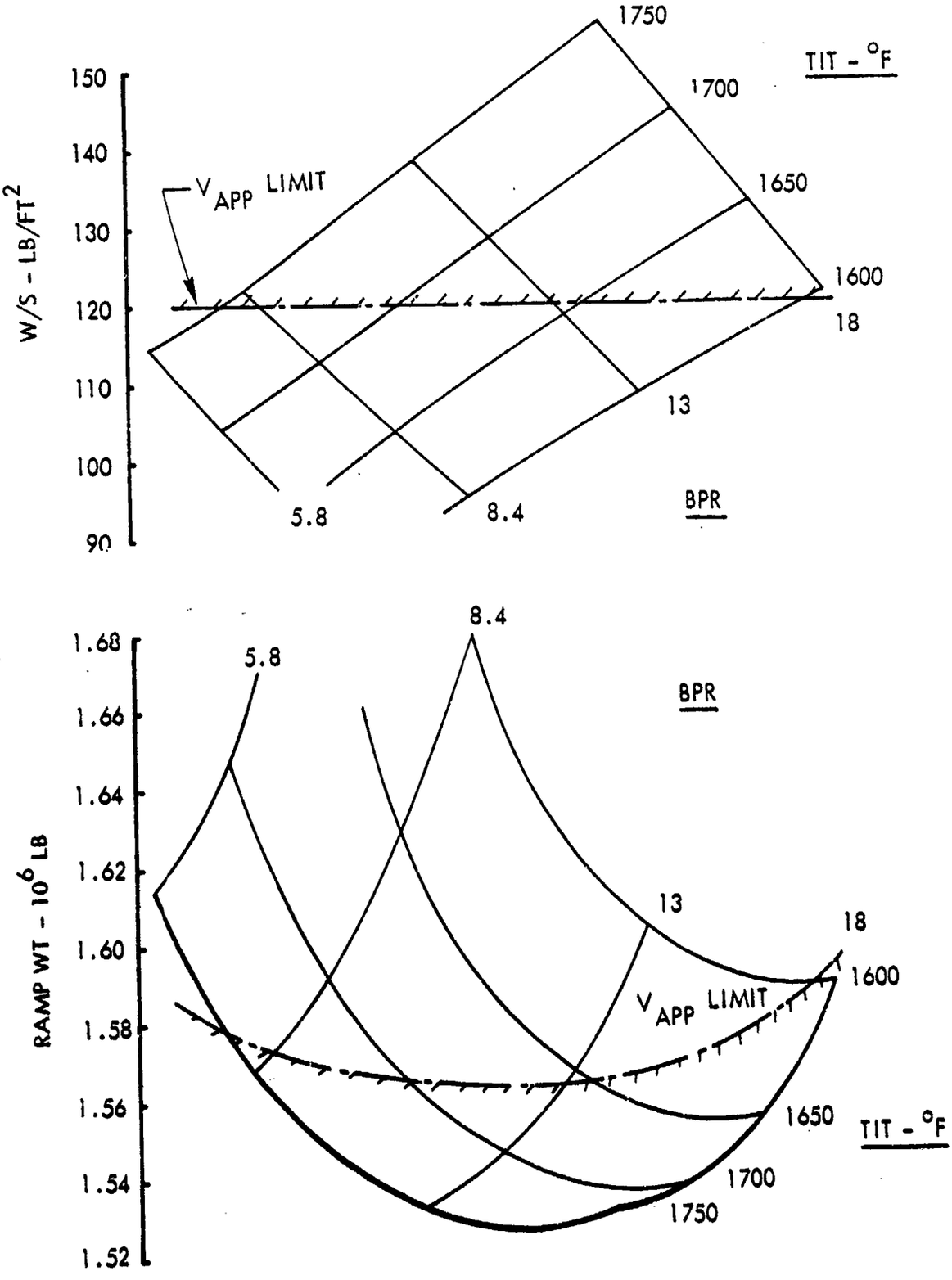

Figure 5-1. Reference Aircraft Parametric Data, 26,000-ft Altitude

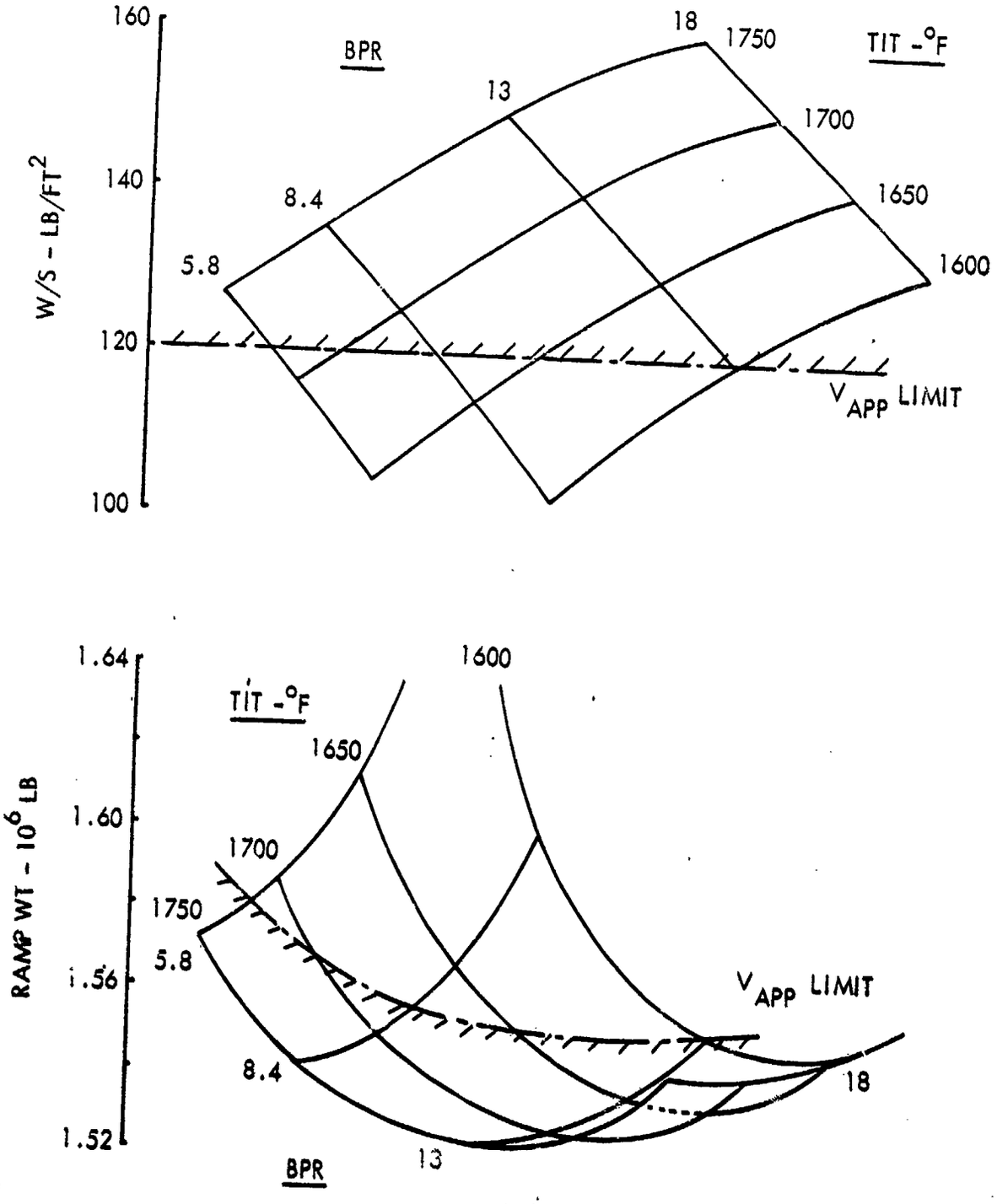

Figure 5-2. Reference Aircraft Parametric Data, 31,000-ft Altitude

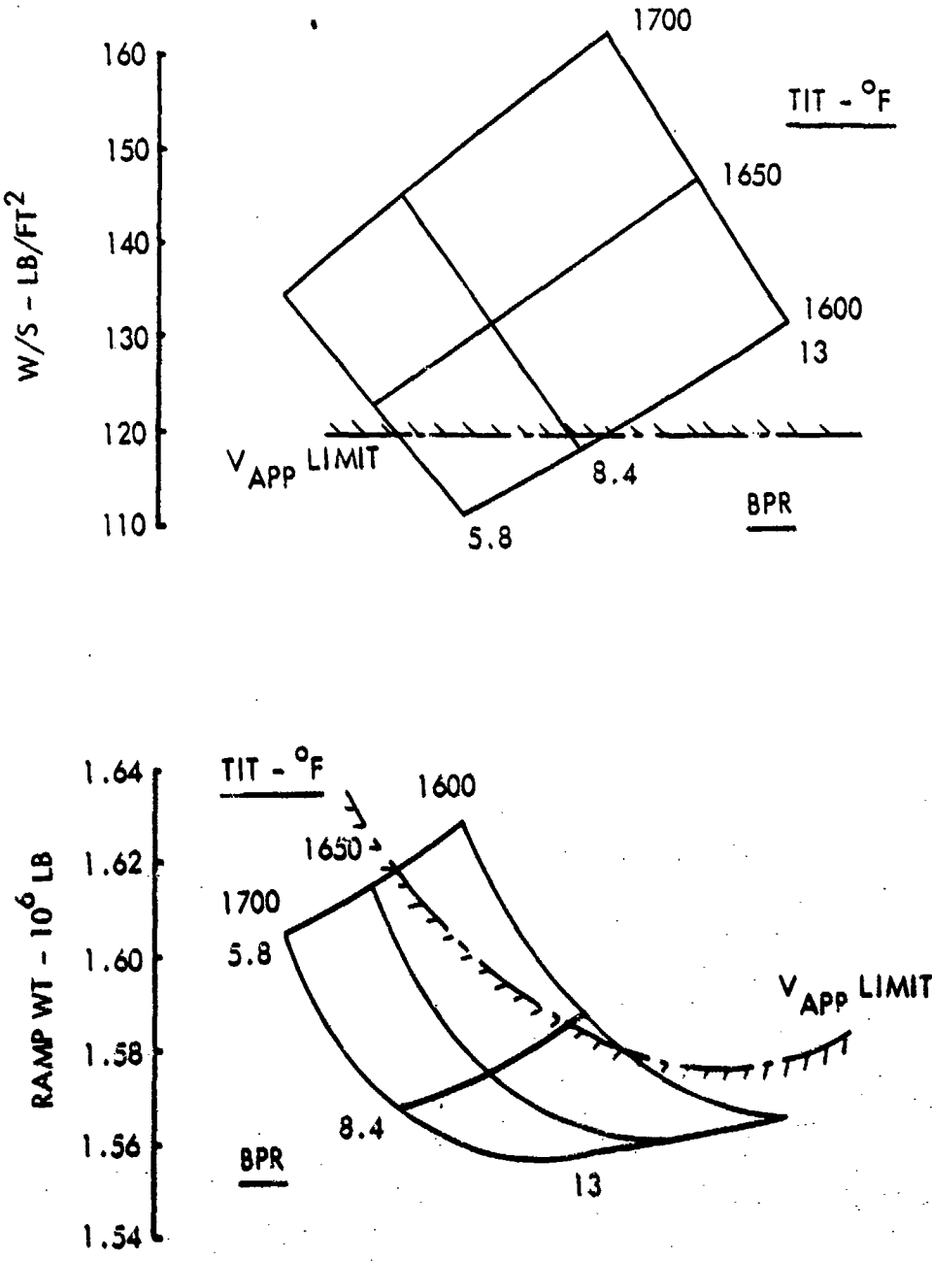

Figure 5-3. Reference Aircraft Parametric Data, 36000-ft Altitude

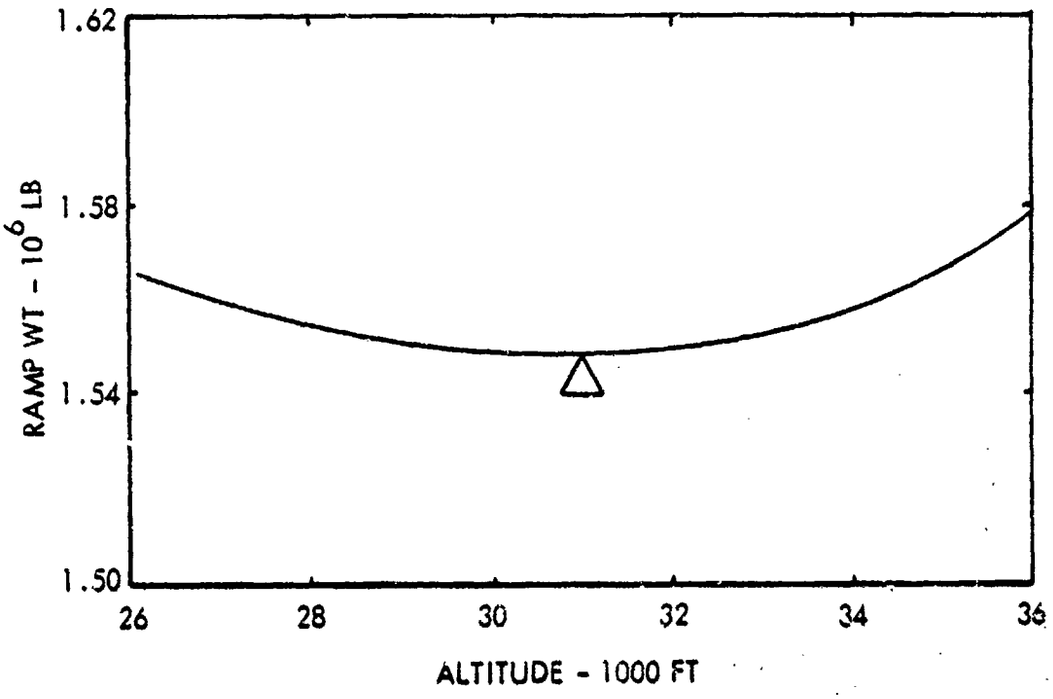

Figure 5-4. Reference Aircraft Altitude Optimization

Selection of the optimum engine bypass ratio was made based on the data in Figure 5-2 for the optimum altitude. The approach speed limiting line on the ramp weight graph shows the optimum bypass ratio to be between 8.4 and 13. Through interpolation, it appeared that a bypass ratio of 11.5 was optimum. However, due to the flatness of the curve between the 8.4 and 13 bypass ratio values, the value of 8.4 was selected for use on the reference aircraft. The weight penalty of 0.38 percent imposed by this off-optimum selection was deemed insignificant in comparison with minimizing the technology risk associated with the higher bypass-ratio engine.

5.2 REFERENCE AIRCRAFT CHARACTERISTICS

The reference aircraft design established in the parametric study is depicted in Figure 5-5. Pertinent design features of the aircraft are summarized in Table 5.1, and a weight statement is presented in Table 5.2. The geometric aspect-ratio value of 7.50 is shown in Table 5.1; an effective aspect-ratio value of 9.87 was achieved through the end-plating effect of the wingtip-mounted vertical surfaces.

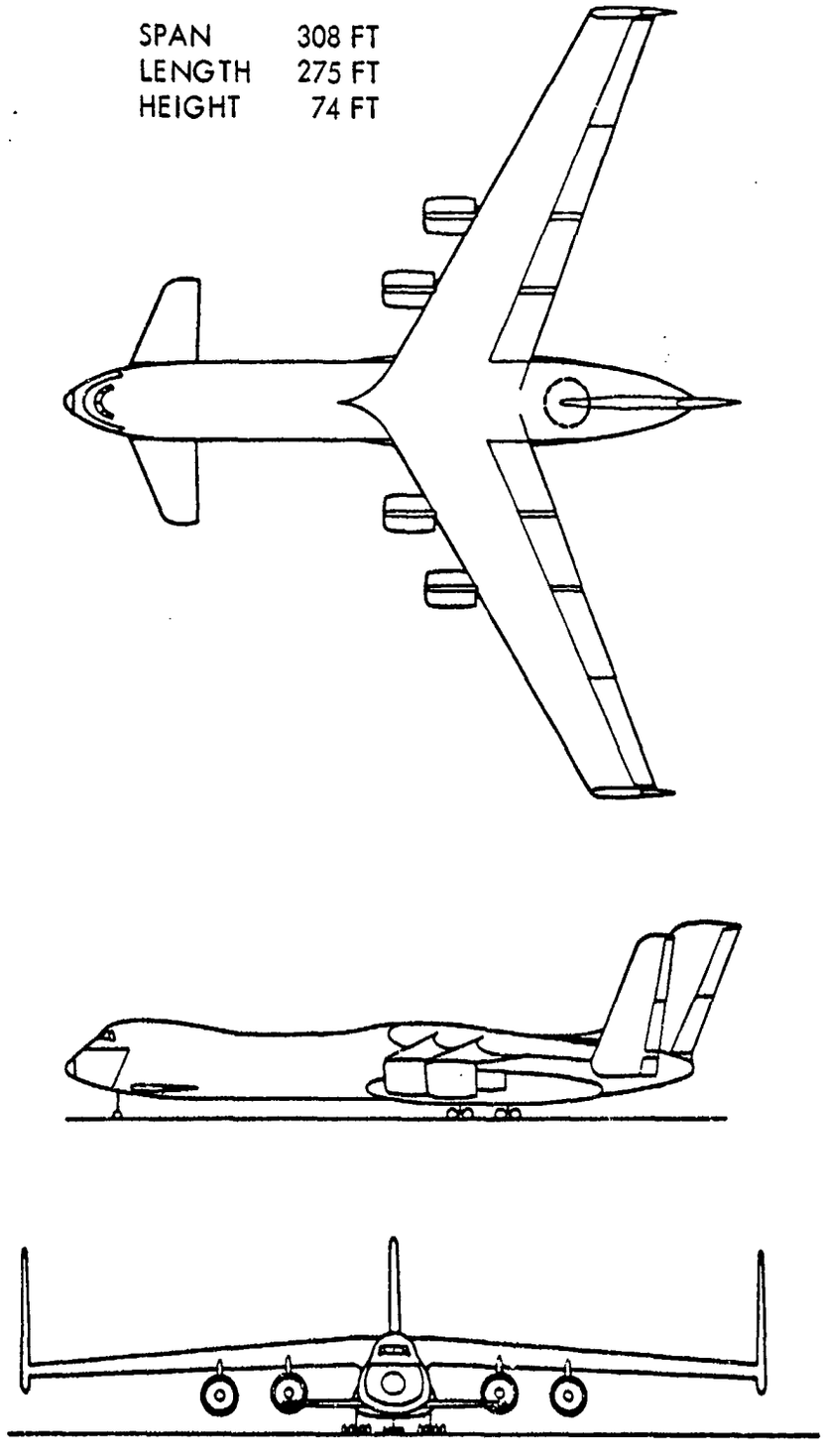

Figure 5-5. Reference Aircraft Layout

TABLE 5.1. REFERENCE AIRCRAFT DESIGN CHARACTERISTICS

Cruise Mach Number	0.75
Cruise Altitude	31,000 ft
Wing Sweep Angle	30 deg
Wing Loading	120 psf
Aspect Ratio	7.50
L/D	22.59
Cruise Lift Coefficient	0.508
Field Length	10,000 ft
Propulsion	
Reactor Size	230 MW
No. Engines	4
Engine Thrust, SLSD	84,823 lb
Engine Design JP TIT	1673°F
Areas, ft^2	
Wing	12,630
Canard	1,194
Verticals	3,698

TABLE 5.2. REFERENCE AIRCRAFT WEIGHT SUMMARY

	Lb
Wing	147,969
Horizontal	7,180
Verticals	12,187
Fuselage	104,708
Landing Gear	65,989
Nacelle and Pylon	23,821
Propulsion	
Engines Installed	81,042
Nuclear Subsystem	391,260
Engine HX & Ducts	122,711
Auxiliary Cooling	12,978
Fuel System	3,137
Systems and Equipment	48,898
Operating Weight Empty	1,021,881
Payload	400,000
JP Fuel	134,610
Ramp	1,556,491

The range of travel for the center of gravity for the reference aircraft is shown in Figure 5-6. These data were estimated based on the weight summary in Table 5.2 and the assumption that the payload and fuel were distributed uniformly in the fuselage and wing, respectively. The center of gravity is at 16 percent of the wing mean aerodynamic chord (MAC) for the reference mission ramp weight. The wide envelope, relative to a conventional aircraft, is due to the payload center of gravity being far forward of the wing. In actual practice, this would probably restrict the loadability of the aircraft more so than for a conventional aircraft.

The weight and balance data were used to check the aerodynamic performance and propulsion characteristics of the reference aircraft and to develop a more detailed breakdown of the nuclear subsystem.

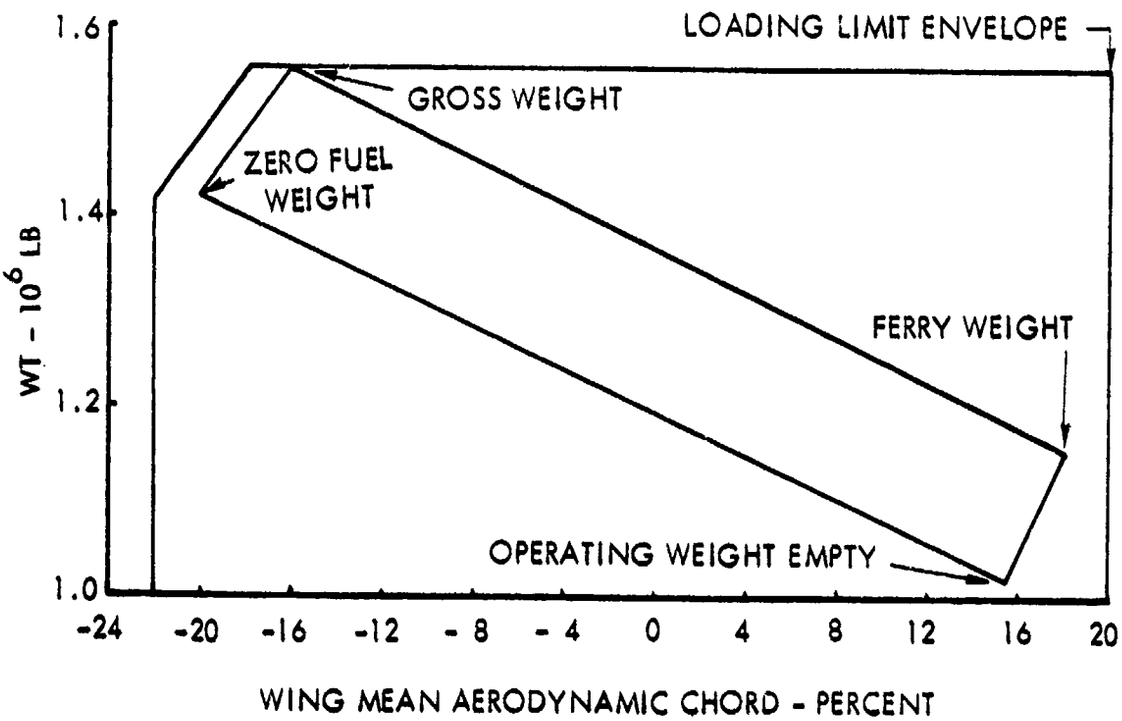

Figure 5-6. Reference Aircraft Center-of-Gravity Envelope

5.2.1 Aerodynamic Performance

An assessment was made of the drag buildup for the reference aircraft design, using methodology similar to that described in Section 3.2.2. The drag for each of the major aircraft components and the total drag buildup are listed in Table 5.3. A lift-to-drag ratio of 22.59 was obtained for the aircraft based on the drag estimate and the cruise lift coefficient of 0.508 given by the drag polar in Figure 5-7. Note that the nacelle drag has been listed as zero on this table since it is accounted for in the thrust data for the engine.

TABLE 5.3. DRAG BUILDUP

PROFILE DRAG		INDUCED DRAG	
Wing	0.00572	Cruise Lift Coefficient	0.508
Fuselage	0.00247	Efficiency Factor	0.92
Pylons	0.00010	End Plating Correction	1.3283
Nacelles	0.00000*		
Horizontal Tail (Canard)	0.00052	Induced Drag	0.00926
Vertical Tails	0.00166		
		TOTAL DRAG	
Total for Components	0.01047	Profile Drag	0.01183
Interference	0.00055	Induced Drag	0.00926
Roughness	0.00033	Trim Drag	0.0004
Miscellaneous	0.00048	Compressibility Drag	0.00100
Total Profile Drag	0.01183	Total	0.02249

Lift/Drag Ratio = 0.508/0.02249 = 22.59

* Nacelle profile drag included in engine thrust data

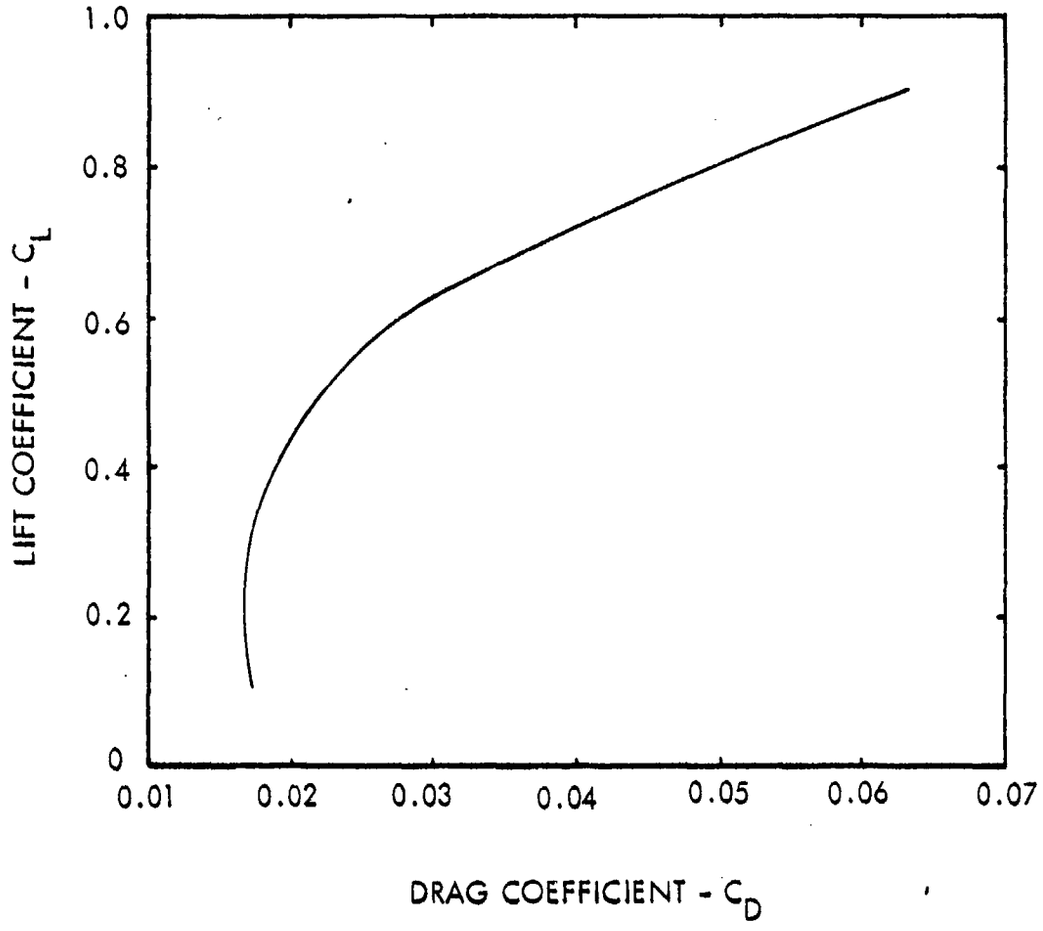

Figure 5-7. Reference Aircraft Drag Polar

Data from the drag polar were used to determine the aircraft flight envelope in Figure 5-8. The left portion of the graph is for the best rate of climb speed of 250 kts (calibrated). The right portion of the graph depicts the speed capabilities for two cases. One case is for operation only on nuclear power with a TIT of 1600°F. The second case represents operation on chemical fuel with a TIT of 1673°F. The top portions of the curves between M = 0.65 and the design point speed are the maximum cruise altitudes achievable while retaining a 300 fpm climb capability.

The high-lift system on the reference aircraft is comprised of 95-percent span leading-edge slats and 75-percent span, double-slotted trailing-edge flaps. The leading-edge slats are formed from, and when retracted become, the wing leading-edge from the

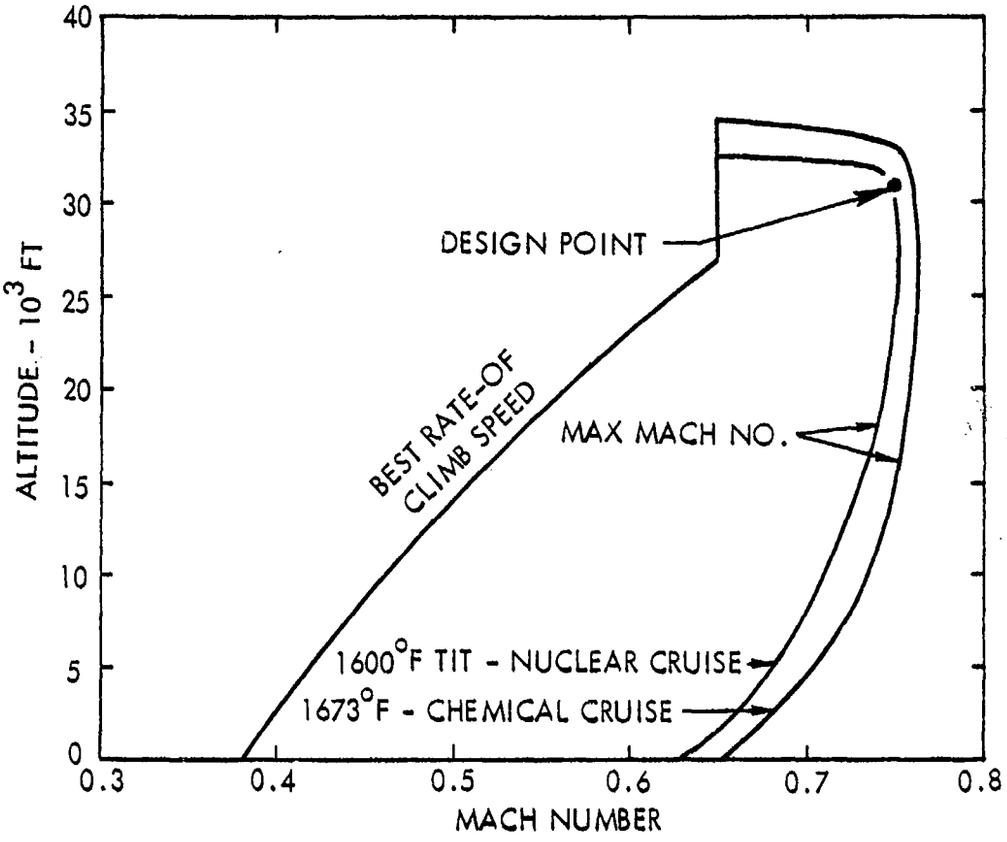

Figure 5-8. Reference Aircraft Altitude - Mach Number Flight Envelope

3-percent chord position on the lower surface to the 14-percent chord position on the upper surface. The trailing-edge flaps are a 30-percent chord design with a maximum chordwise extension of 7 percent. The lift and drag characteristics of the high lift system are summarized in Table 5.4.

TABLE 5.4. HIGH-LIFT SYSTEM DATA

Double-Slotted Flap with Leading-Edge Slat				
	Deflection Angle, deg	$C_{L_{max}}$	$C_{L_{TO}}$	$C_{D_{TO}}$
Takeoff	20	2.37	1.642	0.1564
Landing	40	3.02	1.786	0.2223

The field length over a 50-ft obstacle with all engines operating was computed for a 93°F hot day at sea level. The data used in the calculations and the resulting takeoff performance are presented in Table 5.5.

TABLE 5.5. TAKEOFF DISTANCE DETERMINATION

Maximum Takeoff Lift Coefficient	2.37
Takeoff Lift Coefficient at 120% Stall Speed	1.64
Takeoff Weight	1,556,491 lb
Wing Area	12,630 ft^2
Takeoff Speed	154 kts
Ground Roll Distance	8,970 ft
Distance to Climb to 50 Ft	1,030 ft
Normal Takeoff Distance	10,000 ft
Engine-Out Climb Gradient	0.01959

Derivation of the landing performance is presented in Table 5.6. The landing weight of 1,519,546 lb corresponds to the aircraft ramp weight less the ground maneuvering and takeoff fuel and the enroute climb fuel. The landing sequence is based on a normal 3-deg glide slope at 1.3 times the stall speed, and a touchdown speed equal to 1.1 times the stall speed. Three seconds were allotted for free roll after touchdown, followed by full braking and spoiler deployment. Reverse thrust was not used.

TABLE 5.6. LANDING DISTANCE DETERMINATION

Maximum Landing Lift Coefficient	3.02
Landing Lift Coefficient at 130% Stall Speed	1.79
Landing Weight	1,519,546 lb
Landing Approach Speed	140 kts
Touchdown Speed	119 kts
Distance from 50-ft Obstacle Height to Touchdown	1,730 ft
Ground Roll Distance	3,350 ft
Total Distance	5,080 ft

The flight control systems were found to be adequate for the established design criteria. The canard surface size was verified to be sufficient for both standard critical cases of stall out of ground effect and of nose-wheel liftoff at 80 percent of stall speed for the most forward center-of-gravity condition. A check of the basic static longitudinal stability confirmed that the aircraft design was consistent with conventional aerodynamic practice of having the aircraft center of gravity forward of the neutral stability point for the tail-off configuration.

5.2.2 Propulsion System

5.2.2.1 Engine

Part of the parametric study to define the optimum reference aircraft included variations of engine bypass ratio and TIT. As a result of that study, a turbofan engine was selected with a bypass ratio of 8.4 and turbine inlet temperatures on JP fuel of 1873°F for takeoff and 1673°F for cruise. Further definition of the nuclear-powered gas turbine engine for the reference aircraft was based on the Pratt & Whitney Aircraft study engine, the STF 477 (Ref. 11). The STF 477 is an advanced technology turbofan engine with low energy consumption characteristics envisioned for the late 1990s. The performance and installation characteristics of the STF 477 are, however, regarded as goals and can be achieved only after an intensive research and development program is undertaken to bring the advanced propulsion technology to the state required for incorporation into development powerplants.

The STF 477 basic cycle bypass ratio was retained, but the installation geometry and scaling characteristics were extrapolated to approximately 84,800 lb of rated thrust to meet the requirements of the reference aircraft. A table of the baseline engine performance and installation parameters is shown on Table 5.7. The baseline engine was installed in a separate exhaust/short duct nacelle for the reasons discussed in Section 3.2.3.2. The pressure losses assumed for the inlet and exhaust duct are typical for large bypass engines of this type. The nacelle drag value shown on Figure 5-9 is the sum of several drag components. One of the drag components is surface friction drag, both freestream over the fan cowl and exhaust efflux scrubbing over the gas generator cowl. Another component is the pressure drag forces of the nacelle forebody and afterbody due to the momentum spillage of the inlet and to the afterbody boat-tail effects.

An additional increment accounted as nacelle drag is the momentum penalty of the fan air bled for nacelle compartment cooling. The environment airbleed and accessory power loads were extrapolated from existing C-5 and C-141 data as representative of the requirements for a military transport of this configuration.

TABLE 5.7. CHARACTERISTICS OF THE BASELINE ENGINE AND INSTALLATION

ENGINE			
Rated Thrust, lb	84,800		
Bypass Ratio	8.4		
Fan Pressure Ratio	1.3		
Overall Pressure Ratio	12		
Turbine Inlet Temperature, °F			
Takeoff: (SLS) JP Fuel	1873		
Cruise: (31,000 ft, M = 0.75)			
JP Fuel	1673		
Nuclear	1600		
INSTALLATION (Per Engine)		Takeoff	Cruise
Inlet Pressure Losses $\Delta P/P_2$		0.01	0.003
Duct Pressure Losses			
Fan $\Delta P/P_F$		0.015	0.015
Core $\Delta P/P_c$		0.008	0.008
Mid-stage Compressor Airbleed, lb/sec		2.9	2.00
Turbine Power Extraction, hp		150	150
Nacelle Drag from Figure 5-8, lb		64	1432

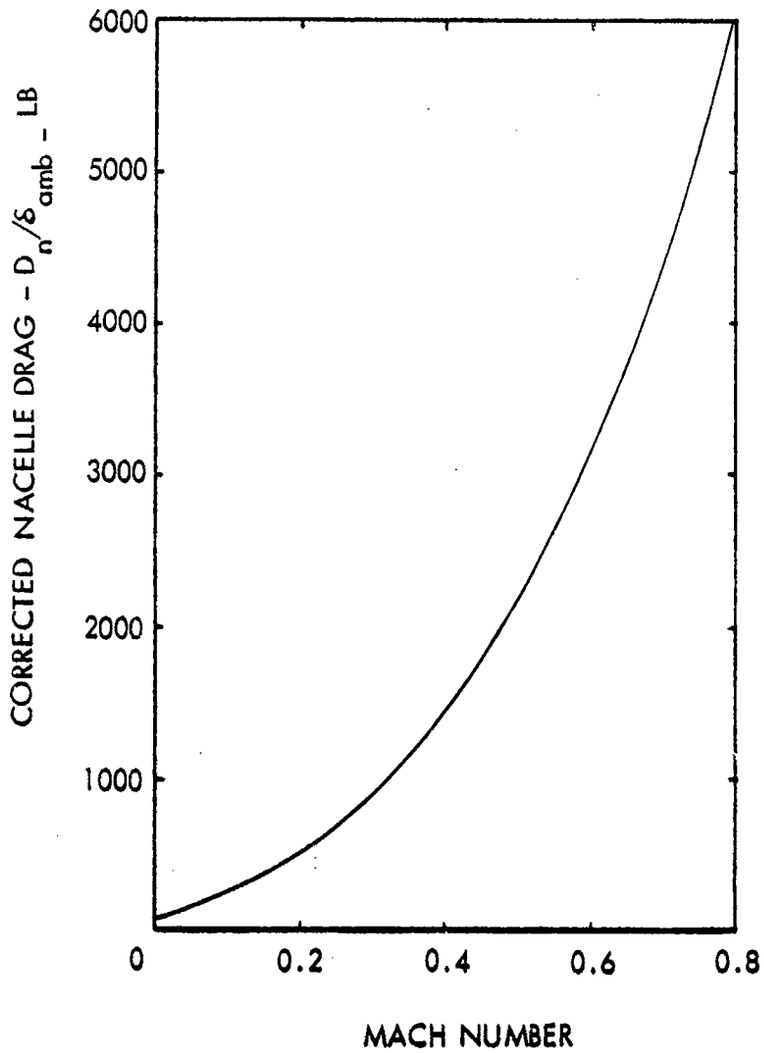

Figure 5-9. Nacelle Drag Characteristics for Baseline Engine. Rated Thrust - 84,800 lb. $\delta_{amb} = P_{amb}/14.7$ psia

5.2.2.2 Nuclear Subsystem

The reference aircraft required a nuclear subsystem thermal power rating of 230 MW. Using this power rating and the other six major input parameters (lifetime, burnup, coolant velocity, etc.) given in Section 3.2.3.1, the nuclear subsystem weight was calculated using the COP-DS computer code. The resultant computer output listing for this case is given in Table 5.8. This resulting nuclear subsystem weight is based

TABLE 5.8. NuERA II COP-DS DATA FOR REFERENCE AIRCRAFT NUCLEAR SUBSYSTEM

Input Values	
Reactor Power Level	230 MW
Average Atom Percent Burnup of Fuel	11.4
Core Lifetime	10,000 hr
Reactor Outlet Temperature	1800 °F
Coolant Velocity	27.8 ft/sec
Dose Rate Criterion	5 mr/hr
Impact Velocity	250 ft/sec
Power Plant Weight Summary (lb)	
Reactor Subassembly	44,466
Reactor Shield	177,334
Heat Exchanger and Piping Shields	46,573
Auxiliary Equipment	12,043
Containment Vessel	99,508
Structure	4,000
Coolant	2,500
Miscellaneous Components	5,000
Total Nuclear System Weight	391,424
Power Plant Geometry Summary (in.)	
Containment Vessel Outer Diameter	219.2
Containment Vessel Thickness	2.1
Reactor Pressure Vessel Length	86.0
Reactor Pressure Vessel Inner Diameter	48.2
Active Fueled Core Diameter	27.7
Active Fueled Core Length	21.4
Total Core Length	45.7
Shield Outer Diameter, Primary Radial Direction	177.3
Shield Outer Diameter, Transverse Radial Direction	150.1
Shield Outer Length, Vertical Direction	171.7
Volume of Core	33,899 in^3
Volume of Shielded Reactor Subassembly	2,617,718 in^3
Envelope Volume of Containment Vessel	5,515,795 in^3
Volume of Auxiliary Equipment	113,510 in^3
Packing Fraction	0.484

TABLE 5.8. NuERA II COP-DS DATA FOR REFERENCE AIRCRAFT NUCLEAR SUBSYSTEM (CONT.)

Nuclear Subassembly Weight Summary (lb)	
Core	9,203
Fuel (Uranium Nitride)	2,193
Radial Reflector (Tungsten and Nickel)	9,287
Axial Reflector (Tungsten)	1,345
Radial (Side) Shield (Tungsten)	10,656
Axial (End) Shield (Columbium-1 Zirconium)	4,141
Coolant (Lithium-7)	644
Pressure Vessel (Columbium-1 Zirconium)	4,035
Control System	3,500
Insulation and Support Structure	3,000
Nuclear Subassembly Geometry Summary (in.)	
Core Diameter (With Filler Strips)	30.7
Thickness of Core Support Barrel	0.3
Thickness of Radial Reflector	6.1
Thickness of Axial Reflector	3.5
Thickness of Radial (Side) Shield	2.3
Thickness of Axial (End) Shield	5.9
Thickness of Pressure Vessel	1.0
Thickness of Top Support Plate	2.0
Thickness of Bottom Support Plate	0.5
Plenium Height	13.4
Pressure Vessel Outer Diameter	50.2
Pressure Vessel Length	86.0
Radiation Dose at 20 Feet from Core Center Line (mr/hr)	
Primary Radial Direction (Direct)	4
Transverse Radial Direction (Direct)	450
Vertical Direction (Direct)	490
Primary Radial Direction (Direct + Air Scat. + Secdry.)	5
Reactor Shield Weight Summary (lb)	
Inner Shield (Zirconium Hydride)	
Primary Radial Direction	37,243
Transverse Radial Direction	20,516
Vertical Direction	71,693
Total	129,473

TABLE 5.8. NuERA II COP-DS DATA FOR REFERENCE AIRCRAFT NUCLEAR SUBSYSTEM (CONT.)

Outer Shield (Lithium Hydride)	
Primary Radial Direction	8,543
Transverse Radial Direction	6,543
Vertical Direction	32,776
Total	47,861
Reactor Shield Geometry Summary (in.)	
Thickness of Inner Shield	
Primary Radial Direction	30.5
Transverse Radial Direction	19.3
Vertical Direction	17.4
Thickness of Outer Shield	
Primary Radial Direction	30.3
Transverse Radial Direction	27.9
Vertical Direction	22.5
Auxiliary Equipment Weight Summary (lb)	
Heat Exchangers	6,228
Piping	1,283
Pumps	4,531
Core Weight Summary (lb)	
Fuel	2,193
Clad (Astar 811C)	2,508
Axial Reflector	1,345
Top and Bottom Support Plates	456
Shim (Yttrium Hydride and Boron Carbide)	309
Structure	253
Filler Strips (Nickel)	1,780
Support Barrel	360

TABLE 5.8. NuERA II COP-DS DATA FOR REFERENCE AIRCRAFT NUCLEAR SUBSYSTEM (CONT.)

Reactor Parametrics

Effective (Fueled) Core Diameter	27.7 in
Active (Fueled) Core Length	21.4 in
Mission Gas Length	11.8 in
Number of Shim Rods	6
(Delta)/K due to Burnup	0.108
(Delta K)/K Cold to Hot	-0.022
Peak Power to Average Power, Flattened	1.05
Minimum Power to Average Power, Flattened	0.80
Critical Enrichment of Unzoned Reactor	0.66
Centerline Enrichment Required by Power Flattening	0.60
Outermost Zone Enrichment	0.84
Reactor Coolant Delta Temperature	400°F
Centerline Fuel Hotspot Temperature	3450°F
Thickness of the Clad	0.020 in.
Diameter of Fuel Pin Including Cladding	0.295 in.
Number of Fuel Pins	5516
Volume Fraction of Fuel in Core	0.455
Volume Fraction of Clad in Core	0.169
Volume Fraction of Coolant in Core	0.204

Reflector provides control for cold-to-hot swing plus shutdown margin.
Shims provide control for burnup.

on the NuERA II dose rate criteria of 5 mr per hr at 20 ft from the core center forward and aft during operation and at 20 ft from the core center in any direction one-half hour after shutdown of the reactor. With this criteria, the outer boundary of the shield is an elliptical cylinder with ellipsoid shaped top and bottom, as shown in Figure 5-10.

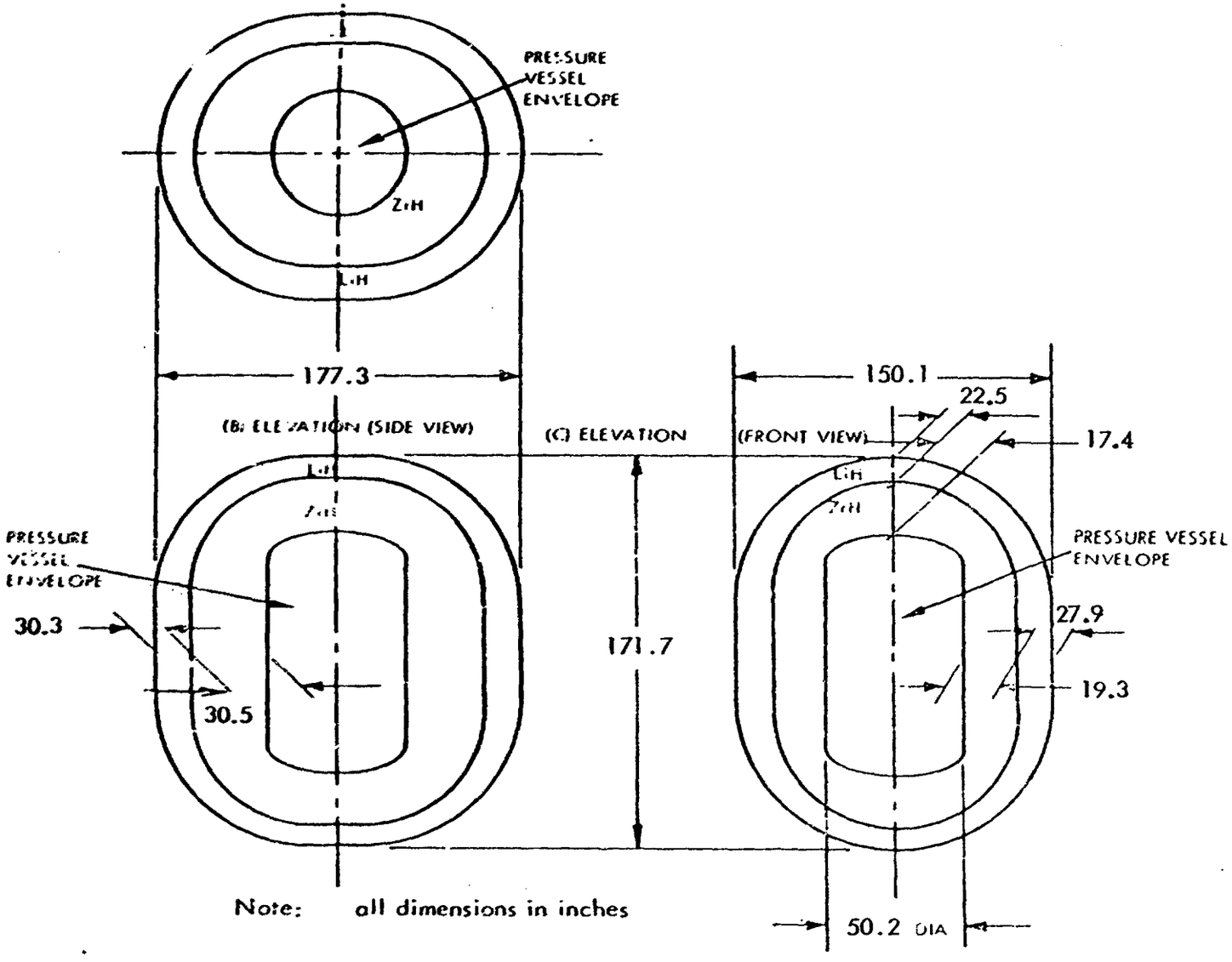

Figure 5-10. NuERA Aircraft Shield Arrangement (230 MW)

6.0 SENSITIVITY ANALYSES

Sensitivity of the selected reference aircraft to variations in performance requirements, advanced levels of technology, alternate philosophies for nuclear operation and alternate mission applicability were evaluated to determine where the greatest benefits can be obtained.

6.1 PERFORMANCE

The sensitivity of the reference aircraft ramp weight was assessed for variations in the three mission performance requirements of cruise Mach number, emergency recovery range, and takeoff distance. The results of these assessments are summarized in Table 6.1.

TABLE 6.1. PERFORMANCE SENSITIVITY STUDY RESULTS

Mach Number	0.65	0.75*	0.85		
Δ Ramp Weight	-1.65%	0	4.60%		
Emergency Range, n.m.	1000*	2000			
Δ Ramp Weight	0	10.4%			
Takeoff Distance, ft	8000	9000	10,000*	11,000	12,000**
Δ Ramp Weight	1.29%	0.45%	0	-0.45%	-0.45%

* Reference Aircraft Design Value
** Limited by Minimum Engine TIT of 1600°F

6.1.1 Cruise Mach Number

Two alternate cruise Mach numbers of 0.65 and 0.95 were considered for the reference aircraft. The 10,000-ft field length requirement was retained, but alternate cruise altitudes were investigated for each Mach number. For the lower speed, an altitude of

26,000 ft was found to give the lightest weight aircraft. The minimum weight aircraft for the Mach 0.65 cruise speed was established by the approach speed limit, as indicated on Figure 6-1.

At the higher speed, the reference aircraft altitude of 31,000-ft was found to give the best results. As for the lower cruise Mach number, the approach speed limit established the minimum weight aircraft on Figure 6-2. The 36,000-ft altitude curve has also been included on this figure in case there is interest in reducing the approach speed limit, thereby driving the design altitude to the higher value to minimize aircraft weight.

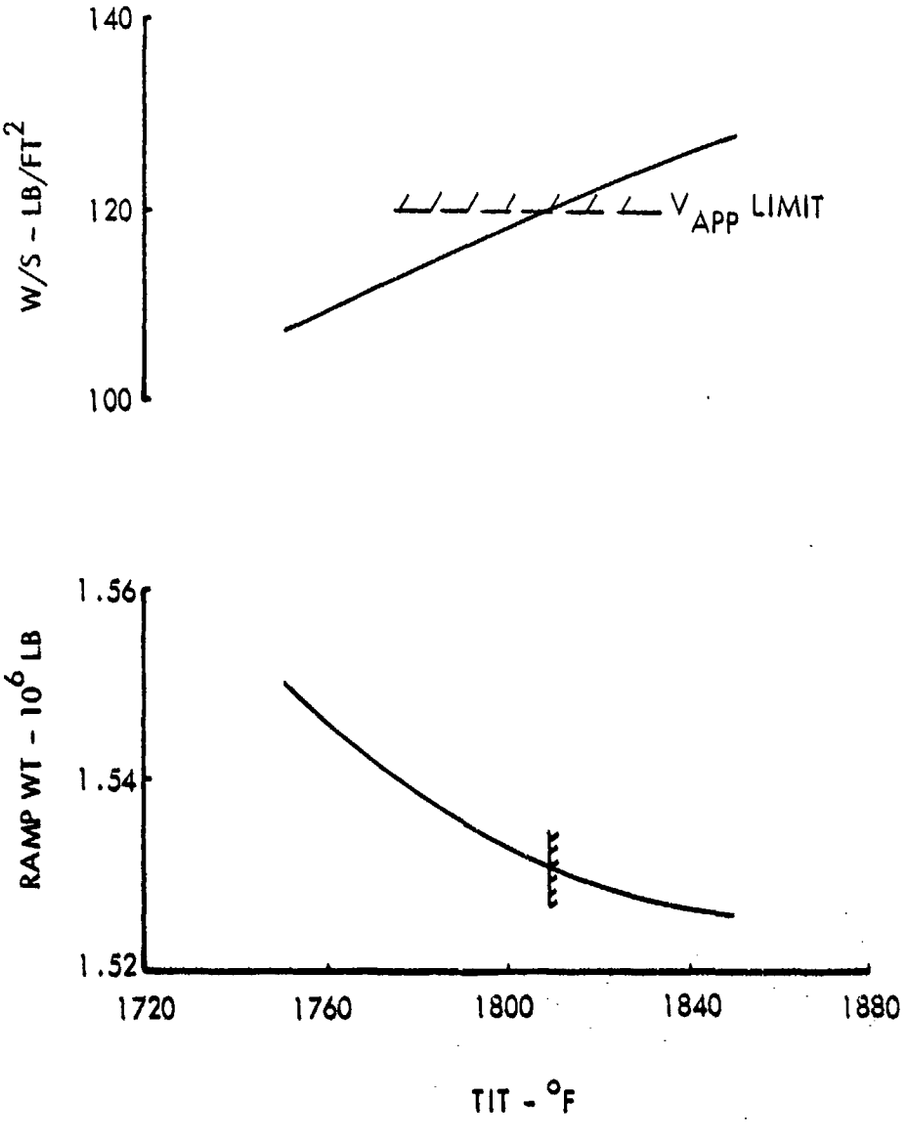

Figure 6-1. Ramp Weight Determination for 0.65 Cruise Mach Number. BPR = 8.4, Altitude = 26,000 ft, TOD = 10,000 ft.

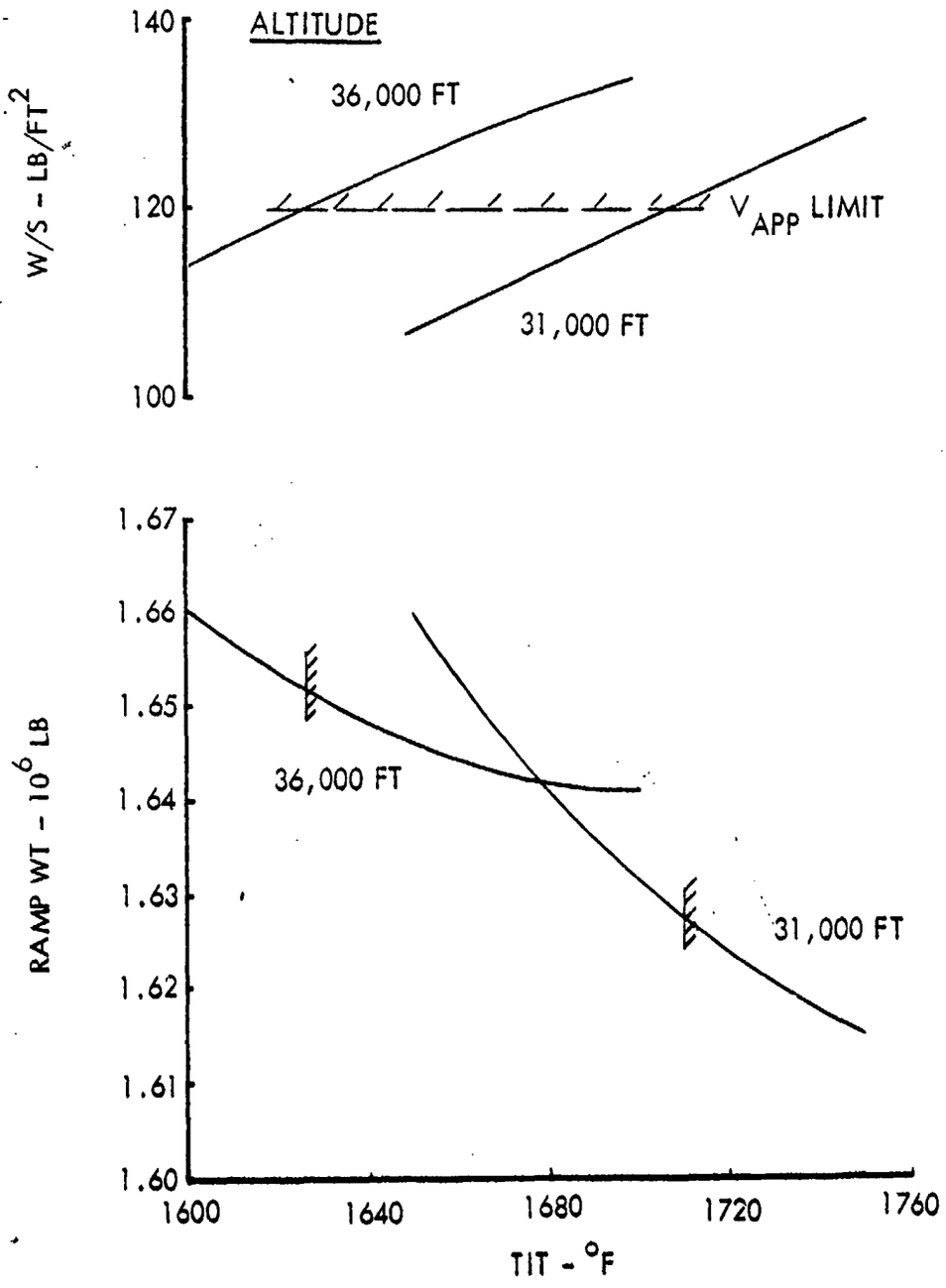

Figure 6-2. Ramp Weight Determination for 0.85 Cruise Mach Number. BPR = 8.4, TOD = 10,000 ft.

As indicated by the summary curve in Figure 6-3, a small weight savings of 1.65 percent can be obtained by reducing the cruise Mach number from 0.75 to 0.65. The effect of increasing the Mach number by the same increment to 0.85 produces a relatively larger weight penalty of 4.60 percent.

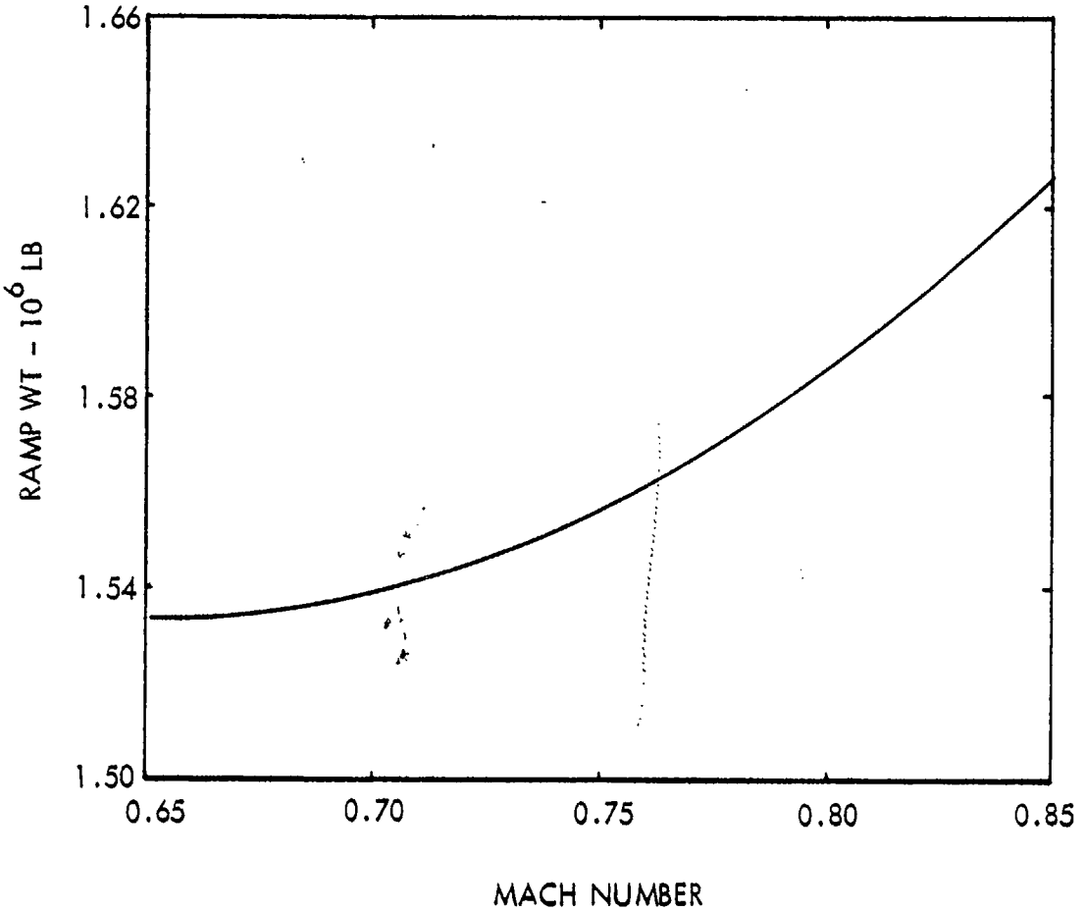

Figure 6-3. Effect of Cruise Mach Number on Reference Aircraft Weight. BPR = 8.4, TOD ≐ 10,000 ft.

6.1.2 Emergency Recovery Range

The requirement to carry enough JP fuel for an additional 1000 n.m. of emergency recovery range resulted in a 10.4-percent increase of the reference aircraft ramp weight. In reoptimizing the aircraft for this additional range requirement, the only input parameters to be varied were the wing aspect ratio and the engine TIT. The latter was forced to change for the 10,000-ft field length requirement to be satisfied. As a result of the reoptimization, the aspect ratio of the reference aircraft changed from 7.50 to 8.25 and the engine TIT increased from 1673°F to 1698°F.

6.1.3 Field Length

The effects of alternate field length requirements on the ramp weight of the reference aircraft were assessed simultaneously with changes in engine bypass ratio - one of the technology sensitivity studies. The results of the analysis are presented in Figures 6-4 to 6-6. With the approach speed limitation imposed, less than a two-percent variation in ramp weight was realized as the field length requirement was increased from 8000 ft to 12,000 ft, assuming the best engine bypass ratio and TIT. As an illustration, for an 8000-ft field length requirement, an engine bypass ratio of 12.7 and a 1700°F TIT give the minimum ramp weight. For a 12,000-ft field length, the minimum weight occurred for an engine bypass ratio of 9.0 and a TIT of 1600°F.

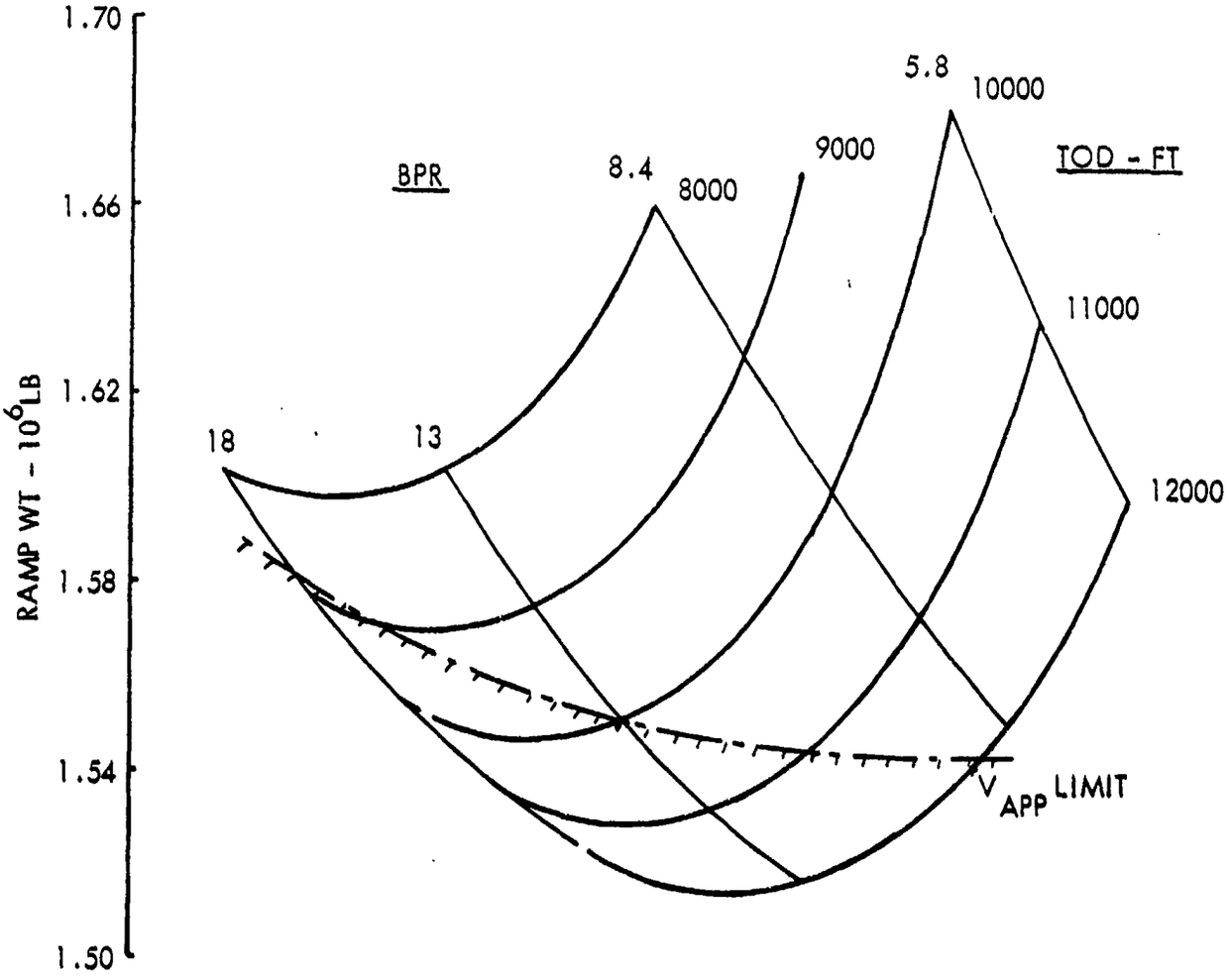

Figure 6-4. Effects on Ramp Weight of Engine Bypass Ratio and Field Length, TIT = 1600 °F.
M = 0.75, Altitude = 31,000 ft.

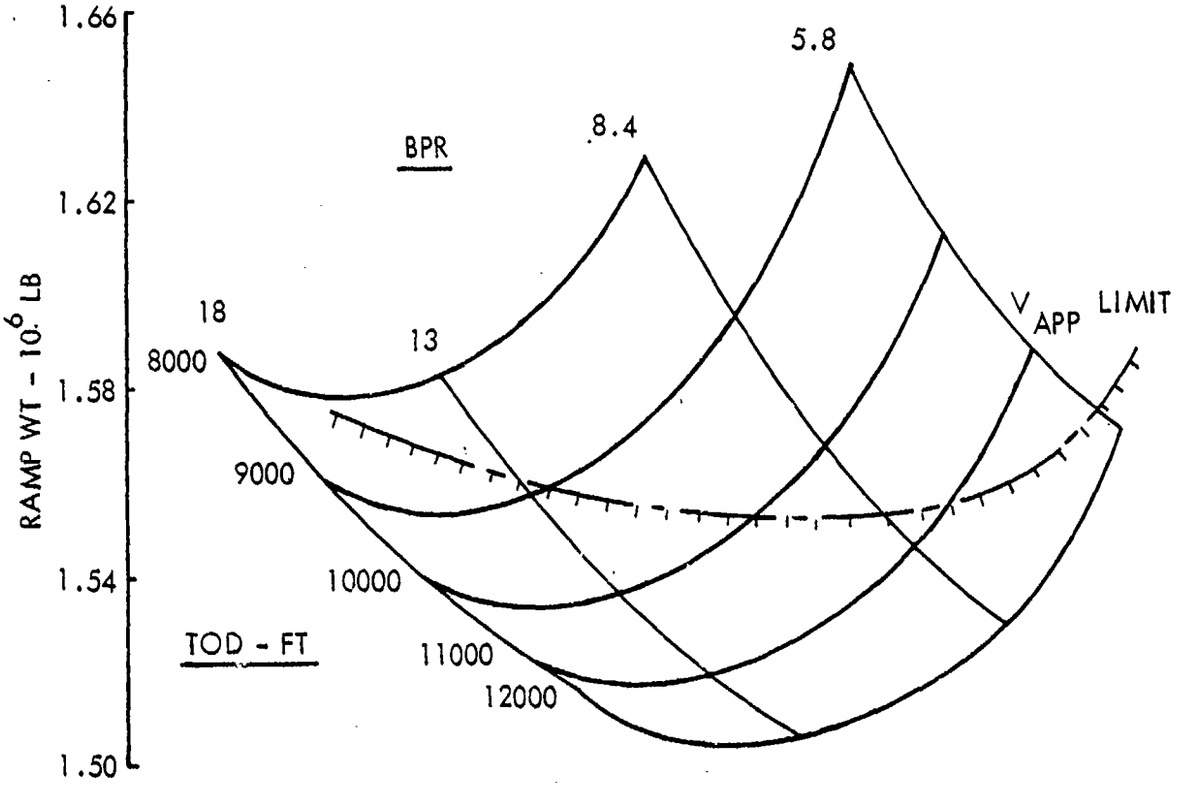

Figure 6-5. Effect on Ramp Weight of Engine Bypass Ratio and Field Length, TIT = 1650 °F. M = 0.75, Altitude = 31,000 ft.

6.2 TECHNOLOGY

Four technology areas, suggested by the technology assessment results in Appendix A, were examined for their effect on the reference aircraft design. Alternate levels were considered for engine bypass ratio, the percent of structural weight in composite materials, and the TIT of the engine during nuclear cruise. Laminar flow control (LFC) was applied to the aircraft wing and vertical surfaces, as an additional technology feature. The results from these technology sensitivity studies are summarized in Table 6.2.

6.2.1 Engine Bypass Ratio

The engine bypass ratio results were obtained by cross-plotting the data shown previously in Figures 6-4 to 6-6. For this sensitivity, the field length was held constant at 10,000 ft.

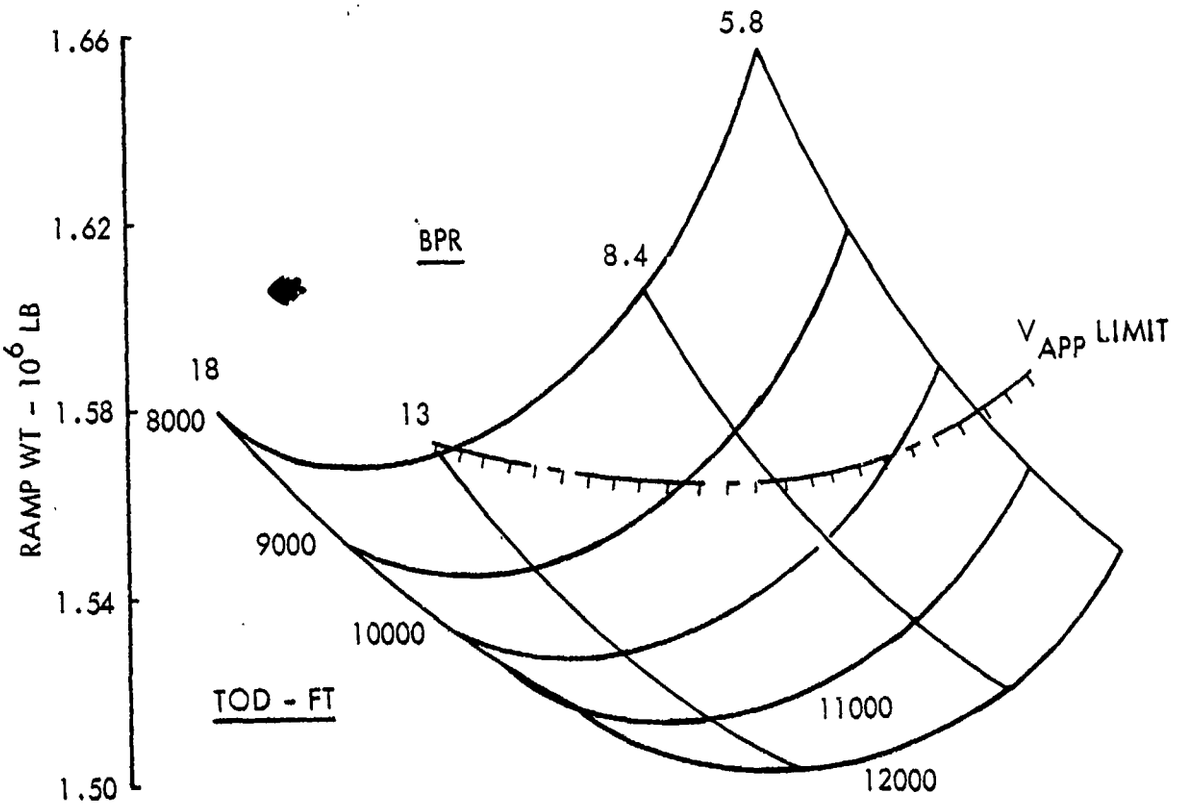

Figure 6-6. Effect on Ramp Weight of Engine Bypass Ratio and Field Length, TIT = 1700 °F. M = 0.75, Altitude = 31,000 ft.

TABLE 6.2. TECHNOLOGY SENSITIVITY STUDY RESULTS

Engine Bypass Ratio	5.8	8.4*	13.0	18.0
Δ Ramp Weight	1.61%	0	-0.29%	-0.29%
Composite Material Level, %	0	20	40*	60
Δ Ramp Weight	13.51%	4.98%	0	-4.21%
Nuclear Cruise TIT, °F	1600*		1800	
Δ Ramp Weight	0		-1.05%	
Laminar Flow Control	None*	Wings & Verticals		
Δ Ramp Weight	0	-3.61%		

* Reference Aircraft Design Value

6.2.2 Composite Materials

The reference aircraft design uses composite materials for 40 percent of the structural weight. This level was arbitrarily chosen for this study, but in a detailed design effort, the level of composites would be selected on the basis of minimizing the aircraft costs. Such a costing exercise was outside the scope of this program. However, the effects of alternate levels of composites on the aircraft weights were investigated.

In reoptimizing the reference aircraft for composite material levels of 0, 20, and 60 percent of the structure, the only other input parameters to be varied were the wing aspect ratio and the engine TIT. The latter was forced to change for the 10,000-ft field length requirement to be satisfied. Values for these parameters for each of the composite levels are presented on Figure 6-7, along with the percent variation in the ramp weight of the reference aircraft.

Composite material levels greater than 60 percent were not considered. Generally, higher levels require that composite materials be used for non-optimum structures or for minimum gage elements. The result is a considerable economic penalty for little or no weight savings.

6.2.3 Nuclear Cruise TIT

Chemical-fueled engines operate at TITs in excess of 2500°F to achieve good efficiency. When modified for nuclear power, the engines experience considerable performance degradation due to the low TIT of 1600°F dictated by material limitations of the engine heat exchanger. Material improvements to permit higher TITs are not expected by the year 2000 unless considerable research in this area is initiated in the near future. To determine if a concentrated effort in material development is warranted, the potential benefit from a 200°F improvement in engine TIT was investigated, with a corresponding increase in reactor outlet temperature.

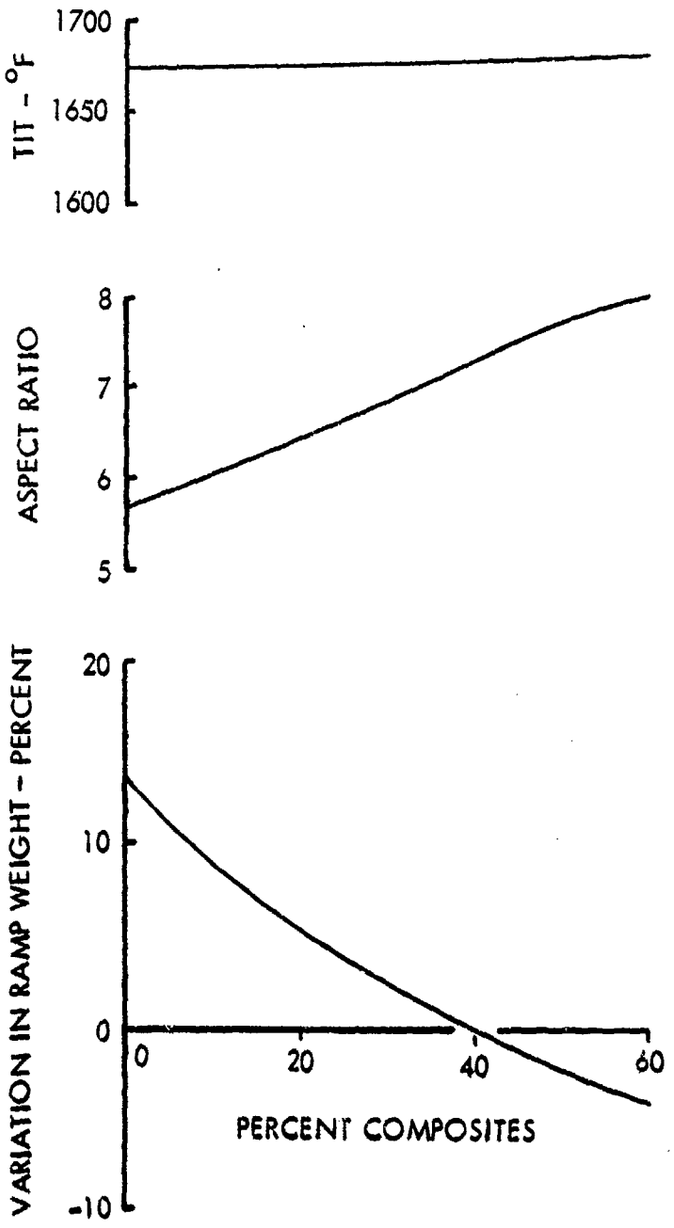

Figure 6-7. Composite Material Sensitivity Results.
M = 0.75, Altitude = 31,000 ft,
W/S = 120 psf, TOD = 10,000 ft.

Figure 6-8 shows the parametric sizing data used to evaluate the effect of an 1800°F TIT for the engine during nuclear cruise. Aircraft wing loading and aspect ratio and engine design TIT were the input parameters; the latter was varied to achieve the 10,000-ft field length requirement. The approach limitation established the minimum ramp weight for this sensitivity study.

As noted earlier in Table 6.2, only a 1.05 percent improvement in ramp weight was realized with the higher nuclear cruise TIT for the engine. Considerably greater improvements had been anticipated. Analysis of the data verified that reductions in engine size occurred and that the engine efficiency had increased, as reflected by smaller specific fuel consumption values. Further analysis revealed that these gains were partially offset by increases in the nuclear subsystem weight. A simple explanation for the increased nuclear subsystem weight is that the weight is proportional to the product of reactor outlet temperature and operational lifetime. Since the reactor outlet temperature increased by 200°F while the operational lifetime remained constant, the weight of the subsystem was forced to increase.

6.2.4 Laminar Flow Control (LFC)

Several technology concepts were assessed in Appendix A as to the potential benefits from their applicability. LFC was one of the more promising concepts due to the possible gains in cruise lift-to-drag ratio and the resulting reduction in nuclear subsystem weight. As a sensitivity study, LFC was applied to the reference aircraft. Extensive use was made of Lockheed's* recent LFC background in performing this analysis. The wing and three vertical stabilizers were laminarized. The canard surface was excluded from laminarization because of its distant location relative to the other laminarized surfaces, and the uncertain design problems of combining the canard's spanwise blowing system with a LFC glove.

* R. F. Sturgeon et al, "Study of the Application of Advanced Technologies to Laminar Flow Control Systems for Subsonic Transports," NASA CR-133949, Lockheed-Georgia Company, 1976. (Ref. 13)

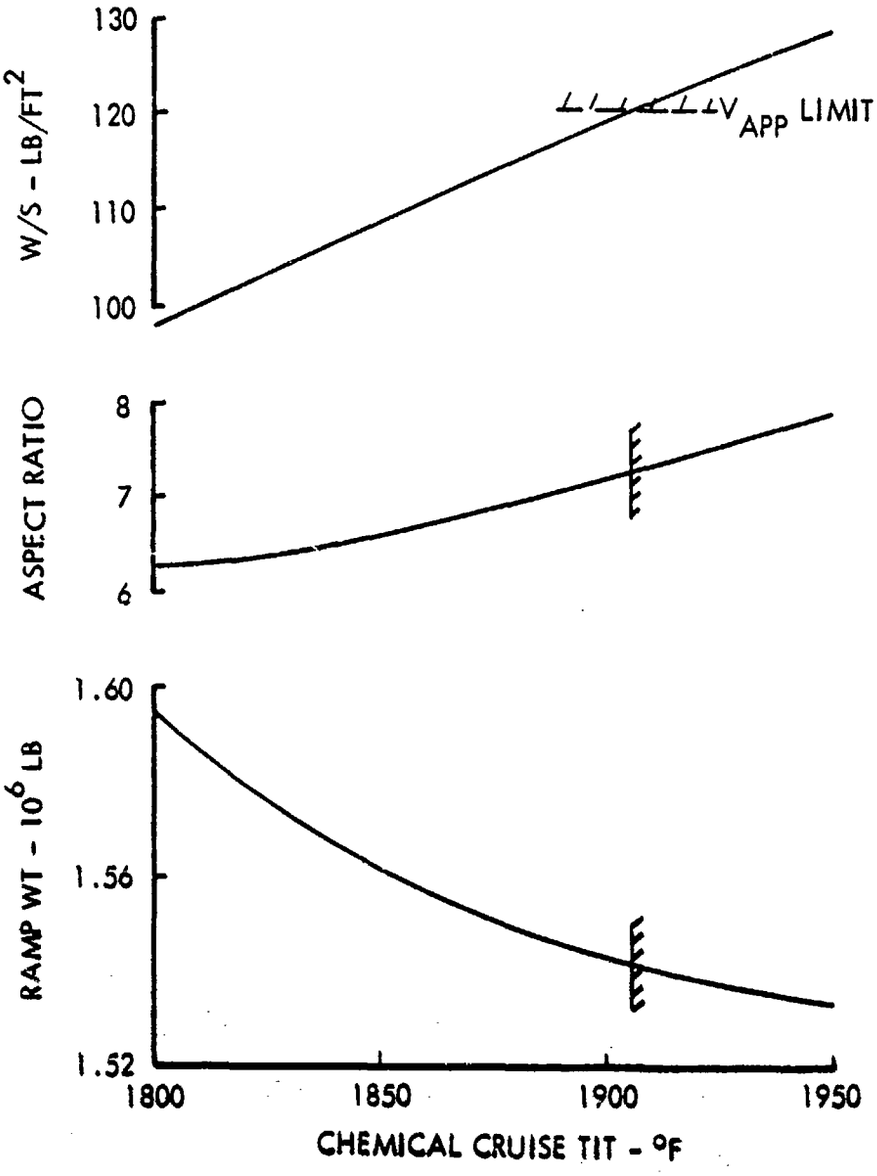

Figure 6-8. Aircraft Sizing for Nuclear Cruise TIT of 1800 °F. BPR = 8.4, TOD = 10,000 ft, M = 0.75, Altitude = 31,000 ft.

Suction for the LFC system was supplied by two LFC engines ducted to gloves on the wing and the vertical stabilizers. These engines were buried in the aft portion of the fillet at the intersection of the fuselage and wing lower surface.

The LFC gloves on the wing and fuselage-mounted vertical stabilizer extended spanwise for the total length and chordwise from the 3 to 75-percent chord locations. The LFC gloves on the wingtip-mounted vertical stabilizers covered the region between the 15

percent spanwise station and the tip on the inner surface and the entire outer surface span. The chordwise distribution was the same as for the wing.

The additional weights of the gloves were based on the total upper and lower surface areas and the estimated glove thicknesses. Weights for the LFC engines and ducts, and the LFC engine fuel requirements were estimated according to the procedures outlined in Ref. 13.

Parametric data are presented in Figure 6-9 for reoptimizing the reference aircraft with LFC. Wing aspect ratio and engine TIT were varied to satisfy the 10,000-ft field length requirement and to minimize the ramp weight. These data were generated at a wing loading of 120 psf which corresponds to the approach speed limit for this configuration.

The aspect ratio for the minimum weight point was unchanged from the 7.50 value of the reference aircraft. However, the engine TIT did increase by approximately 100°F over that of the reference aircraft. Larger ramp-weight reductions than the 3.61 percent value in Table 6.2 had been anticipated. Analysis of the data for the reoptimized aircraft revealed that the weights of the LFC gloves and equipment cancelled much of the benefit from its high cruise lift-to-drag ratio of 28.95. Also, in a chemical-fueled aircraft much of the benefit from the application of LFC is derived through a substantial reduction in fuel weight and a reoptimization of the wing sized by fuel volume requirements. Neither a significant fuel weight reduction or a wing reoptimization is realized by nuclear aircraft when LFC is applied.

6.3 NUCLEAR OPERATION

Guidelines for the nuclear subsystem in the reference aircraft were:

- A dose rate of 5 mr/hr at 20 ft in all directions from the reactor center.
- All JP fuel to be stored in the wing and not used as reactor shielding.
- The reactor to be inoperative during takeoff, climb, and emergency range cruise.

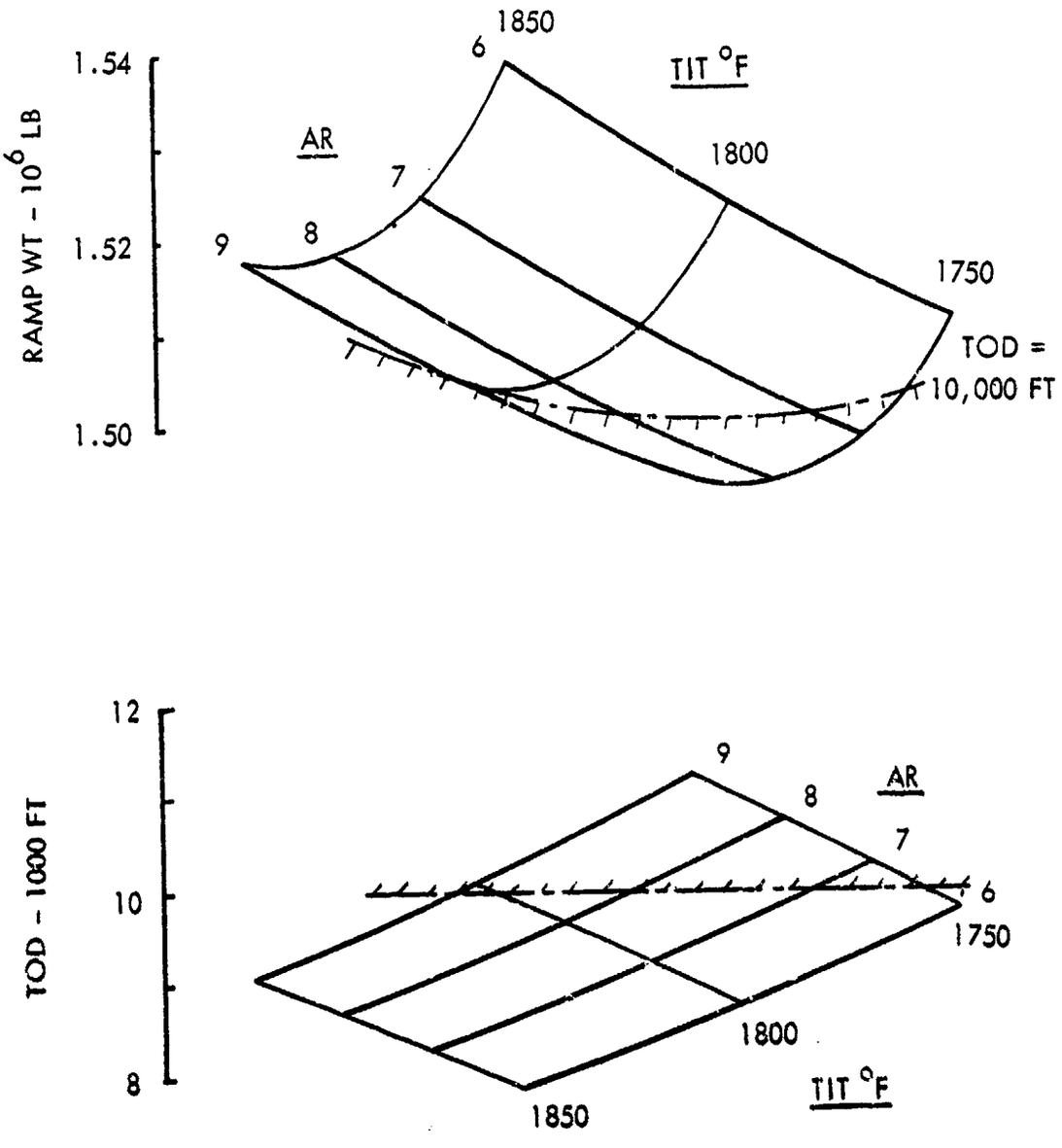

Figure 6-9. Aircraft Sizing for Laminar Flow Control.
Wing and Vertical Laminarized.
BPR = 8.4, W/S = 120 psf, M = 0.75
Altitude = 31,000 ft.

These guidelines are what the name implies, guidelines for the nuclear subsystem. Depending upon the level of safety required and demonstrable, variations to these guidelines may be in order. One portion of this study was devoted to assessing the effects of alternate guidelines on the reference aircraft design. The results of that assessment are listed in Table 6.3 and discussed subsequently.

TABLE 6.3. NUCLEAR OPERATION SENSITIVITY STUDY RESULTS

Distance to Dose Rate Applicability, ft	15	20*
Δ Ramp Weight	+1.81%	0
Shaped Shield	No *	Yes
Δ Ramp Weight	0	-2.48%
Emergency JP Fuel Used for Shielding	No *	Yes
Δ Ramp Weight	0	-5.74%
Reactor Used for Takeoff & Emergency Cruise	No *	Yes
Δ Ramp Weight	0	-7.88%
Combination of Preceding Three	No*	Yes
Δ Ramp Weight	0	-13.1%

* Reference Aircraft Design

6.3.1 Dose Rate Applicability Distance

In the reference aircraft, a bulkhead was placed 20 ft forward of the reactor center. At this distance, the dose rate had diminished to the guideline criterion of 5 mr/hr. The diameter of the nuclear subsystem containment vessel measured 18.2 ft. This meant that a 10.9-ft long section existed in the fuselage between the bulkhead and the containment vessel for reactor instrumentation and control systems. These systems require only 100 ft^3 of space out of approximately 2500 ft^3 available in the 10.9-ft long section. The effect of reducing this unused space by removing a 5-ft long portion of this fuselage section was investigated.

By removing the 5-ft section, the dose rate criterion was in effect changed to being 5 mr/hr at 15 ft from the reactor center. This reduction in distance for dose rate applicability required increased shielding weight with corresponding changes in other nuclear subsystem components, as shown by comparing the data in the first two columns of Table 6.4. The increase in nuclear subsystem weight exceeded the savings in fuselage weight, and produced the weight penalty indicated on the result summary of Table 6.3.

TABLE 6.4. WEIGHT SUMMARY FOR REACTOR SHIELDING VARIATIONS

Dose Rate Criteria	5 mr/hr at 20 ft forward and aft	5 mr/hr at 15 ft forward and aft	5 mr/hr at 15 ft forward	5 mr/hr at 15 ft forward with JP-4*
Reactor Subassembly	44,470 lb	41,970 lb	41,970 lb	41,970 lb
Reactor Shield	177,330	191,580	170,190	137,200
Heat Exchanger and Piping Shields	46,570	50,050	50,050	50,050
Auxiliary Equipment	12,040	12,040	12,040	12,040
Containment Vessel	99,510	102,620	102,620	79,220
Structure	4,000	4,000	4,000	4,000
Coolant	2,500	2,500	2,500	2,500
Miscellaneous Components	5,000	5,000	5,000	5,000
Additional JP Tankage				9,320
Total Nuclear System Weight	391,420 lb	409,760 lb	388,370 lb	341,300 lb

* 95,000 lb of JP-4

6.3.2 Shield Shaping

Since there are no manned positions aft of the reactor in the reference aircraft, a reduction in the aft shield thickness was investigated. By reducing the aft shield thickness to the values of the lateral shield thickness, a nuclear subsystem weight reduction of 21,390 lb was realized. The weight breakdown for this modification is shown in the third column of Table 6.4. This approach is conservative, since the same after-shutdown criterion is applicable and the scattering sources due to aft radiation leakage are much lower. The higher (500 mr/hr) dose rates from the sides, top, bottom and aft directions during operation were set to limit the air-reflected dose rate to approximately 1 mr/hr while maintaining the 5 mr/hr shutdown dose rate.

Actually, if not for the after-shutdown limit of 5 mr/hr in all directions after 30 min, the aft direction could be shielded less than the sides and still maintain about 1 mr/hr in scattered dose rate at the crew locations. Radiation in the aft direction would require at least two air scattering events to reach crew locations, rather than a single air

scatter from the lateral directions,and the crew dose rate from double air scatter would be negligible. Scattering from the bare surface metal of the aircraft wing and fuselage is slight. However, the portion of the wing containing JP-4 fuel is about 10-ft thick and has an appreciable albedo (radiation reflection coefficient) of 0.1. Assuming geometric attenuation inversely proportional to the square of the distance from the wing to a detector point, and very conservatively assuming the entire fuel-containing wing area is exposed to the same flux as the closest region, the reflected dose rate from the wing would be 0.22 mr/hr. This is negligible.

Only the inboard engines are near enough to the fuselage (about 25 ft) to produce any significant scatter source. Proceeding as with the wing region and noting that the engines are 50 ft from the reactor, the dose rate at possible crew locations in the aircraft is negligible since the engines have much less surface area than the fuel-containing portion of the wing.

The wing support structure location directly above the fuselage is most favorable as a scatter source from geometric considerations. However, since impingent radiation must traverse a longest path-length slant trajectory through the primary shield, the direct radiation level at the wing support locations is much less than 5 mr/hr. Hence the support structure can also be ignored as a scatter source.

With the reduction in nuclear subsystem weight for the shaped shield, a weight savings of 2.48 percent was realized, as noted in Table 6.3 for the reference aircraft.

6.3.3 Use of JP Fuel for Shielding

Some chemical, JP-4, fuel is carried for use during takeoff, climb, descent and landing and to provide a chemically-fueled emergency cruise capability if the reactor should have to be prematurely shut down in flight. Because of its availability and its characteristics, consideration has been given to the use of this fuel as shielding, thereby reducing the weight of the reference shield material.

The use of JP fuel as shielding material impacts the design and weight of the primary shield and containment vessel diameter. The basic NuERA II system did not use JP shielding because of its design guidelines, however, a brief analysis of the use of JP fuel as a shield was included in Ref. 3. These data were used to determine the JP fuel shield geometry and the resulting primary shield weight reduction for this study. Some of the pertinent considerations of the JP fuel shielding analysis given in Ref. 3 are repeated herein for completeness.

The basic shielding characteristics of JP-4 fuel for neutrons and gammas are shown in Figure 6-10. It is apparent that JP-4 is a relatively good neutron shield material because of its hydrogen content. Based on density and removal cross section, it is approximately two-thirds as effective as lithium hydride (LiH) on a linear basis. Hence, any shield concept employing fuel outside the containment sphere would especially relieve the neutron shield requirements of the primary shield around the reactor. Such a tradeoff would ultimately be limited by the capture and activation sources generated in the containment sphere material, which would be important because of the increased neutron leakage incident on this region.

In the reference aircraft, 95,000 lb of JP fuel are available for use as shielding. This fuel must be available for use when needed, and therefore, must be stored external to the containment vessel. For the purposes of this study, it was assumed to be stored in a constant thickness tank surrounding the spherical containment vessel. The shielding effect of the fuel allows the LiH thickness to be reduced and therefore the containment vessel diameter to be reduced. The smaller containment vessel diameter in turn allows the inside diameter of the fuel tank to be reduced which increases the thickness occupied by the 95,000 lb of fuel. Through an iterative process, the weight estimates shown in the fourth column of Table 6.4 were derived. They include a reduction of lithium hydride thickness by 15.4 in. in all directions and a fuel thickness of 22.5 in. in all directions.

The data in Table 6.4 show that the use of 95,000 lb of JP fuel as shielding allows a reduction of 47,070 lb in nuclear system weight. The net effect of this savings was to

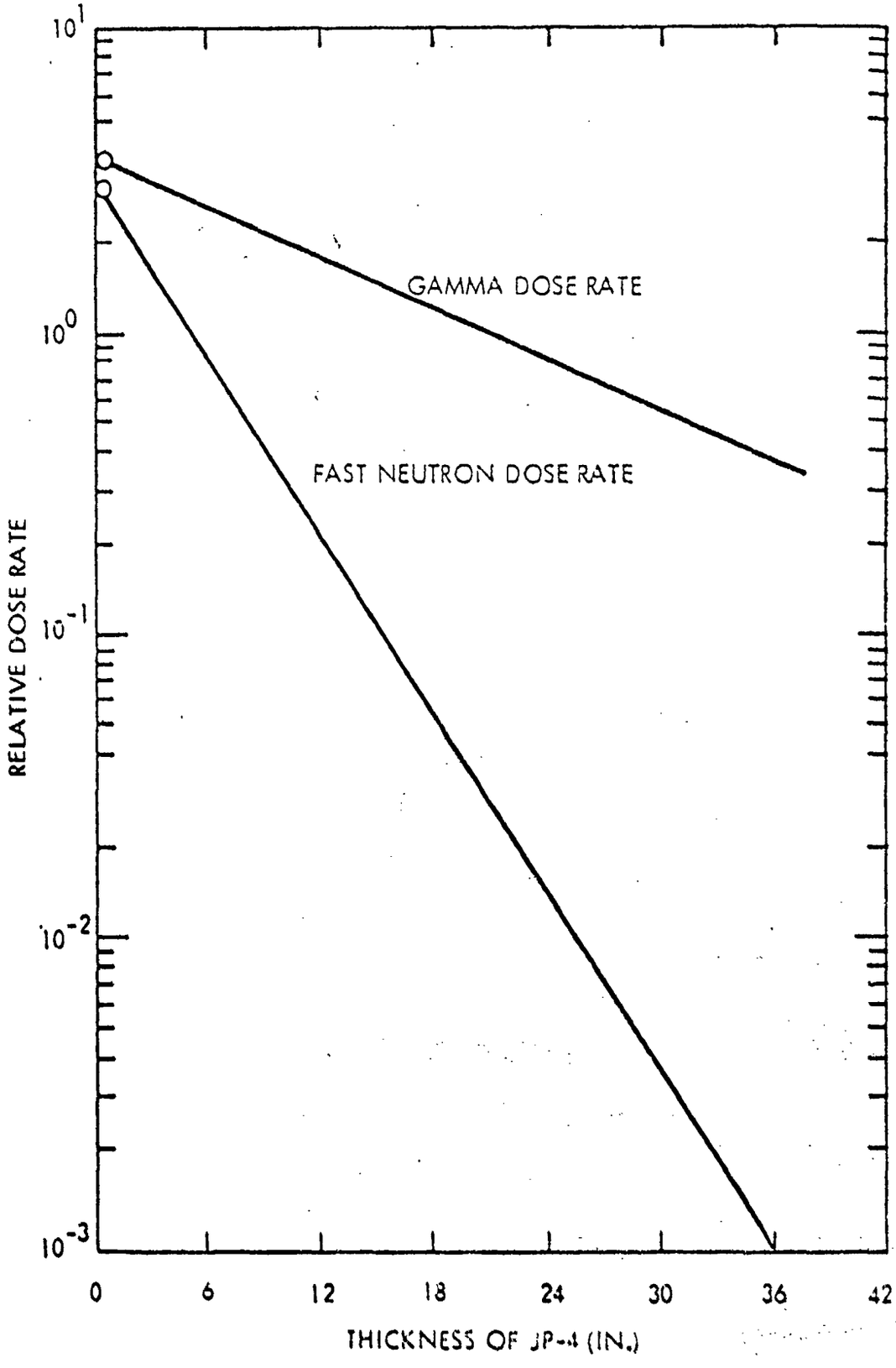

Figure 6-10. Radiation Attenuation Characteristics of JP-4 Fuel

reduce the ramp weight of the reference aircraft by 5.74 percent, as noted in Table 6.3.

The significant weight scvings by thinning the LiH region, made possible by using the JP-4 recovery fuel as an auxiliary radiation shield, is not without potential problems which must be considered. It must be assured that the quality of the fuel is not reduced because of radiation damage to an extent such that the fuel would be unsatisfactory when needed. Another consideration is that of increased heating rate and/or radiation damage to the containment vessel because of effectively moving some of the shield material to a location outside of the containment vessel. Another similar effect that must be considered is that the containment vessel becomes a source of increased gamma radiation through its exposure to a higher neutron flux. All of these potential problems were examined for the case under study, and it was determined that the substitution of JP fuel for a portion of the lithium hydride shield would be acceptable. The results of the examinations are summarized below.

The shielding changes summarized in Table 6.4 are the result of substituting JP fuel for a portion of the LiH on the basis of achieving the same neutron attenuation. This is conservative because the thickness of fuel also provides greater gamma attenuation than does the thickness of the LiH removed.

The flux level incident on the containment vessel in the reference aircraft shield configuration is at most 490 mr/hr. This is increased to 89 R/hr after the removal of 15.4-inches of LiH which is allowable when 95,000 lb of fuel are used as shielding. If it is conservatively assumed that all of the fuel would see this dose rate for the total 10,000 full power hours, the energy absorbed in the fuel would be on the order of 9×10^7 ergs/gm. Tests* have shown that degradation of fuel performance, thermal stability, or sludging does not occur until exposures of approximately 2×10^9 ergs/gm. It is therefore clear that degradation of the fuel is not a problem in this case. However, prudence would indicate that good operating procedures would be to transfer fuel after

* J. F. Kircher and R. E. Bowman, "Effects of Radiation on Materials and Components," Reinhold Publishing Corp., 1964. (Ref. 14)

each flight from the shield tank to the tanks used for takeoff and landing. This would help to insure that no unusual fuel degradation would occur if unexpectedly high localized radiation streaming should occur. Further, at this energy deposition rate, no significant heating of the fuel will occur.

The after-shutdown dose rate 20-ft from the reactor center in the lateral directions was determined to be 3.7 mr/hr for the NuERA II base case, 0.04 mr/hr of which came from activation of the containment vessel. The increased neutron flux level arising from removal of 15.4-in. of lithium hydride results in an increase of the containment source to 7.2 mr/hr. The 22.5-in. thick layer of JP-4 would attenuate the radiation source by a factor of 4.3 to a level of 2.5 mr/hr which is acceptable. It does mean, however, that any JP-4 used from the shield tank should be replaced before maintenance is accomplished.

6.3.4 Alternate Reactor Utilization

The guideline to have the reactor inoperative during ground proximity operations evolved more than a decade ago as a safety measure consistent with the existing technology development. At that time, there was no accepted method for containing the radioactive elements of a hot reactor in the event of an aircraft crash. Since more than two-thirds of large aircraft flight-related accidents occur during taxi, takeoffs and landings, the safest approach was to have the reactor inoperative for these phases of flight.

In recent years, NASA* has demonstrated the feasibility of a spherical metal shell to contain the reactor system elements during a crash. While this concept requires additional development, it appears the guideline on reactor operation can be relaxed. Such an approach was adopted for this sensitivity study. The reactor was assumed to be fully operational during all normal flight phases with chemical fuel augmentation available for the high thrust phases of takeoff and climb. During the emergency cruise

* R. L. Puthoff, "A 1055 Ft/Sec Impact Test of a Two-Foot Diameter Model Nuclear Reactor Containment System Without Fracture," NASA TM X-68103, June 1972. (Ref. 15)

phase, the reactor was assumed to be at half power, and chemical fuel augmentation supplied the additional thrust requirements.

The reference aircraft design was reoptimized for this alternate reactor utilization philosophy, thereby achieving a 7.88 percent reduction in ramp weight, as shown in Table 6.3. In the reoptimization, the reference aircraft aspect ratio was reduced from 7.50 to 6.55. The engine TIT required for the 10,000-ft field length dropped from 1673°F to 1638°F, while the wing loading of 120 psf remained constant due to the approach speed limitation.

6.3.5 Alternate Operational Philosophy

The preceding three nuclear system guidelines, which were beneficial in reducing aircraft weight, were applied jointly to determine the total effect of a more liberal nuclear operating philosophy. In summary, the alternate guidelines permitted special shaping of the shielding, use of emergency range JP fuel for shielding, and the reactor at full power during all normal flight operations and at half power for emergency cruise.

Figure 6-11 contains the parametric data from which the optimum alternate reference aircraft was selected. The alternate aircraft has a 13.1 percent lower ramp weight than the reference aircraft. This total savings is less than the sum of the three options considered individually, as noted in Table 6.3, because of the compounding effects. Less emergency range JP fuel was required, and hence the benefits from using the JP fuel for shielding were smaller. Also, the reactor system was smaller so that less savings were realized for shaping the shield.

Pertinent design features of the alternate aircraft are summarized in Table 6.5 and a weight statement is presented in Table 6.6. In external appearance, the alternate aircraft is very similar to the reference aircraft shown in Figure 5-5 with only slight differences in the wing planform. The flight envelope for the alternate aircraft is presented on Figure 6-12.

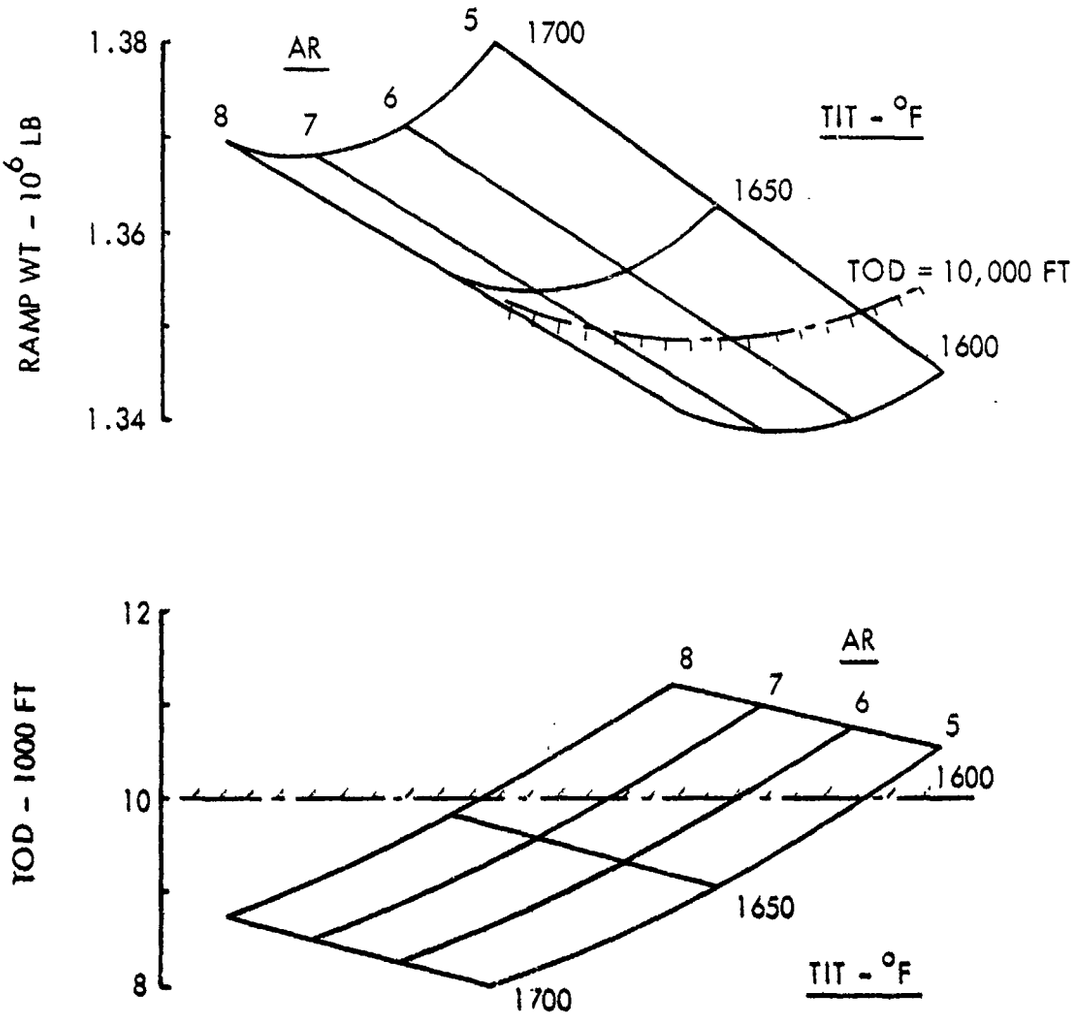

Figure 6-11. Alternate Nuclear Philosophy Aircraft Sizing Data

TABLE 6.5. ALTERNATE REFERENCE AIRCRAFT DESIGN CHARACTERISTICS

Cruise Mach Number	0.75
Cruise Altitude	31,000 ft
Wing Sweep Angle	30 deg
Wing Loading	120 psf
Aspect Ratio	6.40
L/D	21.38
Cruise Lift Coefficient	0.508
Field Length	10,000 ft
Propulsion	
Reactor Size	218 MW
No. Engines	4
Engine Thrust, SLSD	74,208 lb
Engine Design JP TIT	1629°F

TABLE 6.6. ALTERNATE REFERENCE AIRCRAFT WEIGHT SUMMARY

	Lb
Wing	105,973
Horizontal	6,497
Verticals	10,616
Fuselage	107,614
Landing Gear	59,050
Nacelle and Pylon	20,343
Propulsion	
Engines Installed	70,590
Nuclear Subsystem	346,819
Engine HX & Ducts	114,097
Auxiliary Cooling	12,355
Fuel System	1,939
Systems and Equipment	45,822
Operating Weight Empty	901,715
Payload	400,000
JP Fuel	51,405
Ramp Weight	1,353,120

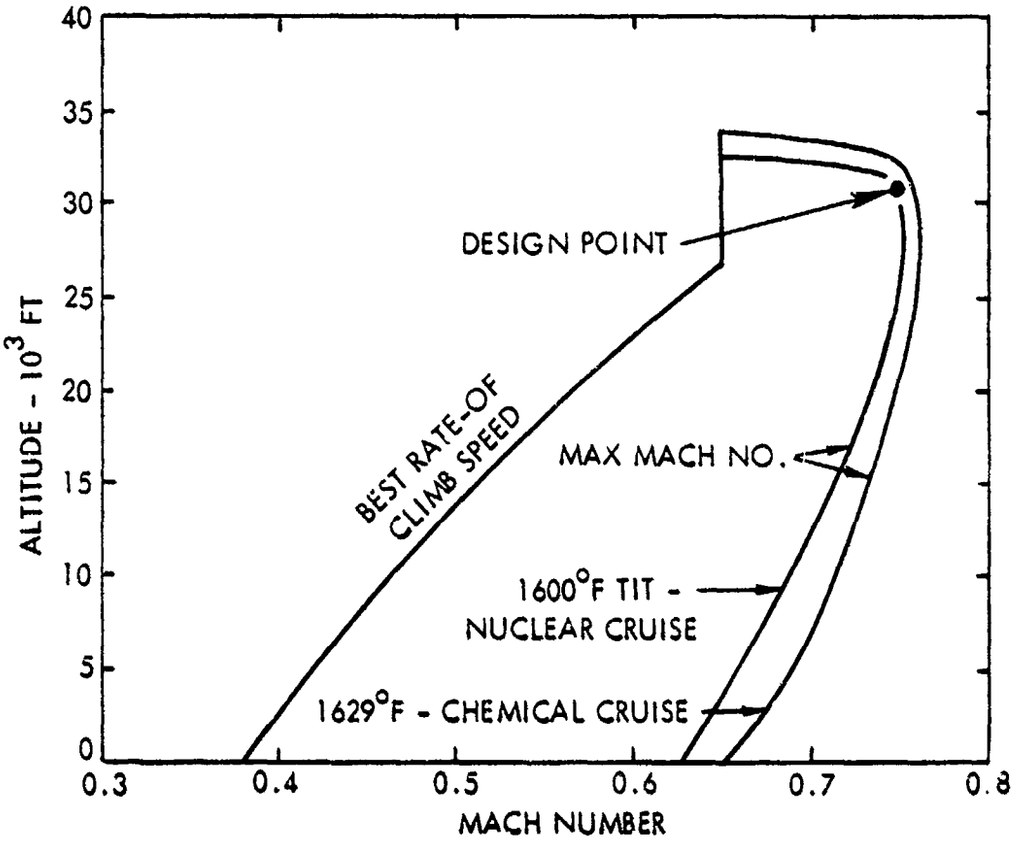

Figure 6-12. Alternate Aircraft Altitude - Mach Number Flight Envelope

6.4 ALTERNATE MISSIONS

The available volume inside the fuselage of the reference aircraft was configured for containerized or palletized cargo and for outsized and mobile equipment. The interior could just as easily have been configured for personnel accommodations, computers, communications systems, and other specialized equipment required for a variety of alternate missions. Extensive reconfiguration of the fuselage interior for alternate missions was not undertaken in this study due to a lack of data on mission requirements. However, this does not preclude the use of the reference aircraft for other applications.

Prime alternate missions, which could readily be accomplished with appropriate versions of the reference aircraft include:

- o Airborne Weapons Launcher
- o Tanker
- o Airborne Command Post
- o Airborne Warning and Control
- o Sea Lane Control
- o Anti-Submarine Warfare
- o Airborne Battle Platform

Figure 6-13 shows a possible arrangement concept of a delivery system for an airborne weapons launcher mission. This system is suitable for either the Air Force Air Launched Cruise Missile (ALCM) or the Navy Sea Launched Cruise Missile (SLCM). Both are considered to be long range cruise missiles with their 1500 to 2000 n.m. range capability. In size, these missiles weigh approximately 3000-lb each, and are about 21-ft long and 2-ft in diameter.

The delivery system consists of mechanized storage racks for transporting the missiles aft to a delivery elevator and bomb-bay door. The length of the racks are dependent upon the number of missiles to be carried. Depending upon the mission definition, a portion of the fuselage forward of the racks could be configured for personnel if a long time on station is envisioned prior to missile launch.

In a tanker mission role, modular tanks for carrying JP fuel could be positioned in the cargo compartment, similar to loading containerized cargo. Due to the heavier fuel density relative to that of the containerized cargo, the height of the fuel tanks would be about one-fifth that of the containers to achieve a uniform payload distribution over the entire floor area. Thus, there would be plenty of space for inter-connecting the tanks in a relatively short period of time. Booms for refueling other aircraft would be

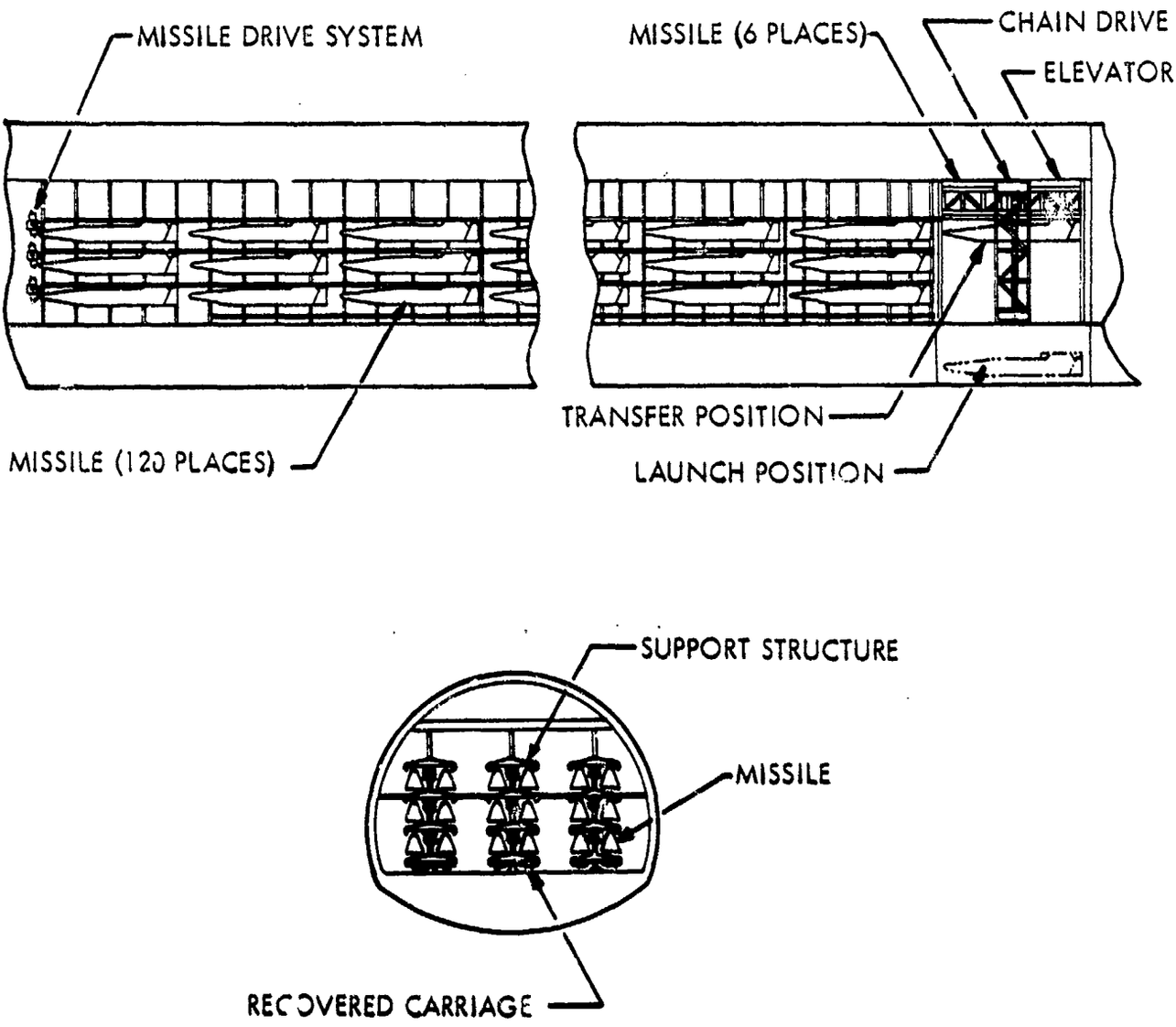

Figure 6-13. Long Range Cruise Missiles - General Arrangement

positioned in the aft fuselage behind the reactor and at each wingtip. More than adequate space exists at all three locations for a boom operator.

The reference aircraft is capable of serving as a joint military/civil airlift transport. No changes would be made to the reference design unless some compromises are made on military and civil requirements. Due to the more stringent military design specifications, the reference aircraft would suffer weight penalties relative to an aircraft designed for the civil market. For example, the heavy floor structure required by the military for wheeled and tracked vehicles would be eliminated in a commercial transport. The commercial approach might conceivably consist of just an integral container-rail system without any floor.

7.0 ECONOMIC ANALYSES

Costs of the reference aircraft were estimated following accepted military and civil practices. In both cases, the breakdown of the cost into its various elements is in such detail that the portions of the total life-cycle cost allocated to research, development, production and operation are readily discernible. All of these cost estimates are in constant January 1975 dollars, without allowance for any future inflation or escalation. Also included are the cost sensitivities to variations in fuel price and nuclear propulsion research and development.

7.1 MILITARY COSTING

Twenty-year life-cycle costs (LCC) of the reference aircraft in military service were estimated using a previously developed methodology* which incorporates the intent of the pertinent Air Force regulations and guidelines.** Figure 7-1 gives a breakdown of the various elements that contribute to military life-cycle costs. As illustrated in the figure, the two major categories are the total acquisition cost and the system operation and support cost. Following the breakdown further, the acquisition cost consists of the production program cost and the total research, development, testing and evaluation (RDT&E) cost.

7.1.1 RDT&E Costs

Table 7.1 summarizes the cost estimates presented in Appendix E for the prototype validation and full-scale development phases of the RDT&E program. The validation

* "Advanced STOL Transport (Medium) Study, Cost and Schedule Data," Volume VII, Technical Report ASD/XR 72-22, Lockheed-Georgia Company, 1972. (Ref. 16)

** "Cost Analysis, USAF Cost and Planning Factors," AFR 173-10, Department of the Air Force, 1975. (Ref. 17)
"Program Management," AFR 800-2, Department of the Air Force. (Ref. 18)
"Work Breakdown Structures for Defense Material Items," MIL-STD 881A. (Ref. 19)
"Operating and Support Cost Estimates, Aircraft Systems," Defense Systems Acquisition Review Council, May 1974. (Ref. 20)

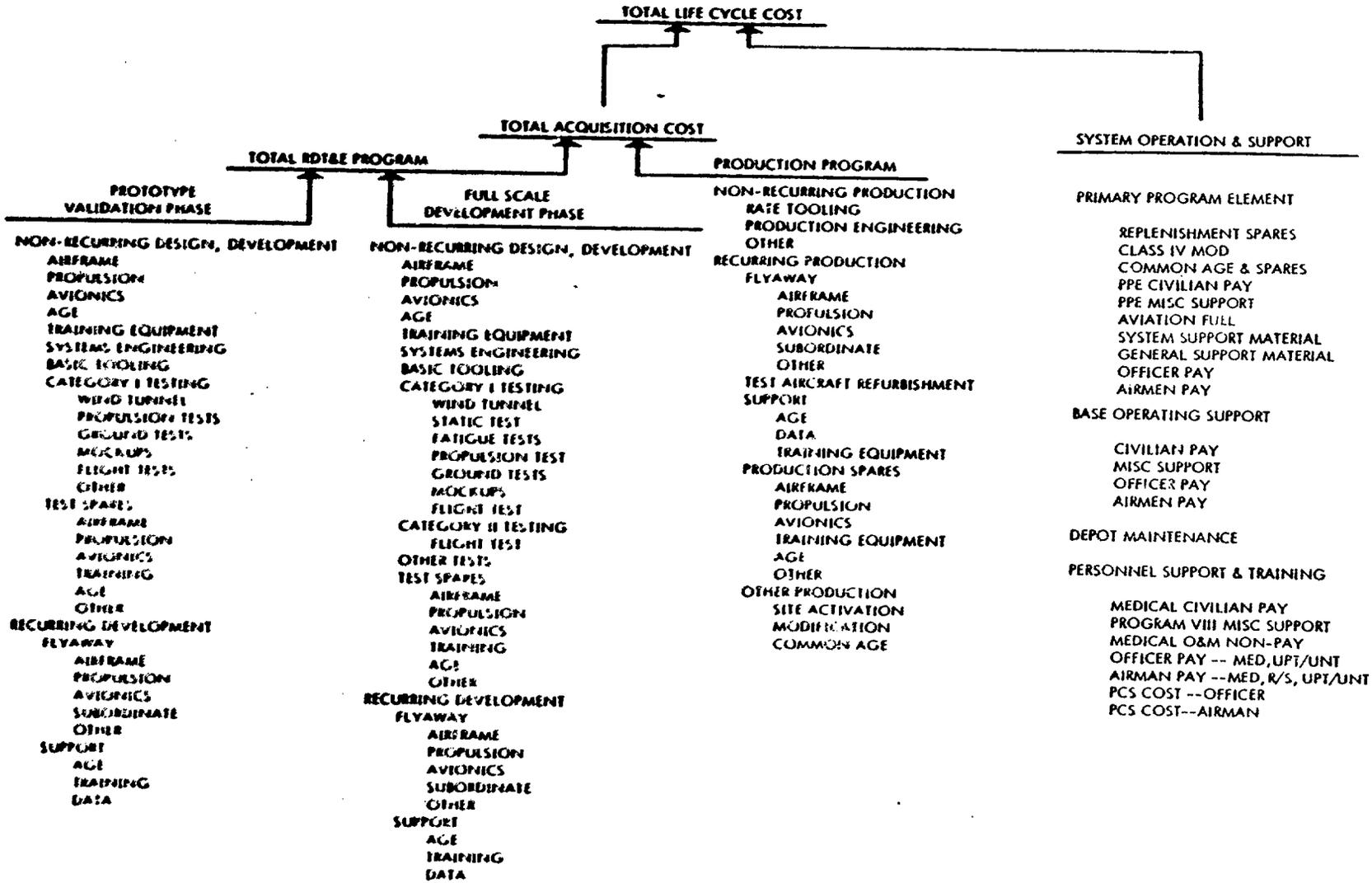

Figure 7-1. Life-Cycle Cost Elements

TABLE 7.1. SUMMARY OF MILITARY RDT&E PROGRAM COSTS

	Prototype Validation (2 Aircraft) Million $		Full-Scale Development (4 Aircraft) Million $	
Conceptual Studies	1.2		3.7	
Non-Recurring Design & Development				
Aircraft	182.6		411.9	
Propulsion*	0.0		0.0	
Nuclear Subsystem	1372.5		877.5	
Avionics*	0.0		0.0	
System Engr. & Management	9.1		61.8	
Basic Tooling	190.0		544.6	
System Test	75.9		474.0	
Test Spares	26.6		110.2	
Total Non-Recurring R&D		1857.9		2483.7
Recurring Development				
Airframe	342.7		575.4	
Propulsion	29.4		54.2	
Nuclear Subsystem	78.9		157.8	
Avionics	1.0		2.0	
ECO's	13.7		32.6	
Total Flyaway		465.7		822.0
Unit Flyaway	232.8		205.5	
Support	2.4		70.2	
Total Recurring Development		468.1		892.2
Total		2326.0		3375.9
Total RDT&E				5701.9

* Included with Vendor Cost of Item Listed under Recurring Costs

phase is intended to prove the operational capability and feasibility of an aircraft. For costing purposes, it encompassed the design, development, and limited testing of two prototype aircraft.

Sometime after completion of the prototype validation phase, a decision is made to begin the follow-on, full-scale development phase which entails an RDT&E program of design, development, and fabrication of four flight-test aircraft, including propulsion and all the mission subsystems. Static and fatigue test articles are included along with Category I and II test programs in estimating the costs. In addition, the test cost includes allowances for the many subsystem qualification, reliability and maintainability checks that must be performed.

The non-recurring costs associated with the R&D program for the nuclear subsystem were estimated to be 1.75 billion dollars with an additional 0.5 billion dollars required for facilities. Of all the elements in the total RDT&E cost of 5.7019 billion dollars, the 40 percent represented by the nuclear subsystem non-recurring cost of 2.25 billion dollars probably has the greatest uncertainty of any. The reasons are severalfold. Firm definition of the specific development program which will be necessary requires extensive study and agreements by all government agencies involved. It also requires more detailed propulsion systems and nuclear subsystem design so that the specific R&D efforts needed can be better quantified. Further, the cost is very dependent upon the specific type of reactor which is chosen for development and the specific program requirements imposed during the development.

A nominal R&D program duration of fifteen years was assumed for the costing analysis as representative, based on the experiences of the Aircraft Nuclear Propulsion (ANP) and the NERVA nuclear rocket programs. Significant changes to the schedule would probably increase the costs.

As a basis of comparison, the nuclear system R&D costs for the ANP and NERVA programs were reviewed. Both of these programs were terminated before the systems were proven. This consideration would indicate that a completed development program

would incur greater costs. Of course, the dollar inflation over the intervening years would also increase the magnitude of costs today. However, there are additional factors which would tend to lower the costs. The reactor design guidelines today are considerably simpler and the technology base is improved significantly. Both the ANP and NERVA programs were redirected several times; the Government Accounting Office documented seven basic reorientations of the ANP program during a ten year period. The cost estimates for this study are based on the assumption of no study redirections.

Total costs of 1.04 billion dollars were incurred between 1946 and 1961 on the ANP program with an estimated 1.0 billion additional dollars needed for completion. Between 1955 and 1972, a total of 1.4 billion dollars were expended on the NERVA program. When these costs are adjusted for estimated effects of redirection, completion, inflation, and different scope, the total estimate of 2.25 billion dollars for this study appears to be reasonable. Significant cost increases could accrue from extensive program redirections or from the selection of a reactor without a firm technology base. Conversely, the R&D costs associated with the nuclear subsystem development for aircraft propulsion could be reduced by sharing the basic reactor development for another application, such as a surface effects ship.

In the non-recurring cost category, no allocation was made for either engines or avionics. Both of these items were assumed to be purchased from the manufacturer with the R&D cost included in the purchase price. Thus, the total costs of each of these items are listed in the recurring cost category.

7.1.2 Production Costs

The value and versatility of the computer model used to cost the production aircraft is the result of the model logic. The various aircraft subsystems were costed separately and then combined to obtain the cost of the total aircraft. The flexibility of the model, which permits ready addition of new subsystems and accurate costing of the individual subsystems, provides a large improvement over parametric models which use aircraft physical and performance data to derive costs.

Production costs generated by the model for the reference aircraft are presented in Table 7.2. Labor and material rates were derived for each of the subsystems listed through the "Total Empty Manufacturing Cost" category in the table. (Actual values for these subsystems are tabulated in Appendix E.) Learning curve slopes of 75 and 89 percent for labor and material, respectively, were used to develop the costs for 250 production units. The values shown in the table represent the average unit costs for this fleet size.

Cost of the nuclear subsystem was estimated using a procedure similar to that for the aircraft. Specific materials required for each of the major components of the subsystem were discussed with suppliers of raw materials to establish a basic material cost per pound. Whenever a choice of material grades was available for a particular component, such as shielding and the working fluid, the material with the higher purity level, usually designated for nuclear service, was selected. Manufacturing costs for each component were determined based on the type of material and the ease or difficulty of fabrication, and were added to the raw material cost. The manufacturing cost estimate was tempered by the experience gained during the manufacture of similar type items for the reactors tested during the NERVA program and components fabricated for the Fast Flux Test Facility.

Each of the major components of the nuclear subsystem and the associated costs are listed in Table 7.3. An uncertainty factor of 1.5 was applied to account for the numerous small components which were not individually included. Assembly of all the components inside the containment vessel and an engineering checkout of the subsystem was estimated to be an additional 5 million dollars. With fuel priced at $0.65 per million Btu, the total cost of the initial nuclear subsystem increased to 35.6 million dollars with the addition of fuel for 10,000 hours of operation.

Production costs for the first six nuclear subsystems were assumed to be constant. Between the sixth and twenty-fourth units, a learning curve slope of 85 percent for reducing the unit production cost was judged reasonable based on the experience with other nuclear systems. After the twenty-fourth unit, the production costs were assumed to remain constant. The learning curve effect was taken into account in determining

TABLE 7.2. MILITARY PRODUCTION COST

	Thousand $ Per A/C	
Wing	10,860	
Tail	1,340	
Body	7,230	
Landing Gear	1,834	
Flight Controls	913	
Nacelles & Pylons	3,291	
Engine Installation	125	
Fuel System	225	
Lube System	2	
Instruments	415	
Hydraulics	239	
Electrical	263	
Electronics Racks	157	
Furnishings	384	
Air Conditioning	304	
APU	180	
Final Assembly	3,241	
Production Flight	1,576	
System Integration	1,883	
Total Empty Mfg. Cost		34,462
Sustaining Engineering	2,606	
Prod. Tooling Maint.	3,656	
Quality Assurance	3,745	
Airframe Fee	9,228	
Airframe Cost		53,697
Engine Cost with Fee and Warranty	9,694	
Avionics Cost	500	
Nuclear Subsystem	22,229	
Nuclear Secondary Systems	4,285	
Engine Heat Exchangers	3,214	
Equipment GFE/CFE	2,757	
Total Support	3,073	
Total Production Spares	17,813	
Total Recurring A/P Unit Cost		117,262

TABLE 7.3. NUCLEAR SUBSYSTEM COST SUMMARY

Component	Material	Weight (lb)	Cost (10^6 $)
Containment Vessel	Haynes-188	99,507	1.9
Reflector and Shields	Nickel and Tungston	21,286	1.1
Inner Shield	Zirconium Hydride	129,472	1.7
Outer Shield	Lithium Hydride	47,861	1.1
Primary Fluid	Lithium - 7	644	1.4
Pressure Vessel	Columbium 1% Zirconium	4,035	1.0
Pipe	Columbium 1% Zirconium	1,283	1.1
Support Plates	Columbium 1% Zirconium	3,000	0.7
Primary Pumps	Columbium 1% Zirconium	4,531	3.0
Intermediate HX	Columbium 1% Zirconium	6,228	4.0
Total Cost for Major Components			17.0
Uncertainty Factor			x 1.5
Total Cost for Nuclear Subsystem Components			25.5
Assembly and Engineering Checkout			5.0
Assembled Nuclear Subsystem Cost			30.5
Fuel (at $0.65 per million Btu)			5.1
Total			35.6

the nuclear subsystem cost in Table 7.2 for the reference aircraft. The value shown represents the average price for the total fleet of 250 aircraft without nuclear fuel.

A similar approach was followed to derive the costs for the nuclear ducting, auxiliary cooling, and instrumentation. Various components of this secondary system are listed in Table 7.4 along with the estimated costs. The nuclear subsystem learning curve effect was also applied to the nuclear secondary system and is reflected in the value for the secondary system in Table 7.2.

TABLE 7.4. SECONDARY SYSTEM COST SUMMARY

Component	Material	Weight (lb)	Cost (10^6 $)
Hot Duct			
Pipe, Hangers & Valves	Haynes-188	20,936	1.50
Insulation	Alumina Silica	16,160	0.20
Working Fluid	NaK 78%	6,978	0.05
Cold Duct			
Pipe, Hangers & Valves	Haynes-188	9,743	0.70
Insulation	Alumina Silica	11,189	0.13
Working Fluid	NaK 78%	7,611	0.06
Pumps and Motors	Haynes-188	7,176	0.75
Intermediate Heat Exchanger	Haynes-188	4,909	0.90
Pipe and Insulation	Haynes-188	884	0.03
Instrumentation & Control	---	2,000	1.00
Total Secondary System Cost			5.32

7.1.3 Acquisition Costs

The total military acquisition cost for a fleet of 250 reference aircraft was estimated to be 34.797 billion dollars. The derivation of this value is presented in Table 7.5.

TABLE 7.5. MILITARY ACQUISITION COST DERIVATION

	Million $
Military Recurring Cost	28,846
Refurbish Test Aircraft	20
Initial Personnel Training	3
Modification & Update Kits	2
Total Recurring Production Cost	28,871
Total Non-Recurring Production Cost	224
Total Production Cost	29,095
Total RDT&E	5,702
Total Acquisition Cost	34,797
Unit Acquisition Cost	139

The military recurring cost shown is the product of the unit production price of 117 million dollars from Table 7.2 and a fleet size of 246 aircraft. Four additional aircraft were produced for the RDT&E program and are accounted for therein. However,

some refurbishment of these four aircraft is required which will also involve limited personnel training and modification kits.

The total production cost includes 224 million dollars for non-recurring costs expended for tooling and production engineering. The RDT&E cost was previously shown in Table 7.1.

7.1.4 System Operation and Support Costs

The Air Force has designed a Budget Annual Cost Estimating (BACE) Model to provide a standard approach for developing individual aircraft annual operating cost estimates for planning studies. Basically, the model computes the annual operating functions which are closely identified to a squadron or which can be allocated to individual squadrons of aircraft. The cost elements and equations of this Air Force model are part of Lockheed's military costing model, which was used to determine the annual and 20-year life-cycle operating and support costs.

The manpower required to perform the operation and support of the aircraft system is presented in Table 7.6. The values shown are for a crew ratio of 2.25 and for aircraft annual utilization rates of 1080 hr in peacetime and 2160 hr in wartime.

Estimates of the system operation and support costs are summarized in Table 7.7; further breakdowns of the summarized cost elements are included in Appendix E. The first column of cost data in the table is for 20-year operation of the fleet, the next two are for annual operation of a squadron and the fleet, and the last is for hourly operation of a single aircraft. Generally, Air Force data and recommendations (Ref. 17) were the source of cost factors and unit element values used in the cost estimates. Since nuclear propulsion systems are not addressed in Ref. 17, special approaches were dictated to evaluate the cost elements affected by nuclear power.

Replenishment spares, the first element of the primary program listing in the table, is one of the items requiring a separate evaluation. For a comparably-sized JP-fueled

TABLE 7.6. PERSONNEL REQUIREMENTS FOR SQUADRON OPERATION AND SUPPORT

Type of Personnel:	Officers	Airmen	Civilians	Total
Flight Crew	144	36	0	180
Maintenance	23	1010	128	1161
Security	0	55	0	55
Wing Base Staff	8	9	0	17
Primary Program Element	175	1110	128	1413
Base Operating Support	4	181	38	223
Medical Support	5	16	4	25
Total	184	1307	170	1661
16 Aircraft/Squadron		15.625 Squadrons		

aircraft, a value of $362 per flight hour would be recommended. An additional $1079 per flight hour was included for nuclear subsystem replenishment. This extra cost is incurred by the removal, refueling, and refurbishment of the nuclear subsystem after each 10,000 hours of nuclear operation. Certain components of the nuclear subsystem, besides the fuel elements, will require replacement at the time of refueling because of unavoidable destructive disassembly, component wear-out, or end of component design life. Only through extensive design studies could the particular components requiring

TABLE 7.7. MILITARY OPERATING COSTS

	20-Year Fleet Operation Million $	Annual Squadron Operation Million $	Annual Fleet Operation Million $	Hourly Aircraft Operation $/Hr
Replenishment Spares	7,782	24.90	389	1,441
Class IV Mod & Spares	2,636	8.44	132	488
Common AGE & Spares	613	1.96	31	113
Misc. Support	25	0.08	1	5
Aviation Fuel	3,259	10.43	163	604
System Support Material	1,706	5.46	85	316
General Support Material	567	1.81	28	105
Civilian Pay	625	2.00	31	116
Officer Pay	1,178	3.77	59	218
Airmen Pay	3,274	10.48	164	606
Maintenance Pay	3,759	12.03	188	696
Total Primary Program	25,424	81.36	1,271	4,708
Base Operating Support	914	2.93	46	169
Depot Maintenance	9,540	30.53	477	1,767
Personnel Support & Training	780	2.50	39	144
Total Operating Cost	36,658	117.32	1,833	6,788

replacement be identified. Consistent with the intent of this study, a very cursory analysis indicated that 50 percent of the non-fuel nuclear subsystem cost would be reincurred at each refueling cycle for refurbishment labor and material.

Refueling will not occur until well after the 24th nuclear subsystem has been produced, beyond which the production cost of the system without fuel will have been reduced through the effect of the learning curve from the initial 30.5 million dollars shown in Table 7.3 to a constant 22.04 million dollars. The $1079 per flight hour for replenishment spares is 50 percent of the constant production cost prorated over a 10,000-hr nuclear design lifetime. For this cost estimation, the average mission was assumed to be one day in duration and cover 10,500 n.m. During this mission, JP fuel will be used for one-half hour for the takeoff, climb, and landing phases of flight and nuclear power will operate for 23.5 hours of cruise time. This gives 24 flight hours for every 23.5 hours of nuclear operation.

A total of 45.66 maintenance manhours per flight hour was used in calculating other maintenance elements. Of this total, 3.16 hours are for maintenance of the engine heat exchanger and the secondary nuclear system components, all of which are external to the nuclear containment vessel. Due to its very high design reliability, no maintenance is envisioned for the nuclear subsystem except at refueling, and that has been included in replenishment spares. Maintenance material costs of $75 per flight hour were included for the engine heat exchanger and secondary nuclear system components.

The aviation fuel element includes the cost of both the nuclear fuel at $0.65 per million Btu and the JP fuel at $0.40 per gal. For the assumed one-day mission range of 10,500 n.m., JP fuel is used for the first 189 n.m. as the aircraft takes off and climbs to its 31,000-ft cruise altitude.

The total 20-year life-cycle cost to the military for the fleet of 250 aircraft is 71,455 million dollars. This value was obtained by combining the 20-year fleet operating cost of 36,658 million dollars from Table 7.7 with the total acquisition cost of 34,797 million dollars from Table 7.5.

7.2 CIVIL COSTING

Measures of the costs of aircraft operating in the commercial environment differ somewhat

from those used by the military. In the area of acquisition costs, most of the differences are of a bookkeeping nature. However, alternate philosophies are pursued in the areas of operating and life cycle costs. Some of the differences between the military and civil costing approaches are pointed out by comparison during the derivation of the civil acquisition, direct operating and life-cycle costs.

7.2.1 Acquisition Costs

Civil R&D costs for the reference aircraft of Section 5.2 and the alternate reference aircraft of Section 6.3 were generated using a Lockheed costing model which has shown excellent correlation with recent large civil aircraft programs, such as the L-1011. The major elements contributing to the total civil R&D cost of approximately 5.5 billion dollars for the reference aircraft are presented in Table 7.8. No costs are listed for avionics and engine R&D since they are included in the production costs for these systems.

TABLE 7.8. CIVIL R&D COSTS

	Million $
Develop Tech Data	58.9
Design Engineering	1309.1
Development Tooling	1225.2
Development Test Article	293.0
Flight Test	150.7
Special Support Equipment	15.7
Development Spares	193.6
Engine Development*	0.0
Avionics Development*	0.0
Reactor Development	2250.0
Total R&D	5496.2
Unit R&D for 250 Aircraft	21.9

* Included in Cost of Vendor Item Purchased During Production

The reactor development cost of 2.25 billion dollars is the same value which was used for the total military reactor R&D. To account for the high level of composite material usage, the design engineering and development tooling values include increases of 34 and 76 percent, respectively, over the values for an all-aluminum aircraft.

A comparison of the military RDT&E costs in Table 7.1 with the civil R&D costs shows the final values to be quite similar. The greater number of breakdowns in the levels of military costs are the result of the military approach of dividing the R&D program into prototype and full-scale development phases.

Civil production cost elements are identical to those shown previously in Table 7.2 for the military with the exception of the last three elements. Rather than repeat the major portion of that prior table, the simpler approach illustrated in Table 7.9 was adopted for presenting the derivation of the civil acquisition cost for the reference aircraft. The 117.3 million dollar unit production cost of the military aircraft is the initial value listed. By deducting the values of the last three military-oriented cost elements in Table 7.2, the civil production cost was reached. With the addition of the unit civil R&D cost, the unit civil flyaway cost of 115.6 million dollars was obtained.

TABLE 7.9. CIVIL ACQUISITION COST DERIVATION

		Million $
Unit Military Production Cost from Table 7.5.		117.3
Less Military-Oriented Items		23.6
Equipment GFE/CFE	2.757	
Total Support	3.073	
Total Production Spares	17.721	
Adjusted Unit Cost		93.7
Plus Unit Civil R&D from Table 7.8.		21.9
Unit Civil Flyaway Cost		115.6
Total Acquisition Cost for 250 Aircraft		28,900

A similar approach was followed for the alternate reference aircraft. With a total civil R&D cost of approximately 5.14 billion dollars and a unit flyaway cost of 106.4 million dollars, the comparative cost benefits from adopting the alternate nuclear design philosophy are readily apparent in the 7.9 percent savings. Detailed cost breakdowns for this alternate aircraft are included in Appendix E.

7.2.2 Direct Operating and Life-Cycle Costs

Direct operating cost (DOC) data for the reference and alternate aircraft were estimated using the revised 1967 Air Transport Association (ATA)* methodology updated to January 1975 dollars. Several modifications and additions to the methodology were developed to handle the various features and ramifications of the nuclear propulsion system.

No changes were made to those equations in the methodology which cost hull insurance, airframe maintenance material, engine maintenance materials, maintenance burden, and fuel costs since these equations are dependent on updated input values or other derived costs which were escalated to 1975 dollars. An escalation factor of 1.594, which allowed six percent per year inflation for the eight years between 1967 and 1975, was applied to the crew cost and additional crew cost equations. The maintenance labor rate was escalated from $4.00 per hour to $6.50 per hour, thereby escalating both the airframe and engine maintenance labor costs. The average annual utilization was assumed to be 3000 hours. A 20-year period and a residual value of zero were used for depreciation. This depreciation period is consistent with the 20-years used for the life-cycle costs (LCC).

Values are compared in Table 7.10 for the various elements which contribute to the direct operating cost of the two aircraft on a trans-oceanic flight of 3500 n.m. Costs for both the JP fuel and the nuclear energy used on the trip are included in the fuel and oil element. The two nuclear system elements cover all of the nuclear propulsion

* "Standard Method of Estimating Direct Operating Costs of Turbine Powered Transport Aircraft," Air Transport Association, 1967. (Ref. 21)

TABLE 7.10. TYPICAL OPERATING COST BREAKDOWNS FOR 3500 N.M. TRIP

Element	Dollar Cost for	
	Reference Aircraft	Alternate Aircraft
Crew	3,777	3,640
Fuel and Oil	6,570	5,618
Insurance	6,528	6,005
Aircraft Labor	1,235	1,106
Aircraft Material	3,310	3,053
Engine Labor	684	615
Engine Material	2,162	1,928
Nuclear System Labor	342	308
Nuclear System Material	609	588
Maintenance Burden	3,454	3,099
Depreciation (Includes Spares)	26,604	24,844
Total	55,275	50,804
DOC, ¢/ATNM	7.90	7.26
Unit 20-Year LCC, Million $	392	360

components external to the containment vessel. As in the military costing, nuclear subsystem refueling and refurbishment costs are included as spares and were depreciated.

The effect of variations in average trip distance on the direct operating costs and the unit 20-year life-cycle costs for both aircraft are illustrated in Figure 7-2 with the alternate aircraft enjoying an eight percent relative cost benefit. Two factors are responsible for the higher costs at the shorter ranges. The first is that the ratio of JP fuel to nuclear energy for the trip is greater for shorter ranges. Since the cost of JP fuel per unit of energy exceeds the cost of nuclear power, increasing cost penalties are incurred at shorter ranges. For the longer ranges, this ratio is almost constant.

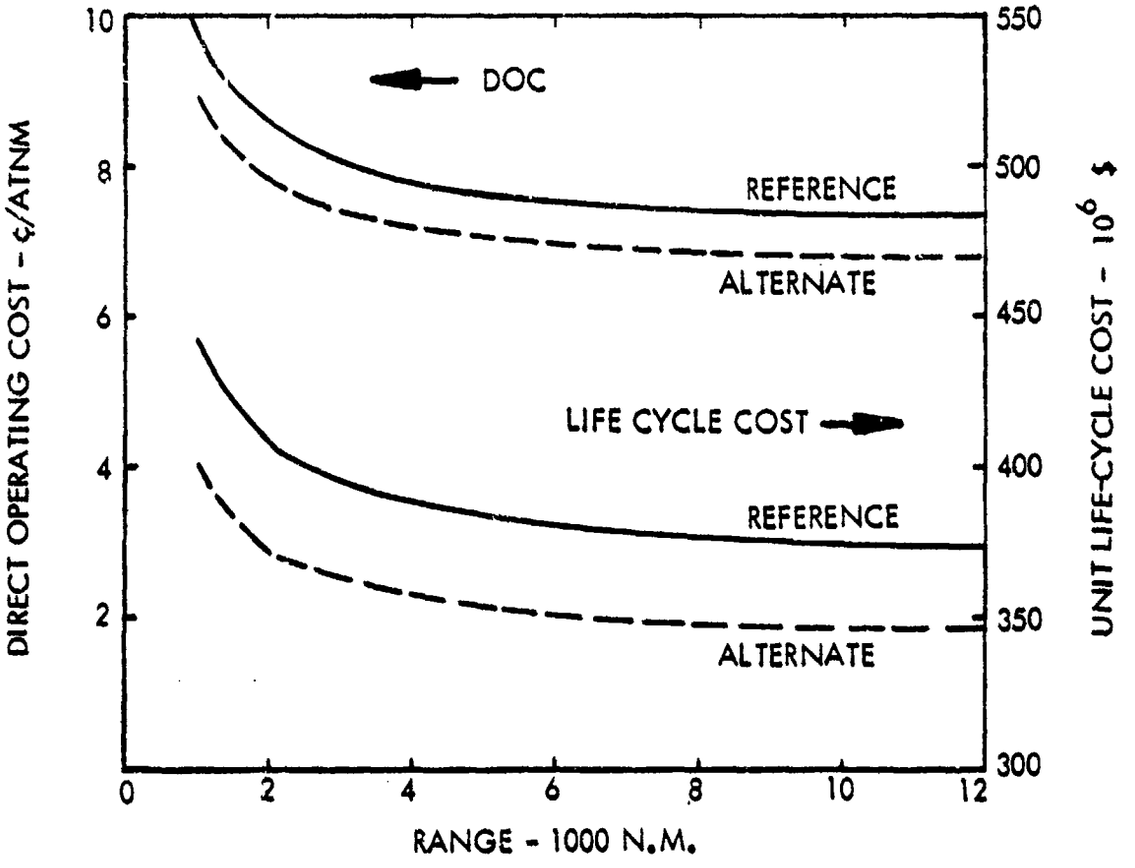

Figure 7-2. Effect of Trip Distance on Operational Costs

The second factor contributing to the higher costs is the difference between cruise speed and block speed. This reflects the portion of the mission which is flown at less than cruise speed, an indication of short range mission inefficiency. For long range missions, this difference becomes negligible.

The military and civil LCC are not comparable because of the differences in various standard operational parameters and in the approaches as to which items are included in the cost. For example, the annual utilization rate for the military is 1080 hours per year while the commercial value is 3000 or higher. Further, these military costs include an estimate of indirect operating costs but the commercial costs do not.

7.3 COST SENSITIVITIES

Studies were performed to assess the sensitivities of the costs of the reference aircraft to increasing fuel costs and to variations of the nuclear R&D cost. Figure 7-3 shows the effects of increasing the fuel costs by 50 and 100 percent over the baseline costs of $0.40 per gal for the JP fuel and $0.65 per million Btu for the nuclear energy. An average increase of 10 percent was experienced by the direct operating and life-cycle costs for a 100-percent increase in fuel costs.

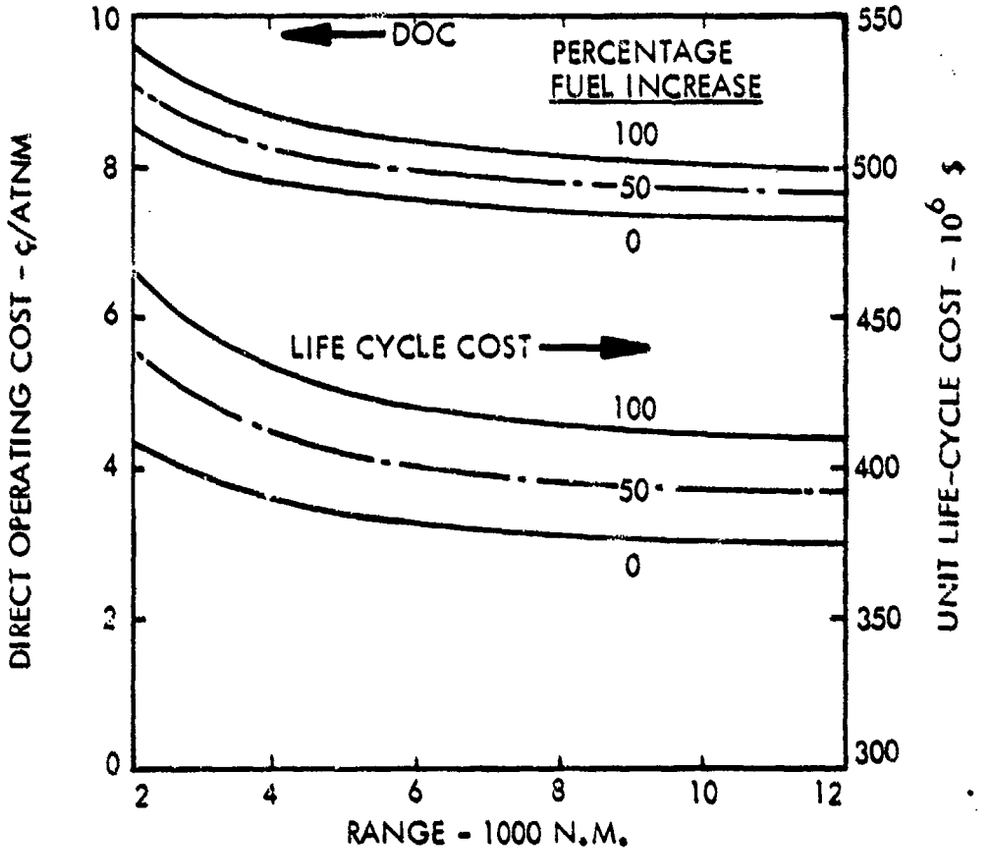

Figure 7-3. Fuel Cost Sensitivity Results

With a fair degree of certainty, it can be said that the development cost for a nuclear system will be large. The uncertainty arises in attempting to establish how large. For this study, the nuclear R&D cost was estimated to be 2.25 billion dollars. The effect of 50-percent variations in this estimate, as shown in Figure 7-4, was to produce only a two percent variation in life cycle costs. Thus, while it can be surmised that the development cost will be large, it can be concluded that its effect will not be significant relative to the total aircraft system operation.

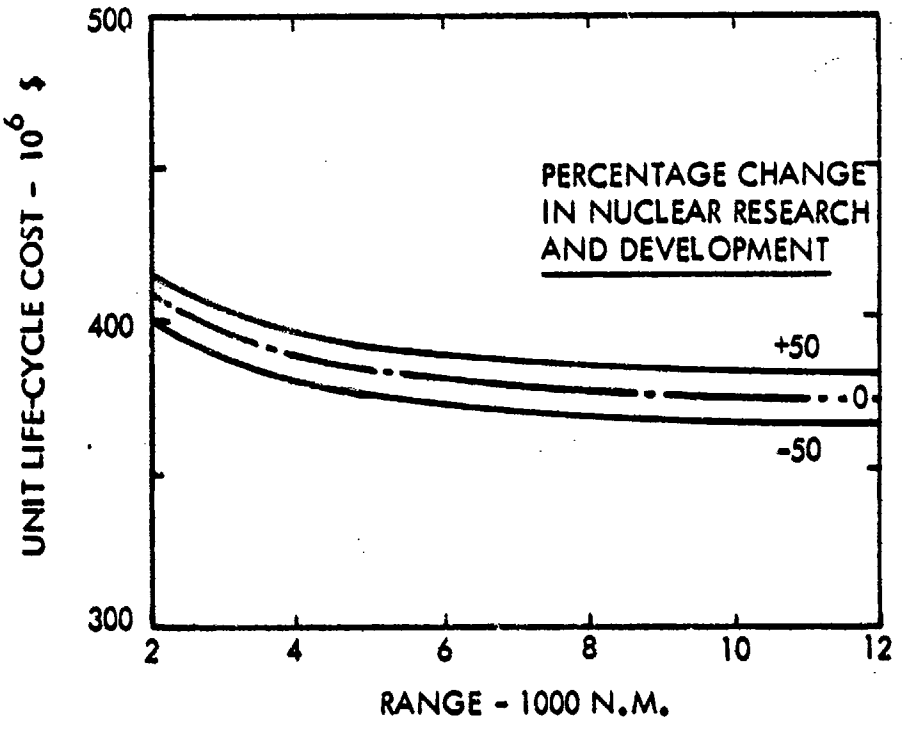

Figure 7-4. Nuclear Research and Development Sensitivity Results

8.0 COMPARISON WITH JP-FUELED AIRCRAFT

Any attempt to compare nuclear-powered and JP-fueled aircraft is difficult and frustrating because optimum utilization of either aircraft is realized for radically different missions. The JP aircraft is best at intercontinental ranges while the nuclear aircraft excels over global distances. Rather than develop the two aircraft concepts for mission ranges which would be unsuitable for both or prejudiced in favor of one, another approach was selected. This approach recognizes that the nuclear-powered reference aircraft design has been developed and costed for a particular mission payload. Instead of trying to compare the reference aircraft with a JP-fueled aircraft with an arbitrary range capability, the approach was to determine what must be the design range of a JP-fueled aircraft that has the same payload and either the same gross weight or the same life-cycle cost as the reference aircraft.

Several JP-fueled aircraft designs were developed as part of this determination. The mission specifications and the economic guidelines for these designs were the same as those imposed on the nuclear aircraft. Further, the JP and nuclear aircraft have equivalent technology levels, identical cruise speeds, and common values for many other characteristics to give as fair a comparison as possible.

8.1 JP-FUELED AIRCRAFT SIZING

A conventional configuration, similar to that investigated for the application of nuclear power, was selected for sizing the JP-fueled aircraft. The 20-deg wing sweep angle of the conventional nuclear configuration was retained for the JP aircraft. This configuration has a T-tail empennage mounted on the aft fuselage, the fuel is carried in the wing, and all of the cargo is loaded in the fuselage. The fuselage cross-section is identical to that of the nuclear aircraft. It will accommodate outsized equipment and/or three rows abreast of containerized cargo. The fuselage length of 238 ft is shorter than for the conventional nuclear aircraft by the 22 ft required for the reactor.

Five range values of 3500, 5500, 7500, 10,000, and 12,000 n.m. were chosen for developing JP aircraft design data from which the cross-over ranges for equal weights and costs could be determined. The initial parametric sizing effort was directed toward identifying the optimum initial cruise altitude and engine bypass ratio values. The results in Figure 8-1 for this initial effort are for the 7500 n.m. range. The minimum ramp weight was established by the 140-kt approach speed limit and its

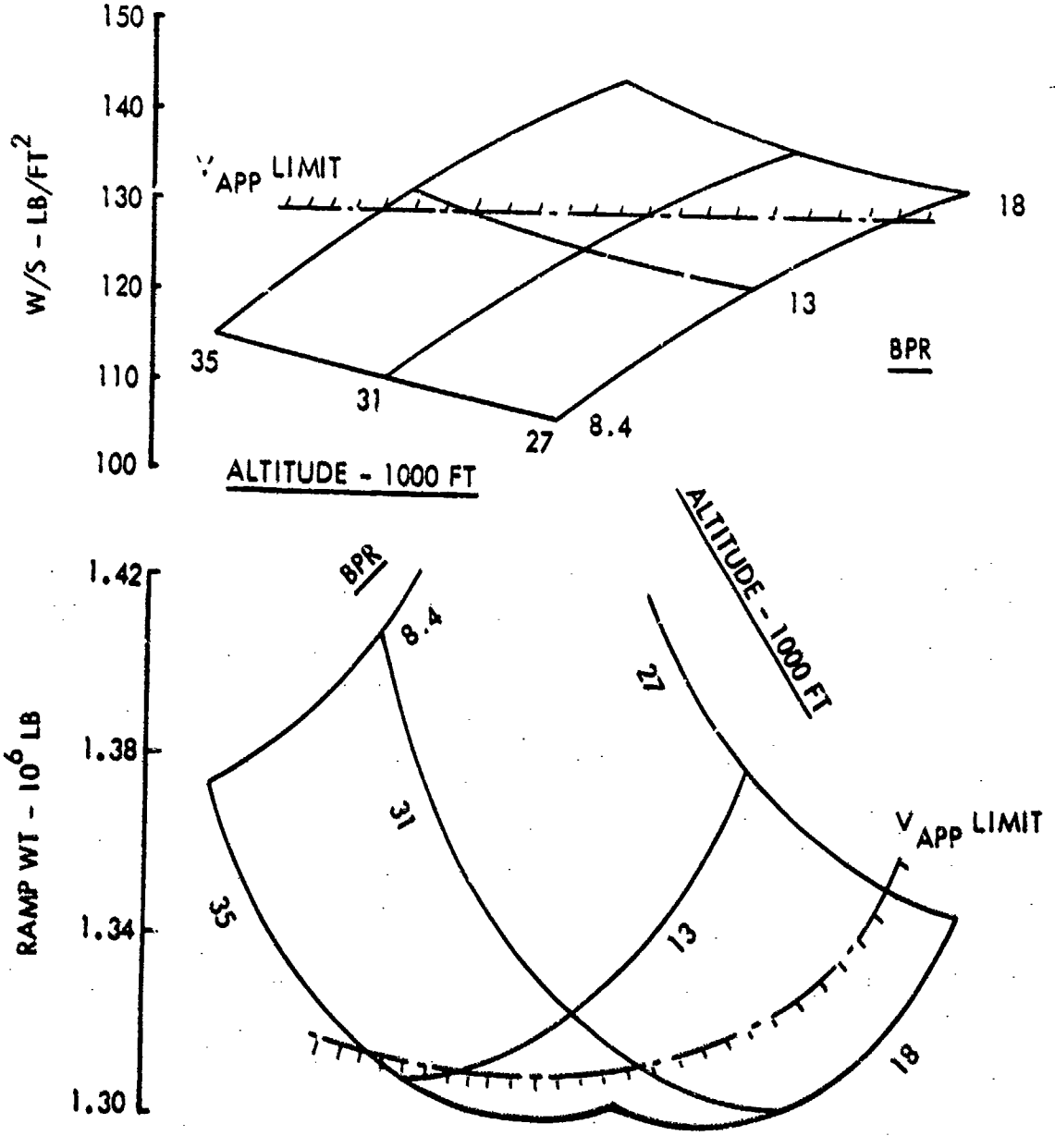

Figure 8-1. Cruise Altitude and Engine Bypass Ratio Optimization for JP-Fueled Aircraft. Range = 7500 n.m. TOD = 10,000 ft.

equivalent wing loading of 129 psf. As illustrated on the figure, the minimum weight was for an initial cruise altitude of 33,000 ft and an engine bypass ratio of approximately 13. These two parametric values were held constant in generating the matrix of design point data in Figures 8-2 to 8-6 for the five mission ranges. The

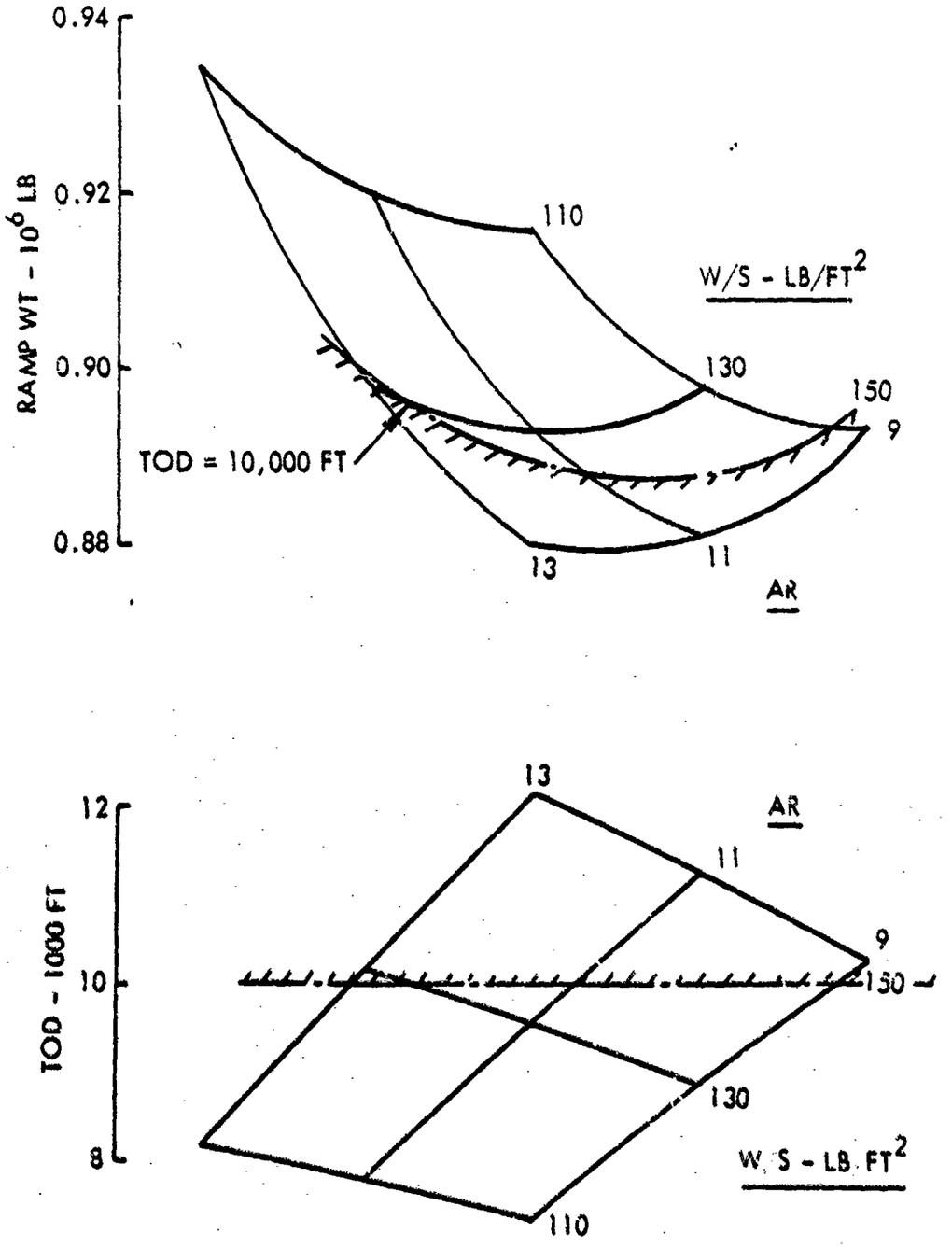

Figure 8-2. JP-Fueled Aircraft Optimization for 3500 N.M. Range

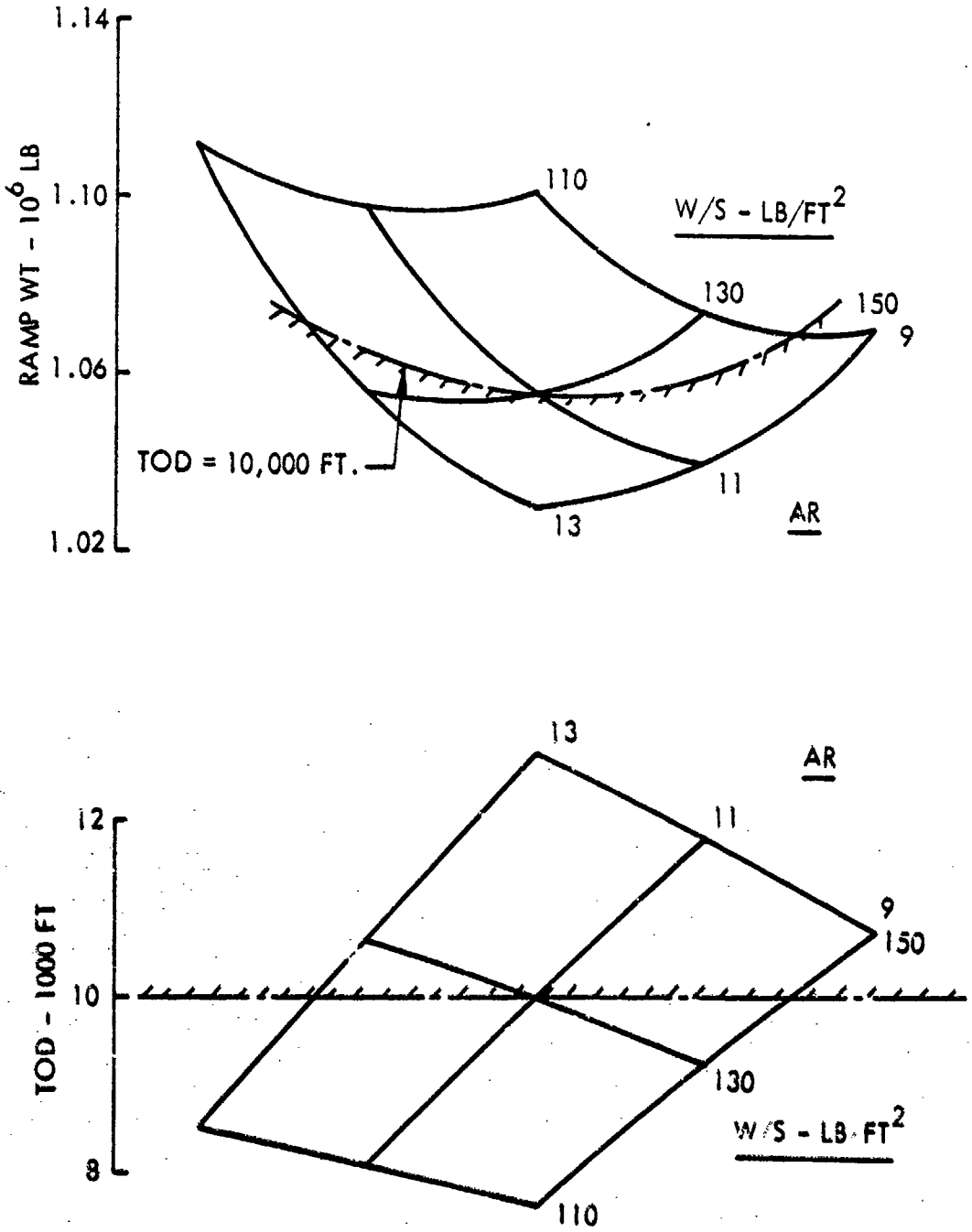

Figure 8-3. JP-Fueled Aircraft Optimization for 5500 N.M. Range

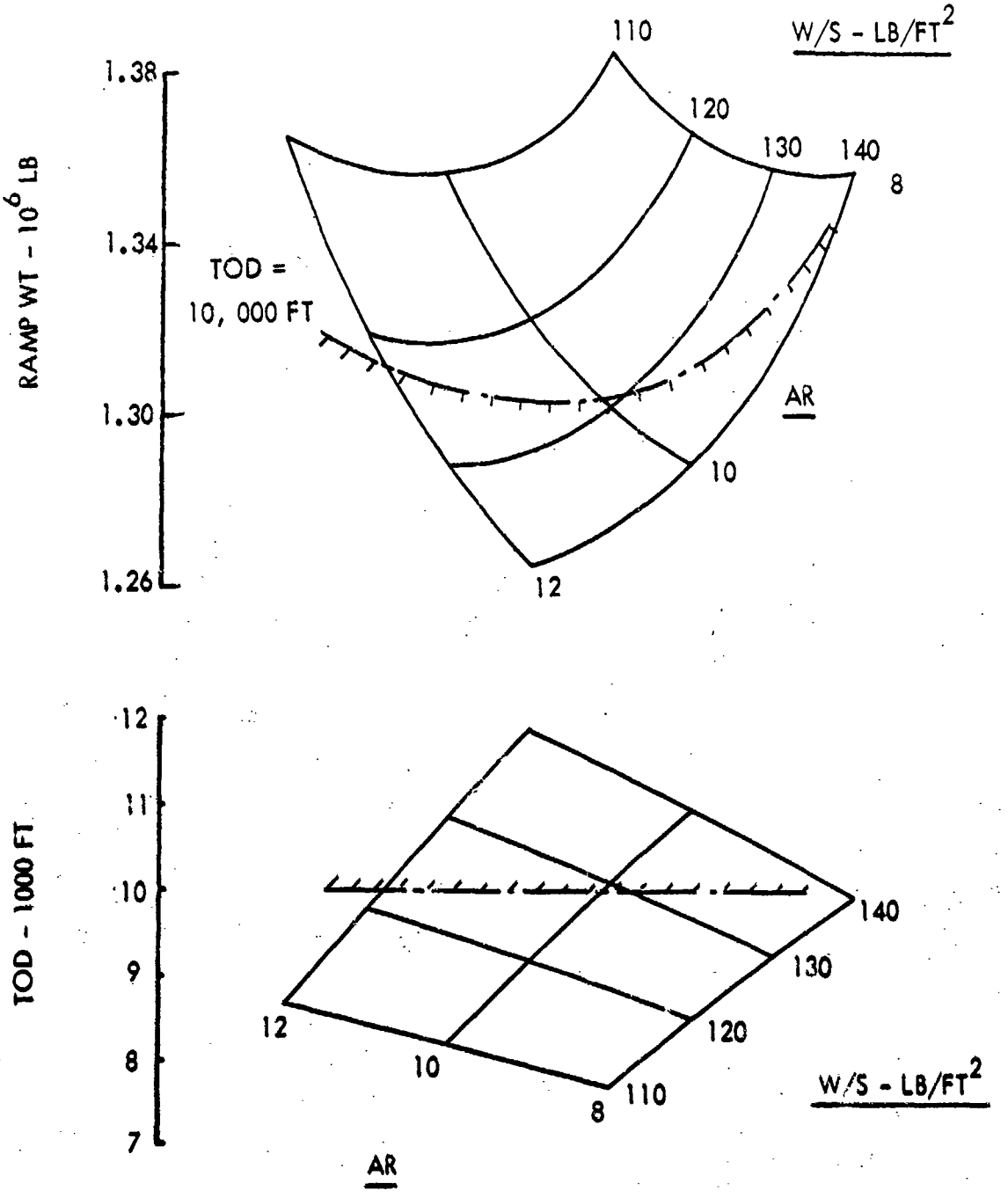

Figure 8-4. JP-Fueled Aircraft Optimization for 7500 n.m. Range

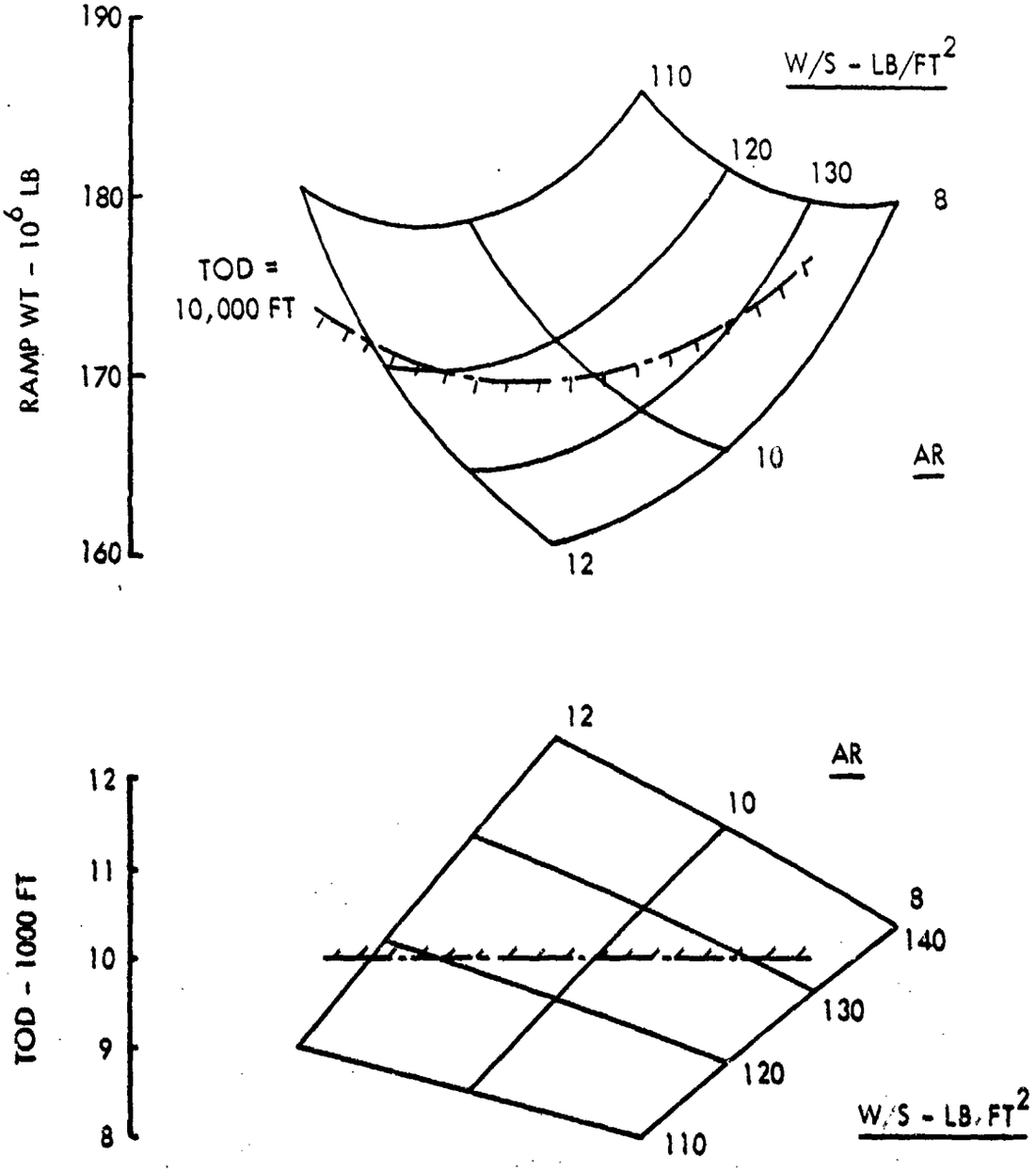

Figure 8-5. JP-Fueled Aircraft Optimization for 10,000 n.m. Range

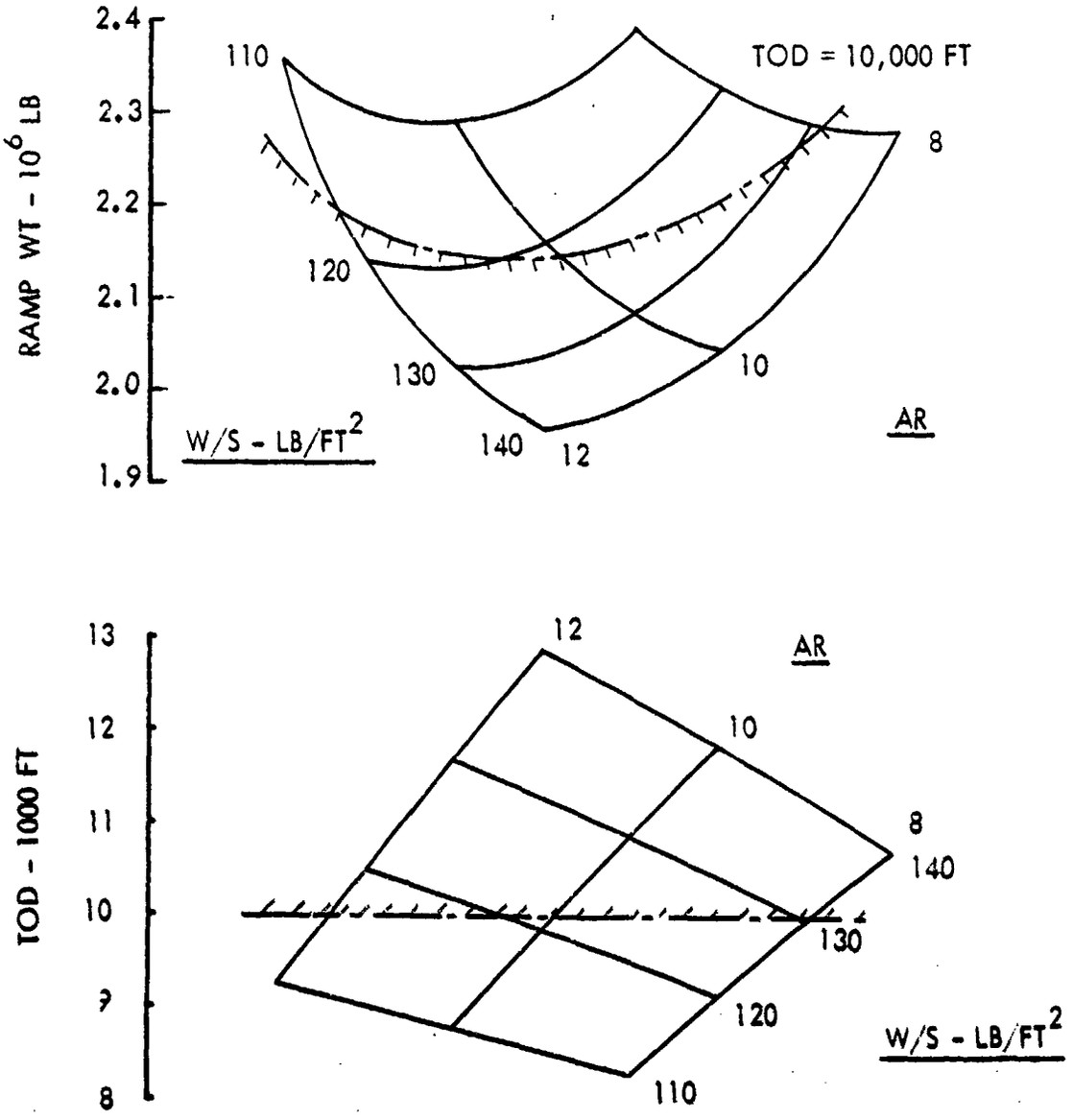

Figure 8-6. JP-Fueled Aircraft Optimization for 12,000 n.m. Range

minimum weight aircraft for each range was defined by the 10,000-ft field length curve. Data for the optimum design point for each range were combined on Figure 8-7. Superimposed on this figure are the ramp weights of the reference and alternate nuclear aircraft. The intersection points define the design ranges of 9200 and 7850 n.m. for JP aircraft with the same ramp weights as the two nuclear aircraft.

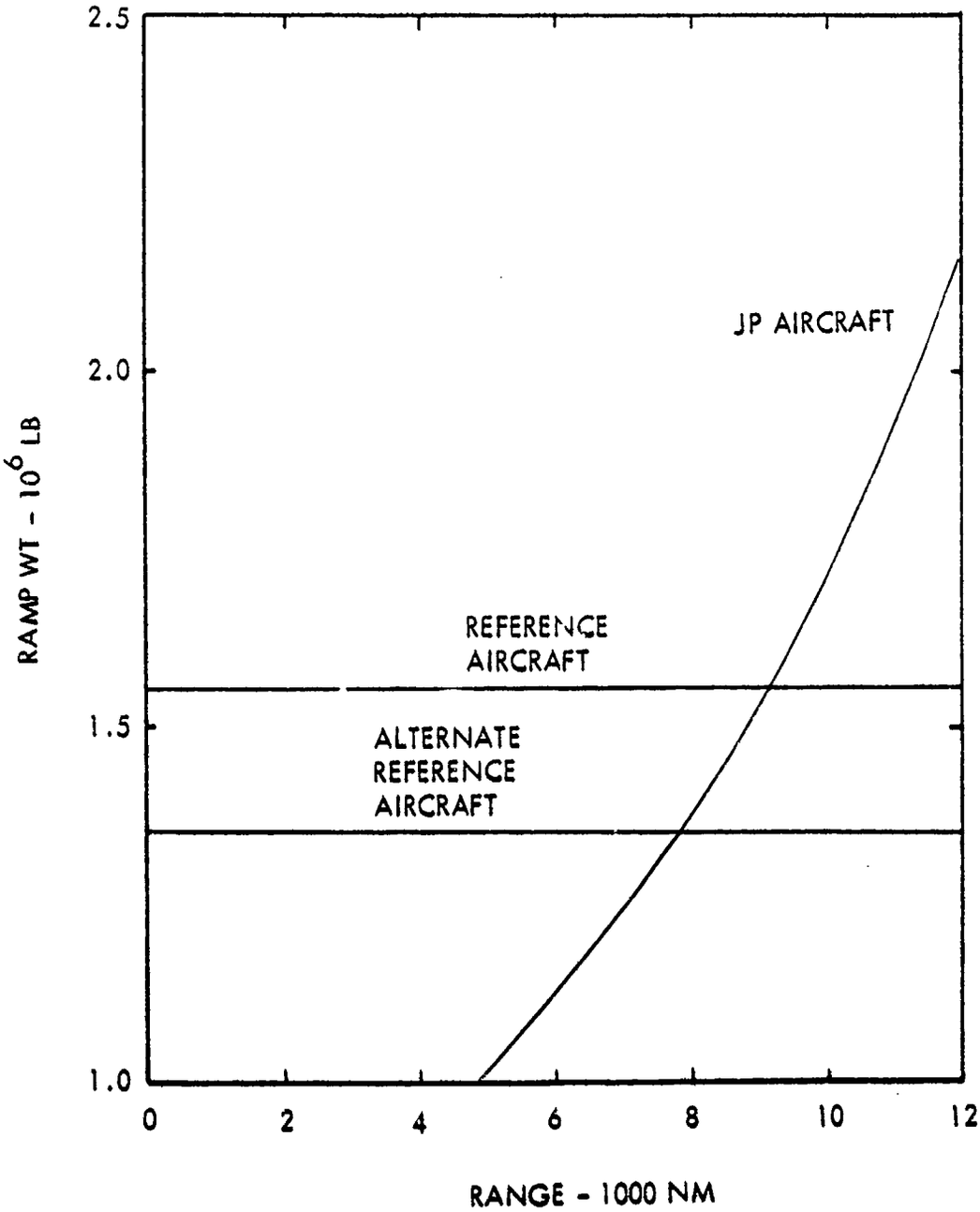

Figure 8-7. Nuclear and JP-Fueled Aircraft Cross-Over Ranges for Equal Ramp Weights

The 9200 n.m. range aircraft is illustrated in Figure 8-8. A weight summary for the aircraft is included in Table 8.1, the design features are listed in Table 8.2, and a cost breakdown is presented in Table 8.3. The wing loading is less than the maximum allowed by the 140-kt approach speed limit. Also, the cruise lift coefficient value of 0.573 falls well below the maximum design value of 0.706 for a 20-deg wing

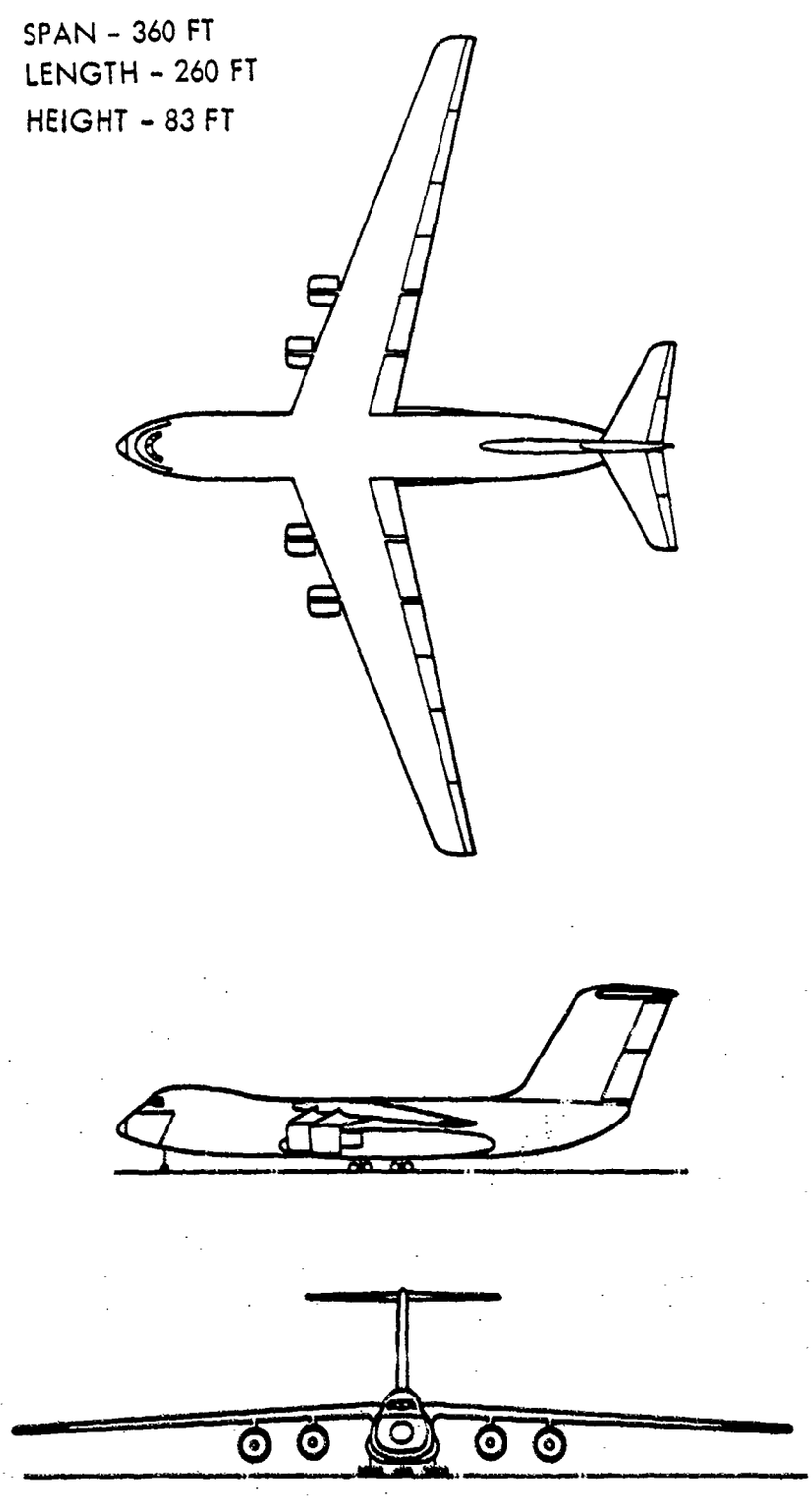

Figure 8-8. Equivalent Weight JP-Fueled Aircraft

TABLE 8.1. WEIGHT SUMMARY FOR 9200 N.M. RANGE JP AIRCRAFT

	Lb
Wing	180,969
Horizontal	9,417
Vertical	8,760
Fuselage	78,794
Landing Gear	53,892
Nacelles and Pylons	19,628
Propulsion	72,587
Systems and Equipment	51,357
Operating Weight	475,404
Payload	400,000
Fuel	681,087
Ramp Weight	1,556,491

TABLE 8.2. DESIGN CHARACTERISTICS OF 9200 N.M. RANGE JP AIRCRAFT

Cruise Mach Number	0.75
Cruise Altitude	33,000 ft
Wing Sweep Angle	20 deg
Wing Loading	123.5 psf
Aspect Ratio	10.5
L/D	23.76
Cruise Lift Coefficient	0.573
Field Length	10,000 ft
No. Engines	4
Engine Thrust, SLSD	88,284 lb
Engine Bypass Ratio	13
Wing Area	12,323 ft^2
Horizontal Area	1,759 ft^2
Vertical Area	2,307 ft^2

TABLE 8.3. PRODUCTION COST BREAKDOWN FOR 9200 N.M. RANGE JP AIRCRAFT

	Thousand $ Per Aircraft	
Wing	13,319	
Tail	1,910	
Body	5,440	
Landing Gear	1,498	
Flight Controls	1,005	
Nacelles	2,711	
Engine Installation	610	
Instruments	192	
Hydraulics	263	
Electrical	264	
Electronics Racks	157	
Furnishings	370	
Air Conditioning	237	
APU	180	
Final Assembly	1,400	
Production Flight	681	
System Integration	860	
Total Empty Manufacturing Cost		31,097
Sustaining Engineering	2,314	
Production Tooling	3,246	
Quality Assurance	3,326	
Airframe Fee	8,297	
Airframe Cost		48,280
Engine Cost	10,032	
Avionics	500	
Research & Development	12,993	
Total Flyaway Cost		71,805

sweep. The excellent performance of the aircraft is due in part to its high aspect ratio value of 10.5.

Mission capabilities of the equivalent weight JP-fueled aircraft are summarized on Figures 8-9 and 8-10. With decreases in mission payload, the aircraft range is not restricted by fuel volume limitations as it increases to the maximum, or ferry, range of 13,600 n.m. Station-keeping characteristics of the aircraft are presented in

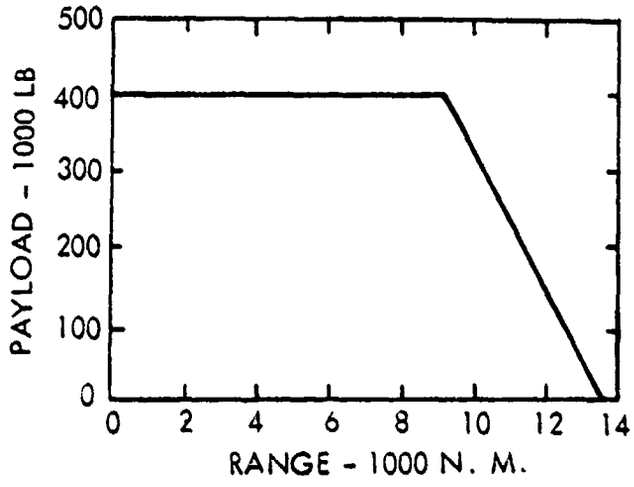

Figure 8-9. Payload-Range Characteristics of Equivalent Weight JP-Fueled Aircraft

Figure 8-10 for variations in mission radius and payload. Flight to and from the mission station was at the cruise speed of 436 kts, while the maximum endurance speed for station-keeping was 125 kts.

Throughout this study, every effort has been made to include those technologies, design features and costs projected to be characteristic of the 2000 time period. The one noticeable exception is that of fuel price. Both the JP fuel price of $0.40 per gal and the nuclear energy cost of $0.65 per million Btu represent today's values. With decreasing fuel availability in the future, fuel prices will increase over and above the increment due to inflation. Recognizing this future trend, the effects of increasing

To find the design range of a cost equivalent JP aircraft, civil life-cycle costs were computed and plotted in Figure 8-11 for the optimum aircraft for each of the range values. Similar cost data for the two nuclear aircraft were superimposed on the figure to establish the design ranges for the equal-cost JP aircraft. The cost cross-over ranges of 11,950 and 11,100 n.m. relative to the reference and alternate reference nuclear aircraft, respectively, are somewhat greater than those determined for equal ramp weights.

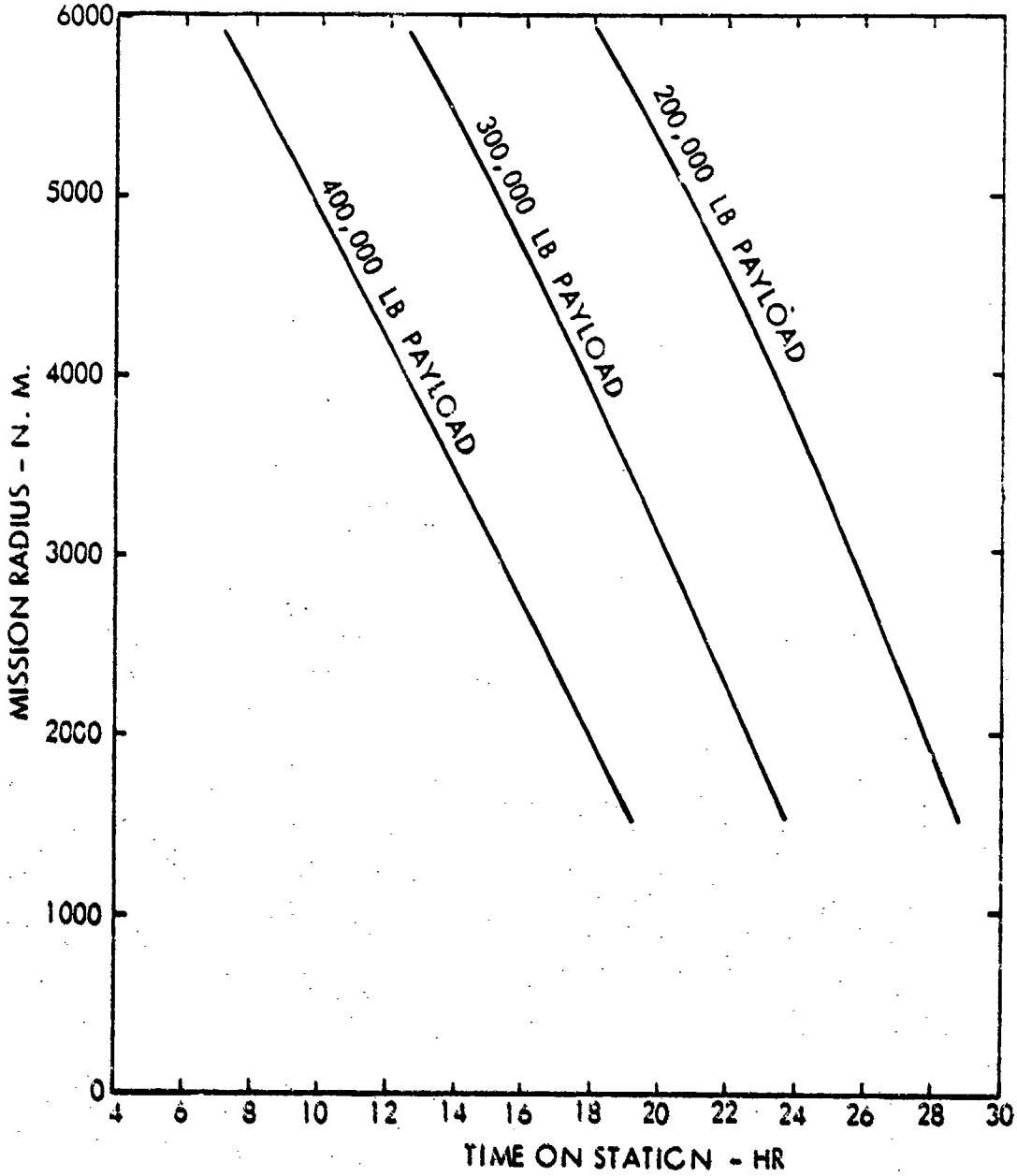

Figure 8-10. Mission Endurance of Equivalent Weight JP-Fueled Aircraft

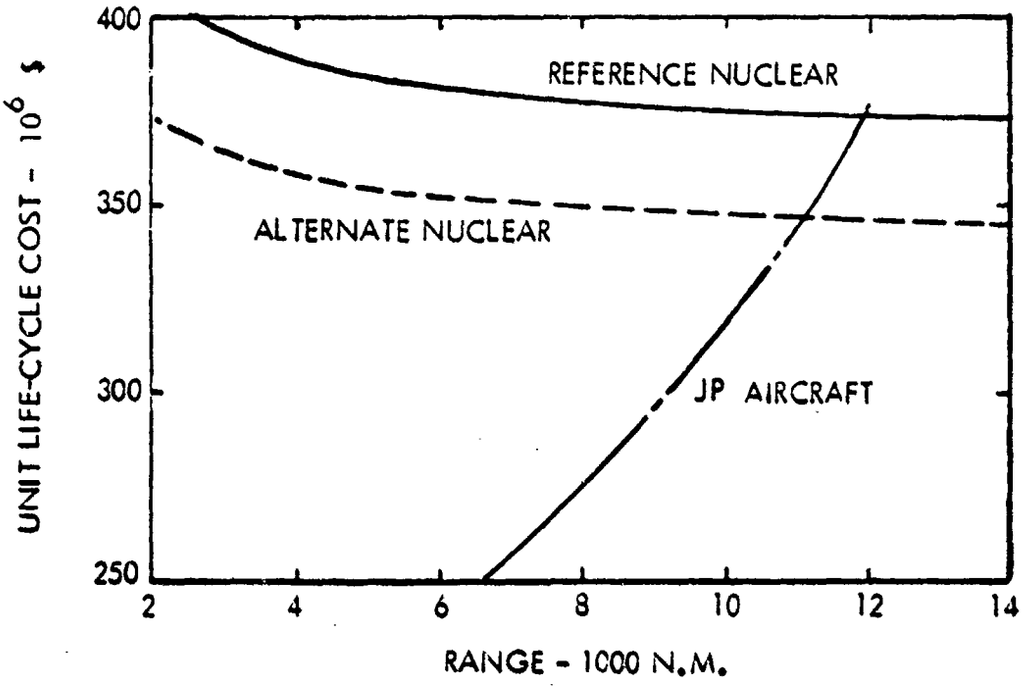

Figure 8-11. Nuclear and JP-Fueled Aircraft Cross-Over Ranges for Equal Life-Cycle Costs (JP fuel at $0.40/gal.; nuclear fuel at $0.65/million BTU)

the fuel prices were investigated. As shown by the results on Figure 8-12, the range for equal life-cycle costs drops to 6100 n.m. relative to the reference nuclear aircraft for a 300-percent fuel price increase. Similar data on Figure 8-13 for the alternate nuclear aircraft show a cross-over range of ~700 n.m. for the 300-percent fuel price increase. Thus, the prospects for airborne nuclear power will be considerably enhanced in the future.

8.2 AIRCRAFT COMPARISON

Both the nuclear-powered and the JP-fueled aircraft were designed for the same mission of carrying 400,000 lb of cargo at a cruise Mach number of 0.75. The JP aircraft was designed for a range of 9200 n.m. to achieve a ramp weight identical to that of the nuclear aircraft; the range of the nuclear aircraft is limited only by crew endurance.

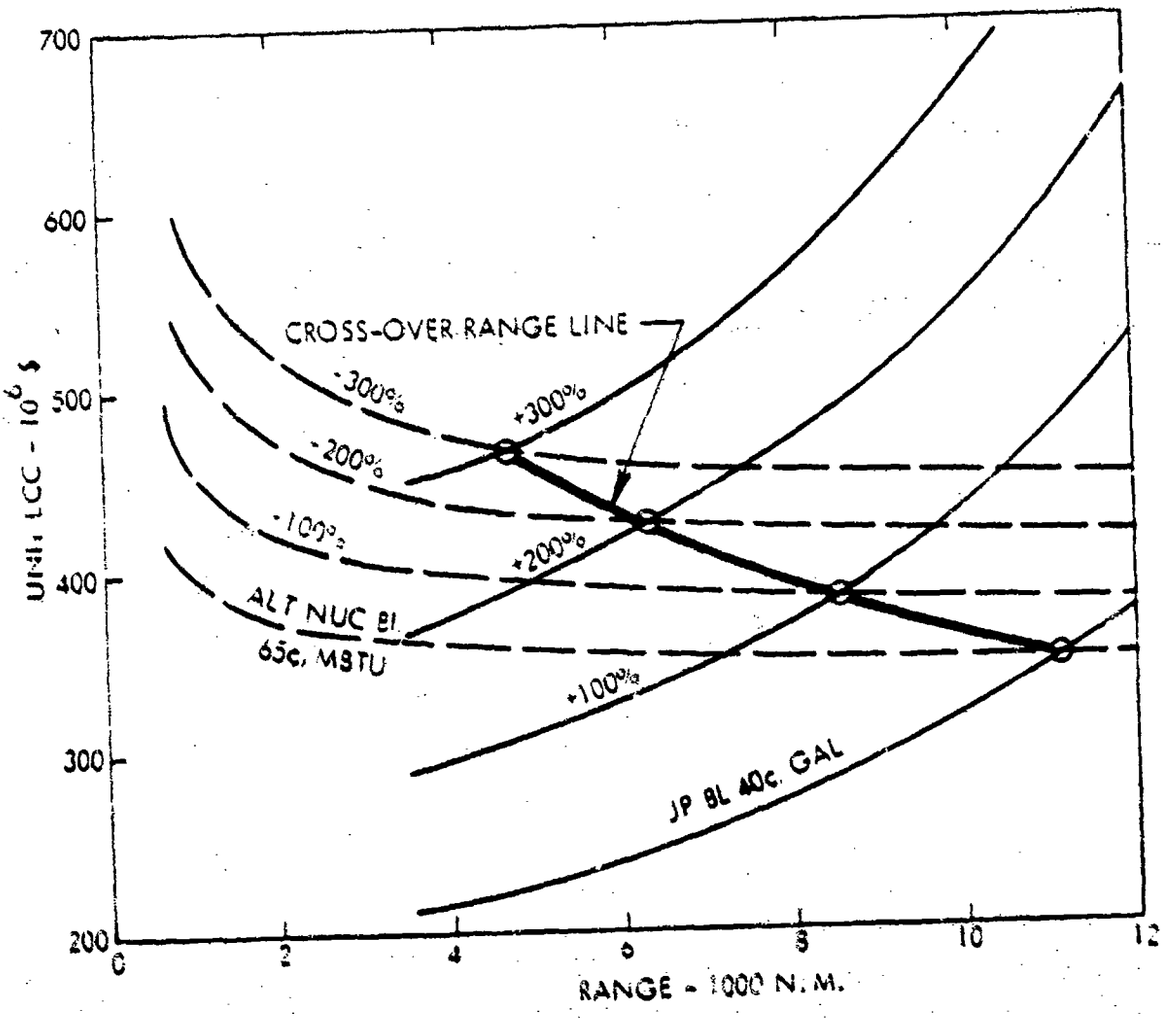

Figure 8-12. Sensitivity of Cross-Over Range to Fuel Price for Reference Nuclear Aircraft

The JP aircraft begins cruise at an altitude of 33,000 ft and slowly increases its cruise altitude as fuel is burned to minimize fuel consumption. The nuclear aircraft maintains a constant cruise altitude of 31,000 ft for optimum performance. Since the true airspeed is slightly greater for the nuclear aircraft, its productivity will be slightly greater than that of the JP aircraft for the same mission range.

Overall dimensions of the two aircraft are similar, as noted in Table 8.4, with the chemical-fueled aircraft requiring slightly more terminal area - the product of wing span and overall length. The differences in fuselage lengths and overall lengths for the two aircraft reflect the effect of the space occupied by the reactor. Characteristic

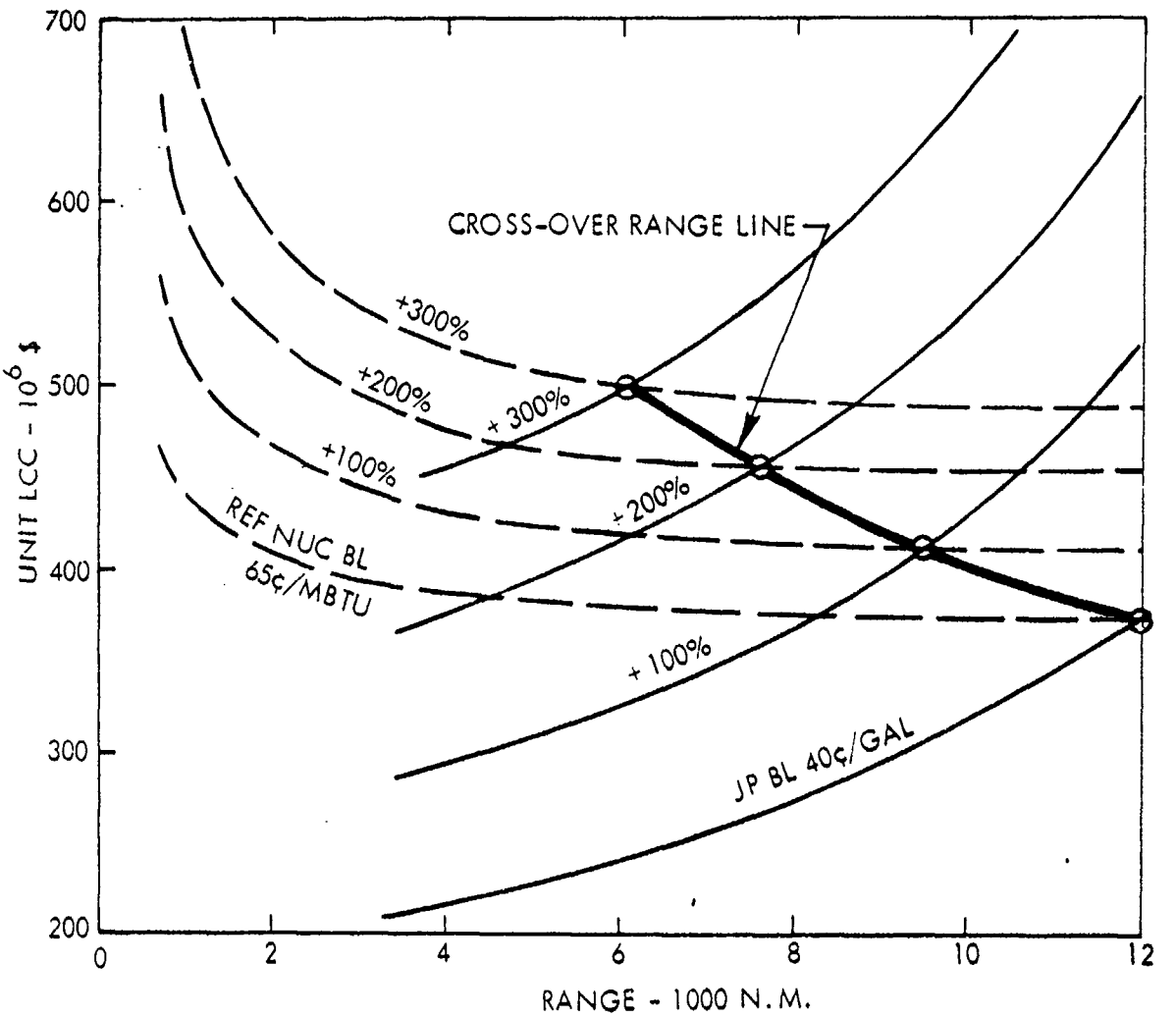

Figure 8-13. Sensitivity of Cross-Over Range to Fuel Price for Alternate Nuclear Aircraft

layout features of the two configurations are responsible for considerable differences in the empennage moment arms and resulting surface areas.

The wing areas are approximately the same for the two aircraft. However, the beneficial drag reduction achieved through the higher aspect ratio value for the JP aircraft is partially offset by the higher wing weight, as shown in Table 8.5. Contributing to the JP aircraft wing weight, is the additional structural weight required by downbending criticality of the wing due to the fuel load during taxi.

TABLE 8.4. AIRCRAFT GEOMETRY COMPARISON

	Nuclear	Chemical
Wing		
Span, ft	308	360
Sweep, deg	30	20
Area, ft^2	12,630	12,323
Aspect Ratio	7.5	10.5
Overall Length, ft	275	260
Maximum Height, ft	75	83
Fuselage Length, ft	260	238
Fuselage Equivalent Diameter, ft	27	27
Cargo Compartment Size, ft	25 x 13.5 x 164	
Empennage Areas, ft^2		
Horizontal	1194	1759
Vertical	3698	2307

TABLE 8.5. AIRCRAFT WEIGHTS COMPARISON

	Nuclear	Chemical
Structure		
Wing	147,969	180,969
Horizontal Tail	7,180	9,417
Vertical Tail	12,187	8,760
Fuselage	104,708	78,794
Landing Gear	65,989	53,892
Nacelle and Pylon	23,821	19,628
Propulsion		
Engine Installation	81,042	65,530
Fuel System	3,137	7,057
Nuclear Subsystem	391,260	-
Engine HX, Ducting and Auxiliary Cooling	135,689	-
Systems and Equipment	48,898	51,357
Operating Weight Empty	1,021,881	475,404
Payload	400,000	400,000
Fuel	134,610	681,087
Ramp	1,556,491	1,556,491

Empennage weight differences are caused by the variances in surface areas. The greater fuselage weight for the nuclear aircraft includes the structure for attaching and housing the reactor. Additional landing gear weight for the nuclear aircraft is necessitated by its higher landing weight. The inefficiencies and additional size of the engine due to the installation of the heat exchanger resulted in higher engine weights for the nuclear aircraft. The weights of the fuel system and of the systems and equipment are higher for the chemical-fueled aircraft because of the larger quantity of JP fuel carried.

A comparison of the performance characteristics listed in Table 8.6 shows that the chemical-

TABLE 8.6. AIRCRAFT PERFORMANCE COMPARISON

	Nuclear	Chemical
Cruise Mach Number	0.75	0.75
Cruise Altitude, ft	31,000	33,000
Cruise Lift/Drag Ratio	22.59	23.76
Wing Loading, psf	120.0	123.5
No. Engines	4	4
Engine Thrust, Uninstalled, lb	84,823	88,284
Engine Bypass Ratio	8.4	13.0
Takeoff Field Length, ft	10,000	10,000
Landing Approach Speed, kts	140	137

fueled aircraft enjoys a 5 percent better cruise lift-to-drag ratio as a result of its higher wing aspect ratio and wing loading. The difference in engine thrust levels is basically due to the different cruise altitudes and engine bypass ratios.

Costs for the two aircraft are compared in Table 8.7. The higher unit engine cost for the chemical-fueled aircraft is a direct function of its higher thrust rating. The difference in the airframe prices is due largely to the additional fuselage length for housing the reactor and the structure for attaching it. The resulting 61 percent greater cost of the nuclear aircraft is partially offset by its cheaper unit energy cost for operation. For this particular comparison, the direct operating and life-cycle costs of the nuclear aircraft exceed those of the chemical aircraft by 23 percent.

TABLE 8.7. AIRCRAFT COST COMPARISON*

	Nuclear	Chemical
Unit Cost, Million $		
Engine	2.4	2.5
Reactor Subsystem	22.2	-
Airframe	53.7	48.3
Aircraft	115.6	71.8
20-Year Life-Cycle	375	304
DOC, ¢/ATNM	7.40	5.98
Fleet 20-Year Life-Cycle Costs, Billion $	93.8	76.0

* 9200 n.m. range

9.0 CONCLUSIONS

Parametric studies were performed for several aircraft configurations to determine the minimum ramp weight concept with the application of nuclear power. Similarly, several nuclear propulsion cycles were analyzed to ascertain the minimum weight and minimum development risk concepts. Using the selected configuration and cycle, an optimum aircraft was developed for a reference mission to carry a 400,000-lb payload on nuclear power and to have an emergency chemical fuel recovery range of 1000 n.m. A competitive chemical-fueled aircraft was also designed for the reference mission payload. Conclusions reached as a result of these parametric studies, design efforts, and the subsequent comparison are as follows:

1. The canard configuration exhibited smaller ramp weights than either the spanloader or conventional configurations for the 400,000 and 600,000-lb payload cases under consideration. For the larger payload, the canard aircraft was one percent lighter than the spanloader aircraft and 4.3 percent lighter than the conventional aircraft. For the smaller payload, the canard was 4.8 and 9.8 percent lighter than the conventional and spanloader aircraft, respectively.

2. The canard configuration has the potential for achieving greater benefits from alternate nuclear design approaches than do the other two configurations. This is the result of the reactor placement in the aft end of the fuselage of the canard with cargo and personnel adjacent to only one side of the reactor. In the conventional aircraft, cargo and personnel are in close proximity to the reactor on two of its sides. The spanloader configuration has cargo and personnel on three sides of the reactor. As the reactor system becomes less isolated, more stringent shielding design is necessitated, with attendant weight penalties. The canard configuration has the most isolated reactor placement and hence, is able to benefit substantially from special shaped shielding concepts.

3. Adoption of the alternate nuclear operation and design philosophy offers the greatest potential for reducing aircraft weight and cost. For the reference mission canard aircraft, a 13.1-percent reduction in ramp weight was achieved by applying this alternate philosophy to the aircraft design. The first feature of this philosophy is to shape the shield to satisfy standard dose rate limitation criteria in all directions normally occupied by personnel but to relax the criteria in those directions which are inaccessible. The second feature is to use the emergency range chemical fuel for shielding, thereby permitting a reduction in the amount of regular shield material. The third feature is to operate the reactor during all flight phases, using half reactor power for emergency cruise and full reactor power for takeoff and climb. Chemical fuel is used during these power critical phases to augment the reactor and provide the additional thrust required.

   Safety is not compromised by adopting this alternate philosophy. In effect, this alternate philosophy yields a better engineering solution for a design than is possible with the previous approach.

4. Studies to assess the sensitivity of the reference canard design to several alternate technology applications revealed that the use of composite materials was most beneficial in reducing aircraft ramp weight. For 20, 40 and 60 percent of the aircraft structure in composite materials, the ramp weight of an all aluminum aircraft was reduced by 8.53, 13.51 and 17.72 percent, respectively.

   In addition to composite materials, the alternate technologies considered included laminar flow control (LFC), higher bypass ratio engines, and a higher engine turbine inlet temperature (TIT) for nuclear cruise. With LFC on the wing and vertical surfaces, a 3.61-percent reduction in ramp weight was achieved. Less than a two percent variation in ramp weight was evident for engine bypass ratios between 5.8 and 18.0. Increasing the engine TIT during nuclear cruise by 200°F, also had little effect on ramp weight, yielding an improvement of about one percent.

All of these advanced technology applications will require additional development and production costs, the extent of which could not be assessed within the scope of this study. Based on the experience gained from previous studies concerned with the application of these four advanced technologies, it appears that composite materials is the only one that offers sufficient benefits to offset the expected additional cost.

5. Studies on the sensitivity of the reference aircraft design to variations in the mission parameters of cruise Mach number, takeoff distance and emergency range revealed that the increased emergency range imposed the greatest penalty. The aircraft ramp weight was increased by 10.4 percent when the emergency range was doubled to 2000 n.m. Variations in takeoff distance between 8000 and 12,000 ft have little effect with less than a 1.75 percent change in ramp weight. Decreasing the cruise Mach number from the reference value of 0.75 to 0.65, saved a marginal 1.65 percent in ramp weight. Increasing the cruise Mach number to 0.85 had a somewhat greater effect with a 4.6-percent weight penalty.

6. Of the various nuclear propulsion cycles analyzed, only the non-recuperated closed Brayton cycle with a dual-mode engine was found to be lighter in weight than the base case open Brayton cycle. However, the difference in weight was judged to be more than balanced by the greater background and design certainty associated with the open Brayton cycle. Until further development work is completed for other cycle concepts, the open Brayton cycle should serve as the basic nuclear propulsion cycle.

7. Nuclear power gives the lighter ramp weight and lower life-cycle cost aircraft for global range missions while chemical JP fuel appears to be better for intercontinental mission ranges. For mission ranges less than 9200 n.m., the JP-fueled aircraft has a lighter ramp weight than the reference nuclear aircraft. The converse is true for mission ranges exceeding 9200 n.m. If the alternate nuclear operation and design philosophy is adopted, the cross-over range value is reduced to 7850 n.m. In terms of life-cycle costs, the

cross-over ranges are 11,950 and 11,100 n.m. relative to the reference and alternate nuclear aircraft, respectively. However, for a 300-percent fuel price increase because of energy shortages, these cross-over ranges are reduced to 6100 and 4700 n.m., respectively. Thus, the prospects for airborne nuclear propulsion to long range missions will be considerably enhanced in the future.

8. The nuclear R&D cost was estimated to be 2.25 billion dollars. Due to the uncertainty associated with this estimate, 50-percent variations of this estimate were investigated and were found to produce only a two percent change in life-cycle cost. Thus, while it can be surmised that the nuclear development will be large, it can be concluded that it will have a small effect on the total aircraft systems operation.

10.0 RECOMMENDATIONS

Before a nuclear-powered aircraft can become a reality, considerable research and development effort will be required. System studies are needed to define the design requirements for the aircraft and to determine the optimum configuration characteristics. Technology development programs must be continued, and in some cases initiated, to advance the state of the art in the areas of propulsion, aerodynamics and flight controls, structures and materials, and noise reduction. Several study recommendations in these areas must be pursued within the immediate future if nuclear aircraft are to become operational by the year 2000.

10.1 NUCLEAR PROPULSION SYSTEM

The total nuclear propulsion system is the pacing technology area in the development of a nuclear aircraft. While all elements of the total propulsion system require further development, some need more than others. To aid in the discussion of recommended development programs, the total propulsion system is considered to be composed of the engine, the heat transfer system, and the nuclear subsystem which includes the reactor, shielding and containment structure. Before discussing each of these three major sub-areas, one recommendation will be made concerning the total system. In the propulsion cycle analyses of this study, the non-recuperated closed Brayton cycle with dual-mode engines was found to be the lightest weight cycle. However, it was not selected for use on the reference aircraft because of the minimal investigations and data base of this cycle.

It is recommended that future studies be initiated to confirm, and quantify with more certainty, the characteristics of the non-recuperated closed Brayton cycle with dual-mode engines. The investigations of this study have been sufficient to show that such a propulsion system is potentially very attractive from weight considerations. Several other attractive characteristics of this cycle, as outlined previously in Section 4.4, give further impetus to the recommendation to study this cycle in more detail.

10.1.1 Nuclear Subsystem

Two basic types of nuclear reactors are prime candidates for nuclear aircraft propulsion systems. One type is a liquid-metal-cooled fast reactor as typified by the NuERA II concept. The other prime concept* is a gas-cooled, graphite-moderated, epi-thermal reactor based on the proven technology of the nuclear rocket reactors. The liquid-metal-cooled NuERA nuclear subsystem was used in this study because of its extensive parametric data base for aircraft application. Such a data base is non-existent for the gas-cooled reactor. Therefore, it is recommended that a similar parametric data base be established for the gas-cooled reactor.

It is further recommended that both types of reactors then be included in a total systems integration study of a nuclear powered aircraft to select the more promising concept. Regardless of which type reactor is selected, there will remain a substantial technology undertaking to develop and demonstrate both the components for and a flight-weight system with the power, life, temperatures and safety needed for aircraft application.

10.1.2 Engines

Due to material limitations of the nuclear heat exchanger in the engine, design temperatures and pressures of the nuclear gas turbine were considerably lower than those predicted for advanced chemical-fueled gas turbines. Consequently, it became necessary in this study to "redesign" an advanced engine to achieve a more optimum match between cruise and takeoff performance. It would have been more satisfactory to have had a parametric data set for an advanced engine preliminary design somewhat consistent with the requirements of a nuclear aircraft. Ideally, this preliminary engine design could exhibit technology levels similar to those of the Pratt & Whitney STF 477 engine, but with combustor pressure losses and temperatures that are compatible with nuclear power applications. It is recommended that such a data set be developed by

* R. E. Thompson, "Lightweight Nuclear Powerplant Applications of a Very High Temperature Reactor (VHTR)," Westinghouse Advanced Energy Systems Division, Paper 759164, 10th IECEC, 1975. (Ref. 22)

an engine manufacturer for parametric variations of bypass ratio, fan pressure ratio, turbine inlet temperature, etc. It is further recommended that the engine data set be used in a total aircraft system integration study.

Another area recommended for investigation is the design and integration of the engine heat exchanger in the open Brayton cycle to insure that the optimum tradeoff of exit temperature and heat exchanger design is maintained. The proper design and integration of the heat exchanger into the gas generator can have a large impact on the engine performance, on the external drag of the engine/nacelle installation, and on the total weight of the propulsion system.

10.1.3 Heat Transfer System

The heat transfer system is an integral part of the total propulsion system, with a strong mutual interdependence between it and the nuclear subsystem. Eventually, a decision will be reached on a gas-cooled versus a liquid-metal-cooled reactor. That decision cannot be made without taking into account the heat transfer system.

Technology developments are required for both gas and liquid metal heat transfer systems before any decision can be made. A review of the current status and of the technology tasks envisioned for both systems are discussed in Reference 23.* Both systems require technology development and demonstration in a flight-weight design at the temperatures, pressures and lifetime for aircraft application. It is recommended that sufficient material development and system fabrication be undertaken to demonstrate concept feasibility for both gases and liquid metals to permit one type of heat transfer media and reactor to be selected.

* J. C. Muehlbauer, "Nuclear Power for Aircraft," LG74ER0068, Lockheed-Georgia Company, May 1974. (Ref. 23)

10.2 AERODYNAMICS AND FLIGHT CONTROLS

Considerable analytical and experimental efforts are needed to complete the establishment of a data base for supercritical airfoils, which were assumed to be standard state-of-the-art technology for the reference aircraft. Similar efforts are recommended for the relatively large wingtip-mounted vertical surfaces and for the free floating canard with spanwise blowing. For both control surfaces, limited data were extrapolated considerably for application on the reference aircraft. Verification of the estimated performance characteristics through wind-tunnel testing is essential to assure concept feasibility.

One potential problem area requiring further study is the influence of the canard surface on both the wing and the engines. There is a possibility that the canard tip vortices may impinge on one or more engines with unacceptable performance degradation. Extensive analyses and testing will be required to determine the extent of the problem and to eliminate it, if one exists. Similar studies are recommended concerning possible interference effects of the canard on the wing lift distribution.

Studies are recommended to define the overall requirements for load alleviation, active controls, and high lift systems. Wind-tunnel tests of the complete configuration, including the control surfaces, in both high and low-speed regimes will be required to confirm the aircraft performance evaluations.

Current aircraft flying qualities criteria will probably not be adequate or applicable to a nuclear aircraft because of its size, weight, interia distribution, and types of controls. It is suggested that C-5 criteria studies be extended to encompass the peculiarities of the reference nuclear aircraft configuration. Particular attention should be directed toward the effectiveness requirements of the large area, short moment-arm vertical surfaces for yaw, the effect of the roll requirements on the wingtip-mounted verticals, and the response of the aircraft to conventional and non-conventional types of control.

A preliminary study is recommended to establish flying qualities criteria which would be correlated with current large aircraft flight-test experiences. Subsequently, further validation is recommended using ground-based simulators.

10.3 STRUCTURES AND MATERIALS

The reference aircraft was designed with a somewhat arbitrarily-chosen level of composite materials of 40 percent of the total aircraft structural weight. Parametric variations of the level of composite material application produced the expected result on aircraft weight. However, the limited scope of this study precluded establishing the optimum level of composite application to minimize aircraft life-cycle costs. It is recommended that the aircraft designed for the composite sensitivity analysis of this study be investigated in sufficient detail to develop cost data for the major structural subsystems of these aircraft, and then ascertain the optimum level of composites for minimum cost.

Studies are recommended to determine the effects of the large wingtip-mounted verti:als on the wing structural design and flutter. Multi-station analyses of the wing and vertical structures are needed for typical flight conditions to check the strength and weight estimates for these structural elements. It is also recommended that potentially-critical flutter cases be investigated to confirm that an unacceptable low flutter speed is not encountered and that the vertical tail design and placement are satisfactory. If any flutter problems are encountered, then part of the study should include a systematic investigation of the most promising passive means of increasing flutter speed, and an evaluation of the benefits from active flutter-suppression concepts.

10.4 NOISE

Noise certification and community noise analysis studies need to be performed for the reference aircraft if it is to serve as a joint military/civil cargo transport. The recommended study should identify the nacelle acoustic design requirements for

compliance with applicable regulations anticipated for the year 2000. Further, the airframe noise minimum should be investigated, and the impact of applying expected technology advances should be assessed. Part of the end result should be the nacelle acoustic design and acoustic footprints for takeoff and landing.

11.0 REFERENCES

1. "Innovative Aircraft Design Study, Task II," Air Force Request for Proposal F33615-76-R-0112, March 31, 1976.

2. "Technical and Economic Assessment of Swept-Wing Span-Distributed Load Concepts for Civil and Military Air Cargo Transports," NASA Request for Proposal, June 24, 1976.

3. J. E. Werle et al, "High Temperature Liquid Metal Cooled Reactor Technology," Westinghouse Astronuclear Laboratory Final Report on Contract AF33(615)-69-C-1430, Vol. 1-3, March 1970.

4. W. M. Johnston, J. C. Muehlbauer et al, "Technical and Economic Assessment of Span-Distributed Loading Cargo Aircraft Concepts," NASA CR-145034, Lockheed-Georgia Company, 1976.

5. "Airplane Strength and Rigidity" Series, MIL-A-8860 Series, Department of Defense.

6. "Airworthiness Standards: Transport Category Airplanes," Federal Aviation Regulations, Part 25 (FAR 25), Federal Aviation Administration, Department of Transportation, 1974.

7. E. A. Starke, Jr., "The Fatigue Resistance of Aircraft Materials, The Current Frontier," LG76RR0001, Lockheed-Georgia Company, September 1976.

8. J. C. Muehlbauer, "Analytical Investigations of Containment Concepts and Criteria for Airborne Nuclear Reactor Systems," Technical Report AFFDL-TR-71-56, Lockheed-Georgia Company, June 1971.

9. S. F. Hoerner, "Fluid Dynamic Drag," Published by the Author, 1958.

10. T. P. Higgins et al, "Study of Quiet Turbofan STOL Aircraft for Short Haul Transportation," NASA CR-2355, Lockheed Aircraft Corporation, 1973.

11. D. E. Gray, "A Study of Turbofan Engines Designed for Low Energy Consumption," NASA CR-135002, Pratt & Whitney Aircraft Corporation, April 1976.

12. "Flying Qualities of Piloted Airplanes," Military Specification MIL-F-8785B(ASG), 1969.

13. R. F. Sturgeon et al, "Study of the Application of Advanced Technologies to Laminar Flow Control Systems for Subsonic Transports," NASA CR-133949, Lockheed-Georgia Company, 1976.

14. J. F. Kircher and R. E. Bowman, "Effects of Radiation on Materials and Components," Reinhold Publishing Corp., 1964.

15. R. L. Puthoff, "A 1055 Ft/Sec Impact Test of a Two-Foot Diameter Model Nuclear Reactor Containment System Without Fracture," NASA TM X-68103, June 1972.

16. "Advanced STOL Transport (Medium) Study, Cost and Schedule Data," Volume VII, Technical Report ASD/XR 72-22, Lockheed-Georgia Company, 1972.

17. "Cost Analysis, USAF Cost and Planning Factors," AFR 173-10, Department of the Air Force, 1975.

18. "Program Management," AFR 800-2, Department of the Air Force.

19. "Work Breakdown Structure for Defense Material Items," MIL-STD 881A.

20. "Operating and Support Cost Estimates, Aircraft Systems," Defense Systems Acquisition Review Council, May 1974.

21. "Standard Method of Estimating Direct Operating Costs of Turbine Powered Transport Aircraft," Air Transport Association, 1967.

22. R. E. Thompson, "Lightweight Nuclear Powerplant Applications of a Very High Temperature Reactor (VHTR)," Westinghouse Advanced Energy Systems Division, Paper 759164, 10th IECEC, 1975.

23. J. C. Muehlbauer, "Nuclear Power for Aircraft," LG74ER0068, Lockheed-Georgia Company, May 1974.

24. O. Helmer, "Analysis of the Future - The Delphi Method," Report No. P3558, The Rand Corporation, 1967.

25. M. D. Marvin, "Liquid Metal-to-Air Heat Exchanger Design Study," AFAPL-TR-74-12, General Electric Company, 1974.

26. A. W. Thorley and C. Tyzack, "Corrosion Behavior of Steels and Nickel Alloys in High-Temperature Sodium," Proceedings of a Symposium, Vienna, 28 Nov. 1966.

27. "Engineers Guide to Thermal Insulations," Materials Engineering, May 1970.

28. "Nuclear Aircraft Feasibility Study," School of Engineering Air Force Institute of Technology, Wright-Patterson Air Force Base, Ohio, March 1975.

29. F. L. Robson et al, "Analysis of Nuclear Propulsion and Power Conversion Systems for Large Subsonic Aircraft," United Aircraft Research Laboratories, AFAPL-TR-72-47, September 1972.

APPENDIX A. TECHNOLOGY ASSESSMENT

A technology assessment was performed to determine the advanced technology items and design features which were incorporated into the basic nuclear aircraft designs or were considered in technology sensitivity studies. For this assessment, the list in Table A.1 was compiled of technology items potentially capable of improving overall aircraft performance, of reducing the total system cost, of adding to the operational flexibility of the aircraft, and/or of solving some design problem.

The Delphi Method* was used to evaluate the applicability and the development status by the year 2000 for each technology item. A minimum of three specialists in each of the major disciplines, e.g., Aerodynamics, Propulsion, Structures, etc., was selected to implement the Delphi Method. Each specialist independently evaluated items in his discipline, using the format of the sample evaluation in Figure A-1.

Following the standard Delphi procedure, the averaged results of the evaluations were submitted to the specialists for consideration in possibly revising their original assessments. The averaged results from this assessment iteration were the technology levels used in Sections 3.0, 5.0 and 8.0 for the aircraft designs and in the sensitivity studies of Section 6.0.

The technology evaluation included an assessment of current and projected status in the year 2000, of the level of applicability, of the probability of attaining the future status, and of the potential effects of the technology item on aircraft drag and fuel consumption and on system weight and cost. Comments by the specialists identified special problems, features, and other important factors. Typically, they commented on the sensitivity of the technology application to aircraft size, reliability and maintainability effects, cost and dependence upon other technology development programs, recognized technology spinoffs, safety characteristics, and similar considerations.

* O. Helmer, "Analysis of the Future - The Delphi Method," Report No. P3558, The Rand Corporation, 1967. (Ref. 24)

TABLE A.1. TECHNOLOGY ITEMS EVALUATED

Aerodynamics

- Supercritical Wing
- Laminar Flow Control
- Upper Surface Blowing
- Externally Blown Flaps
- Internally Blown Flaps
- Winglets
- Oblique Wing
- Variable Cambered Wing
- Boundary Layer Control
- High Aspect Ratio Wing
- Streamline Contouring
- Area Ruling
- Powered Lift
- Propulsion Lift
- Augmentor Wing
- Variable Sweep Wing

Stability & Control

- Active Controls
- Relaxed Static Stability
- Stability Augmentation System
- Ride Control System
- Load Alleviation System
- Gust Alleviation System
- Fly-By-Wire System
- Flutter Suppression System

Propulsion

- Nuclear Propulsion
- High Bypass-Ratio Engines
- Dual Cycle Engines
- Regenerative Engines
- Variable Geometry Engines
- High-Speed Propellers
- Prop-Fans

Structures & Materials

- Metallic Structures
- Composite Structures
- Crashworthy Structure
- High Strength Alloys
- Titanium Alloys
- Composite Materials

Systems

- Multiple Redundancy Avionics
- Automatic Subsystem Monitoring
- Solid State Electronics
- Air Cushion Landing System
- Comfort Systems
- Safety Systems
- Survival Systems

TECHNOLOGY ITEM: Composites

CONCEPT APPLICABILITY (Circle C - critical, (S) - significant, M - minor, N - none)

TECHNOLOGY ASSESSMENT

	Status*	Level	Percent Probable	Effect** (% Change Relative to 1976)			
				Drag	Weight	Fuel	Cost
1976	G	10%	90%				
1985	E	35%	80%		-15		5
1995	E	60%	90%		-20		0
2000	E	65%	90%		-25		-15

* Use E - excellent, G - good, F - fair, P - poor
** Use minus sign to show a decrease

COMMENTS:

Sensitivity to Aircraft Size: Insensitive to aircraft size if level of applicability is expressed as a percentage of aircraft weight. Early level of use will depend on amount of potential secondary structural applications on proposed aircraft.

Reliability & Maintainability: Much better than current secondary structure of aluminum and fiberglass-faced honeycomb (25% of present maintenance).

Cost: Cost increases in 1985 are due to limited fabrication experience and development. After 1985, cost reductions occur through improved manufacturing techniques.

Technological Spinoffs: Sports equipment, transportation vehicles, specialized structural elements.

Safety: No problem.

Other: The present concern over water absorption will be solved by 1985.

Figure A-1. Typical Technology Evaluation

Figure of Merit (FOM) values were calculated for each technology item and used in selecting the important items for the aircraft design and sensitivity studies. The FOM was defined as the product of the future status and the applicability. Numerical values were assigned to the predictions in these two areas according to the code:

Applicability	Value	Status
C - critical	10	E - excellent
S - significant	6	G - good
M - minor	3	F - fair
	1	P - poor
N - none	0	

All technology items judged to be of critical applicability automatically qualified for further consideration. Additional items were selected based on the FOM values according to the guidelines:

Evaluation	Procedure
FOM > 60	Item selected
60 ≥ FOM ≥ 30	Item selection dependent upon possible effects and comments
FOM < 30	Item disregarded

FOM values greater than 60 indicate relatively low risk development items with a high degree of applicability. FOM values less than 30 indicate poor risk development items with a low level of applicability.

Table A.2 shows the projected applicability, development status, FOM, and benefit results for each of the technology items. The benefit values are the algebraic averages of the effects of the technology on drag, weight, fuel consumption, and cost. Positive benefit values are desirable, while negative values represent a penalty.

TABLE A.2. TECHNOLOGY ASSESSMENT RESULTS

Aerodynamics	Application[1]	Status[2]	FOM	Benefits	Selection
Supercritical Wing	S	E	60	12.8	Yes[3]
Laminar Flow Control	S	E	60	11.5	Yes[7]
Upper Surface Blowing	N-M	E	15	23.5	No
Externally Blown Flaps	N-M	G-E	12	-8.8	No
Internally Blown Flaps	N-M	G-E	12	26.8	No
Winglets	M-S	E	45	9.3	Yes[7]
Oblique Wing	N-M	G	9	1.5	No
Variable Cambered Wing	M	E	30	5.3	No
Boundary Layer Control	M-S	E	45	8.0	No
High Aspect Ratio Wing	S	E	60	7.8	Yes[5]
Streamline Contouring	M	E	30	4.3	No
Area Ruling	M-S	E	45	4.5	No
Powered Lift	M	E	30	-7.5	No
Propulsion Lift	M	E	30	-7.5	No
Augmentor Wing	N-M	E	10	-7.5	No
Variable Sweep Wing	M	E	30	0.8	No
Stability & Control					
Active Controls	S	E	60	12.1	No[6]
Relaxed Static Stability	S	E	60	9.6	Yes[3]
Stability Augmentation System	S	E	60	7.2	No[6]
Ride Control System	M-S	G-E	36	7.0	No
Load Alleviation System	S	E	60	5.8	No[6]
Gust Alleviation System	S	E	60	7.2	No[6]
Fly-By-Wire-System	S	E	60	-1.2	No[6]
Flutter Suppression System	S	E	60	10.3	No[6]

TABLE A.2. TECHNOLOGY ASSESSMENT RESULTS (Cont)

Propulsion	Application[1]	Status[2]	FOM	Benefits	Selection
Nuclear Propulsion	C	P-F	20	-	Yes[4]
High Bypass-Ratio Engines	S	E	60	2	Yes[5,7]
Dual Cycle Engines	M-S	G-E	36	-0.3	No
Regenerative Engines	M	G	18	7.7	No
Variable Geometry Engines	S	G	36	5.7	No
High-Speed Propellers	M	G	18	9.0	No
Prop-Fans	S	G	36	18.0	No
Structures & Materials					
Metallic Structures	C	E	100	3.0	Yes[3]
Composite Structures	S	E	60	12.7	Yes[3,7]
Crashworthy Structure	S	G	36	-	Yes[4]
High Strength Alloys	S	G-E	48	-12.0	No
Titanium Alloys	S	E	60	0	Yes[3]
Composite Materials	S-C	E	80	23	Yes[3,7]
Systems					
Multiple Redundancy Avionics	C	E	100	5.5	Yes[3]
Solid State Electronics	S-C	E	80	-75.7	Yes[3]
Automatic Subsystem Monitoring	S	E	60	33	Yes[3]
Air Cushion Landing System	M	F	9	-	No
Comfort System	S	G-E	48	-3	Yes[3]
Safety System	C	E	100	0	Yes[3]
Survival System	C	E	100	-8	Yes[3]

1. Applicability Code: C - critical, S - significant, M - minor, N - none
2. Status Code: E - excellent, G - good, F - fair, P - poor
3. Item incorporated into all designs as standard future state of the art
4. Item incorporated into all designs due to concept requirement
5. Items considered as part of normal design optimization
6. Items not included, though highly rated, because of dependence and interface requirements with related systems
7. Item varied in sensitivity studies

As noted on the table, many of the technology items were selected for inclusion on all aircraft designs as standard future state of the art. Items selected for application on a reference aircraft to determine the technology sensitivity included laminar flow control, high bypass ratio engines, and composite material levels. Winglets were selected as a technology sensitivity item in case the conventional configuration emerged as optimum, which it did not. Both the canard and spanloader configurations incorporate vertical endplates on the wing tips as an integral part of the basic design concept. Thus, winglets are not a candidate technology item for these two configurations.

Another item which promises significant potential benefits is the prop-fan. This item was specifically excluded at study initiation due to budgetary constraints, but it merits investigation.

In general, most of the technology items that were rejected lacked applicability for the nuclear aircraft concept, as noted by the none (N) or minor (M) rating. Other rejected items exhibited low FOM ratings or additional costs as reflected by the negative benefit values.

Most of the items in the stability and control area were rejected, in spite of high ratings and potential benefits, because of the interdependence of these items. The high potential benefit values noted for each item are based on the assumption that the other items have also been included in the aircraft design. If the items in this category were considered separately, that is, if the other items were not simultaneously implemented, the potential benefits would be small. The amount of effort required to consider the interaction of all of these items would exceed the intent and scope of this program.

APPENDIX B. DESCRIPTION OF NuERA II REACTOR

The reference reactor used in this study is a liquid-metal-cooled fast reactor as typified by the NuERA II nuclear subsystem concept defined by Westinghouse (Ref. 3) and shown in Figure B-1. In this nuclear subsystem, the reactor coolant is separated lithium which is contained entirely in a refractory metal system. All the primary piping is made of columbium-1 percent zirconium alloy (Cb-1Zr) as are the intermediate heat exchangers, the pumps, and the reactor vessel. The fuel pins, which also are in contact with the lithium, are clad in a tantalum base alloy, ASTAR 811-C. The coolant enters the reactor at 1400°F and is heated to 1800°F. The coolant then enters the intermediate heat exchanger, a counterflow shell and tube exchanger, where it flows through the tubes and is cooled to 1400°F. From the heat exchanger, it flows to the primary coolant circulating pump, an electrically-driven canned-motor centrifugal pump, which returns it to the reactor vessel.

A secondary fluid, liquid sodium-potassium (NaK), is used to transfer the reactor thermal energy to the engines. It leaves the shell of the intermediate heat exchanger at 1700°F and flows to the engine heat exchanger. In this engine counter-flow exchanger, the NaK is cooled to 1300°F as its energy is transferred to the air stream, thereby replacing the normal combustor function in the engine. From the engine heat exchanger, the NaK flows to the secondary coolant circulating pump, an electrically-driven canned-motor centrifugal pump, which returns the coolant to the intermediate heat exchanger. Isolation valves are included in each secondary loop to provide shutoff capability if required in the event of an engine failure.

The reactor, shield, and all primary loop components are installed inside the containment vessel. Secondary coolant pumps and reactor system auxiliaries are located outside of the containment vessel. Components such as pump controllers, gas bottles, shield cooling and the decay cooling auxiliaries are mounted in the aircraft fuselage. The inert gas supply will maintain a pressure of 15 psig in the containment vessel. The control system concept assumes a digital computer control and a battery for critical power supply.

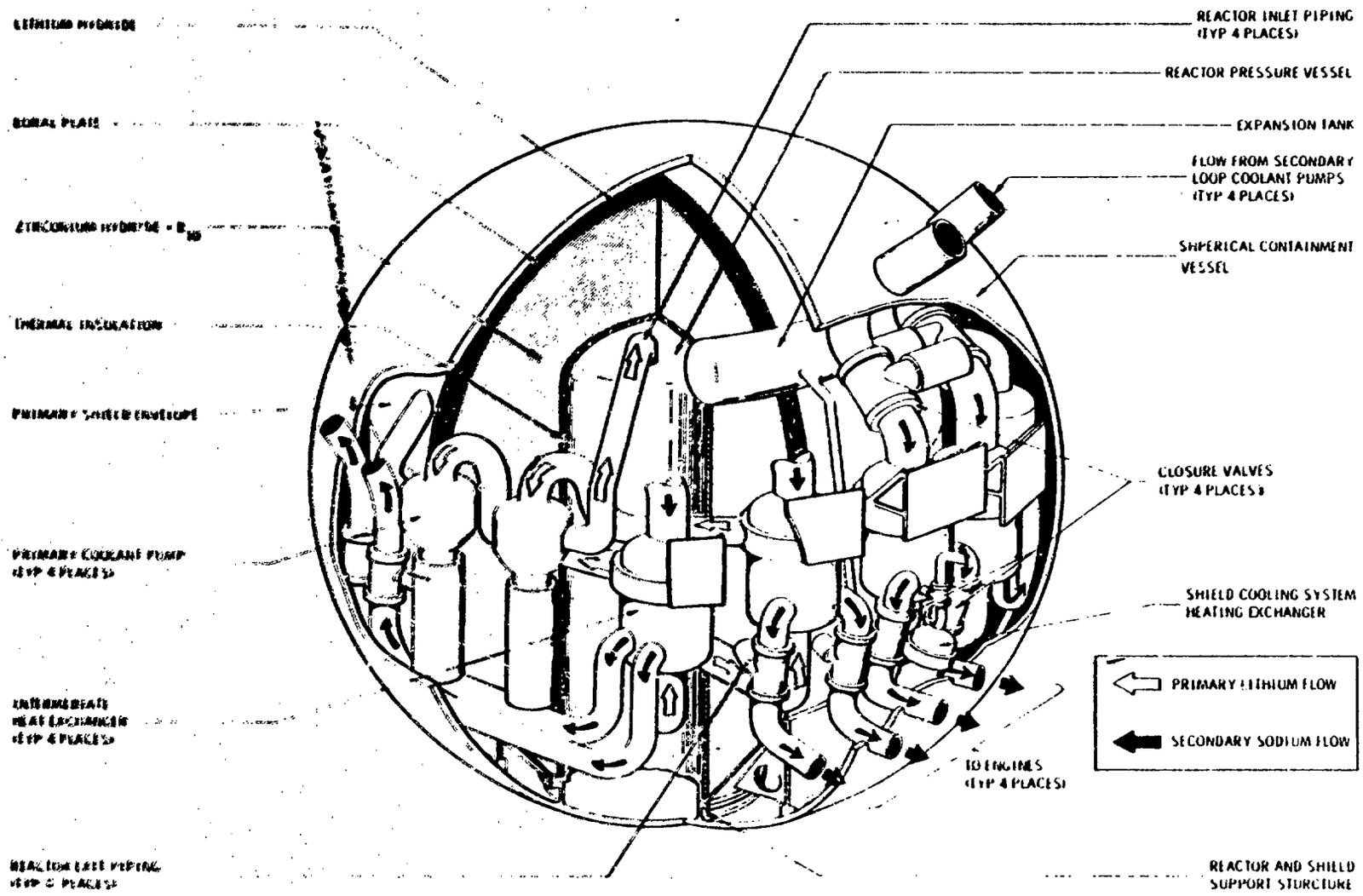

Figure B-1. Reference Reactor Design

As shown in Figure B-1, the reactor with its primary shield is mounted vertically with the vertical centerline laterally offset aft from the center of the spherical containment vessel. The intermediate heat exchangers, primary pumps and the shield coolant system heat exchanger and pumps are installed in the crescent-shaped space provided. The banana-shaped expansion tank is located at the highest point in the compartment, and is connected to one of the reactor outlet lines. The intermediate heat exchangers, primary coolant pumps and expansion tank are supported from the containment shell. The reactor and shield assembly are mounted on a base structure attached to the lower portion of the containment shell.

The primary shield, external to the pressure vessel, completely encloses the reactor and consists of an inner layer of zirconium hydride, and an outer layer of lithium hydride. Inserted between these two major layers is a sheet of boral. The shield is compartmented and hermetically sealed because of materials outgassing and the need to contain the shield coolant.

Shield cooling system components are located both inside and outside of the containment vessel. The shield cooling system is completely independent of the reactor cooling system, having its own primary and secondary loop, both of which contain NaK as the coolant. The primary loop and the system intermediate heat exchanger are located within the containment sphere because the coolant, in passing through the shield in close proximity to the reactor, becomes activated. The secondary shield coolant loop and secondary coolant pump are located outside of the containment sphere. Ultimate heat rejection is achieved by the NaK-to-air heat exchanger, taking heat from the secondary cooling loop and dumping it to ambient air ducted through the heat exchanger.

The decay heat removal system makes use of one of the primary and secondary loops. The latter is modified to contain a bypass loop which is connected to one of the secondary loops and reflects the decay heat through a liquid-metal-to-air heat exchanger. The secondary coolant pump provides the pumping power. The bypass loop is activated by appropriately located flow switching valves.

APPENDIX C. ADDITIONAL ENGINE DATA

Part of the parametric aircraft sizing studies and the sensitivity studies on the reference aircraft addressed variations in cruise altitude and Mach number as well as engine bypass ratio. Typical engine thrust and fuel consumption data used in these analyses are presented in Figures C-1 and C-2. These data are for a "redesigned" engine, based on the Pratt & Whitney STF 477 engine technology, with a nuclear cruise TIT of 1600°F and a chemical-fueled cruise TIT of 1800°F.

The effects of variations in engine design TIT on several engine parameters are shown in Table C.1. The case listed in the third column of the table is the engine for one of the aircraft developed as part of the optimization process in the parametric analyses of Section 3.4. This particular aircraft emerged as optimum from an assessment of the sensitivity of aircraft size to variations in engine design TIT. With a chemical fuel takeoff TIT of 1870°F to meet field length requirements, the engine is operated at a slight partial power setting during nuclear cruise due to the heat exchanger limiting the TIT to 1600°F.

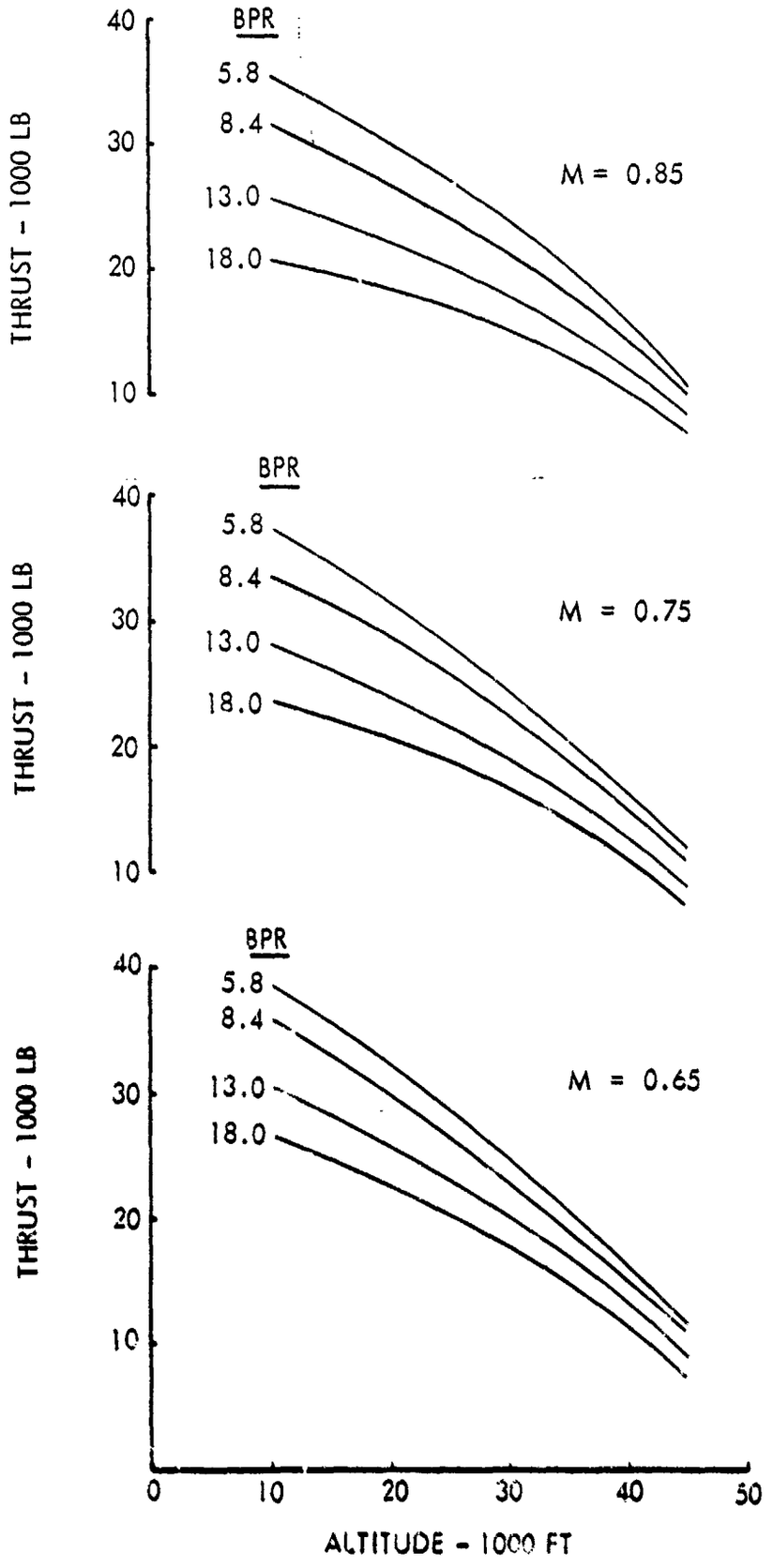

Figure C-1. Typical Engine Thrust Parametric Data

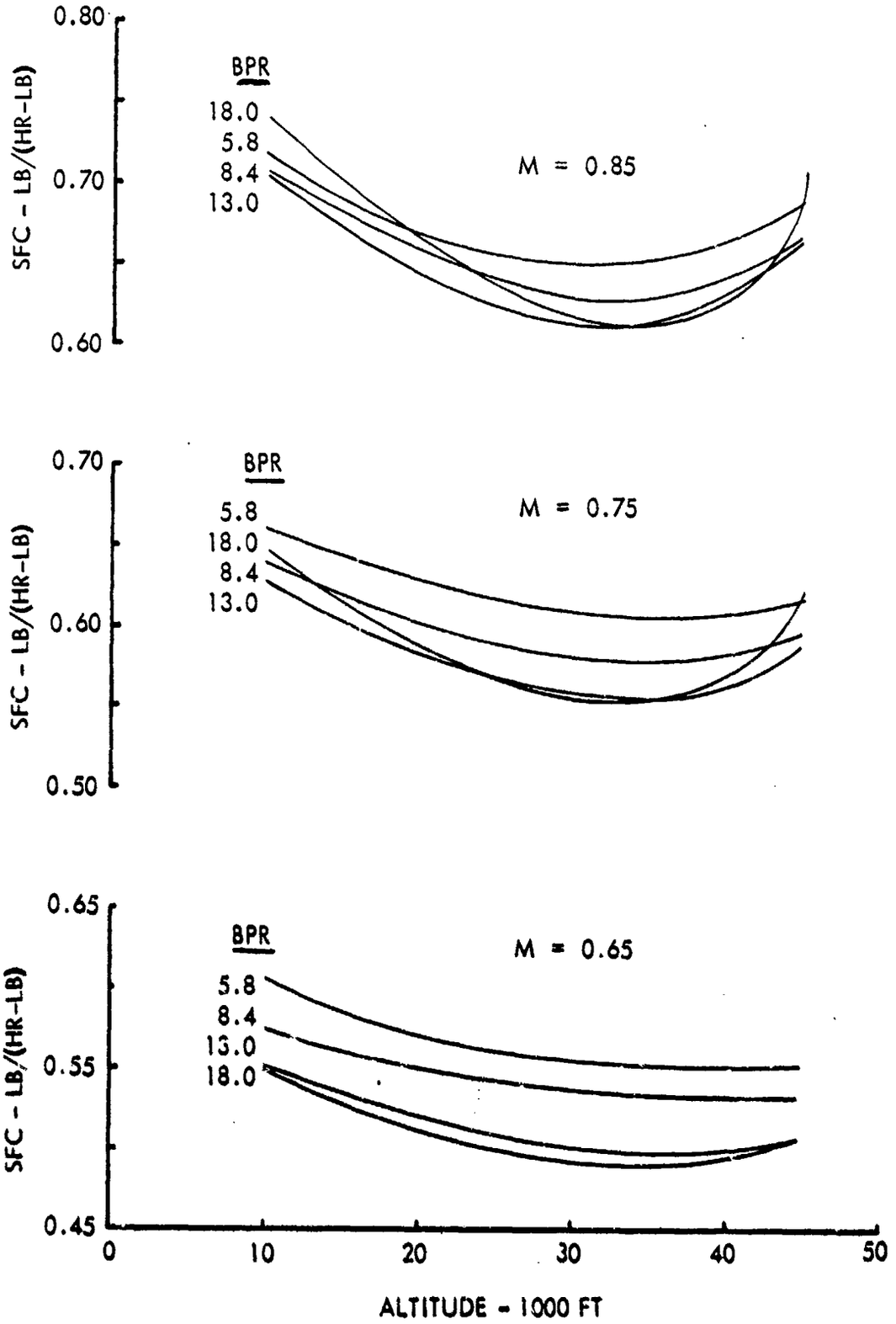

Figure C-2. Typical Engine Fuel Consumption Parametric Data

TABLE C.1. EFFECTS OF TURBINE INLET TEMPERATURE ON ENGINE CHARACTERISTICS

Bypass Ratio = 8.4

Takeoff: (Sea Level Static)

Fuel	JP	JP	JP	JP
Turbine Inlet Temp - °F	2600	2000	1870	1800
Overall Pressure Ratio	40	15	12	10

Cruise: (Altitude = 36,089 ft, Mach Number = 0.75)

Fuel	JP	Nuclear	Nuclear	Nuclear
Turbine Inlet Temp - °F				
Design	2400	1800	1670	1600
Operating	2400	1600	1600	1600

Parameters:

Takeoff Thrust	Base	Base	Base	Base
Combustor Pressure Loss	Base	Base +5%	Base +5%	Base +5%
Bare Engine Weight	Base	Base +12%	Base +15%	Base +17%
Cruise Thrust	Base	Base -31%	Base -16%	Base -7%
Cruise Energy Input Req'd	Base	Base +8.5%	Base +10%	Base +12%

APPENDIX D. PARAMETRIC RELATIONSHIPS FOR PROPULSION SYSTEM EQUIPMENT EXTERNAL TO THE NUCLEAR SUBSYSTEM

Parametric relationships were derived for the various propulsion system components external to the nuclear subsystem so that the aircraft configuration studies could properly account for variations in the weights of these components. Specific components analyzed included the secondary loop, shield cooling system, reactor decay heat removal system, and the reactor instrumentation and control system. Parametric relationships for sizing the sodium-potassium (NaK) to air heat exchanger in the engines were also derived and are included.

D.1 SECONDARY LOOP PIPING

The secondary loop piping is required to transport the heat transfer fluid from the reactor intermediate heat exchangers to the engine heat exchangers. A sodium-potassium liquid metal, NaK 78 (78 weight percent K), was selected as the heat transfer fluid for this application due to its relatively low melting point temperature (12°F). With this melting temperature, pipeline heaters are not required. The assumed pipeline requirements and constraints are shown in Table D.1. Due to the high temperatures (1300 - 1700°F) at which the pipelines must operate, the creep-rupture stress at a 10,000-hr full temperature lifetime was used as the material selection criterion. Haynes 188 was selected as the material for the pipelines, based on the approach in Ref. 25.* The creep-rupture stress value used at 1700°F was 1000 psi and at 1300°F was 8000 psi. Since the pipeline weight and volume are affected by fluid velocity, 40 ft/sec was selected as a reasonable upper limit (Ref. 3).

Ref. 26** shows the corrosion rate to be more or less linear with velocities up to 10 ft/sec. However, there appears to be an inflexion in the range of 10 to 15 ft/sec, above which velocity has very little effect on the rate of metal loss (velocity effects

* M. D. Marvin, "Liquid Metal-to-Air Heat Exchanger Design Study," AFAPL-TR-74-12, General Electric Company, 1974. (Ref. 25)

** A. W. Thorley and C. Tyzack, "Corrosion Behavior of Steels and Nickel Alloys in High-Temperature Sodium" Proceedings of a Symposium, Vienna, 28 November 1966. (Ref. 26)

TABLE D.1. ASSUMED PIPELINE REQUIREMENTS AND CONSTRAINTS

Fluid	NaK 78
Fluid Temperature in Hot Leg	1700°F
Fluid Temperature in Cold Leg	1300°F
Minimum Pipe Thickness	0.1 in.
Maximum Insulation Surface Temperature	200°F
Maximum Fluid Velocity	40 ft/sec
Sink Temperature	
At 30,000 ft Altitude	-2°F
At Minimum Operating Altitude	60°F
Range of Heat Transport per Pipe	20 - 160 MW

have been investigated up to 40 ft/sec). Above 15 ft/sec, the oxygen level in the liquid metal establishes the metal loss rate.

The pipe insulation material, used in this study for weight estimation purposes, is a material composed of alumina-silica fibers combined with binders.* It has a maximum service temperature of 2000°F and a density of 16 lb/ft^3. A mean thermal conductivity of 0.05 Btu/(hr-ft-°F) was used in this analysis.

For this application the effective pipe weight per foot of length may be calculated by the following equation.

$$W_{eff} = \frac{\pi}{4} D_i^2 \quad \rho_{NaK} + \frac{\pi}{4} (D_p^2 - D_i^2) \quad \rho_p + \frac{\pi}{4} (D_o^2 - D_p^2) \quad \rho_{insul.}$$

* "Engineers Guide to Thermal Insulations," Materials Engineering, May 1970. (Ref. 27)

where D_i is the inside pipe diameter in ft.

D_p is the outside pipe diameter in ft.

D_o is the outside insulation diameter in ft.

ρ is the density in lb/ft^3 of the liquid metal, pipe or insulation as denoted by the subscript

The first term is the liquid NaK weight, the second term is the pipe weight, and the third term is the insulation weight. Two other factors normally included are the pumping power penalty and the reactor weight penalty due to the heat loss which increases the reactor size and lowers the engine efficiency. Both terms were found to be small in comparison with the others and were neglected.

Assuming free convection on the outer surface of the insulation, the 30,000-ft altitude ambient conditions require thicker insulation than is required at the minimum operating altitude. When the insulation is sized for the 30,000-ft altitude (200°F surface temperature) but the aircraft is operating at lower altitudes, the surface temperature drops to about 170°F. The piping effective weight relationship is per foot of length, because the total piping weight will be significantly affected by the aircraft configuration.

Two piping configurations were analyzed. The first configuration used separate pipes, one as a supply line to the engine and the other as the return line. Both pipes were insulated with sufficient insulation thickness so that the maximum insulation surface temperature was 200°F. The second configuration used a concentric pipe arrangement with the supply line inside a larger diameter return line. Since the liquid metal has very high heat transfer coefficients, the inner pipe has to be insulated as well as the outer pipe. The net result was that the concentric pipe arrangement was heavier than the two-pipe configuration for the liquid metal case. Therefore, the two-pipe configuration was used as the reference geometry. Similar findings were documented in Ref. 28.*

* "Nuclear Aircraft Feasibility Study," School of Engineering, Air Force Institute of Technology, Wright-Patterson Air Force Base, Ohio, March 1975. (Ref. 28)

With a NaK velocity of 40 ft/sec, a NaK temperature of 1300°F and an insulation surface temperature of 200°F, the pipeline effective weight (includes the weight of the NaK, pipe and insulation) per foot of length is shown in Figure D-1 as a function of the

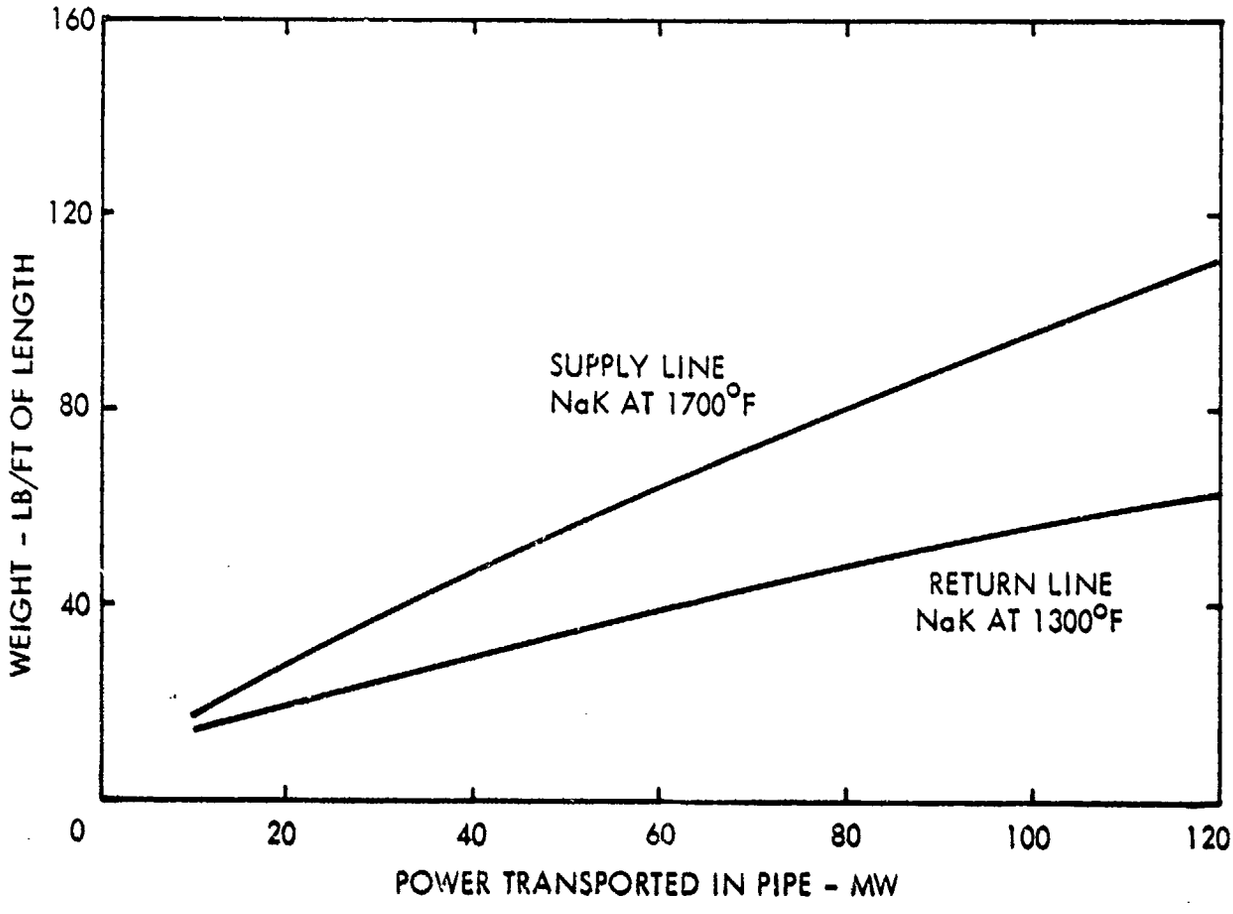

Figure D-1. Pipeline Weight Estimation.
NaK Velocity = 40 ft/sec, Surface Temperature = 200°F

power transported in the pipe. With an allowance for a 20-percent increase in pipe effective weight to account for pipe support and valving, the pipe line weight for the return leg (NaK at 1300°F) for each engine can be approximated by

$$W_c = 3.70 \left(\frac{Q_R}{N_E}\right)^{0.628} \text{ lb/ft of length}$$

and the volume of each return pipeline by

$$V_c = 0.191 \left(\frac{Q_R}{N_E}\right)^{0.542} \text{ ft}^3\text{/ft of length}$$

where Q_R is the reactor power level in MW and

N_E is the number of engines

With the same allowance for pipe support and valving, the pipeline weight for the supply line for each engine can be approximated by

$$W_H = 2.94 \left(\frac{Q_R}{N_E}\right)^{0.792} \text{ lb/ft of length}$$

and the volume of each supply line by

$$V_H = 0.238 \left(\frac{Q_R}{N_E}\right)^{0.575} \text{ ft}^3\text{/ft of length}$$

The pipeline effective weight without the support or valving allowance for the supply line with NaK at 1700°F is also shown in Figure D-1.

The pipeline weight sensitivity to NaK velocity and insulation surface temperature is shown in Figure D-2 for the return piping. An increase in allowable insulation surface temperature from 200°F to 300°F reduces pipeline weight about 20 percent for the velocities investigated. The 40 ft/sec NaK velocity appears near the knee of the curves, such that a significant increase in velocity does not result in a significant decrease in pipeline weight. These same sensitivities for the supply line weight are also shown on Figure D-2. Here again, an increase of 100°F in allowable surface temperature decreases pipe weight about 20 percent over the range of velocities investigated.

D.2 SHIELD COOLING AUXILIARY SYSTEM

In addition to the secondary coolant loops, another active coolant system must penetrate the containment vessel. This is the shield cooling system. During power operation, heat is developed in the reactor shield through gamma radiation absorption and neutron capture. A liquid metal coolant system is used to remove this heat to prevent damage

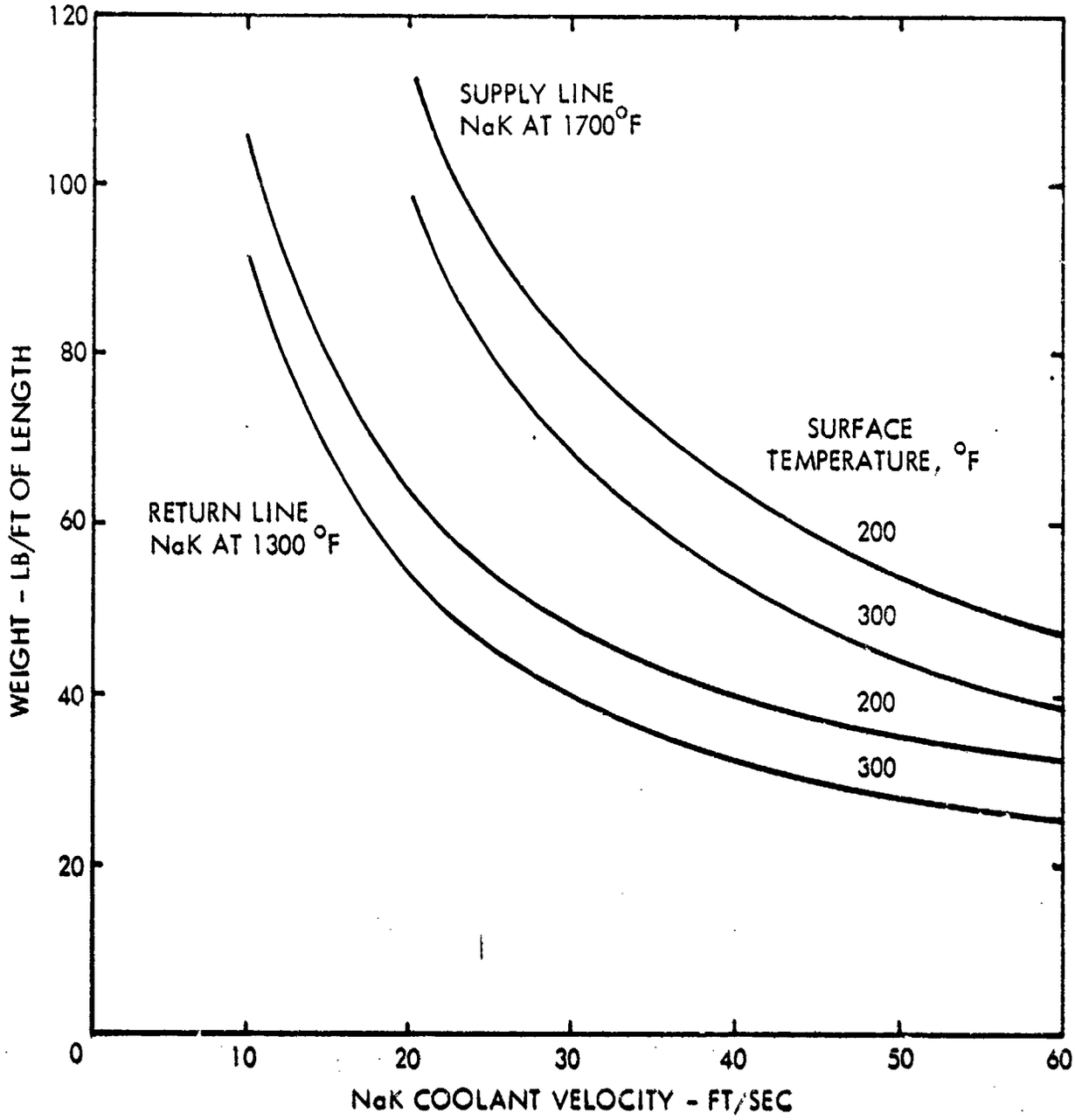

Figure D-2. Effect of Coolant Velocity on Pipeline Weight. 60 MW of Power Transported in Pipe.

to the shield. To avoid activation of this coolant stream, an intermediate heat exchanger is installed inside the containment vessel and a secondary liquid metal loop is used to transfer the heat to a liquid-metal-to-air heat exchanger. The shield cooling system is thus completely analogous to, and consistent with, the secondary loop systems, with the shield cooling coils substituted for the reactor as the heat source and with an air blast heat exchanger substituted for the engine heat exchangers.

The auxiliary systems weights and volumes were first estimated for the reference NuERA II reactor and then scaled for different thermal ratings. For the reference 275 MW thermal output rating, the shield cooling requirement is 7 MW (Ref. 3). With NaK 78 as the coolant and assuming a 200°F rise in the fluid as it passes through the shield, the flow rate requirement is 158 lb/sec. With a pressure loss of 40 psi through the loop and a 60-percent efficient pump and motor, the pumping power requirement is 58 hp.

The size and weight of the pumps and totally enclosed motors were scaled based on data for commercial pumps and motors. It was judged that the decrease in weight due to design for aircraft application would be offset by the increase in weight due to the liquid metal application. Therefore, the pump and motor weight was estimated by

$$W_p = 58.5\ (P_p)^{0.7} \quad \text{lb}$$

and the volume by

$$V_p = 2.12\ (P_p)^{0.6} \quad \text{ft}^3$$

where P_p is the horsepower required by the pump

For the shield cooling system, 30-hp pump units were found to be adequate. These pumps and motors weigh 1260 lb and require a volume of 33 ft^3.

The liquid NaK to air heat exchangers were sized based on heat exchanger data in Ref. 25. Using an air mass flow rate per unit area of 10 lb/ft^2-sec, a specific conductance of 80 Btu/(hr-°F) per pound of finned tube was obtained. Therefore, for the 7 MW heat transfer requirement the finned tube weight would be 1495 lb, and assuming a 1.25 multiplier to allow for ducts and manifolds, the heat exchangers would weigh 1865 lb. Also, based on the above air mass velocity, the volumetric thermal conductance would be 14,000 Btu/hr-°F per cubic foot of the tube matrix.* Therefore, the heat exchanger volume was estimated to be 10.7 ft^3.

* F. L. Robson et al, "Analysis of Nuclear Propulsion and Power Conversion Systems for Large Subsonic Aircraft," United Aircraft Research Laboratory, AFAPL-TR-72-47, September 1972. (Ref. 29)

The pipeline weight for the shield cooling system was based on a conservative NaK velocity of 20 ft/sec, an insulation surface temperature of 200°F and a length requirement of 50 ft. The weight and volumes were scaled for reactor thermal power ratings from 100 to 1000 MW and are shown in Table D.2.

TABLE D.2. WEIGHT AND VOLUME ESTIMATES OF THE AUXILIARY SYSTEMS EXTERNAL TO THE CONTAINMENT VESSEL

Reactor Power - MW		100	275	500	700	1000
Shield Cooling System						
Pumps and Motors	lb	620	1260	1915	2473	3110
	ft^3	17.8	33.0	47.5	58.3	72.5
NaK to Air Heat Exchangers	lb	678	1865	3390	4747	6782
	ft^3	3.9	10.7	19.5	27.2	38.9
Pipes and Insulation	lb	216	407	592	732	916
	ft^3	12.0	20.7	28.6	34.3	41.7
Decay Heat Removal System						
Pumps and Motors	lb	887	1800	2735	3462	4444
	ft^3	24.4	45.2	65.1	79.9	99.3
NaK to Air Heat Exchangers	lb	1456	4004	7280	10192	14560
	ft^3	8.3	22.8	41.5	58.0	82.9
Pipes and Insulation	lb	261	618	1028	1370	1856
	ft^3	20.0	35.9	50.6	61.4	75.4
Secondary Pumps and Motors	lb	1963	5400	9818	13745	19636
	ft^3	13.5	37.1	67.5	94.4	134.9
Total	lbs	6081	15354	26758	36721	51304
	ft^3	99.9	205.4	320.3	413.5	545.6

D.3 DECAY HEAT AUXILIARY SYSTEM

One more system uniquely associated with a reactor power plant is necessary; this is the decay heat removal system. After the reactor is shut down, heat continues to be generated in the core for a short time because of fission induced by sub-critical multiplication of delayed neutrons, and for longer times because of radioactive decay

of fission products, and induced radioactivity of cladding, structural members, etc. The shut-down power level is initially about 15 MW and decays to about one-third of this value in one hour for the reference NuERA reactor. After approximately 80 hours, the power level is still one megawatt. Therefore, the aircraft requires some form of reactor cooling even after it is on the ground. The system selected requires no additional penetrations through the containment shell, and it requires very few components in addition to those already installed in the engine loops. The decay heat removal system consists of an air-cooled heat exchanger in parallel with the engine heat exchanger, with stop valves to isolate the decay-heat-removal heat exchanger from the power loop. Multiple installations for reliability may not be necessary, because the main propulsion engines operating on chemical fuel provide back-up capability for this function. Similarly, the peak heat load that this heat exchanger must carry (the initial load through it) can be somewhat reduced by extending the engine operating time on chemical fuel after reactor shutdown.

The decay heat system was sized for the initial capability to remove 15 MW of decay heat. The same procedure used for estimating the weight and volume of the shield cooling system was used for the decay heat system. The resulting weights and volumes are shown in Table D.2.

D.4 SECONDARY PUMPS, MOTORS AND CONTROLS

The secondary pumps and motors weights and volumes were calculated using the equations given in Ref. 3 for the primary pump and motor (see Table D.2).

The reactor instrumentation and control system was estimated to weigh 2000 lb and require 100 ft^3 of volume independent of reactor thermal power. This estimate was based on one console with a density of 20 lb/ft^3.

The following parametric relationship was used for estimating the weight of the nuclear system components (shield cooling, decay heat removal, secondary pumps, and instrumentation and control) external to the containment vessel:

$$W_T = 2000 + 80.9\,(Q_R)^{0.934} \quad \text{lb}$$

and for volume :

$$V_T = 100 + 2.94\,(Q_R)^{0.756} \quad \text{ft}^3$$

where Q_R is the reactor power level in MW

D.5 ENGINE HEAT EXCHANGER

Characteristics of the engine heat exchangers sized for nuclear cruise were scaled from the engine heat exchanger basepoint design developed by General Electric (GE) (Ref. 25). Pertinent features of the GE design are itemized in Table D.3.

TABLE D.3. CHARACTERISTICS OF BASEPOINT ENGINE HEAT EXCHANGER

Maximum Engine Diameter	8.8 ft
Engine Cruise Thrust on Nuclear Power	12,500 lb
Incremental Engine Length Due to Heat Exchanger	19.7 in.
Engine Turbine Inlet Temperature with Nuclear Power	1600°F
Heat Exchanger Weight*	9300 lb
Engine Weight	22,400 lb

* Includes weights of support structure and liquid metal contained in heat exchanger.

In scaling the GE heat exchanger for this study, the outside diameter of the heat exchanger was restricted to the maximum engine diameter, as determined in sizing the engine for chemical fuel operation. However, the length of the heat exchanger was unrestricted. The relationship used to determine the incremental increase in engine

length due to the heat exchanger is

$$\Delta L = \Delta L_o \, (T/T_o) \, (D_o/D)$$

where ΔL_o is the incremental engine length for the basepoint heat exchanger

T is the engine cruise thrust level in lb

T_o is the basepoint engine cruise thrust level in lb

D_o is the basepoint engine diameter in ft

D is the diameter in ft of the engine sized for operation on chemical fuel

The weight of the heat exchanger was obtained by scaling the GE basepoint heat exchanger in direct proportion to the thrust levels of the engines.

$$W = W_o \, (T/T_o)$$

where W_o is the weight of the basepoint heat exchanger.

APPENDIX E. ADDITIONAL COST DATA

The purpose of this Appendix is to provide more detailed cost breakdowns for some of the economic data which were presented in summary form in the body of this report. Table E.1 contains the manpower estimates and some of the assumptions made in estimating the program costs for the RDT&E, validation and follow-on development phases of the reference nuclear aircraft. The labor and material rates used in deriving the airframe costs for the reference aircraft are listed in Table E.2. Support and operating cost data in Table E.3 provided the basis for the summary data presented in Section 7.1 for the reference aircraft. Table E.4 contains the production cost breakdown for the alternate nuclear aircraft.

TABLE E.1. RDT&E, VALIDATION AND DEVELOPMENT COST DATA FOR REFERENCE NUCLEAR AIRCRAFT

	Program Costs, Million $		Program Effort, Million Manhours	
	Validation Phase	Follow-On Development	Validation Phase	Follow-On Development
Conceptual Phase and Studies	1.236	3.707		
Non-Recurring Design and Development				
Airframe	182.515	411.930	7.800	25.636
Propulsion*	-	-		
Reactor Assy	1372.500	877.500		
Avionics*	-	-		
Systems Engineering and Management	9.126	61.789		
Basic Tooling	190.036	544.567	6.585	18.739
Subtotal, Development	1754.176	1895.786		
Category I Testing				
Wind Tunnel Model and Tests	9.011	9.061	0.377	1.390
Static Test Articles (1)	0.000	61.987	0.000	2.190
Static Tests	0.000	67.829	0.000	2.899
Fatigue Test Articles (2)	0.000	56.273	0.000	1.971
Fatigue Tests	0.000	84.786	0.000	3.623
Propulsion Test Articles*	-	-	-	-
Propulsion Tests*	-	-	-	-
Ground Test Articles (3)	3.480	13.922		
Ground Tests	35.717	99.030	1.526	4.232
Mockups-Engr. and Prod.	7.842	9.436	0.335	0.401
Flight Tests (2277 Hours)	19.875	64.527	0.829	2.913
Category II Testing				
Flight Tests (253 Hours)	0.000	7.170		
Total System Test	75.925	474.021		
Test Spares				
Airframe	18.765	92.021		
Propulsion	7.357	13.539		
Avionics	0.300	1.000		
Training Equipment	0.015	1.003		
AGE, Peculiar	0.155	2.581		
Total Test Spares	26.591	110.174		
Total Non-Recurring RDT&E	1857.929	2483.687		

TABLE E.1. RDT&E, VALIDATION AND DEVELOPMENT COST DATA FOR REFERENCE NUCLEAR AIRCRAFT (CONT.)

	Program Costs, Million $		Program Effort, Million Manhours	
	Validation Phase	Follow-On Development	Validation Phase	Follow-On Development
Number of Aircraft	2	4		
Recurring Development				
Airframe				
Manufacturing Labor	263.043	357.197	11.876	16.126
Manufacturing Material	28.692	63.135		
Equipment, CFE/GFE	16.317	0.000		
Quality Assurance	34.612	39.771	1.544	1.774
Sustaining Engr.		52.103		2.227
Sustaining Tooling		63.243		2.408
Subtotal, Airframe	342.665	575.449		
Propulsion	29.427	54.157		
Nuclear Assembly	78.823	157.647		
Avionics	1.000	2.000		
ECO's	13.707	32.600		
Total Flyaway	465.622	821.852		
Average Unit Flyaway	232.810	205.460		
Support				
AGE, Peculiar	1.546	25.813		
Training Equipment	0.150	10.325		
Data	0.702	34.078		
Total Support	2.398	70.216		
Total Recurring Development	468.020	892.068		
Total RDT&E	2325.949	3375.754		
Total RDT&E, Validation + Development	5701.703			

* Included with Vendor Cost of Item Listed Under Recurring Costs

TABLE E.2. LABOR AND MATERIAL RATES FOR AIRFRAME OF REFERENCE NUCLEAR AIRCRAFT*

	Material Rate, $/lb	Labor Rate, hr/lb
Wing	22.40	3.62
Tail	19.97	3.44
Body	16.95	3.60
Landing Gear	27.25	0.20
Flight Controls	52.03	2.54
Nacelles	51.98	6.18
Instruments	66.41	3.77
Hydraulics	17.61	2.08
Electrical	22.16	2.86
Electronic Racks	50.68	1.46
Furnishings	15.14	2.59
Air Conditioning	50.75	1.25
APU	103.46	1.10

* Based on 100 Production Units and Learning Curve Slopes of 75 Percent for Labor and 89 Percent for Material

TABLE E.3. SUPPORT AND OPERATING COST DATA
FOR REFERENCE NUCLEAR AIRCRAFT

Cost Element	Fleet 20-Year Life-Cycle Cost, Million $	Fleet Annual Operating Cost, Million $	Squadron Annual Operating Cost, Million $	Aircraft Hourly Operating Cost, $
Primary Program (See Table 7.7)	25,420.2	1,271.0	81.34	4707
Base Operating Support	914.3	45.7	2.93	169
Civilian Pay	185.5	9.3	0.59	34
Officer Pay	26.9	1.3	0.09	5
Airmen Pay	533.8	26.7	1.71	99
Miscellaneous Support	168.1	8.4	0.54	31
Depot Maintenance	9,539.9	477.0	30.53	1767
Personnel Support & Training	780.1	39.0	2.50	144
Medical Civilian Pay	19.5	0.9	0.06	3
Medical O&M Non-Pay	79.5	4.0	0.25	15
Officer Pay - Med, UPT/UNT	138.4	6.9	0.44	26
Airmen Pay - Med, R/S, UPT/UNT	293.8	14.7	0.94	54
Program VIII Misc. Support	29.7	1.5	0.09	5
PCS Cost - Officer	47.1	2.4	0.15	9
PCS Cost - Airmen	172.1	8.6	0.55	32
Total Operating Cost	36,654.6	1,832.7	117.29	6788

TABLE E.4. PRODUCTION COST BREAKDOWN
FOR ALTERNATE NUCLEAR AIRCRAFT

	Thousand $ Per Aircraft	
Wing	8,066	
Tail	1,230	
Body	7,727	
Landing Gear	1,643	
Flight Controls	826	
Nacelles	2,907	
Engine Installation	260	
Instruments	419	
Hydraulics	218	
Electrical	259	
Electronic Racks	160	
Furnishings	399	
Air Conditioning	307	
APU	162	
Final Assembly	2,965	
Production Flight	1,461	
System Integration	1,743	
Total Empty Manufacturing Cost		30,752
Sustaining Engineering	2,357	
Production Tooling	3,306	
Quality Assurance	3,387	
Airframe Fee	8,259	
Airframe Cost		48,061
Engine Cost	8,646	
Avionics Cost	500	
Reactor Assembly	21,495	
Nuclear Ducting and Aux. Cooling	4,131	
Engine Heat Exchangers	2,952	
Research & Development	20,568	
Total Flyaway Cost		106,353

LIST OF SYMBOLS

AGE	aerospace ground equipment
ANP	Aircraft Nuclear Propulsion
APU	auxiliary power unit
A/P	airplane
AR	aspect ratio
BPR	engine bypass ratio
C_D	drag coefficient
C_L	lift coefficient
C_l	section lift coefficient
C_n	rate of change of yawing moment coefficient due to sideslip
CFE	contractor furnished equipment
COP-DS	Component Parametric - Design Subroutines
D_n	nacelle drag, lb
DOC	direct operating cost, $
ECO	engineering change order
ETA	engine power setting
FOM	figure of merit
GFE	government furnished equipment
HP	high pressure
HX	heat exchanger
JP, JP-4	jet propulsion fuel

L/D	lift-to-drag ratio
LCC	life-cycle cost, $
LFC	laminar flow control
Li	lithium
LiH	lithium hydride
LP	low pressure
M	Mach number
MAC	mean aerodynamic chord
MW	megawatts
NaK	sodium-potassium
N_E	number of engines
NERVA	nuclear rocket program
NSS	nuclear subsystem
NuERA	Nuclear Extended Range Aircraft
OWE	operating weight equipped
P_{amb}	ambient pressure, psia
$\Delta P/P_C$	engine core duct pressure loss ratio
$\Delta P/P_F$	fan duct pressure loss ratio
$\Delta P/P_2$	engine inlet pressure loss ratio
Q_R	reactor thermal rating, MW
RDT&E	research, development, testing and evaluation
SFC	specific fuel consumption, lb/lb-hr
SLSD	sea-level standard day

T/C	thickness-to-chord ratio
T/C_{eff}	effective thickness-to-chord ratio
TIT	turbine inlet temperature, ^{o}F
TOD	takeoff distance, ft
V_{APP} LIMIT	approach speed limit, kts
W/S	wing loading, lb/ft^2
δ_{amb}	ambient pressure correction
Λ	wing sweep angle, deg